# JOURNAL of the

# *Hydraulics*

# *Division*

## BASIC REQUIREMENTS FOR MANUSCRIPTS

This Journal represents an effort by the Society to deliver information to the reader with the greatest possible speed. To this end the material herein has none of the usual editing required in more formal publications.

Original papers and discussions of current papers should be submitted to the Manager of Technical Publications, ASCE. The final date on which a discussion should reach the Society is given as a footnote with each paper. Those who are planning to submit material will expedite the review and publication procedures by complying with the following basic requirements:

1. Titles should have a length not exceeding 50 characters and spaces.

2. A 50-word summary should accompany the paper.

3. The manuscript (a ribbon copy and two copies) should be double-spaced on one side of 8½-in. by 11-in. paper. Papers that were originally prepared for oral presentation must be rewritten into the third person before being submitted.

4. The author's full name, Society membership grade, and footnote reference stating present employment should appear on the first page of the paper.

5. Mathematics are reproduced directly from the copy that is submitted. Because of this, it is necessary that capital letters be drawn, in black ink, 3/16-in. high (with all other symbols and characters in the proportions dictated by standard drafting practice) and that no line of mathematics be longer than 6½-in. Ribbon copies of typed equations may be used but they will be proportionately smaller in the printed version.

6. Tables should be typed (ribbon copies) on one side of 8½-in. by 11-in. paper within a 6½-in. by 10½-in. invisible frame. Small tables should be grouped within this frame. Specific reference and explanation should be made in the text for each table.

7. Illustrations should be drawn in black ink on one side of 8½-in. by 11-in. paper within an invisible frame that measures 6½-in. by 10½-in.; the caption should also be included within the frame. Because illustrations will be reduced to 69% of the original size, the capital letters should be 3/16-in. high. Photographs should be submitted as glossy prints in a size that is less than 6½-in. by 10½-in. Explanations and descriptions should be made within the text for each illustration.

8. Papers should average about 12,000 words in length and should be no longer than 18,000 words. As an approximation, each full page of typed text, table, or illustration is the equivalent of 300 words.

Further information concerning the preparation of technical papers is contained in the "Technical Publications Handbook" which can be obtained from the Society.

---

HY,PO,SA,ST

## CONTENTS

October, 1957

### Papers

# CONTENTS

# Journal of the
# HYDRAULICS DIVISION
## Proceedings of the American Society of Civil Engineers

### TURBULENCE IN CIVIL ENGINEERING:
### AN INTRODUCTION TO THREE RESEARCH PAPERS

J. M. Robertson,* M. ASCE
for Hydraulics Research Committee
(Proc. Paper 1391)

The "Symposium on Turbulence" for which this paper serves as an introduction is more than a mere collection of papers about turbulence. It is evidence of the hydraulic engineer's interest in learning more about that fundamental subject. Although as engineers we are interested in practical problems, we also desire to understand the basic mechanics of the phenomena that enter into our practice. Thus hydraulic engineers are interested in more than just coefficients. In many instances a clearer understanding of the flow fundamentals has lead to advances in our methods of analysis and design. For example, increased knowledge of turbulence has led to advances in our practical approach to pipe flow problems and sediment transport problems.

Turbulence is a subject of concern to civil engineers in many areas beside just those interested in flow in various channels. Thus, the wind loads on buildings and other structures are variable due to large-scale turbulent fluctuations. The 1952 paper by R. H. Sherlock[1] is an excellent illustration of the structural engineer's concern with turbulence. The group of three research papers which follow are limited to cases of primary concern to hydraulic engineers; however, they do contain information on turbulence fundamental to all areas. Reflecting an interest in turbulence beyond that specified by strictly hydraulic problems, the Committee on Research of the Society's Hydraulics Division has encouraged and sponsored studies and reviews of the nature of turbulent motion. The papers which follow are presented as further evidence of our conviction that the civil engineer, and particularly the hydraulics engineer, desires to be cognizant of turbulence and appreciates this knowledge.

The function of this introduction is to indicate where and how the three research papers conform to the general status of our knowledge of turbulence. Since most of the readers are presumed to be ASCE members, this will be attempted through a review of previous coverages of turbulence in ASCE

publications. The literature on turbulence is voluminous and far exceeds that in ASCE publications; an attempt is made therefore to assess the adequacy of such a coverage.

## ASCE Publications on Turbulence

Presentation of the "modern" theory of turbulence to ASCE members dates back to the 1936 paper by Hunter Rouse[2] and the 1939 paper by A. A. Kalinske.[3] Rouse's presentation was principally concerned with the effects on flow in pipes—head loss and velocity distribution relations. Analytically, the results presented were based on the phenomenological theories of Prandtl's mixing length and von Karman's similarity hypothesis both very valuable concepts today for practical problems. In concluding his paper, Rouse noted the need for a complete rational analysis of the inner mechanism of turbulence movement. Kalinske presented many of the basic concepts of "the statistical theory of turbulence" initiated by G. I. Taylor—the correlation coefficient, length scales, spectrum of turbulence, etc. The knowledge of turbulence was correlated with the solutions of certain practical hydraulic problems; energy dissipation, suspended material transport, etc. Kalinske's experimental data were primarily obtained by laborious photographic techniques; he indicated a great need for an instrument, like the hot-wire anemometer used in air, that could be used for turbulence measurements in water.

A review of the ASCE Transactions and Proceedings since the papers by Rouse and Kalinske indicates papers on turbulence and suspended material by Dobbins [4] (1943), Vanoni [5] (1944), Camp [6] (1945), Ismail [7] (1951); papers on energy conversion by Kalinske[8] (1944) (based on work sponsored by the Hydraulic Research Committee) and Bakhmeteff and Allen[9] (1945) (also based on an investigation under the auspices of this committee). Concern with atmospheric turbulence is represented by the paper by Sherlock[1]. More recently we have the 1953 paper by Bauer[10] on the turbulent boundary layer on steep slopes and the 1955 paper by Ross[11] on the turbulent boundary layer in adverse pressure gradients. We have also papers by Bennett and Lee [12] (1955) on boundary layer transition and by Einstein and Li [13] (1956) on the laminar film or sublayer.

These are interesting papers—all of them from a turbulence consideration and many of them from the standpoint of practical hydraulics problems. It is significant to note that they are primarily concerned with one or the other of the practical problems introduced by Rouse or Kalinske.

Referring to the papers which follow it is quite appropriate that two of them involve solutions to the need expressed by Kalinske for a turbulence measuring instrument for use in water. The hot-wire anemometer (so satisfactory for use in air) is not suitable in water and two of its hydraulic cousins are described. A third cousin, the hot-film anemometer, has recently appeared[14] but is not discussed. The experimental results to be presented in the three papers also help us in our progress towards fulfilling the need expressed by Rouse twenty years ago for an understanding of the turbulence mechanism. However, progress in this direction is quite slow and there is much yet to be learned.

### Status of Turbulence Knowledge

To assess the extent to which the ASCE, through its publications, is keeping up on turbulence it is necessary to take a quick look at the overall progress in the field.

Activity in the field of turbulence during the present century has been concentrated in three periods: in 1925-30 when the phenomenological theories of Prandtl, von Karman, etc. were developed; again in 1935-37 when the statistical theory of turbulence saw rapid development and the first real measurements of turbulence were obtained; and again in the 1947-53 post war period. In this last period a recent review[15] of the significant papers on the measurement of turbulence indicates the publication of twenty-nine such, with eight in the year 1951. Although theoretical development continued, this was principally a period of learning from experiment more and more about the nature of turbulence.

It would obviously require a paper several times this in length to present an adequate review of the present status of our knowledge on turbulence. However, a few remarks will be attempted in the hopes of giving a glimpse of what we know or think we know. It has been noted that Kalinske introduced certain of the basic elements of "the statistical theory of turbulence." In spite of this most of our applications have been in terms of the results of the phenomenological theories involving the mixing length, momentum transfer, etc. As of today, most of the leading turbulence researchers have discarded these concepts. Although it is true that actual measurements of turbulence discredit the mixing length approach, we are not in a position to replace it with a better theory for practical solutions. Therefore, we continue to use it, but with caution. The statistical theory of turbulence, which for a long time has been limited to the rather idealized case of homogeneous isotropic turbulence,[16] is just starting to be used in an attack on the more complicated case of turbulence in shear flows.

The three research papers which follow faithfully reflect this introduction of the statistical theory in to shear flow problems. The study of correlation coefficients and frequency spectrum measurements in the first paper is a direct result of attempts to tie in with the statistical theory. The research reported did not progress as far with the statistical theory as some have,[17] due primarily to limitations in experimental equipment. In two of the three papers this was a direct result of the fluid medium used, namely water. The fact that progress in water has been as good as it has is very encouraging.

From the temporal-mean velocity standpoint our understanding has changed little since the summary paper by Rouse. We still conceive of a thin laminar film separating the wall from the turbulent flow. It is true there are various indications that our idealized picture of this is not correct and that even the laminar film contains turbulence fluctuations which, however, decrease in magnitude as the wall is approached. But the laminar film concept is still valuable and useful. Outside this thin film the turbulent velocity profile is found to follow the logarithmic type relation due to Prandtl and von Karman. However, the 25 year old concept of a universal profile, deduced from Nikuradse's experiments, is now known to be a poor approximation. A single logarithmic law does not adequately describe the velocity variation from the edge of the laminar film to the center of the pipe or outer edge of the boundary layer. Instead the logarithmic velocity distribution applies for

a distance of about ten or fifteen percent of the pipe radius from the wall. Outside of this region, in the central or core region of pipe flow, other relations apply. Description of the velocity distribution in these several regions is still based on phenomenological concepts.

Progress towards our understanding of turbulent shear flows (i.e. pipes and boundary layers) is being made with the aid of energy balance considerations as well as the statistical theory. In this additional approach, one considers the production, convection, diffusion and dissipation of the turbulent energy. Basic discussions along these lines were introduced by von Karman (1937) and Prandtl (1945). The approach is very similar to the analysis utilized by Bakhmeteff and Allen.[9] Some very interesting results of this approach are now apparent. It is found that, although turbulence production and dissipation are very high near the wall, there is significant transport and diffusion of turbulent energy to other regions.

## Future Plans of Hydraulics Research Committee

This present symposium is not a summary of our knowledge of turbulence, with civil engineering applications and interests, but rather a report on some current researches into turbulence. Your Committee on Research of the ASCE Hydraulics Division feels that it should do more in this regard than just collect groups of papers when they become available. With this idea in mind, discussions have been held with several members of our profession who are active in the turbulence field.

This has led to an indication of specific phases of turbulence that should and can be summarized in papers at this time. Some of these are as follows: application of basic ideas of turbulence to liquid mixing problems; application to micrometeorology or surface runoff, to flow through porous media, open channels, hydraulic structures and tidal estuaries; and effects of turbulence on sediment transport, river pollution problems and heat transfer in flumes and rivers. Along this line we have the suggestion that the sediment suspension problem should be amenable to analysis, following energy balance considerations. If so, such an analysis could give us a much better understanding of suspension.

It is impossible to predict the extent to which the above subjects will be reported in the near future. However, it is hoped that at least some of them will be.

## Acknowledgment

The author would like to acknowledge the cooperation of the authors of the three research papers in making this symposium a coherent whole. His thanks are due them for having such interesting and pertinent material to report. The participation of A. A. Kalinske, R. B. Banks and W. D. Baines in the discussions mentioned in the last part of this paper is gratefully acknowledged.

In the review of turbulence knowledge, reference has been limited principally to ASCE papers. The reason for this is obvious but it is not meant to imply that no other papers on the subject exist.

## REFERENCES

1. Sherlock, R. H., "Variation of Wind Velocity and Gusts with Height," Trans. ASCE, Vol. 118, 1953, pp. 463-508.

2. Rouse, Hunter, "Modern Conceptions of the Mechanics of Fluid Turbulence," Trans. ASCE, Vol. 102, 1937, pp. 463-543.

3. Kalinske, A. A., "Relation of the Statistical Theory of Turbulence to Hydraulics," Trans. ASCE, Vol. 105, 1940, pp. 1547-1600.

4. Dobbins, W. E., "Effect of Turbulence on Sedimentation," Trans. ASCE, Vol. 109, 1944, pp. 629-678.

5. Vanoni, V. A., "Transportation of Suspended Sediment by Water," Trans. ASCE, Vol. 111, 1946, pp. 67-133.

6. Camp, T. R., "Sedimentation and the Design of Settling Tanks," Trans. ASCE, Vol. 111, 1946, pp. 895-958.

7. Ismail, H. M., "Turbulent Transfer Mechanism and Suspended Sediment in Closed Channels," Trans. ASCE, Vol. 117, 1952, pp. 409-446.

8. Kalinske, A. A., "Conversion of Kinetic to Potential Energy in Flow Expansions," Trans. ASCE, Vol. 111, 1946, pp. 1043-1102.

9. Bakhmeteff, B. A. and Allen, W., "The Mechanism of Energy Loss and Fluid Friction," Trans. ASCE, Vol. 111, 1946, pp. 1043-1102.

10. Bauer, W. J., "Turbulent Boundary Layer on Steep Slopes," Trans. ASCE, Vol. 119, 1954, pp. 1212-1242.

11. Ross, D., "A Physical Approach to Turbulent-Boundary-Layer Problems," Trans. ASCE, 1956, Vol. 121, pp. 1219-1254.

12. Bennett, H. W. and Lee, C. A., "An Experimental Study of Boundary Layer Transition," Proc. ASCE, Vol. 81, 1955, Paper No. 796.

13. Einstein, H. A. and Li, H., "The Viscous Sublayer Along a Smooth Boundary," Proc. ASCE, Journal Engineering Mechanics Division EM2, April 1956, Paper 945.

14. Ling, S. C. and Hubbard, P. G., "The Hot-Film Anemometer: A New Device for Fluid Mechanics Research," Journal of the Aeronautical Sciences, Vol. 23, 1956, pp. 890-891.

15. Cooper, R. D. and Tulin, M. P., "Turbulence Measurements with the Hot-Wire Anemometer," NATO, AGARDograph 12, August 1955.

16. Batchelor, G. K., "The Theory of Homogeneous Turbulence," Cambridge University Press, 1953.

17. Townsend, A. A., "The Structure of Turbulent Shear Flow," Cambridge University Press, 1956.
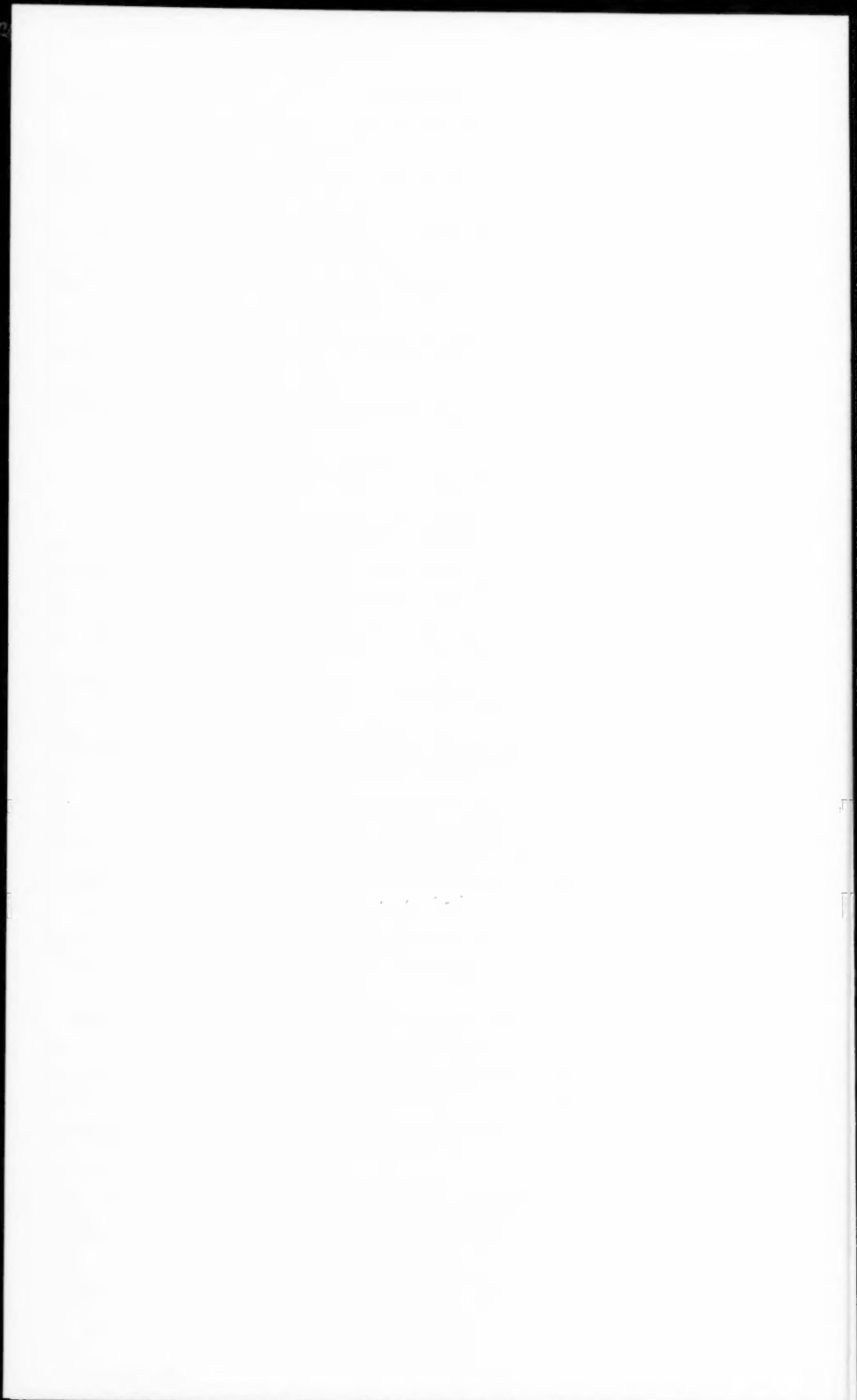
Journal of the

# HYDRAULICS DIVISION

## Proceedings of the American Society of Civil Engineers

TURBULENCE IN CIVIL ENGINEERING:
MEASUREMENTS IN FREE SURFACE STREAMS*

Arthur T. Ippen** M. ASCE and Fredric Raichlen*** J.M. ASCE
(Proc. Paper 1392)

Various turbulence phenomena in free surface streams were investivated
by means of a combination of a total head tube with a capacitance type pres-
sure transducer. Design criteria for the instrument are given as well as a
series of performances data derived from turbulence measurements.

## SYNOPSIS

Certain turbulence characteristics of free surface streams were deter-
mined in the laboratory by means of a combination of a total head tube with a
capacitance type pressure transducer. The design criteria for such an
instrument are given together with performance data.

The experimental studies covered primarily boundary layer growth in a
high velocity stream, the relative turbulence intensity, the properties of the
auto-correlation coefficient and of the mean intensity spectrum in relation to
depth. The purpose of the studies was to check the instrument performance
in relation to turbulence properties known from hot wire measurements in air
streams.

In general, satisfactory agreement was found and it may be concluded that
an instrument of this type gives reliable values of mean velocities, root mean
square values of the turbulent velocity fluctuations in the direction of the
mean flow and the scales of macro turbulence in water.

## INTRODUCTION

Turbulent motion in fluids is of interest to hydraulic engineering in connection with many practical problems. These include in general the mechanism of energy dissipation and the correlated mixing processes of waters with different temperatures, salinities, oxygen content and solid suspensions. More specifically the transport of sediment in streams and by wave action along beaches and the diffusion of waste waters in streams and reservoirs may be mentioned.

Knowledge concerning the statistical properties of turbulent streams has been rapidly advanced in recent years through the development and extensive experimental application of the hot-wire anemometer for turbulent air flows. However, a suitable instrument for water has been lacking, although many methods have been tried. The hot wire is affected by the impurities in the water, which do not permit a constant calibration to be maintained.[1] The study of particle motion with oil droplets or other suspensions is very cumbersome and unsuited to the exploration of local conditions.

The following study reports summarily on a program initiated in 1950 at the Hydrodynamics Laboratory of M.I.T. to combine the familiar Pitot tube, normally used for mean velocity determination, with a rapidly responding pressure pickup, so as to register the time history of the instantaneous pressures exerted by the turbulent flow on the tip of the tube.

Of all the systems considered initially the capacitance type pressure cell proved to be the most suitable pickup with respect to possible sensitivity and frequency response. In the gage developed the dynamic head existing at a given point in the flow is converted to a pressure, which is transmitted through the tube to the pressure cell, where it causes a minute deflection of a clamped circular diaphragm. This deflection reduces the small airgap between the diaphragm and a fixed electrode and results in a change in capacitance, which is electronically amplified and recorded.

For each point in the flow field, these records must permit an adequate definition of the state of turbulence by means of the following statistical parameters:

1. The root mean square of the velocity fluctuations in the direction of mean motion: $\overline{u'^2}$

2. The auto-correlation factor $R_{(\tau)}$, which compares these random fluctuations at one point with time. It is defined as:

$$R_{(\tau)} = \frac{\lim\limits_{T\to\infty} \int_0^T u'(t)\, u'(t+\tau)\, dt}{\overline{u'^2}} \tag{1}$$

wherein $\tau$ indicates a delay time in seconds.

3. The mean intensity spectrum, which gives the distribution of mean power in the turbulence as a function of the frequency. The portion of kinetic energy for a frequency interval df is defined by $\overline{u'^2}\, W(f)df$ wherein according to the Wiener-Khinchine theorem the spectrum function is:

$$W(f) = 4\int_0^\infty R_{(\tau)} \cos \omega\tau \, d\tau \tag{2}$$

In general, the turbulent kinetic energy of the flow is given by the mean square of the fluctuations, while the distribution of the auto-correlation factors with respect to delay time results in definitions of certain turbulent eddy characteristics. The smallest eddies in the flow are defined by the shape of the correlation curves near their origin and are described by the scale of micro-turbulence $\lambda$ . By contrast, the entire area under the auto-correlation curve defines the scale of macro-turbulence or the mean eddy size. The total area under the mean intensity spectrum employed here is evidently only the portion of the total kinetic energy of turbulence defined by $\overline{u'^2}$. The spectrum function as defined by Equation (2) represents a comparison of the auto-correlation function over its entirety with cosine functions of various frequencies $\omega$ .

## Mechanics of Total Head Tube-Pressure Cell Combination

Before discussing the gage actually used in these turbulence investigations, the basic mechanics of such an instrument along with the criteria to be employed in design will be described.

A schematic drawing of the gage is shown in Figure 1. The gage consists essentially of two parts; the total head tube which is inserted in the flow, and the pressure transducer mounted above the flow to which this tube is directly connected. At one end of the pressure chamber is a flexible diaphragm firmly clamped to the chamber walls around its periphery. A fixed electrode is placed a small distance away from the membrane separated by a thin air gap. A change in the instantaneous total head at the tube tip causes a change in pressure at the diaphragm face with a resulting deflection of the membrane. This deflection is recorded by electronically measuring the change in capacitance between the fixed electrode and the diaphragm. By proper static calibration this change in capacitance can be directly related to an instantaneous change in total head.

Considering the total head tube inserted in an open channel and aligned with the direction of mean flow the instantaneous total head recorded by this gage is:

$$H_t = H + h_s = \frac{(U + u')^2}{2g} + \frac{p'}{\gamma} + h_s \qquad (3a)$$

wherein:  $U$ = temporal mean velocity in the x direction
$u'$ = turbulent velocity fluctuation in the x direction
$p'$ = turbulent local pressure fluctuation
$h_s$ = mean hydrostatic head on the tube tip

Thus also:

$$H = H_t - h_s = \frac{U^2}{2g} + \frac{Uu'}{g} + \frac{u'^2}{2g} + \frac{p'}{\gamma} \qquad (3b)$$

The values of $H$ and $H_t$ are varying in random fashion. Assuming that the gage records the instantaneous values of $H_t$ correctly it is seen that the difference between the instantaneous velocity $u = \sqrt{2gH}$  and the temporal

mean velocity $U$ is primarily dependent upon the product $\frac{Uu'}{g}$. While the $\frac{u'^2}{2g}$ and $\frac{p'}{\gamma}$ terms are of the same order of magnitude, they are normally not in phase. Thus it is conceivable that for very small values of $u'$ approaching zero the turbulent pressure $\frac{p'}{\gamma}$ exceeds in value the other turbulent terms. However, assuming for example $u'_{max} = .10\ U$ and thus $\frac{u'^2}{2g} = .01\ \frac{U^2}{2g} \approx \frac{p'}{\gamma}$ it is apparent that the maximum contribution of $\frac{p'}{\gamma}$ to H when $u' = o$ is only of the order of one percent and its influence on $u'$ not more than 5%. The errors inherent in the instrument are given in more detail in reference (4).

The method employed in the analysis of time histories of instantaneous head will be taken up later. Of importance is the fact that the dominant random quantities in the above equation must be recorded by an instrument, which will not distort these fluctuations felt at the tip of the tube. It is clear from dynamic considerations that the design criterion of prime importance for accurate measurement of these fluctuations is the natural frequency of the gage.

In order to determine the natural frequency theoretically, the mechanical system of the gage is represented by a one-dimensional system composed of a spring (the diaphragm), a mass (the combined effective mass of the water in the impact tube and the pressure chamber), and a dashpot for viscous damping. By using this approach to the problem, many graphs and parameters familiar to engineers can be used. This one-dimensional analysis has been shown satisfactory from both experimental and theoretical considerations.(4)

For the system described above, the natural frequency can be obtained either by the use of Lagrange's equation or by adding up the forces acting on the system; i.e., the sum of the inertial, spring and viscous forces being set equal to the sum of the externally applied forces. In both methods the following major assumptions are made in the evaluation of the resonant frequency.

1. Velocity distributions in the tube and in the diaphragm well are uniform and may be related by the continuity equation:

$$m_1 = m_2\ \frac{A_2}{A_1}$$

where,   $m_1$ = the velocity of water in the tube

         $m_2$ = the velocity of water in the diaphragm well

         $A_1$ = the area of the tube bore

         $A_2$ = the area of the diaphragm well

2. The kinetic energies of the water in the diaphragm well and of the diaphragm are considered small compared to the kinetic energy of the water in the tube, since $\left(\frac{A_2}{A_1}\right)^2 \gg 1$.

3. The effect of viscous damping on the resonant frequency of the instrument is assumed to be small.

The expression defining the natural frequency of the gage, in units of cps, derived by this type of analysis is thus:

$$f_m = \frac{1}{2\pi}\left(\frac{A_1}{A_2}\right)\sqrt{\frac{k}{\rho A_1 L_1}} \tag{4a}$$

where,  $k$ = spring constant of the diaphragm
 $L_1$ = tube length
 $\rho$ = density of water

The spring constant of the diaphragm treated as a circular membrane clamped at its edge is:

$$k = \frac{16\pi E h^3}{a^2\left(1-\xi^2\right)} \tag{4b}$$

where,  $a$ = radius of the diaphragm
 $h$ = thickness of the diaphragm
 $E$ = modulus of elasticity of the diaphragm
 $\xi$ = Poisson's ratio = .30

The instrument first developed at the Hydrodynamics Laboratory and used for the initial turbulence studies described herein is designated as Gage 1 and is shown in Figure 2. The "pressure pick-up" which was inserted in the flow was a small tube, with a vertical leg 6 in. long and a 2 in. horizontal leg. The tube was of stainless steel with a 1/8 in. outside diameter and a 1/16 in. inside bore diameter. It was connected directly to the pressure transducer which was located above the water surface. The diaphragm was 0.0075 inches thick and 1 in. in diameter and was made of beryllium copper with a modulus of elasticity of $15 \times 10^6$ psi. The brass electrode, 0.938 in. in diameter, was insulated from the gage housing by a sheath of hard rubber and was separated from the diaphragm by an air gap of no less than 0.0025 inches. A small cylinder valve attached to the pressure cell allowed the system to be filled by flushing water through the diaphragm well and out through the impact tube.

With these physical characteristics of Gage 1, a natural frequency of 15.4 cps is obtained from Equations 4a and 4b.

At first glance, this frequency response appears to be too low for an instrument to be used in turbulence measurements. However, the results obtained with this instrument are in good agreement with those obtained using a modified version of Gage 1 (designated as Gage 2) having a ten times higher natural frequency. This would indicate that the major portion of the turbulent energy in the type of flow investigated is of low frequency. This conclusion will be supported by experimental data presented in connection with the results of turbulence investigations with Gage 2.

### Turbulence Measurements with Gage 1

The major portion of the measurements with Gage 1 and its successors was carried out in an open channel in the laboratory. This flume has

aluminum walls, a glass bottom and is 45 ft. long and 4 ft. wide. The slope of the flume can be varied fully from zero to 0.1 ft. per ft. The mean velocities ranged from 4 to 10 fps and the depth of flow was varied from 1 to 3 inches. The circulation of water is accomplished by pumping from a large reservoir in the basement of the laboratory through a 10 x 6 in. Venturi for metering purposes and a 10 in. gate valve into a closed transition section. This section transforms the flow cross-section from a circular one of 10 in. diameter to a rectangle 10 in. x 4 ft. After this the flow passes upward to the elevation of the flume bottom and into the nozzle section, where several honeycomb baffles eliminate large scale disturbances. The flow is accelerated rapidly through a 4 ft. wide adjustable nozzle and enters the so-called high velocity flume with a free surface with practically negligible turbulence.

E. M. Lowry, Jr.[2] in 1951 used Gage 1 to investigate the variation of the temporal mean velocity and of the root mean square of the turbulent velocity fluctuations depthwise in a uniform free surface flow. The results obtained (see Figure 3) were compared to measurements of Laufer[3] made in an air stream in a rectangular test section at a comparable Reynolds number and indicated good agreement.

In obtaining the mean velocities and the root mean square values of the turbulent velocity fluctuations, it was assumed that each horizontal line on the Brush recorder paper that was used for signal display corresponded to a particular velocity head found by static calibration of the gage. Knowing the head of water H necessary to cause a given deflection on the recorder, the

velocity was obtained from the relation $u = \sqrt{2gH}$ . Thus, in analyzing the record, it was assumed that every time the trace touched or crossed a particular horizontal line on the recorder paper, a certain velocity associated with that line existed instantaneously. Designating the frequency of occurrance of the velocity as f, and the total velocity at that point as u, the expression

$$U = \frac{\Sigma f \cdot u}{\Sigma f} \tag{5}$$

was used to determine the value of the temporal mean velocity U for a record of suitable length. For each record so analyzed, the value of the root mean square of the velocity fluctuations was computed from:

$$\sqrt{u'^2} = \sqrt{\frac{\Sigma f \cdot (u - U)^2}{\Sigma f}} \tag{6}$$

These expressions actually evolve from Equation 3 after neglecting the pressure fluctuations, p'.

Immediately downstream from the nozzle of the flume a turbulent boundary layer begins to develop which grows from the bottom and eventually extends over the full depth of the flow within a distance dependent upon the flow conditions established. For more detailed confirmation of the applicability of the gage Lowry investigated this boundary layer growth at stations every six inches downstream from the exit of the nozzle for a distance of four feet. The thickness of the turbulent boundary layer was determined by varying the tube

submergence slowly from the smooth glass bottom of the flume upwards in the flow until the velocity fluctuations existing in the boundary layer and observed in the record decreased to a few short intermittent bursts and eventually disappeared. The values of the boundary layer thickness as shown for two runs in Figure 4 appear in good agreement with the well known expression:

$$\frac{\delta}{x} = \frac{0.38}{R_x^{1/5}} \tag{7}$$

where, $\delta$ = boundary layer thickness
$x$ = distance downstream
$R_x = \dfrac{U_{max} \cdot x}{\nu}$

Water surface elevations and theoretical boundary layer displacement thicknesses are also given.

In addition the statistical distribution of the velocity fluctuations about the temporal mean velocity was found nearly Gaussian in form which is to be expected for a random variable. This is shown in Figure 5 for numerous points at the same station.

In 1952, D. L. Favin constructed an electrodynamometer at the laboratory and J. P. Lawrence[5] incorporated it into the circuit of Gage 1 to obtain, directly, values of the temporal mean velocity and the mean square of the fluctuations. This dynamometer consisted essentially of two sets of interacting coils, one set fixed and the other set suspended by a spring. When a current is imposed in both sets, an angular deflection of the novable set is experienced which is proportional to the mean of the product of the applied currents.

The actual values of interest can be obtained by applying the following currents to the coils:

1. By imposing a constant current on one set of coils and a fluctuating signal from the gage on the other set, the value of the temporal mean velocity was determined.

2. By removing the D.C. level of the signal and sending only the A.C. portion through both the fixed and the movable coils, a squaring and meaning effect is produced from which the mean square of the fluctuating velocity component is determined.

A typical example of Lawrence's results of the variation of the relative mean velocity and relative turbulent intensity with relative depth for Reynolds number value of $R = 210,000$ is shown in Figure 6. The different check points that were made both with a Prandtl tube and at a later time with Gage 1 are also given in this figure illustrating the reproducibility of the data obtained with this instrument. Figure 7 gives a summary of results for relative turbulence intensities obtained for a wide range of Reynolds numbers.

The dynamometer is also capable of giving correlation factors directly; however, this possibility was not pursued, since a magnetic recording and playback of the record would have been required for auto-correlation or a duplicate instrument for space correlation. Instead the attention was directed

towards the development of a gage with much higher natural frequency.


## Turbulence Measurements with Gage 2

### Mechanical Features

This new instrument denoted as Gage 2, was designed for a natural frequency of better than ten times that of the original capacitive element. Referring to Equations 4a and 4b, it is seen that this can be accomplished in several ways by:

1. increasing the spring constant k of the diaphragm
2. increasing the area ratio, $A_1/A_2$
3. decreasing the impact tube length

Of most practical significance is the increase of the spring constant of the diaphragm. Hence, in the first version of Gage 2 the diameter of the diaphragm in Gage 1 was retained while the thickness was increased from 0.0075 in. to 0.030 in. This change alone will result in a natural frequency of approximately eight times that of Gage 1; i.e., approximately 112 cps. The possibility of viscous damping to attain a relatively flat response curve was investigated by dividing the internal portion of the gage into essentially two parts; (1) a damping chamber that could be oil-filled for viscous damping and (2) an impact tube connection that would be water-filled and separated from the damping chamber by a thin secondary diaphragm. It was found that mechanical damping even with the damping well filled with an extremely viscous oil was not appreciable. However, the secondary diaphragm was nevertheless retained, with the gage completely water-filled, in order to achieve a higher frequency response. Since it was found that a small amount of air trapped in the gage would substantially reduce the frequency response of the instrument, the gage was filled while submerged in a container of deaerated water.

The features of this modified gage may be seen in Figure 8-a, a schematic drawing of Gage 2, along with Figures 8-b and c showing photographs of the instrument and of its associated electronics.

A typical set of records obtained using Gage 1 and Gage 2 is shown in Figure 9. In these cases the gages were positioned in the high velocity flume approximately 2 ft. downstream from the nozzle exit. This station is upstream from the point where the turbulent boundary layer reaches the water surface. The first record for each gage was obtained outside of the turbulent boundary layer where the small fluctuations evident in the signal may be considered to be low intensity free stream turbulence. The second set of records for each gage was obtained near the channel bottom: i.e., within the boundary layer and thus the shear zone.

It was found at a later date that the secondary diaphragm mentioned above introduced certain instabilities in Gage 2. For this reason, it was eliminated and the resultant decrease in the natural frequency was compensated for by increasing the thickness of the primary diaphragm still further by a factor of two (from 0.030 in. to 0.060 in.). This increased the calculated natural frequency of Gage 2 to approximately 255 cps.

Due to the frequency limitations of the Brush Recorder used in conjunction with Gage 1, a Dumont type 322 dual beam oscilloscope was employed with Gage 2 with the signal being fed into one beam of the oscilloscope while

simultaneously a square wave of 60 cps was displayed on the other. The latter afforded both a time and a reference trace for the signal as illustrated in the lower portion of Figure 9. Recordings were made by photographing the oscilloscope by means of an open-shutter, 35 mm. motion picture camera.

## Data Analysis and Auto-Correlations

A micro-film viewer was used in the analysis of the data and a transparent grid was placed over this enlarged record with time intervals assigned to the vertical grid lines by means of the 60 cps square wave. Using this grid arrangement, values of the amplitude of the signal were obtained from the record at equally spaced time intervals. Approximately 1200 such points were then submitted to the Digital Computer Laboratory of M.I.T. where a program had been evolved for obtaining values of the auto-correlation factor from $\tau = 0$ to $\tau_t = 300 \ \tau_0$, where $\tau_0$ is the time spacing of the raw data points.

Employing the method described above, auto-correlation curves were obtained at one depth in each of two flows having Reynolds numbers of 52,000 and 54,300. These results are presented in Figures 10 and 11.

It is apparent that these curves have both a high and a low frequency periodicity superimposed on the random portion. In examining the form of the numerator of the auto-correlation function (Equation 1), it is seen that for a periodic signal, a periodicity occurs in the correlation function with the same frequency as that in the signal but with no phase relation. The high frequency component is due to the natural frequency of the gage and affords a method of experimentally determining the frequency response of the instrument (240 cps in this case compared to 255 cps calculated theoretically).

By the use of the correlation curve, two characteristic lengths have been defined by Taylor[6] which help to describe the properties of the turbulent flow field in more detail. The scale of micro-turbulence, associated with the smallest eddies in the flow is defined as the intercept, on the time or distance axis, of a parabola fitted to the correlation curve in the vicinity of the origin. In order for this parameter to be used in this investigation confidence must be placed in the portion of the correlation curve in the vicinity of $\tau = 0$. With this type of gage, where the mechanical system can be said to be composed of essentially a spring, a mass and a dashpot, the signal becomes distorted near the resonance and at forcing frequencies greater than the natural frequency (240 cps or $\tau = 0.00415$ sec). Therefore, reliable information cannot be obtained from the correlation curves in this region, and hence, the scale of micro-turbulence cannot be determined.

The second length termed the scale of macro-turbulence, L, is associated with the entire turbulent field and is a measure of the average eddy size present. It is defined in units of time as:

$$L_\tau = \int_0^\infty R(\tau) \, d\tau \tag{8}$$

A macro-scale larger in one case than another indicates that the auto-correlation curve falls off more gradually, and there is better correlation at greater delay times in the former as compared to the latter.

As has been shown by Dryden[7] and Laufer,[3] a curve of the form

$$R(\tau) = e^{-\tau U / L_x} \qquad (9)$$

can often be fitted to the correlation curve away from the origin for cases of a high turbulence Reynolds number. With this function fitting the data, then:

$$L_\tau = \int_0^\infty e^{-\tau U / L_x} \, dt = \frac{L_x}{U} \qquad (10)$$

The macro-scale was determined from these curves first by eliminating the 240 cps component from the curves received from the Digital Computer Laboratory by a three point averaging process. In this manner a correlation curve consisting of 300 weighted mean values of the correlation factor was constructed. The curves so resulting were then averaged by eye, the final smoothed curves being shown in the above mentioned figures. This facilitated the subtraction of any low frequency periodicities from the correlation curve before proceeding with the determination of the macro-scale. A cosine function having the same amplitude and period as the predominant low frequency component was subtracted from the smoothed correlation curves. The ordinates of the curve which resulted after the cosine function was removed comprised the curve to which Equation (9) was fitted to determine $L_x$. The first third of these points was then plotted on semi-logarithmic paper, $\ln R(\tau)$ vs $\tau$. Since the function $e^{-\tau U / L_x}$ treated in this manner reduces to a straight line, this was a relatively simple method of determining the mean eddy size. The analytical expression fitted in this manner shows rather good agreement with the meaned experimental data away from the origin. From this curve fitting process the values of $L_x/y_0$ were obtained for the relative depths of .157 and .510 as 2.95 and 3.66 respectively.

The magnitude of these results is reasonable, since other investigators have found that the scale $L_y$ in a depth-wise direction is approximately 1/3 to 1/2 of that in the downstream direction. If this factor is applied to these results with $y_0 = 1.27$ and 1.09 in., the depth-wise macro-scale would be of the same order as the depth of the flow. In addition to this, Townsend[8] has indicated that "eddies of downstream length . . . over three times the boundary layer thickness, contain much of the turbulent energy . . . ."

Mean Intensity Spectra

The mean intensity spectrum, which is the cosine transform of the auto-correlation function determines the distribution of turbulent energy with frequency. The Digital Computer Laboratory which assisted in the evaluation of the mean intensity spectra used a finite length of data in determining the cosine transform of the correlation function. Thus instead of an upper limit of infinity in the integral in Equation (2), the limit is actually the effective time length of the correlation curve, $\tau_t$. In addition, the cosine transform is convolved with the cosine transform of a unit step function of length $\tau_t$. Hence, the mean intensity spectrum obtained from the Digital Computer Laboratory and denoted as $W(f)^*$ is actually:

$$W(f)'' = W(f) \frac{sin\ \omega \tau_t}{\omega} \tag{11}$$

If a periodicity exists in the signal, this periodicity will be apparent as a spike at that frequency in the mean intensity spectrum caused by the quantity W(f). On both sides of the spike will be a series of peaks and troughs of

amplitude $\tau_t / \frac{n\pi}{2}$ , wherein n = 3, 5, 7, 9, . . . occurring with a period of 0.8 $\tau_t$ due to the term $\frac{sin\ \omega \tau_t}{\omega}$ .

A typical example of the mean intensity spectra obtained from the Digital Computer Laboratory is shown in Figure 12 for three frequency ranges; 0-25 cps, 0-75 cps and 0-250 cps.

Apparent in this curve is a negative spike at zero frequency. This point on the mean intensity spectrum corresponds to the ordinate of the auto-correlation curve at $\tau = \infty$; i.e., the mean or D.C. level of the auto-correlation curve. The primary data from which these curves were obtained were taken from the record about an assumed mean velocity level. Therefore, if this assumed mean level is correct, the auto-correlation curves should approach a line of zero correlation in the results received from the Digital Computer Laboratory. However, if this value is incorrect and the Computer fails to remove all the D.C. level from the signal in computing the auto-correlation factor, the line of zero correlation obtained with its assistance will possess either a positive or a negative value. A negative value of this line of zero correlation, such as was actually experienced, resulted in the negative spike at the origin of the mean intensity spectrum.

Periodicities below 5 cps are evident in this spectrum and are believed to be caused by periodic components in the flow. The apparent irregularity of this spectrum can be attributed to the term $\frac{sin\ \omega\ \tau_t}{\omega}$ in Equation (11) which super-imposes curves of this form throughout the spectral range, its effect being most noticeable on either side of the predominant periodicities.

A procedure was developed to smooth these curves by fitting the curve $\frac{sin\ \omega\tau_t}{\omega}$ to the peaks and troughs on either side of the predominant spikes caused by the periodic components in the flow. In this manner a mean intensity was obtained at each predominant periodicity which would be the actual relative intensity with the absence of the spike and the elimination of the effect of the sine term in Equation (11). Minor protuberances were removed from these curves by eye. The smoothed curve obtained in this manner from Figure 12 is shown in Figure 13.

Using the exponential expression $e^{-\tau U/Lx}$ for the correlation function and the definition for the mean intensity spectrum; i.e., Equation (2), the following analytic expression is obtained for the spectrum function:

$$W(f) = \frac{4\ Lx/U}{1 + (2\pi f\ Lx/U)^2} \tag{12}$$

This expression was fitted to the smoothed mean intensity spectrum obtained in the manner described above. The value of the turbulence macroscale employed in this reference curve was that obtained from the autocorrelation curve. The agreement between experimental function and analytic reference points in Figure 13 indicates that the low frequency periodicities were successfully removed in the first $L_x$ evaluation; i.e., using the autocorrelation curve of Figure 11.

The mean intensity spectrum shows a rapid decrease in energy with increasing frequency, with over 50% of the turbulent energy lying below 5 cps. The natural frequency of the instrument is evident in Figure 12 as a band of low amplitude spikes from approximately 200 to 235 cps. Thus both the autocorrelation curve and the mean intensity spectra can be employed to evaluate the natural frequency of such an instrument.

A loss of sensitivity of the electronic circuit was experienced in subsequent experiments which could not be corrected electronically without completely redesigning this circuit. However, this was improved by decreasing the thickness of the primary diaphragm from 0.060 to 0.045 in. Though this lowered the natural frequency of the instrument to approximately 150 cps, it is evident from an examination of the mean intensity spectrum that this is high enough to record the turbulent fluctuations with little distortion.


## Turbulence in the Wake of a Cylinder

The primary objective of this phase of the investigation was to measure variations in the temporal mean velocity, the root mean square of the turbulent velocity fluctuations and the scale of macro-turbulence in the wake of a right circular cylinder in super-critical open channel flow, thereby demonstrating the applicability of a total head tube-pressure cell combination in such investigations. A brass cylinder with a diameter $d = 1$ in. was used for testing in the high velocity flume in the laboratory. The cylinder was placed with its vertical axis 18 ft. from the nozzle exit, on the centerline of the flume, and with the following uniform flow characteristics established:

$$y_0 = 1.34 \text{ in.} \qquad\qquad U = 6.28 \text{ fps}$$
$$R = 58,500 \text{ (Reynolds No.)} \qquad F = 3.31 \text{ (Foude No.)}$$

Measurements were made using the improved instrument, Gage 2, in the wake of the cylinder within the region enclosed by the standing waves emanating from the body and at three stations downstream from the centerline of the cylinder, at $x/d = 40$, 50, and 70. At each station the velocity traverses were made near the centerline of the flume and at a fixed distance of $y = 0.84$ in. from the channel bottom.

It must be remembered that the wake investigated is not that of a cylinder in two-dimensional flow, but is also subject to shear conditions imposed by the channel bottom.


### Mean Velocity Distribution

Figure 14 represents graphically the results obtained in the temporal mean velocity phase of the wake study and is plotted as the ratio of the local temporal mean velocity U to the upstream mean velocity, $U_0$ computed at a relative depth $y/y_0 = 0.63$ vs. the ratio of the perpendicular distance from

the centerline of the wake to the cylinder diameter, $z/d$. As a basis of comparison at different stations downstream from the test cylinder, two equations were employed; the first was a function of the form of the Gaussian normal distribution:

$$\frac{u_2}{U_o} = c e^{-K(z/d)^2} \tag{13}$$

$$where \ u_2 = 1.06 \ U_o - U$$

Equation (13) showed good agreement with experimental data at the three downstream stations. The second expression was one derived by Schlichting.[9]

$$\frac{b}{d} = \sqrt{10} \ \beta \left( C_w \frac{x}{d} \right)^{1/2} \tag{14}$$

$$1 - \frac{U}{U_o} = \frac{5}{9} C_w \frac{d}{b} \left[ \ell - \left( \frac{z}{b} \right)^{3/2} \right]^2 \tag{15}$$

where:

$2b$ = the width of the wake

$\beta = \ell/b$

$\ell$ = Prandtl mixing length

$C_w$ = coefficient of drag

$d$ = diameter of cylinder

$U$ = temporal mean velocity in wake

$x$ = distance measured downstream from the cylinder in the direction of flow

$z$ = distance measured perpendicular to and from the centerline of the wake

$U_o$ = upstream mean velocity at distance $y$ from bottom

The quantity $\beta$ was evaluated experimentally; one set based on assumptions relating the mixing length to the macro-scale in a longitudinal direction and an additional set listed as $\beta_{exp.}$ modified to agree with the data $z/d = 0$. These are:

| $x/d$ | $\beta$ | $\beta_{exp.}$ |
|---|---|---|
| 40 | 0.144 | 0.174 |
| 50 | 0.219 | 0.242 |
| 70 | 0.245 | 0.245 |

These values are quite close to the constant found experimentally by Schlichting; $\beta = 0.207$. Reference (4) contains a detailed discussion of this phase of the investigation.

Intensity of Turbulence

Figure 15 illustrates graphically the variation of the ratio of the root mean square of the velocity fluctuations to the mean stream velocity, $\sqrt{u'^2}/U_0$, with distance $z/d$. A decrease of turbulence intensity with distance downstream along with the transverse variations is indicated. The general trend of these results is in agreement with experiments of Townsend[11] and of Roshko[12] performed with negligible boundary layer effects in air streams at subsonic velocities. The locations of intensity maxima observed by these investigators are also presented for comparison. At $x/d = 70$ the turbulence intensity has practically returned to the value of the undisturbed flow upstream at the equivalent relative depth.

Auto-Correlation Studies

The auto-correlation curves shown in Figures 16, 17, and 18 for the velocity fluctuations are for points on or near the centerline of the wake at $x/d = 40, 50, 70$, respectively. They were obtained in accordance with the method described previously after the effect of the hydrostatic head and the mean velocity had been removed from the signal.

The exponential function, Equation 9, fitted these curves quite well away from the origin as can be seen from the figures. In the case of the auto-correlation function at $x/d = 70$, it was necessary to first subtract a cosine function of about 3.6 cps from the curve to obtain a better fit. This frequency is of the same order of magnitude as that experienced in the previously mentioned uniform flow investigations. The periodicities at the natural frequency of the gage (140 cps) are barely perceptible indicating that the turbulence gage is capable of measuring accurately the major portion of the spectrum of turbulent energy in the wake.

The scale of macro-turbulence, $L_x$, was determined by the procedure described previously and is presented in Figure 19 as the variation of $(L_x/d)^2$ with distance downstream on or near the centerline of the wake.

A marked increase in $L_x$ with distance downstream is seen from this figure, which may be explained as follows: Near the cylinder the body tends to break up the eddy pattern in the approaching flow and substantially reduces the size of the macro-scale below its free stream value. With distance downstream the smaller eddies produced by the obstacle would tend to dissipate more rapidly than the larger eddies, thereby producing an increase in $L_x$ with $x$. Since the value of $L_x$ at the farthest station downstream is of the same order of magnitude as values obtained with Gage 2 in fully developed turbulent flow at comparable Reynolds numbers, a general return to upstream turbulence conditions is indicated. This same trend has been observed by other investigators in the flow behind grids. A curve of the form:

$$\left(\frac{L_x}{d}\right)^2 = K\left(\frac{x}{d} - \frac{x_o}{d}\right) \tag{16}$$

was fitted to the experimental data, showing the dependence of $L_x$ on $x^{1/2}$ in the core of the wake. The dependence of lateral macro-scale on $x^{1/2}$ has been found to hold downstream from a grid where the flow is known to be

isotropic.[13,14]  Thus the longitudinal scale would also vary in the same
manner.  In all these considerations the vorticity generated by the interaction
of the cylinder with the non-uniform flow of approach in the channel has been
ignored.  It would be of interest to investigate the entire problem in more de-
tail.  The present aim was confined however to establishing the general
validity of results obtained with the instrument developed.


## CONCLUSIONS

The studies presented indicate that an instrument consisting of a total head
tube-pressure cell combination may be designed with sufficient frequency
response to measure essential turbulence characteristics.  The character-
istics of a number of turbulent flows have been determined and have been
found in essential agreement with comparable results obtained with the
generally accepted hot-wire technique in airstreams.

In general the following advantages may be stated:

1.  The instrument is suited for use in water, maintains its calibration and
is mechanically simple.

2.  It may be built for laboratory as well as field use and for clean water
as well as for liquids with suspensions.

3.  Its mechanical features in relation to its natural frequency response
are readily determined by a one-dimensional vibrational analysis.

4.  The instrument records with sufficient accuracy the instantaneous
total head at a given point in the flow in the direction of the mean motion.

5.  From these records the turbulent fluctuations of the velocity in that
direction can be determined with satisfactory accuracy.  The error in the
root mean square value of the turbulent component being normally less than
5%.  Auto and cross-correlations, the mean intensity spectra and scales of
the macro-turbulence may be derived also.

The disadvantages are:

1.  Turbulent pressure fluctuations are included in the record and cannot be
extracted.

2.  The temporal mean velocity must be large as compared to the fluctuat-
ing component.  The error due to pressure fluctuations increases as the mean
velocity decreases.

3.  Transverse velocity fluctuations cannot be determined at present with
the instrument.

4.  The micro-scale of the turbulence apparently cannot be determined with
sufficient accuracy.

The claims made for the instrument are obviously not in any way tied to
the present mechanical and electronic assembly, but will apply to any similar
mechanical system.  On balance it may be stated that the instrument provides
a simple but restricted approach to turbulence measurements in liquid flow
and that with adequate development of the electronic components a great
many problems of liquid flow may be explored with respect to their most

important internal flow mechanics.  In the attempt to verify the performance
of the instrument a beginning has been made in that direction with the turbu-
lence studies presented above.


## ACKNOWLEDGMENT

## REFERENCES

1. Macovsky, M. S., "The Measurement of Turbulence in Water," David
   Taylor Model Basin Report No. 670, October, 1948.

2. Lowry, E. M., Jr., "Turbulence Studies from Recordings of Instantaneous
   Pitot Tube Pressures," Master of Science Thesis, Massachusetts
   Institute of Technology, 1951.

3. Laufer, J., "Investigation of Turbulent Flow in a Two-Dimensional
   Channel," NACA Report 1053, 1951.

4. Ippen, A. T.; Tankin, R. S. and Raichlen, F., "Turbulence Measurements
   in Free Surface Flow with an Impact Tube - Pressure Transducer Com-
   bination," Technical Report No. 20, Hydrodynamics Laboratory, Depart-
   ment of Civil and Sanitary Engineering, Massachusetts Institute of
   Technology, July, 1955.

5. Lawrence, J. P., "Reduction of Turbulence Data with an Electrodyna-
   mometer," Master of Science Thesis, Massachusetts Institute of
   Technology, 1953.

6. Taylor, G. I., "Statistical Theory of Turbulence," Proc. Roy. Soc. of
   London, Series A, Vol. 156, 1935.

7. Dryden, H. L., "A Review of the Statistical Theory of Turbulence,"
   Quart, Appl. Math., Vol. 1, 1943.

8. Townsend, A. A., "The Structure of the Turbulent Boundary Layer,"
   Cambridge Philosophical Society Proceedings, Vol. 47, 1951.

9. Schlichting, H., "Lecture Series 'Boundary Layer Theory' Part I Laminar
   Flows and Part II Turbulent Flows," NACA Tech. Mem. 1217 and 1218,
   1949.

10. Rouse, H., Engineering Hydraulics, John Wiley and Sons, Inc., New York,
    1950.

11. Townsend, A. A., "Measurements in the Turbulent Wake of a Cylinder,"
    Proc. Roy. Soc. of London, Series A, Vol. 190, 1947.

12. Roshko, A., "On the Development of Turbulent Wakes from Vortex Streets," NACA Tech. Note 2913, 1953.

13. Batchelor, G. K. and Townsend, A. A., "The Decay of Turbulence in the Initial Period," Proc. Roy. Soc. of London, Series A, Vol. 193, 1948.

14. Batchelor, G. K. and Townsend, A. A., "The Decay of Turbulence in the Final Period," Proc. Roy. Soc. of London, Series A, Vol. 194, 1949.
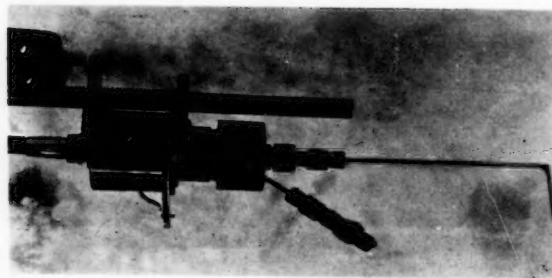
Figure 2.  Photograph of Gage 1
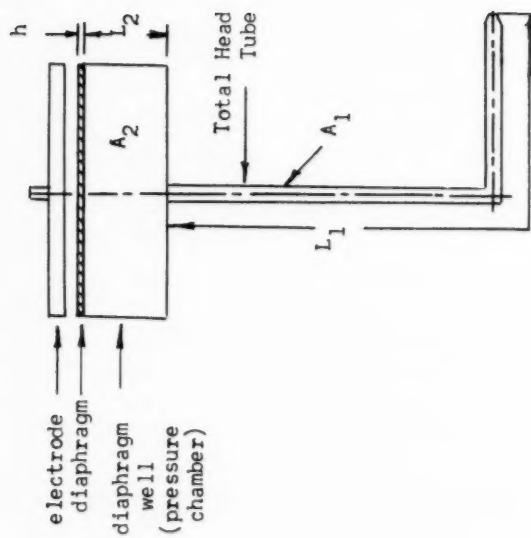


Figure 1.  Schematic Diagram of Gage 1
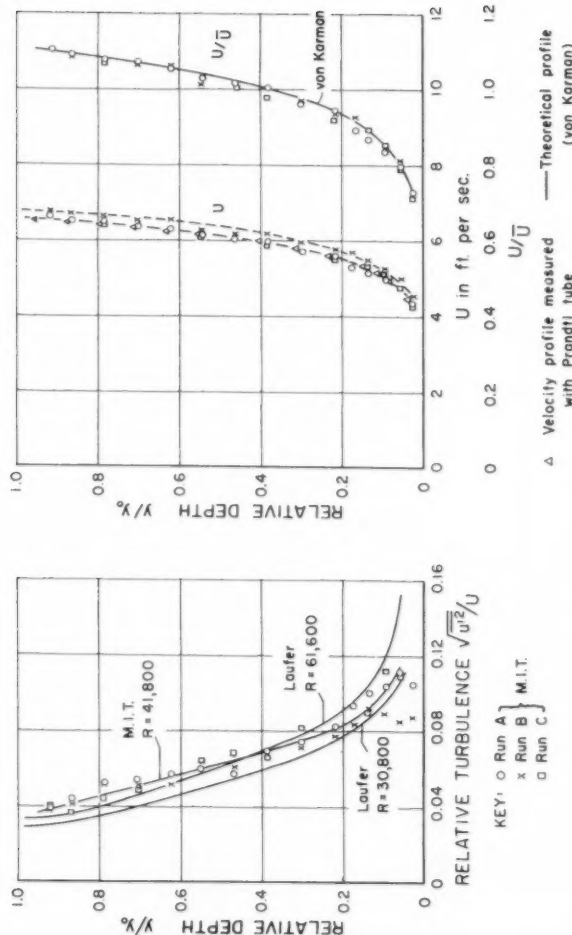
Figure 3.   Turbulence Distribution and Velocity Profiles.
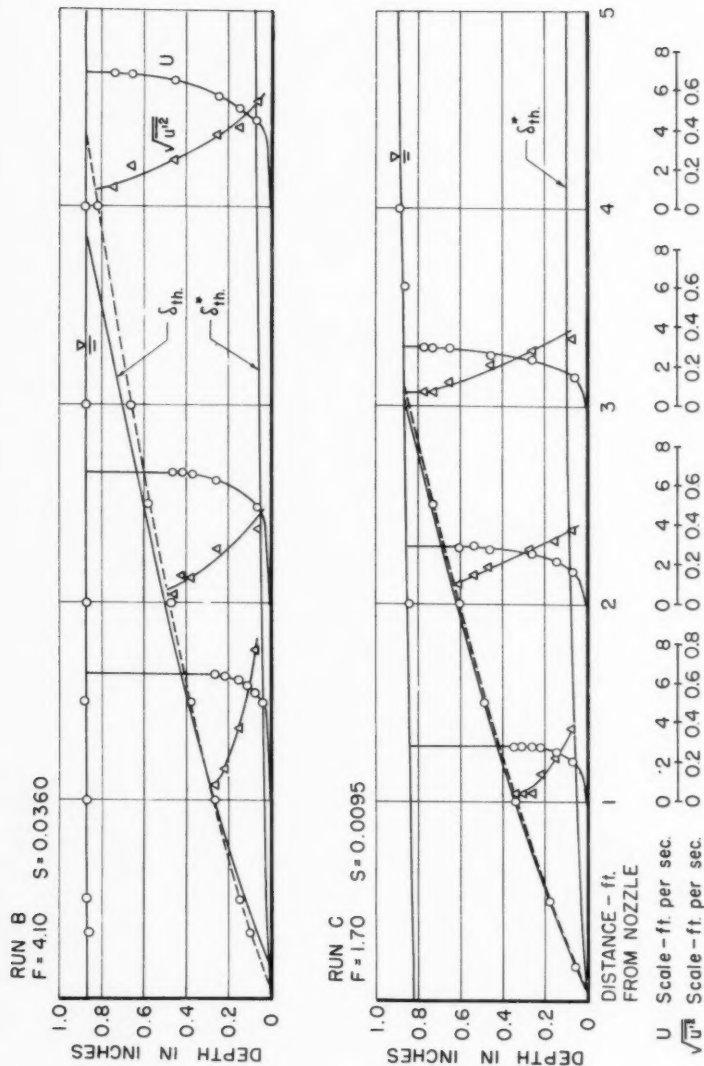
Figure 4. Temp. Mean Velocities, Turbulence Intensities, and Boundary Layer Growth in Channel Downstream of Nozzle.

IV



Figure 7
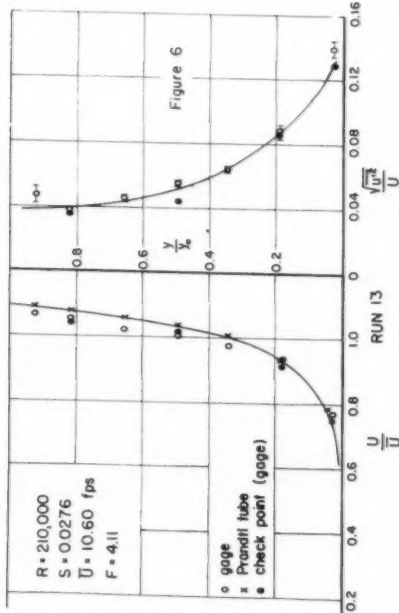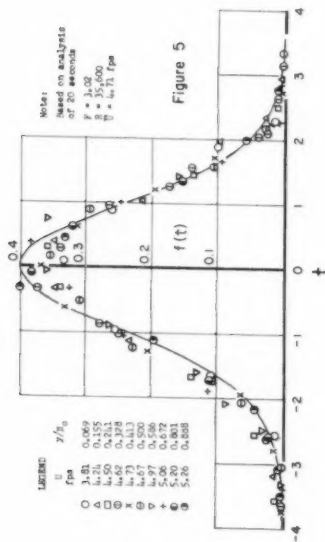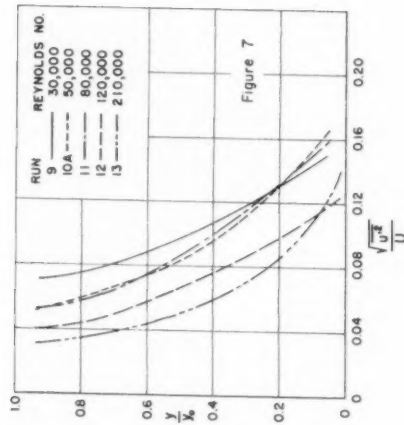


Figure 5



Figure 6

Figure 5.  Comparison of Normalized Fre-
quency Distributions to Normal
Statistical Distribution.

Figure 6.  Velocity Distribution and
Relative Turbulence as a
Function of Depth.

Figure 7.  Relative Turbulence for Vari-
ous Reynolds Numbers.
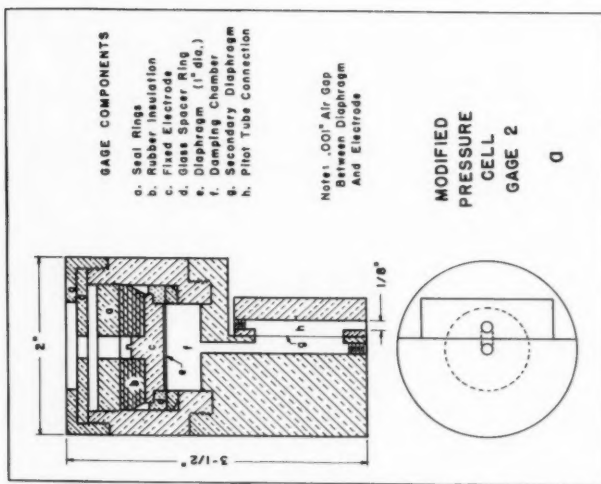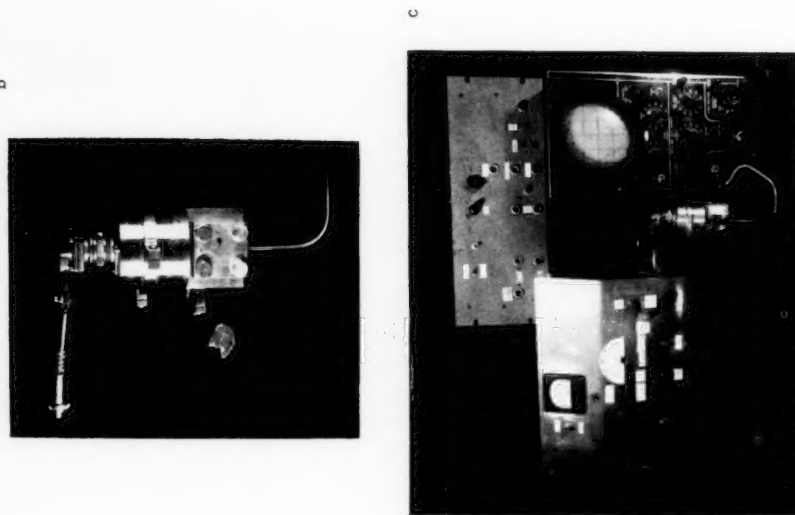
Figure 8. Modified Gage 2.

a. Schematic Diagram of Pressure Cell
b. Photograph of Assembled Gage
c. Gage and Electronic Components

VI



Gage 1

Free stream signal

⊢ 1 Sec. →

Signal within
boundary layer

Gage 2

1/60 sec.

Free stream and
time signal

Boundary layer
and time signal
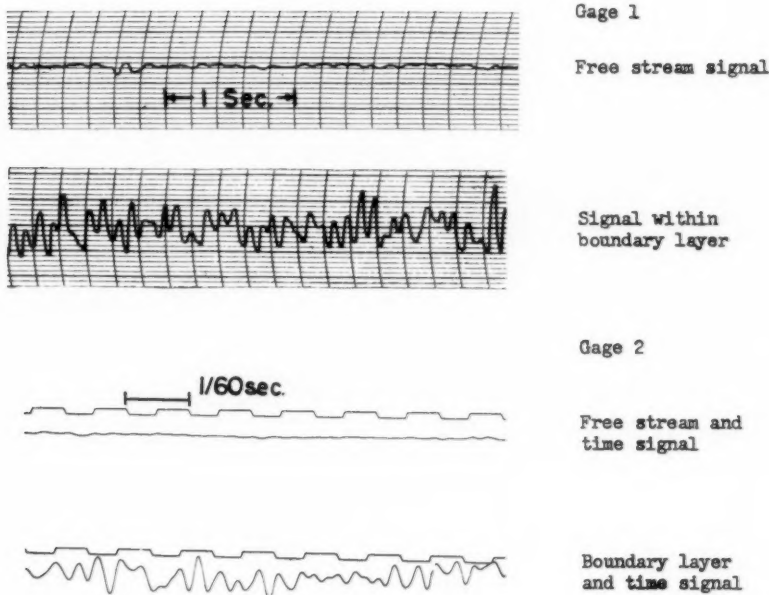
Figure 9.   Samples of signal records



Auto-Correlation Curve

$y/y_0 = 0.157$    $y_0 = 1.27$ in.
Reynolds No. = 52,000
·       experimental data
———     weighted mean of data
—·—   $0.075 \cos(\omega\tau)$
-----   reference curve
$R(\tau) = e^{-\tau U/L_x}$
where    $U = 5.34$ fps
         $L_x = 3.74$ in.
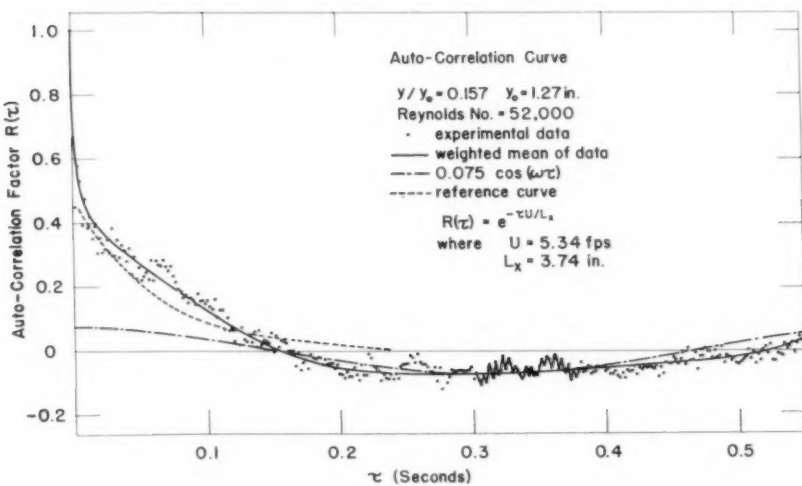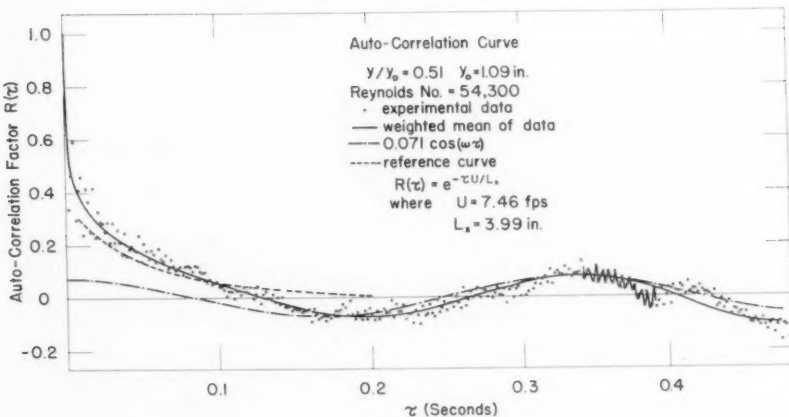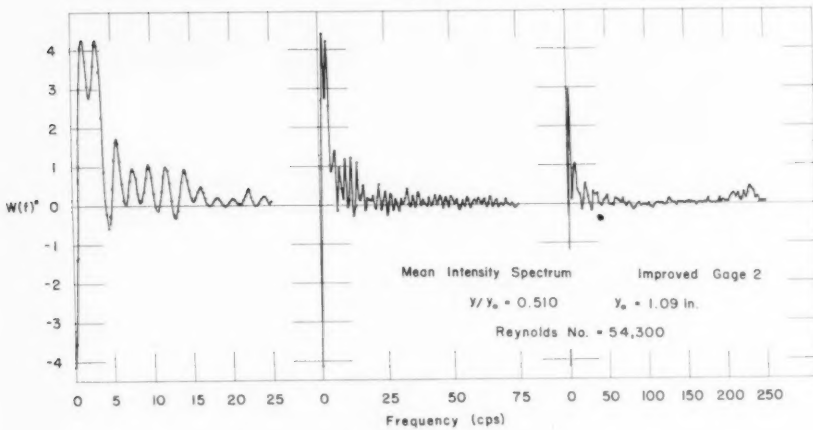
Figure 10.

Figure 11.



Figure 12.
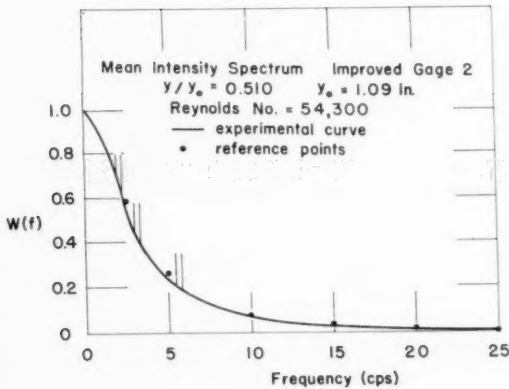


Figure 13.

VIII
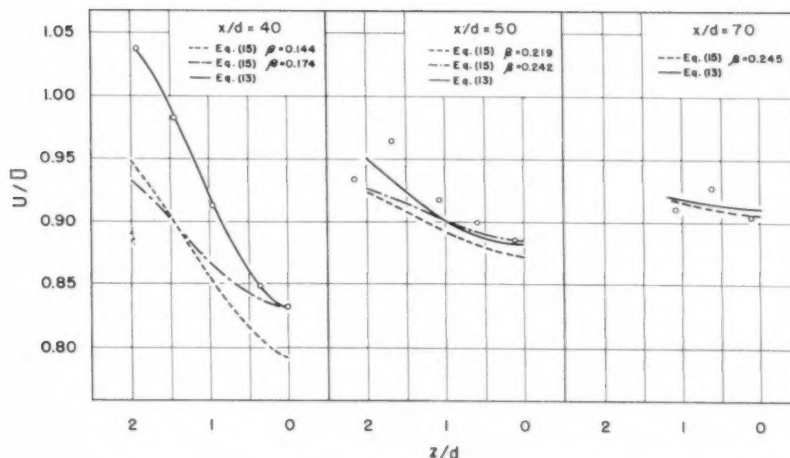


Figure 14.  Mean Velocity Distribution in Wake
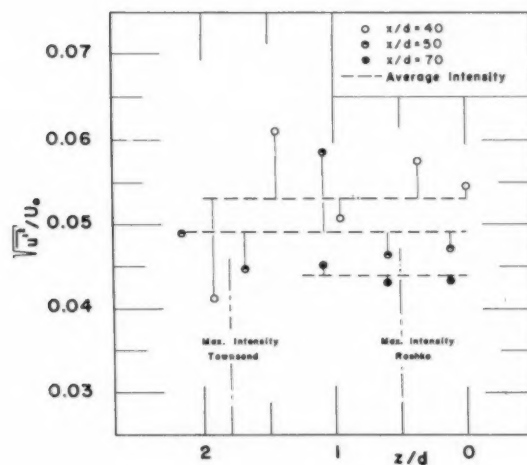


Figure 15.  Turbulent Intensity in Wake

IX
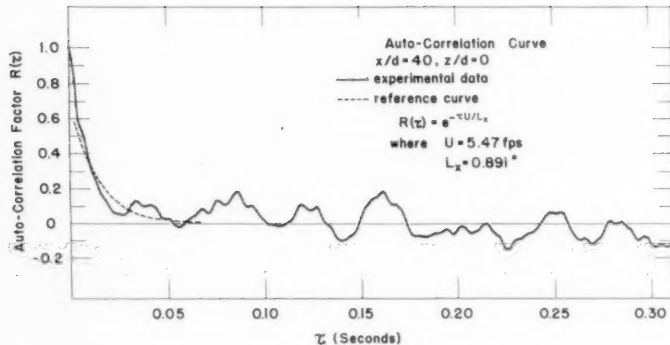


Figure 16.
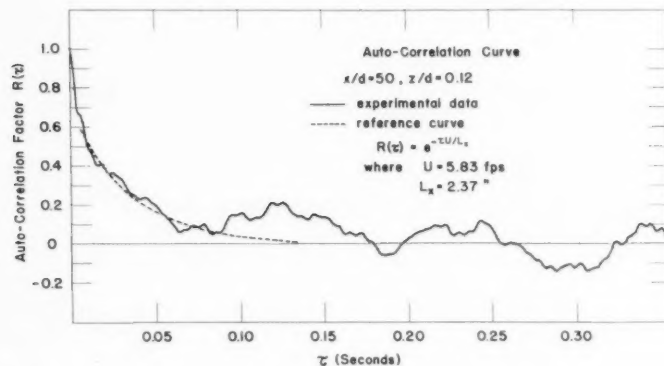


Figure 17.
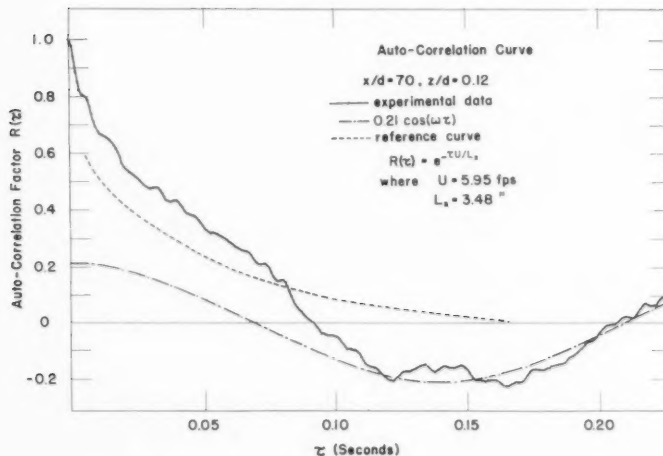


Figure 18.
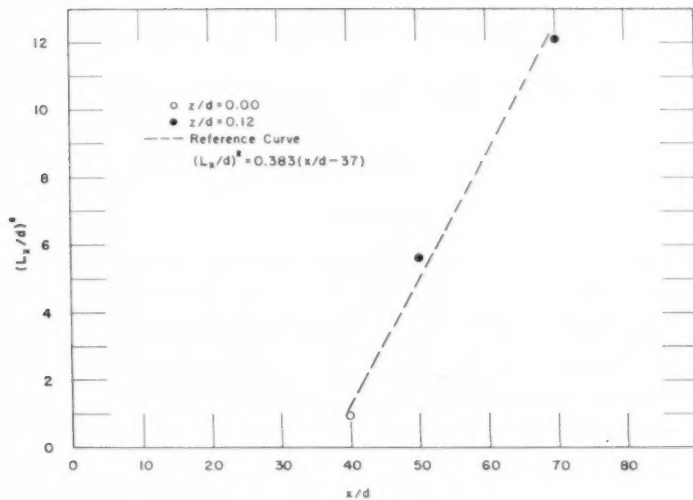
Figure 19.   Variation of Macro-Scale During
             Turbulent Decay in Wake
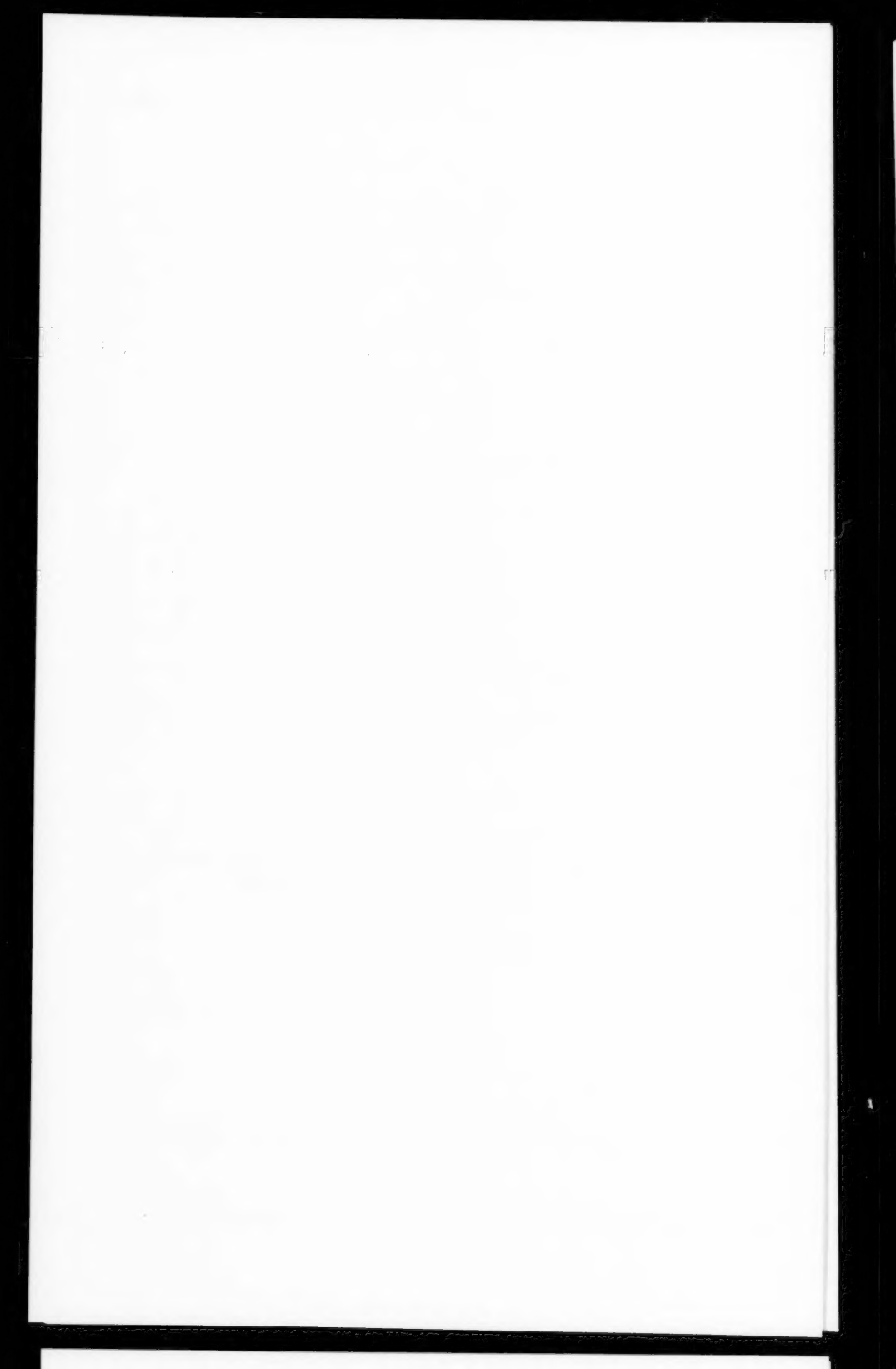
# Journal of the
# HYDRAULICS DIVISION

## Proceedings of the American Society of Civil Engineers

### TURBULENCE IN CIVIL ENGINEERING:
### TURBULENCE IN A DIFFUSER BOUNDARY LAYER

J. M. Robertson* M. ASCE and G. L. Calehuff**
(Proc. Paper 1393)

---

### ABSTRACT

Measurements of turbulence intensity at five stations and shear at one station in the boundary layer on the inside of a 7 1/2 degree conical diffuser are reported. Comparison of the results with those reported for non-pressure gradient boundary layers indicates significant divergence from the universal inner region concept. The microscale of turbulence appears to be remarkably constant although other turbulence quantities are greatly increased as the flow develops in the adverse pressure gradient.

---

### Turbulence in a Diffuser Boundary Layer

The state of knowledge regarding the exact nature of the flow in a turbulent boundary layer developed under the influence of an adverse pressure gradient is best described as incomplete. Information is required, both on the mean flow characteristics and on the nature of turbulence and turbulence processes in the developing boundary layer. Mean flow data have been reported by various investigators; nevertheless, a recent comprehensive study of the situation for plane two dimensional flows by D. Ross[1] has indicated the need for even more information. If, in spite of the relative wealth of literature available on this phase of the subject, it can be described as "incomplete," then the state of knowledge regarding the turbulent aspects of the situation can only be described as "fragmentary." This interpretation has been stated in slightly

stronger terms by G. B. Schubauer and P. S. Klebanoff[2] who commented,
"The real problem is the understanding of the mechanics of turbulent shear
flow under the action of pressure gradient. The solution of this problem de-
pends upon the understanding of the mechanics of turbulence and in this only
rudimentary beginnings have been made."

The random velocity fluctuations known as turbulence must be character-
ized with the aid of certain statistical values, the first of which was introduced
by O. Reynolds. Thus the flow velocity at any time is defined by the relation,
velocity = U + u in the x direction. Here U is the temporal mean velocity
which varies with location and u is the fluctuating component. This random-
ly fluctuating quantity is characterized by u', its root-mean-square (rms)
value, known as the turbulence intensity. From a mean velocity consideration,
turbulent flows with small (as in pipes and channels) or zero (as in boundary
layers) pressure gradients are similar, particularly near the wall. Within a
wall region 10 or 15 percent of the pipe radius or boundary-layer thickness,
the "Law of the Wall" applies and the velocity distribution is given by a
logarithmic relation. Of course, there is a laminar film at the wall if it is
smooth. In the outer portion of the flow, away from the wall, other velocity
relations are more appropriate.

The effect of adverse pressure gradients on turbulent boundary-layer type
flows have been clearly indicated by Ross[1] from a mean flow standpoint.
The "Law of the Wall" associated with the wall shear stress still applies in
the inner region. The flow in this region is singularly unaware of the pres-
sure gradient. In the outer region the flow is greatly modified through the
cumulative effects of the pressure gradient. The velocity profiles become
sharper with inflection points sometimes appearing as the wall shear stress
becomes smaller. Eventually, this becomes zero and the flow separates from
the wall.

The status of our knowledge about the turbulence in flows with negligible
pressure gradients (including pipes and channels) has been well summarized
by G. B. Schubauer.[3] He shows that, except for an intermittency which oc-
curs in the outer part of boundary-layer flows, the turbulence in pipes,[4]
channels,[5] and boundary-layers[6] is in many respects the same. Thus if

the intensities are expressed in terms of the shear velocity $U_\tau = \sqrt{\tau_w / \rho}$

(where $\tau_w$ = wall shear stress and $\rho$ = fluid density) as a function of the

friction wall distance paramenter $y U_\tau / \nu$ (where y = wall distance

and $\nu$ = fluid kinematic viscosity) unique relations result. Understanding of
the turbulence in these flows is elucidated through a detailed study of the
energy processes. Schubauer also shows the similarity for the various flow
cases of the several terms in the turbulent energy balance equation, which
may be written in simplified form

$$P_r + D + C + W = 0$$

where

      $P_r$ indicates the production of turbulent energy from the mean motion

      D, the kinetic energy and pressure energy diffusion across the flow

C,  the convection of turbulent energy by the mean motion, and W, the dissipation of the turbulent energy.

The first of these terms may be expressed in dimensionless form as

$$P_r = \frac{\nu}{U_\tau^4} \overline{uv} \frac{dU}{dy}$$

which is simply calculated. Part of the mean flow energy is directly dissipated; the dimensionless direct-viscous-dissipation rate is given by

$$W_\mu = \frac{\nu^2}{U_\cdot^4} \left(\frac{dU}{dy}\right)^2$$

When integrated across the boundary-layer or conduit $(P_r + W_\mu)$ account for the loss of kinetic energy of the mean flow - some of it going directly to heat through the action of viscosity and the remainder going into the production of turbulence energy. Thus we have a connection between mean flow conditions and turbulence. Some of the turbulence terms involved in the convection and dissipation have been measured so that the trends for C and W are known with some reliability. The diffusion terms are found by balancing the equation and, as summarized in Schubauer's paper, the diffusion is significant.

It has already been remarked that information on the turbulence in adverse-pressure gradient flows is "fragmentary." G. B. Schubauer and P. S. Klebanoff[2] at the National Bureau of Standards, B. G. Newman[7] in Australia and V. A. Sanborn and R. J. Slogar[8] at the NACA have contributed the major portion of the literature available on turbulence in adverse pressure gradients. All of these references describe studies of the plane two-dimensional boundary layer and the first two were concerned primarily with the separation phenomena.

A study of boundary layers in axisymmetric flow was conducted at the Pennsylvania State University from 1946 to 1954. Recently E. M. Uram[9] along with J. W. Holl and J. M. Robertson[10] have investigated the mean flow parameters for an axismmetric boundary layer encountered in a circular diffuser. Near the conclusion of these studies, a two channel, constant-temperature hot-wire anemometer became available for a brief series of turbulence measurements in this facility. Time commitments did not permit a thorough, detailed study of the turbulent processes in the developing boundary layer. Nevertheless, it is hoped that the relatively modest amount of information obtained during the course of this investigation and presented in this paper will contribute toward the advancement of the knowledge regarding turbulent boundary-layer flow phenomena under the action of an adverse pressure gradient.

### Apparatus and Test Procedure

#### Flow Circuit

The turbulence measurements were made in the developing boundary layer of a 7 1/2 degree (total angle) conical diffuser which was also the test facility

for the mean velocity studies[9,10,11] at Penn State. The particular configuration corresponds to the Phase II arrangement reported in the recent papers and was essentially an Eiffel type air tunnel. The diffuser had a 6-inch entrance diameter and increased to a 11 1/4 inch diameter where it discharged freely. The test set up consisted of a 24-inch axial flow fan followed by reducing section, screens and a cast aluminum nozzle. Six diameters of straight conduit separated the nozzle from the start of the diffuser. This promoted the growth of a reasonably thick boundary layer before the start of the adverse pressure gradient.

Holes suitable for the insertion and traversing of instrumentation were provided at a number of stations along the diffuser. The location of those stations at which turbulence measurements were made is shown in Figure 1 along with a dimensional description of the diffuser. A plot of the pressure distribution obtained from the previous studies[9,10] is included. As in other diffuser flows, the initial pressure gradient is comparatively steep. It is seen from this figure that the first measurement station was at or slightly ahead of the start of the strong pressure gradient.

The physical condition of the boundary layer entering the diffuser is defined by the velocity outside the boundary layer $U_1 = 166$ fps and the boundary-layer Reynolds number based on momentum thickness, $R_\theta = 6900$. This was determined at Station 1 in the mean flow investigation.[9,10]

Numerous accurately machined, flanged construction joints in the diffuser section permitted disassembly of the facility to insert the hot-wire probe in the traversing apparatus. For each location, the zero reading of the traverser was adjusted to place the plane of the hot wire at the wall of the diffuser. In this manner, the reading of the traverser was actually the distance of the probe from the diffuser wall. It is estimated that the cumulative radial positional error arising from the initial installation of the probe in the traverser, and the error in the traverser screw, amounted to no more than 0.02 inches. A Pitot tube was positioned in the same measurement plane as the hot wire through an instrumentation hole in the opposite wall. The dynamic pressure, derived from the difference in the Pitot impact pressure and the static pressure obtained from wall piezometers, was used to check the calibration of the hot wire probe and make suitable corrections for any temperature induced drift in the anemometer. The mean flow rate was monitered during the tests by measuring the pressure drop across the nozzle. It remained steady and corresponded very closely to the flow rates developed during the other studies (9,10).

Hot Wire Anemometer

This paper is not primarily concerned with the development and design of hot wire anemometers; therefore, the fine points of the subject will not be discussed here. To those who wish to review this field, we refer to the excellent survey of hot wire anemometry by R. D. Cooper and M. P. Tulin.[12]

The particular instrument used in this investigation was constructed by the Hubbard - Ling Company of Iowa City, Iowa. It is a constant temperature system designed to overcome the two major inherent defects of the hot wire as a velocity measuring device, namely the thermal capacity of the wire and its non-linear conversion of velocity to electrical signals. The frequency response of this hot wire anemometer is $\pm 1$ percent, 0-10 KC, down 10 percent at 25 KC, and the equivalent noise level (relative to mean velocity) is

0.1 percent or less for velocities over 20 fps.

The two channel feature of this instrument along with the signal manipula-
tion possible in the metering circuit enabled the determination of the follow-
ing quantities with relative ease:  U, the mean velocity in the axial direction,*
u', and longitudinal component (rms value) of turbulence and $\lambda_x$, the micro-
scale of turbulence, all using a single wire placed normal to the mean flow
direction.  The use of an X or crossed wire probe enabled the determination
of v', the rms orthogonal component of turbulence and $\overline{uv}$ the Reynolds shear
stress in the xy plane.

## Test Procedure

Calibration of the hot wire probe was conducted prior to each boundary
layer traverse by placing the wire outside the boundary layer, and establish-
ing a mean velocity calibration curve.  In progressing down the diffuser, the
maximum velocity, $U_1$ at any station dropped from 166 fps to 98 fps.  Lower
velocities were obtained for the calibration process by placing a cloth over
the entrance grill of the fan.  This throttled the flow very effectively without
disturbance.

Following calibration of the probe, measurements were taken at frequent
intervals across the boundary layer.  As the wall was approached, the inter-
vals between adjacent measurement stations were systematically reduced
from 1/4 to 1/100 inches.  The probe was then returned to the initial position
outside the boundary layer; during the return, a number of points were re-
peated as a check on the results.  In several instances, the traverses were
repeated on different days as a further check on reliability.

## Results

The change in the mean velocity profile as the boundary layer grows along
the diffuser is illustrated in Figure 2.  Here the local mean velocities have
been reduced to dimensionless numbers in terms of the maximum velocity
measured at each station.  All of the data were derived from hot wire
measurements.  To indicate agreement between hot wire and impact tube
measurements, a curve from Uram's data (at station 6) is also presented.
It can be seen that the hot wire has followed the impact tube measurements
quite faithfully except for the region near the wall.  Here the difference be-
tween the two sources of data are recognizable but are in the wrong direction.
Normally, one would expect the impact tube to read high because of the effect
of turbulence on the impact pressure.  The multiple sets of data, obtained on
different days for Stations 3 and 12 show some shift.  However, it amounts to
only a few of percent, which is within the repeatability limits of the hot wire
anemometer.  In general, the validity of the hot wire mean flow measure-
ments is established.

The mean velocity profiles have also been analyzed to determine the dis-
placement and momentum thicknesses as given by the following definitions:

---

*The mean velocity in the y direction, V is sensibly zero, since the maxi-
mum angle of the streamlines relative to the diffuser axis is 3.75 degrees.
In the absence of secondary motion, the circumferential component W is
zero.

$$\delta^* = \int\left(1 - \frac{U}{U_1}\right)dy$$

$$\theta = \int\frac{U}{U_1}\left(1 - \frac{U}{U_1}\right)dy$$

These are actually two-dimensional definitions rather than the three-dimensional definitions which should apply.[10] However, for comparative purposes, the differences are irrelevant. Comparison of the hot-wire determined momentum and displacement thicknesses with those reported by E. M. Uram[9] are presented in Figure 3. In general, the agreement is good. Also included in this figure is the common shape parameter $H = \delta^*/\theta$. As in the case of other boundary layers, H is seen to increase to a value of about 2.8 as the end of the diffuser (and separation) are approached.[10] These parameters along with the pressure distribution serve to describe the mean flow conditions under which the turbulent boundary layer developed.

The distribution of the relative turbulence intensity at the five measurement stations along the diffuser is illustrated in Figure 4. Turbulence intensity is normally nondimensionalized through division by a reference velocity, in this case the local velocity U. Measurements at Stations 3 and 12 made on different days are indicated by modifications of the basic symbols. Variation from day to day does not seem particularly large. The greatest scatter coincides with the highest turbulence levels, particularly in the case of the single traverse at Station 17. Other investigators have found considerable scatter during measurements of high intensity turbulence.[12]

Curves derived from Klebanoff's[6] investigation of the zero pressure gradient boundary layer are included in both Figures 2 and 4, for comparison with the results found at Station 1 which was essentially in a zero pressure gradient and at the same Reynolds number. These comparisons serve to show that the velocity distribution and turbulence in the boundary layer under study was quite normal prior to its exposure to an adverse pressure gradient. They also indicate a fair degree of reliability in the hot-wire measurements.

The curves of Figure 4 indicate relative intensities which do not permit comparison between sections or even across the boundary layer at the same section. For such comparisons, the absolute intensity u' is more suitable. Schubauer and Klebanoff[2] refer intensities to the velocity outside of the boundary layer in the flow just before the start of the adverse pressure gradient. The intensities measured in this present study were similarly converted to dimensionless rations $u'/U_{10}$ where the initial reference velocity $U_{10}$ was taken at Station 1. From smooth curves drawn through the data, the contour plot of Figure 5 was obtained, showing the variation in turbulence intensity in the boundary layer. This shows a definite peak in the $u'/U_{10}$ values; this peak shifting outward as the flow progressed. The results are compatible with data presented by Schubauer and Klebanoff except the present data seem more internally consistent.

Shear stress and v' measurements were made only at Station 12. The shear stress results are shown in Figure 6. Considerable scatter is apparent in the data, especially in the region of greatest shear. Again, qualitative similarity with the observations of Schubauer and Klebanoff is found.

The longitudinal microscale or dissipation length can be expressed by the

following relation:

$$\lambda_x = \frac{u' U}{\sqrt{\left(\frac{\partial u}{\partial t}\right)^2}}$$

Experimentally, the square root term was found from the hot wire signal with an electronic differentiating current and $\lambda_x$ calculated with the aid of the other measured quantities.

If the turbulence were isotropic, the turbulent-energy dissipation rate would be

$$W_{iso} = \frac{15 \mu u'^2}{\lambda^2}$$

Various researchers have found that when this expression is integrated across the flow, the result may be low by a factor of 2.5 in the simpler flow case of negligible pressure gradient. However, even for such non-isotropic cases, $\lambda_x$ does give an indication of the size of the smallest eddies. The results of the measurements of this length are given in Figure 7. Smooth curves rather than individual data points are presented for the sake of clarity. In the case of Station 3 individual data points are given to indicate the scatter.

## Discussion

The most noticeable feature of the relative intensity curves of Figure 4, other than the rapid increase in this quantity as the flow proceeds, is the occurance of a peak for Stations 6 and 12. Zero pressure gradient boundary layers also display a peak; however, this occurs at wall distances corresponding to the thickness of the laminar film or sub-layer. In the case of Stations 6 and 12, the distance from the peak to the wall is at least several orders of magnitude greater. If this peak is a characteristic feature of adverse pressure gradient boundary layers, its absence at Station 17 is quite unexplainable. For the plane two-dimensional boundary layer with an adverse pressure gradient, Schubauer and Kelbanoff[2] do not seem to have found such a peak.

In the introduction it is pointed out that an inner region exists in boundary layer flows which is independent of external conditions. This inner region is about 10 percent of the boundary layer thickness; this was verified by the mean flow measurements[9,10] in this boundary layer. The inner concept would lead one to expect essential identity of the turbulence in this region.

The measured intensities presented as $u'/U_\tau$ and $v'/U_\tau$ in comparison with the pipe results of Lauffer[4] are shown in Figure 8. In the case of the u' measurements, there is considerable divergence between the values obtained with the X probe and the single wire*. However, this uncertainty is insufficient to invalidate the general results shown. It is obvious from this

---

*The single wire points shown in Figure 8 do not represent actual measurements as in Figure 4, but average values from the measurements.

figure that in the inner region (out to about $\delta/10$) the turbulence intensities are much greater than found in the pipe flow. In the laminar film (thickness = $\delta_1$), these two quantities are probably identical as suggested by the dashed lines. In the outer region, the turbulence intensities reach quite large magnitudes compared to those found in other boundary-layer-type flows. This outer effect is not unexpected since the flow there is the result of upstream generated turbulence.[13]

Additional evidence concerning the high turbulence level in the inner region was obtained through calculation of the turbulence production rate $P_r$. This quantity was determined from mean curves drawn through the shear stress and velocity measurements at Station 12. The direct viscous dissipation rate $W\mu$ was also obtainable. The results of these calculations are shown in Figure 9. Comparison with results for flat plates and pipes[3] show that in the inner region the turbulence production is 5 to 30 times greater while the direct dissipation rate seems to be about the same (or at least insignificant). Again, in the laminar film, it appears that had measurements been made, the values would have been identical. Just as in the case of the intensity, there is a large increase in the production of turbulence in the outer boundary layer region.

Proper understanding of the occurances in boundary layers such as that studied naturally would require evaluation of the other terms in the turbulence energy equation. The necessary measurements to evaluate these should have been made, but the extent of this study was limited by other factors. The high turbulence production rate in the inner region for the adverse pressure gradient case does not appear to have been commented on by other investigators. In retrospect, it seems hardly surprising that this was found since the shear stress in these flows rapidly increases to many times the wall value as the wall distance increases.[13]

The measured shear stress distribution at Station 12 and shown in Figure 6 differs greatly from that found in pipes and zero-pressure gradient boundary layers. In such cases, the shear has a maximum at the wall and decreases monotonically to zero at the outer edge. Peaked shear distribution curves in adverse pressure gradients have been noted previously.[2,7] An explanation for this in terms of the "history" of the flow has been presented elsewhere.[13] At the wall, $\partial\tau/\partial y$ equals $dp/dx$ from the momentum equation, written for the wall streamline. As the pressure gradient is positive, the shear has to increase as one departs from the wall. A theory was presented in 1950 explaining the variation in the wall shear stress, as affected by the local adverse pressure gradient, wall shear stress and boundary layer thickness, and the boundary layer thickness and wall shear stress at the start of the pressure gradient.[13] Figure 6 also presents the calculated shear stress distribution based on this theory. The wall shear stress coefficients used for this calculation were based on pitot tube measurements.[10] The agreement between theory and experiment is seen to be good. The theory gives the total shear, viscous plus turbulent, while the hot wire measurements yield only turbulent shear. This consideration does not affect the comparison of Figure 6 for at a wall distance of 0.1 inches, the viscous shear has been estimated to be 0.2 percent of the measured shear.

The dissipation length $\lambda_x$ results are surprising in that they indicate little variation between stations. It would appear that except near the wall, the smallest eddies had a size of about 0.01 feet. Other recent boundary layer

measurements also indicate little variation.[14,15] Lauffer's results shown in the Figure 7 range from 0.01 to 0.02 feet. As already noted, if the turbulence were isotropic, the dissipation of turbulence into heat would be given by the relation

$$W_{iso} = dE'/dt = 15\nu\, u'^2/\lambda^2$$

$$E' = \frac{\rho}{2}(u'^2 + v'^2 + w'^2)$$

With the essential constancy in $\lambda$ the isotropic dissipation is proportional to $u'^2$. Inspection of Figure 5 indicates that turbulent energy dissipation increases rapidly and has its maximum about the middle of the boundary layer at the downstream stations. One might conjecture that the rate of actual dissipation increases in a similar fashion.

## CONCLUSIONS

Although the turbulence studies were not as extensive as desired and the precision of the data could be improved on, the results are felt to be sufficiently adequate to justify the following conclusions:

1. The turbulence, its rate of production, and its rate of dissipation in an adverse pressure gradient are greatly in excess of similar quantities for zero-pressure-gradient boundary layers.

2. The existence of an inner wall region having universal characteristics, although well established for mean flow conditions, has not been found for turbulence. Thus, the turbulence and its rate of production are far in excess of the zero-pressure-gradient case, even near the wall.

3. The shear stress variation across the boundary layer is reasonably well predicted by the history theory.

4. The longitudinal microscale of turbulence $\lambda_x$ remains remarkably constant across and along the developing boundary layer.

## ACKNOWLEDGMENTS

## REFERENCES

1. "A New Approach to Turbulent Boundary Layer Problems," by Donald Ross, Trans. American Society of Civil Engineers, Vol. 121, 1956, pp. 1219-1254 (Proceedings Separate No. 604, January 1955.)

2. "Investigation of the Separation of the Turbulent Boundary Layer," by G. B. Schubauer and P. S. Klebanoff, NACA Report 1030, 1951.

3. "Turbulent Processes As Observed in Boundary Layer and Pipe," by G. B. Schubauer, Journal of Applied Physics, Vol. 25, January 1954, pp. 188-196.

4. "The Structure of Turbulence in Fully Developed Pipe Flow," by J. Laufer, NACA Report 1174, 1954.

5. "Investigation of Turbulent Flow in a Two-Dimensional Channel," by J. Laufer, NACA Report 1053, 1951.

6. "Characteristics of Turbulence in a Boundary Layer with Zero Pressure Gradient," by P. S. Klebanoff, NACA Report 1247, 1955.

7. "Some Contributions to the Study of the Turbulent Boundary Layer Near Separation," by B. G. Newman, Report ACA-53, Aeronautical Research Consultative Committee, Department of Supply, Australia, March 1951.

8. "Longitudinal Turbulent Spectrum Survey of Boundary Layers in Adverse Pressure Gradients," by V. A. Sandborn and R. J. Slogar, NACA TN 3453, May 1955.

9. "The Growth of an Axisymmetric Turbulent Boundary layer in an Adverse Pressure Gradient," by E. M. Uram, Proceedings 2nd U. S. National Congress of Applied Mechanics, 1954, ASME, pp. 687-695.

10. "Effect of Adverse Pressure Gradients on Turbulent Boundary Layers in Axisymmetric Conduits," by J. M. Robertson and J. W. Holl. To be published in Journal of Applied Mechanics, ASME Paper No. 56-A-25.

11. "Effect of Entrance Conditions on Diffuser Flow," by J. M. Robertson and D. Ross, Trans ASCE, Vol. 118, 1953, pp. 1068-1097.

12. "Turbulence Measurements With the Hot Wire Anemometer," by R. D. Cooper and M. P. Tulin, NATO Agardograph 12, August 1955.

13. "Shear Stress in a Turbulent Boundary Layer," by D. Ross and J. M. Robertson, Journal of Applied Physics, Vol. 21, 1950, pp. 557-561.

14. "Equilibrium Turbulent Flow in a Slightly Divergent Channel," by J. R. Ruetenik and S. Corrsin, 50 Jahre Grenzschichforschung, Fr. Vieweg & Sohn, Braunschweig, 1954.

15. "Etude Experimentale de L'Ecoulement Turbulent dans un Conduit Divergent Parcouru par de L'Air," by J. P. Milliat, (Societe Hydrotechnique de France) LaHouille Blanche, 16 March 1956, pp. 139-159; also Proc. Sixth General Meeting IAHR, 1955, Vol. 4, pp. D18-1-14.
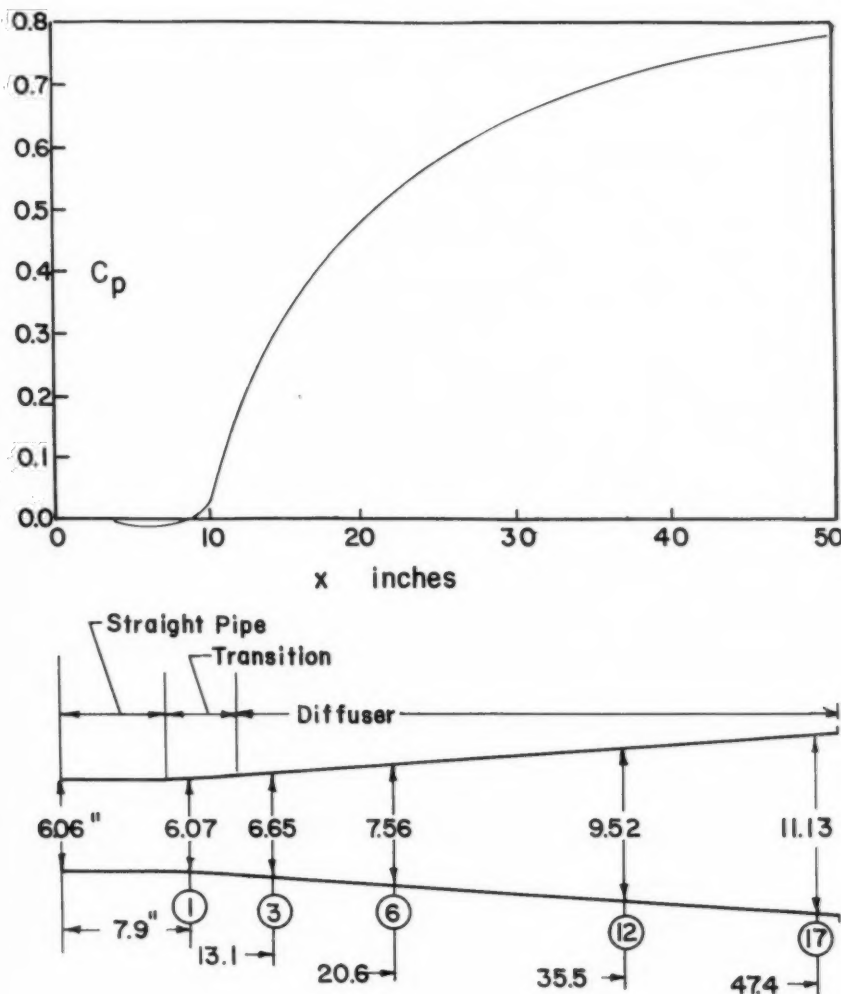
Fig. I  Pressure Distribution and Diffuser Geometry
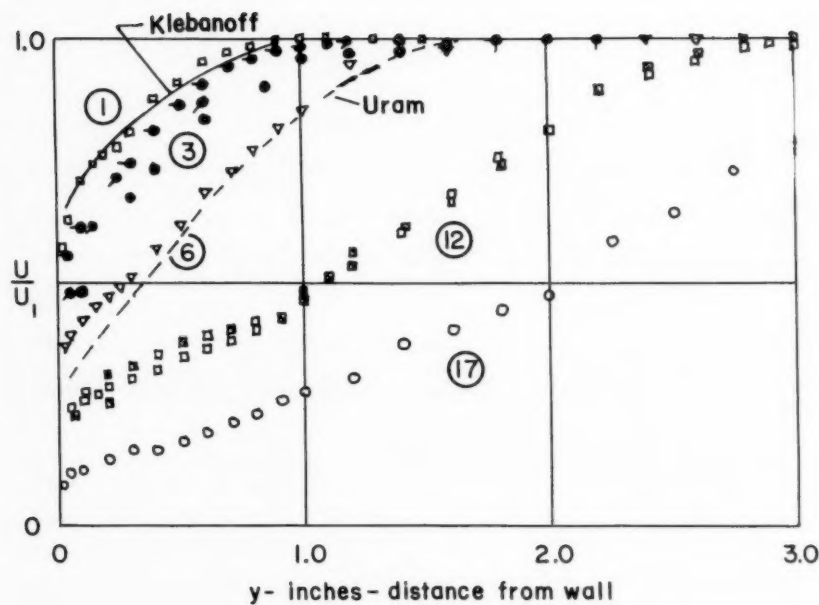
**Fig. 2   Mean-Velocity Profiles at the Several Diffuser Stations**
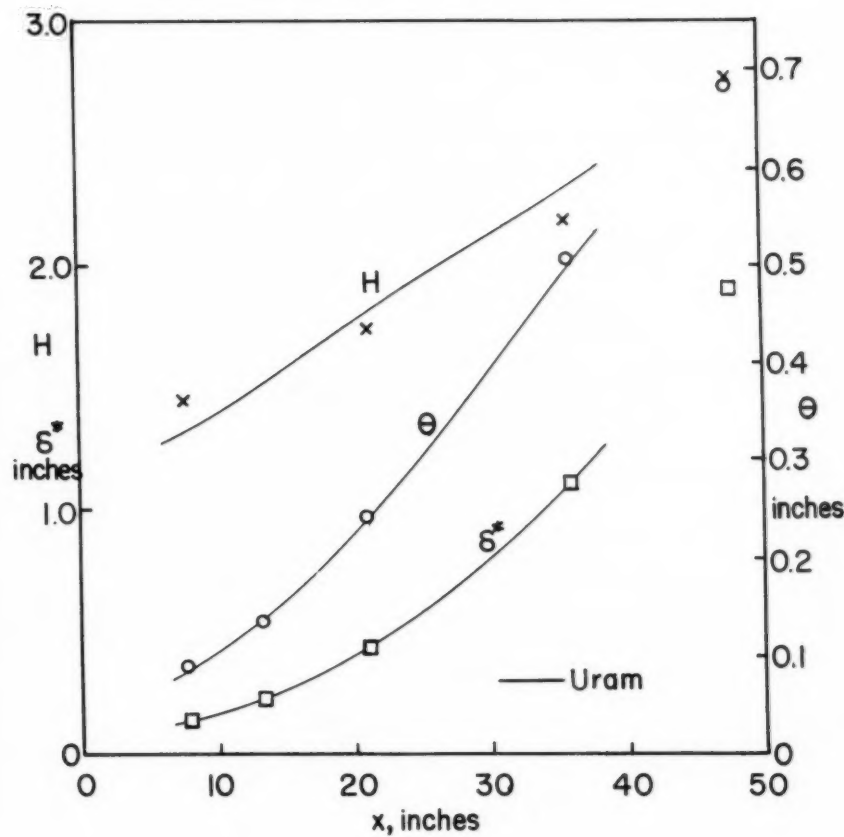
Fig. 3   Longitudinal Variation in Displacement and
Momentum Thicknesses and Shape Parameter
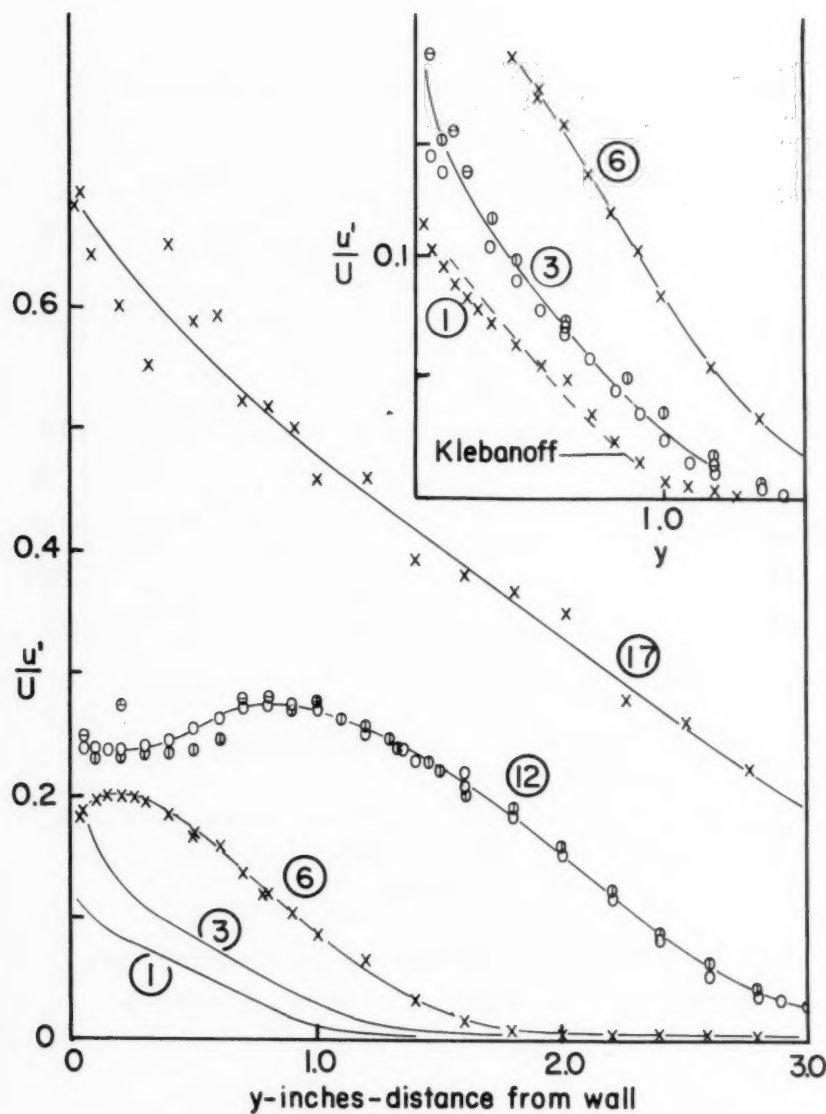
Fig. 4 Transverse Variation in Relative Intensity
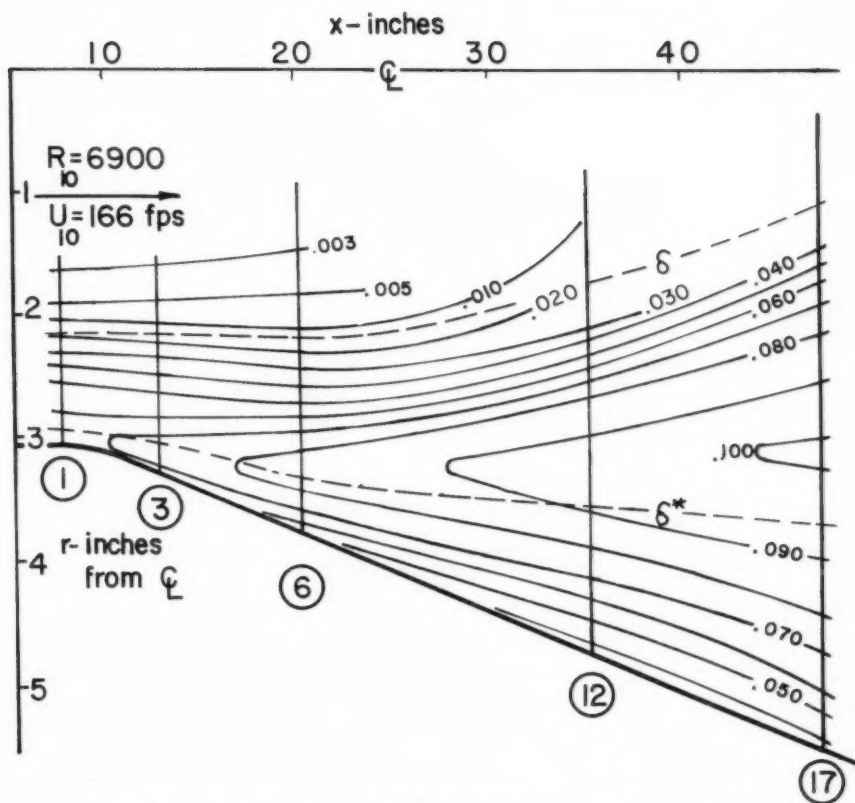
Fig. 5   Contour Plot of Turbulence Intensity $\frac{u'}{U_{10}}$
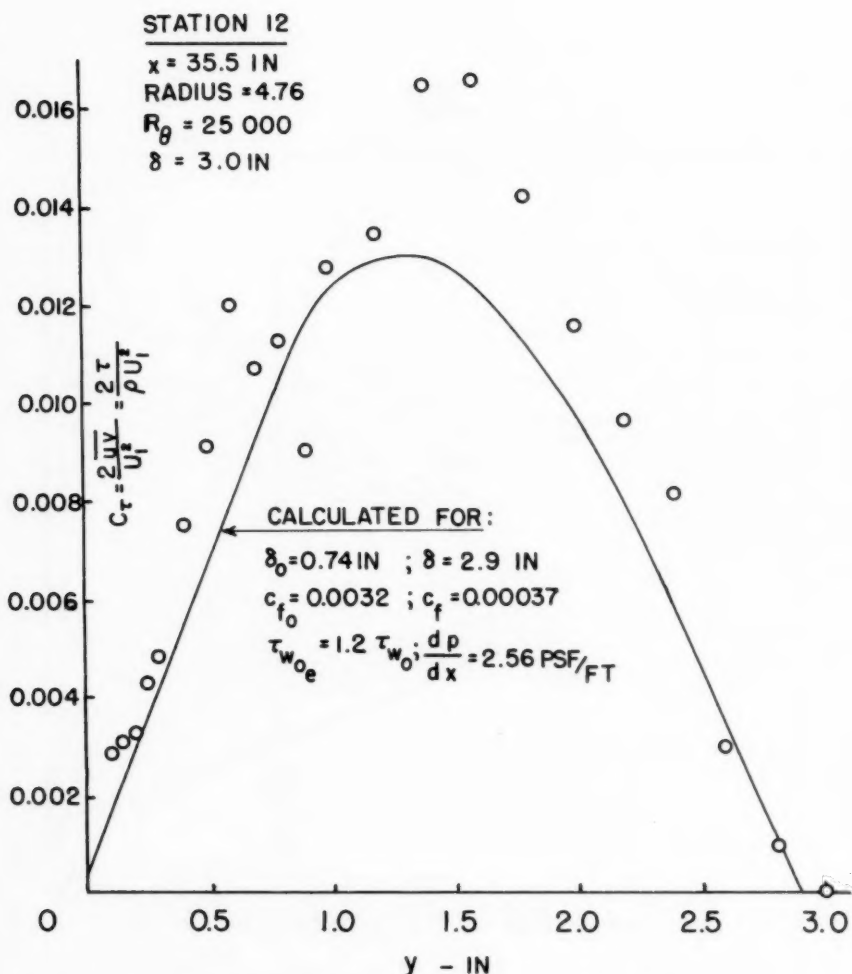
FIG.6  SHEAR STRESS MEASUREMENTS
         COMPARED WITH "HISTORY" THEORY
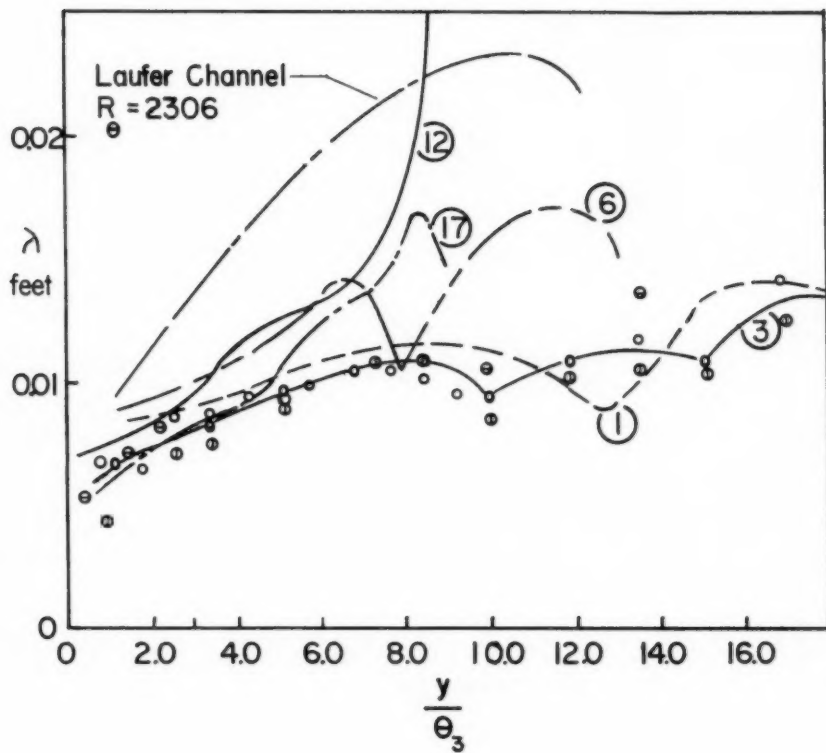
Fig. 7   Turbulence Micro-Scale or Dissipation Length
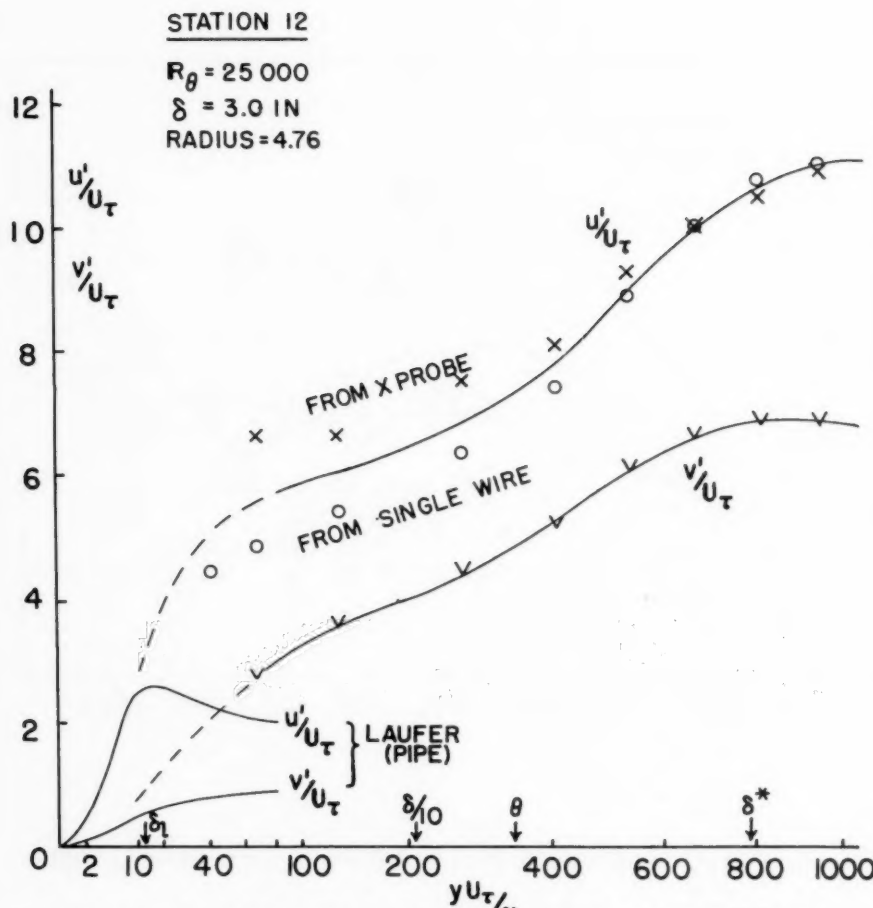
FIG. 8  COMPARISON OF TURBULENCE INTENSITIES
WITH PIPE RESULTS
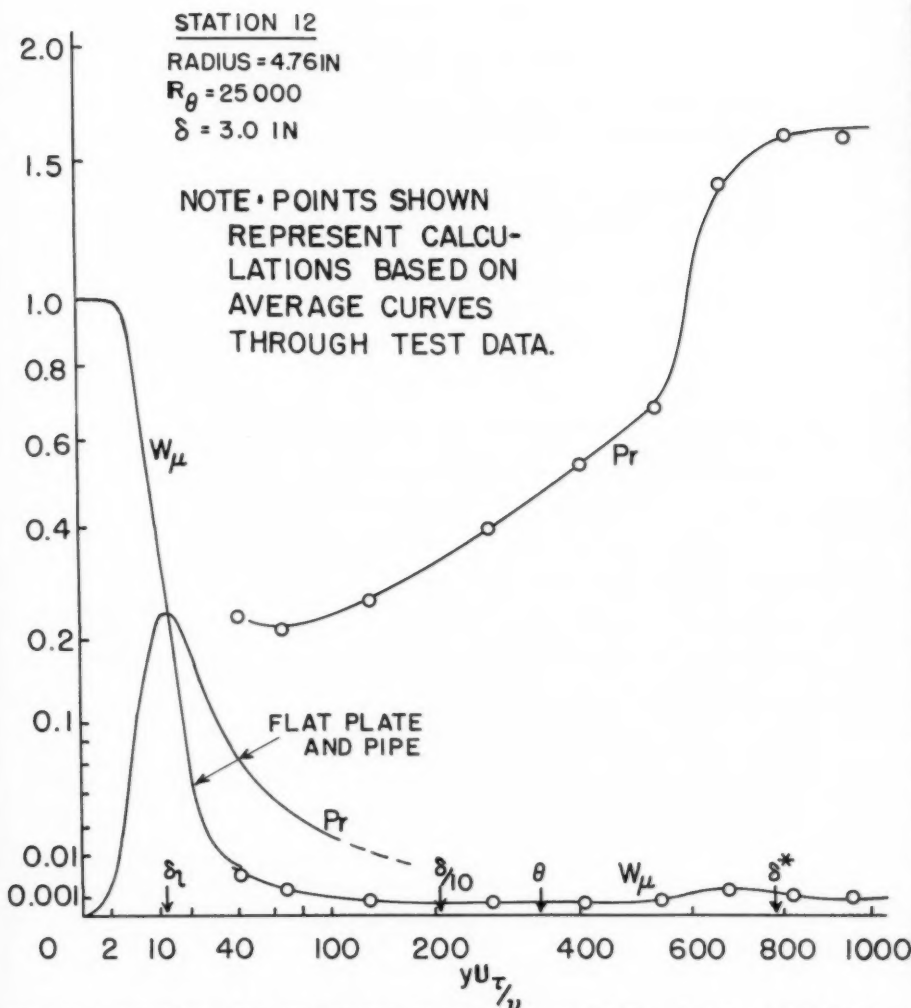
FIG.9 TURBULENCE ENERGY PRODUCTION AND DIRECT
VISCOUS DISSIPATION IN COMPARISON WITH
PIPE AND BOUNDARY LAYER RESULTS

# Journal of the
# HYDRAULICS DIVISION

## Proceedings of the American Society of Civil Engineers

### TURBULENCE IN CIVIL ENGINEERING: INVESTIGATIONS IN LIQUID SHEAR FLOW BY ELECTROMAGNETIC INDUCTION

L. M. Grossman, H. Li and H. A. Einstein[1] M. ASCE
(Proc. Paper 1394)

### INTRODUCTION

The experimental investigation of the component velocity fluctuations in a turbulent fluid requires a method of velocity measurement of high sensitivity, accurate frequency response, and one which will preferably distinguish between motion in various directions. The hot-wire anemometer adequately satisfies these criteria in the case of gas flows but has proven unsatisfactory in the study of the details of turbulent fluctuations in liquid media. It is the purpose of this paper to describe a method of component velocity fluctuation measurement in turbulent liquid flows based upon the induction of an electrical potential field in a continuous medium moving relative to a stationary uniform magnetic field. An analysis of the theoretical basis of the proposed method will be presented, as well as a description of the experimental application to the case of the measurement of the component velocity fluctuations in the fully developed turbulent flow of water in a circular pipe. Attention will be focused upon the physical phenomena underlying the method of electromagnetic induction which will serve to point up the general advantages and limitations of the principle in the experimental investigation of turbulent flows. The directions in which further development appear to be fruitful, will be indicated in a concluding section.

### Electromagnetic Induction in a Fluid in Motion

The physical principle upon which the experimental method is based is Faraday's law of electromagnetic induction which indicates that electromotive forces are induced in a liquid conductor moving relative to a magnetic field, the electric field strength at any point being simply related to the magnetic field strength and the velocity. This fact may be used for investigating the distribution of velocities in a moving liquid, for this distribution can be de-

duced from observations on the e.m.f.'s induced at different points in the
liquid by a known magnetic field.

Let:

$\vec{V}$ = the velocity vector at any point in a fluid

$\vec{B}$ = the magnetic field intensity

$\vec{E}$ = the electric field intensity or induced e.m.f. per unit length

$\vec{i}$ = the induced current

$\sigma$ = the electrical conductivity of the fluid

$\varphi$ = the electrical potential

Faraday's Law of Induction can be formulated as follows. Every changing
magnetic field has associated with it an electric field E; the line integral of
E around any closed circuit is related to the time rate of change of the flux
across the circuit by the basic relation,

$$\oint \vec{E} \cdot d\vec{l} = -\frac{d}{dt} \iint \vec{B} \cdot d\vec{A} \tag{1}$$

where $d\vec{A}$ is the element of area of a surface capping the circuit.

The total magnetic flux through a given circuit appearing as the integral
in the right hand side of equation (1) can change with time for two reasons:

a)  It can change because of changes in the external field with time.
    ("transformer action")
b)  It can change because of motion of the circuit itself or parts of the
    circuit. ("motional induction")

In the case of a flow steady in time relative to a constant external magnetic
field B, only the latter form of induction is operative. If one develops the
form of the right hand side of (1) for a surface itself in motion with the fluid
and applies Ohms Law to relate the current to the electric field, there results
a basic relation for the e.m.f. and the motional induction, namely,

$$\vec{E} = \vec{B} \times \vec{V} + \vec{i}/\sigma \tag{2}$$

The product of magnetic field and velocity is a vector product following the
familiar "Flemings right hand rule".

Since E is the gradient of the potential $\varphi$, one may also write

$$-\nabla \varphi = \vec{B} \times \vec{V} + \vec{i}/\sigma \tag{3}$$

In the case of steady flows the continuity equation for electric charge is

$$\text{div } \vec{i} = 0 \tag{4}$$

so that taking the divergence of both sides of (3) yields

$$\nabla^2 \varphi = \text{div}\left(\vec{V} \times \vec{B}\right) \tag{5}$$

This Poisson equation indicates that for a given magnetic field the potential gradient is uniquely a function of the velocity field and the boundary conditions of the flow.

Under certain conditions the induced current flow is small or identically zero, so that from equation (3) we see that a measurement of the potential gradient at a point where the magnetic field is known is a direct measure of the local velocity. Such a method of velocity measurement has the advantages that: a) it is based upon a universal and fundamental physical principle, b) it is possible to distinguish between velocity components due to the vector nature of the basic relation, c) it yields an instantaneous measure of velocities fluctuating in time, and d) it is insensitive to the physical properties of the fluid medium.

## Application of the Method of Electromagnetic Induction to Local Velocity Measurement

The discussion of Faraday's principle of electromagnetic induction applied to continuous media in motion relative to a fixed magnetic field, led to the fundamental equation for the local potential gradient in terms of the local values of the velocity, magnetic field strength and current density, namely equation (3). If the velocity distribution is known, it is always possible to compute the resultant electrical field, including the potential and current distributions by solving a Poisson equation with suitable boundary conditions.

The central question for experimental application, however, is whether one can deduce the velocity field from a measurement of the distribution of potential gradient. Here one faces the difficulty that the current density in equation (3) is not known a priori, but is rather a function of the velocity field that one wishes to deduce. The local value of the current density appearing in equation (3) is moreover determined by the total velocity vector field, so that the local potential gradient is dependent upon the entire velocity pattern. It might be supposed, at first view, that the influence of induced currents could be reduced by increasing the conductivity of the fluid; but unfortunately

it is the quantity $\frac{1}{\sigma}$ that appears in the fundamental equation, and this quanti-

ty is determined solely by the irrotationality of the induction vector $\vec{B} \times \vec{V}$ .

In the case of the measurement of mean velocity it is always possible to apply the method of electromagnetic induction to determine the velocity distribution experimentally. In such cases one can compute the velocity pattern from measured values of the potential gradient assuming no current flow and then with this assumed velocity distribution compute the induced current flux by the methods previously outlined. A process of successive approximation would then yield the correct velocity distribution. For the case of two-dimensional flow with the vorticity always in the direction of the applied magnetic field the induced current flow is automatically zero. The induced e.m.f. sets up space and surface changes whose electrostatic field exactly balances the induced e.m.f.

The application of the method to the measurement of local turbulent velocity components raises more serious questions. Here there is no possibility of utilizing the simplification of the induction equation for two-dimensional flow, for the velocity fluctuations are conceded to be three dimensional regardless of the mean flow characteristics. In the case of turbulent fluctuations, moreover, one measures the mean square of the potertial gradients

and the expression for the latter deduced from the induction equation by Reynolds' rules of averaging involve product correlations whose magnitude can not easily be estimated a priori.

Consider, for example, the case of pipe flow with the axis as shown and B uniform in the direction of the z axis. Then from
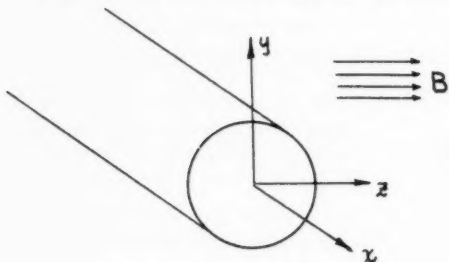
$$\text{grad } \phi = (\vec{V} \times \vec{B}) - \vec{i}/\sigma \quad (6)$$

we have

$$\frac{\partial \phi}{\partial z} = - i_z/\sigma$$

$$\frac{\partial \phi}{\partial y} = - BU - i_y/\sigma$$

$$\frac{\partial \phi}{\partial x} = BV - i_x/\sigma \quad (7)$$

Splitting the velocity components into mean and fluctuating parts, and the same for the current, i.e.

$$U = \bar{u} + u'$$

$$i_x = \bar{i}_x + i_x' \quad (8)$$

and applying the Reynolds rules of averaging we have

$$\overline{\left(\frac{\partial \phi}{\partial z}\right)^2} = \frac{\overline{i_z^2}}{\sigma^2} + \frac{\overline{i_z'^2}}{\sigma^2}$$

$$\overline{\left(\frac{\partial \phi}{\partial y}\right)^2} = B^2\left(\bar{u}^2 + \overline{u'^2}\right) + \frac{2B}{\sigma}\left(\bar{u}\,\bar{i}_y + \overline{u'i_y'}\right) + \left(\overline{i_y^2} + \overline{i_y'^2}\right)/\sigma^2$$

$$\overline{\left(\frac{\partial \phi}{\partial x}\right)^2} = B^2\left(\overline{v^2} + \overline{v'^2}\right) - \frac{2B}{\sigma}\left(\bar{v}\,\bar{i}_x + \overline{v'i_x'}\right) + \left(\overline{i_x^2} + \overline{i_x'^2}\right)/\sigma^2 \quad (9)$$

The expression for the mean square of the fluctuating potential gradients are then,

$$\overline{\left(\frac{\partial \varphi'}{\partial z}\right)^2} = \frac{\overline{L_z'^2}}{\sigma^2}$$

$$\overline{\left(\frac{\partial \varphi'}{\partial y}\right)^2} = B^2 \overline{u'^2} + \frac{\overline{L_y'^2}}{\sigma^2} + \frac{2B}{\sigma} \overline{u' L_y'}$$

$$\overline{\left(\frac{\partial \varphi'}{\partial z}\right)^2} = B^2 \overline{v'^2} + \frac{\overline{L_x'^2}}{\sigma^2} + \frac{2B}{\sigma} \overline{v' L_x'} \qquad (10)$$

It is clear from these relations that provided the presence of induced currents could be neglected that the r.m.s. values of the u and v components could be computed directly from the second and third equations from measured values of the r.m.s. potential gradients. But in the actual case the relations are complicated not only by the unknown current intensities but by the presence of the correlations between velocity and current fluctuations resulting from squaring the induction equation.

Fortunately it is possible to obtain a direct experimental estimate of the intensity of the current fluctuations by utilizing the first of the above equations. This shows that the r.m.s. potential gradient measured in the direction of the magnetic field gives the r.m.s. current in the same direction. The results of this measurement and its interpretation will be discussed in subsequent sections.

### Experimental Program

#### Flow System

The experiments of this research were performed on water flowing in a 2" I.D. lucite pipe. As shown in a schematic diagram, Fig. 1, water was pumped from a reservoir to an entrance head tank I, then passed through a gravel-filled passage to another entrance head tank II. The passage was introduced specifically for the purpose of eliminating large scaleflow disturbance. In order to obtain a smooth flow in the 26' - 6" long pipe of 2" I.D., the pipe entrance was bell-shaped. The bell-mouth was connected to the head tank by a rubber diaphragm. The flexible connection was designed to eliminate the transmission of mechanical vibration between the entrance tank and the experimental pipe. The pipe was arranged horizontally and well supported by nine shock mounts. A heavy masonry support was also placed near the pipe entrance to prevent horizontal movement. The flow discharged from the lucite pipe to an exit tank then drained back to the reservoir, the flow rate being regulated by varying the field resistance of a D.C. motor which was driving the pump. The flow rate was determined gravimetrically.

#### Magnet and Measuring Probe

Magnet—The magnetic field was provided by a direct current electromagnet with 5.75 inch diameter circular pole pieces and a 2-1/2 inch gap. The maximum field intensity was about 9000 gauss. The field strength was practically uniform over the measuring region. D.C. current was supplied by a 110V, 50 KW D.C. generator of the hydro-laboratory of the University

of California, Berkeley.  In order to help eliminate the ripple voltage in the
D.C. supply, a 60-micro-farad condenser was connected across the coils of
the magnet.  An ammeter was used to indicate the current passing through
the coils of the magnet.  The readings of the ammeter were calibrated
against the readings of a standard gauss-meter, which was also used to
check the uniformity of the field.

## Measuring Probe

One electrode, two-electrode, and three-electrode probes were used in
this investigation, the arrangement of the probe depending on the type of
measurement.  A micrometer support for the electrode probe was provided
for traversing the pipe cross-section.  A photograph of the measuring probe
assembly is shown in Fig. 2.

The probe was constructed from 0.0125 inch diameter insulated copper
wires, enclosed in a 0.054 inch O.D. copper tube (the assembly was manu-
factured by the Precision Tube Co., Phila., Pa.), bent into an L shape so that
the wire tips were 3/4" upstream from the stem.  The tips of the wires were
separated by the proper distance and insulated by being painted with glyptal
except at the tips.  At the other end of the probe the electrode wires were
soldered to a microphone connector which was fastened to the micrometer
assembly.

## Electronic Circuits

The signal from the probe was fed to the differential input of a Tektronix
type 122 low level preamplier; the output signal of the preamplier was applied
directly to a Dumont 304-A Cathode Ray Oscillograph.  In addition, the instan-
taneous signal of the preamplier was amplified once again by a single stage
amplifier and fed to a squaring amplifier to obtain the time average square
$\overline{\varphi'^2}$ of the signal.

Two complete channels were provided so that the two input signals from
the probe could be measured at the same time.

The block diagram of the electronic equipment is shown below.
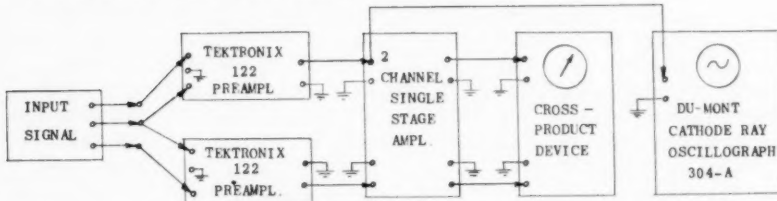


## Results of Measurement

A sample of the oscilloscope record is shown in Fig. 3.  The upper trace
represents the basic amplifier and flow noise without the magnetic field.
The lower one represents the measurement signals with the magnetic field.
This sample was obtained by the input of a two electrode probe with 0.10"
separation at a Reynolds number of $1.0 \times 10^5$.

The results are presented as the square root of the direct readings of the
time average signal by means of the cross-product instrument.  The follow-
ing measurements were made:

(1) RMS potential gradient in the direction normal to the mean flow as a function of radial position in the pipe. A two electrode probe was used for this type of measurement. This arrangement of the probe is shown in Fig. 4. The experimental results of a two electrode probe with 0.025" separation (center to center) are shown in Fig. 4. The abscissa is the fraction of the radius, while the ordinate is the ratio of the reading of the potential gradient to a fractional velocity R.M.S. $\nabla\varphi/B u_*$ The $u_*$ is defined as

$$ u_* = \sqrt{\tau_0/\rho} = \sqrt{f/8}\ \overline{u}_{ave} $$

where   $\tau_0$  is the shear stress at the wall

  $\rho$   is the density

  $f$   is the friction factor

  $\overline{u}_{ave}$  is the average velocity of the pipe flow.

(2) RMS potential gradient in the axial direction as a function of radial position in the pipe—two electrode probe with the arrangement shown in Fig. 5.

(3) RMS potential gradient in the direction of the magnetic field as a function of a radial position in the pipe. Fig. 6 represents the measurement results of this type.

Discussion of Results

With the orientation of the uniform magnetic field perpendicular to the pipe axis as employed in these experiments it is only possible to obtain information on the component velocities in the direction of the mean flow and perpendicular to the mean flow. The experimental information relevant to these velocity component measurements is summarized in the curves of figures 4 through 6. Due to the presence of fluctuating induced currents whose magnitudes can not be estimated a priori, it was thought preferable to present the data in terms of the directly measured root mean square values of the component electrical potential gradients rather than estimated root mean square values of the velocity components. For purposes of comparison the data of Laufer* on velocity component fluctuations in the flow of air through a circular pipe obtained by means of the hot wire anemometer have been plotted in Figs. 4 and 5.

As has been previously discussed (see equation 10), provided that no induced current flow is present, the potential gradient normal, to the flow is a direct measure of the axial velocity component and the potential gradient in the direction of the mean flow represents the normal velocity component. Comparing the measurements of rms potential gradient divided by the uniform and constant magnetic field intensity, to the hot wire velocity measurements of Laufer in air flow, we find first that the distribution of potential gradient as a function of radial position for both the axial and transverse cases follows very closely the corresponding component velocity fluctuation measurements obtained by Laufer and second that the magnitudes compared

---

*J. Laufer, NACA Technical Note 2954, June 1953.

on a dimensionless basis by division by $u_*$ show a marked discrepancy. If the potential gradients per unit magnetic field intensity be interpreted as velocity components, the present set of measurements are consistently lower than those obtained by means of the hot-wire anemometer. We have concluded that the difference is due to the presence of current flow such that the inductional e.m.f. given by the vector product of velocity and magnetic field is greater than the measured potential gradient by the magnitude of the induced current intensity.

Fortunately it is possible to measure at least one component of the current vector, for by the basic induction equation we conclude that the potential gradient in the direction parallel to the magnetic field measures the current flow in the same direction. In Fig. 6 measurements of the r.m.s. current density in the direction of the magnetic field are plotted as a function of the radial position. From equation (10) the magnitude of r.m.s. $\partial \varphi'/\partial z$ is equal

to r.m.s. $i_z'/\sigma$ It may be noted that this quantity is of the correct order of

magnitude to bring the potential gradient measurements into agreement with the data of Laufer if one assumes that the remaining components of current fluctuation are of the same order of magnitude as that measured, and if the correlation between velocity and current fluctuations is of negligible order compared to the other terms of equation (10). Since these hypotheses could not be verified experimentally in the present investigation, the potential gradient data have been reported directly.

From the foregoing discussions of the basic theory of the method of electromagnetic induction and the results of the experimental measurements it will be clear that in order to render the method quantitative for the measurement of fluctuating velocity components it is necessary to measure the three components of the current density. This can be accomplished provided that the orientation of the uniform magnetic field can be varied at will, since the potential gradient parallel to the magnetic field measures directly the current flux in the same direction. For this reason and another to be mentioned shortly, attention is presently being directed to the development of an electrode probe assembly of which a small permanent magnet forms an integral part. Alnico magnets of small size and high flux are currently being investigated for use in a self-contained probe. In addition to the advantage of changing the field direction such a probe assembly offers the possibility of considerably extending the range of flow geometries investigated. These are now limited by the restriction of gap sizes permissible for an electromagnet of high flux density completely enclosing the fluid field.

There is moreover a further application of the method of electromagnetic induction which appears attractive, and is presently being investigated. This is the use of the method as a means of measuring the components of vorticity in a fluid flow. The basic equation for the potential gradient being,

$$\text{grad } \varphi = (\vec{V} \times \vec{B}) - \vec{i}/\sigma$$

(6)

if one takes the divergence of both sides of the equation one has

$$\nabla^2 \varphi = \text{div} (\vec{V} \times \vec{B})$$
$$= \vec{B} \cdot \text{curl } \vec{V} - \vec{V} \text{ curl } \vec{B}$$

(11)

In a uniform magnetic field therefore

$$\nabla^2 \varphi = \vec{B} \cdot \vec{\Omega}$$

(12)

where $\vec{\Omega}$ is the vorticity vector. An electrode probe in the form of a cross enables an experimental measurement of the Laplacian of the potential to be obtained which is a direct measure of the vorticity component in the direction of the known magnetic field. In this application the disturbing influence of induced current patterns is eliminated and with an orientable field the components of the vorticity could be measured separately. Here again the advantages of a self-contained probe-magnet assembly are clear, as is the desirability of an experimental determination of the vorticity in turbulent shear flows.
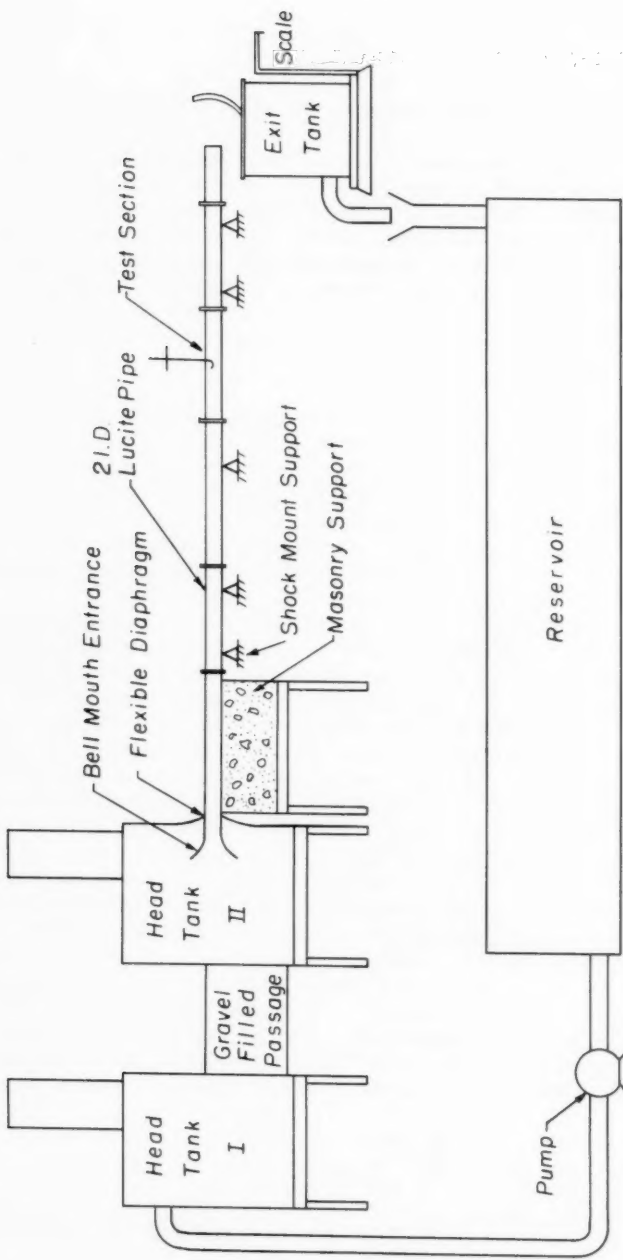
Fig. 1 Schematic Diagram of Flow System
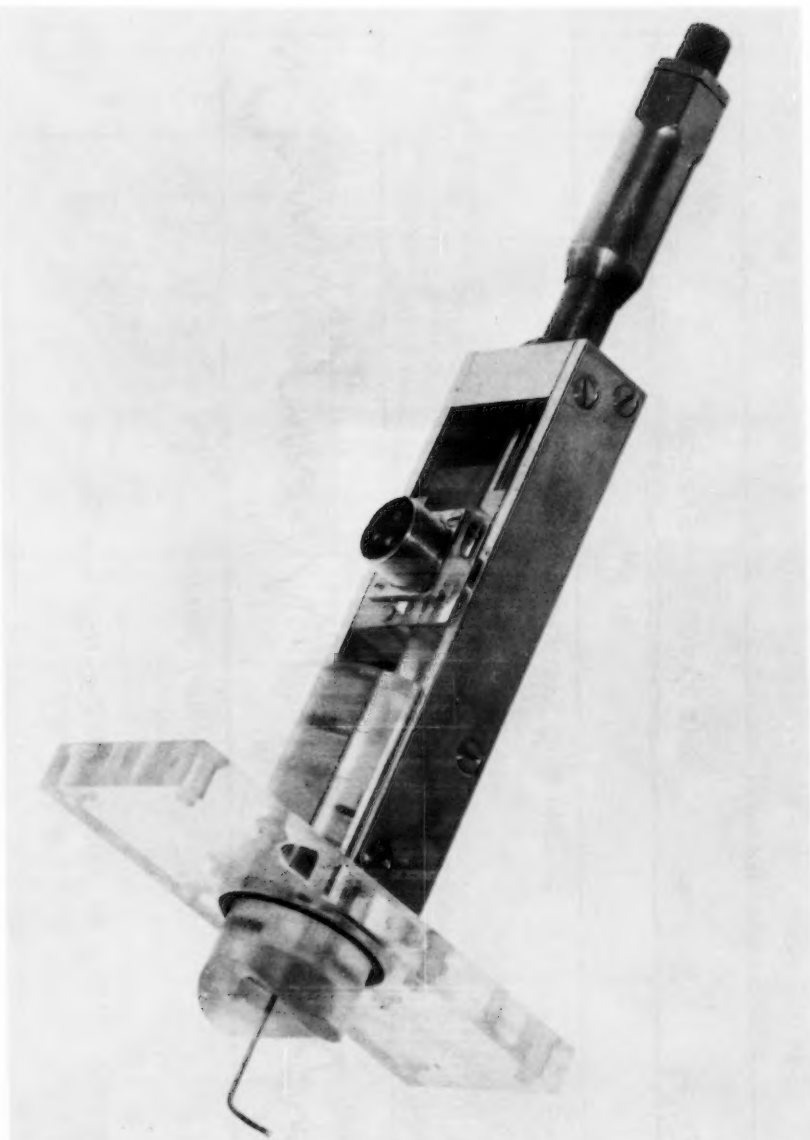
FIG. 2  PROBE ASSEMBLY, SHOWING SHIELDED
ELECTRODES, OUTPUT CONNECTOR AND
MICROMETER TRAVERSING MECHANISM
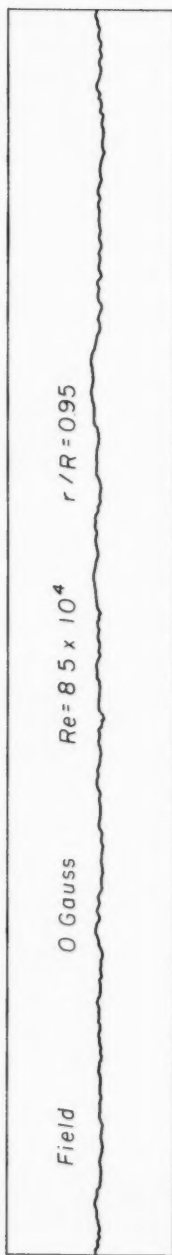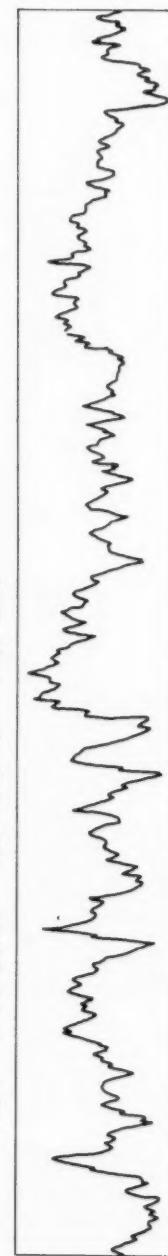
Fig. 3 Sample of Oscilloscope Record
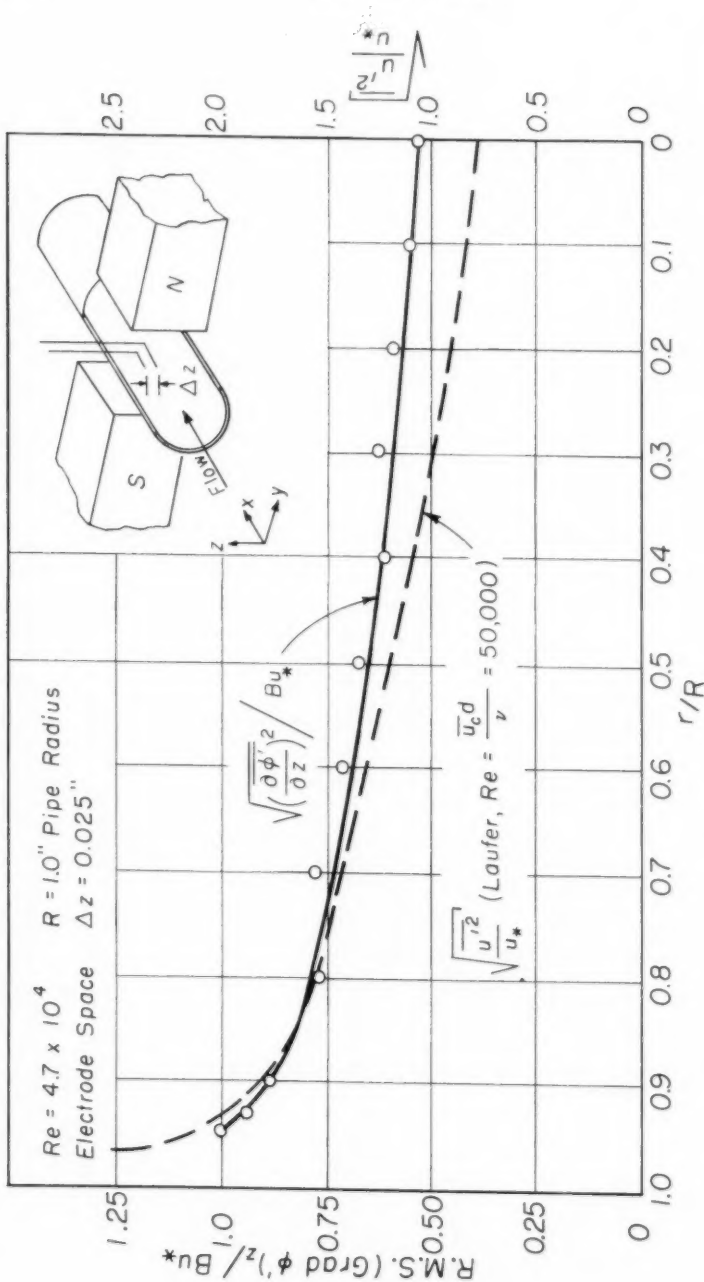
Fig. 4 Measurement of R.M.S. Potential Gradient in the Direction Normal to the Mean Flow as a Function of Radial Position in the Pipe
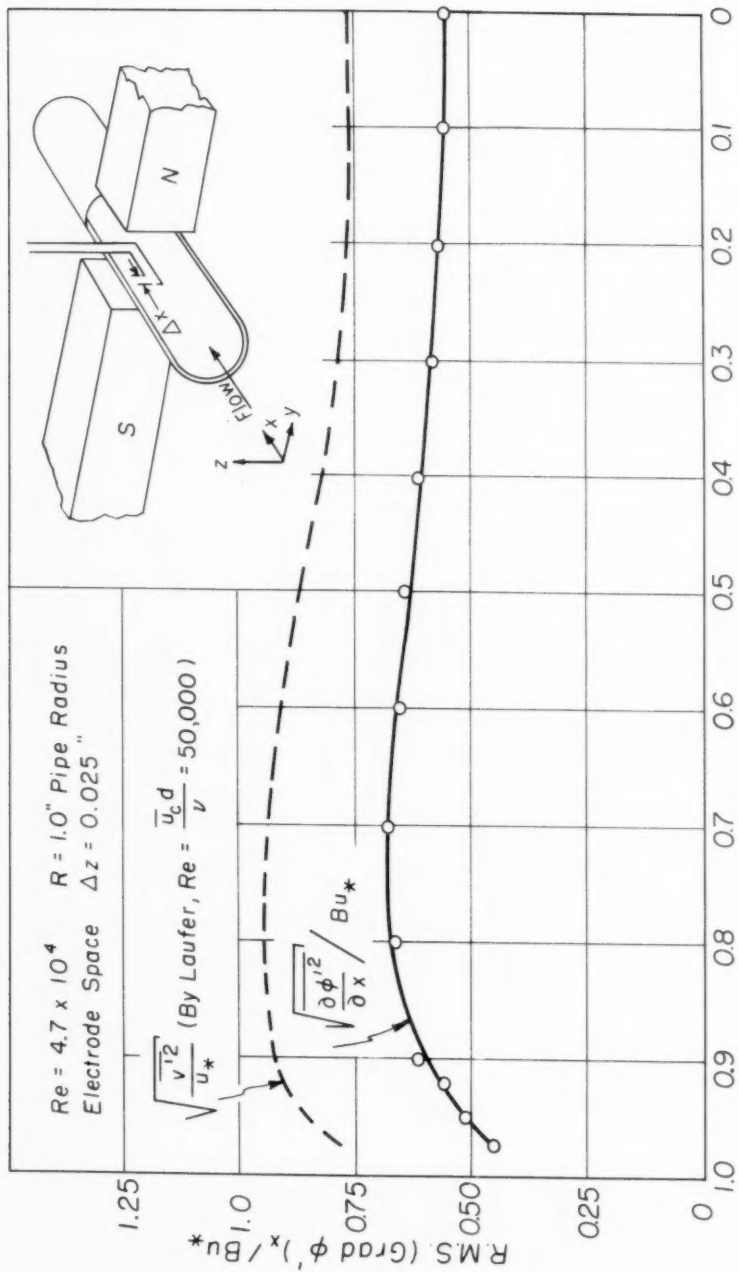
Fig. 5 Measurement of R.M.S. Potential Gradient in the Axial Direction as a Function of Radial Position in the Pipe
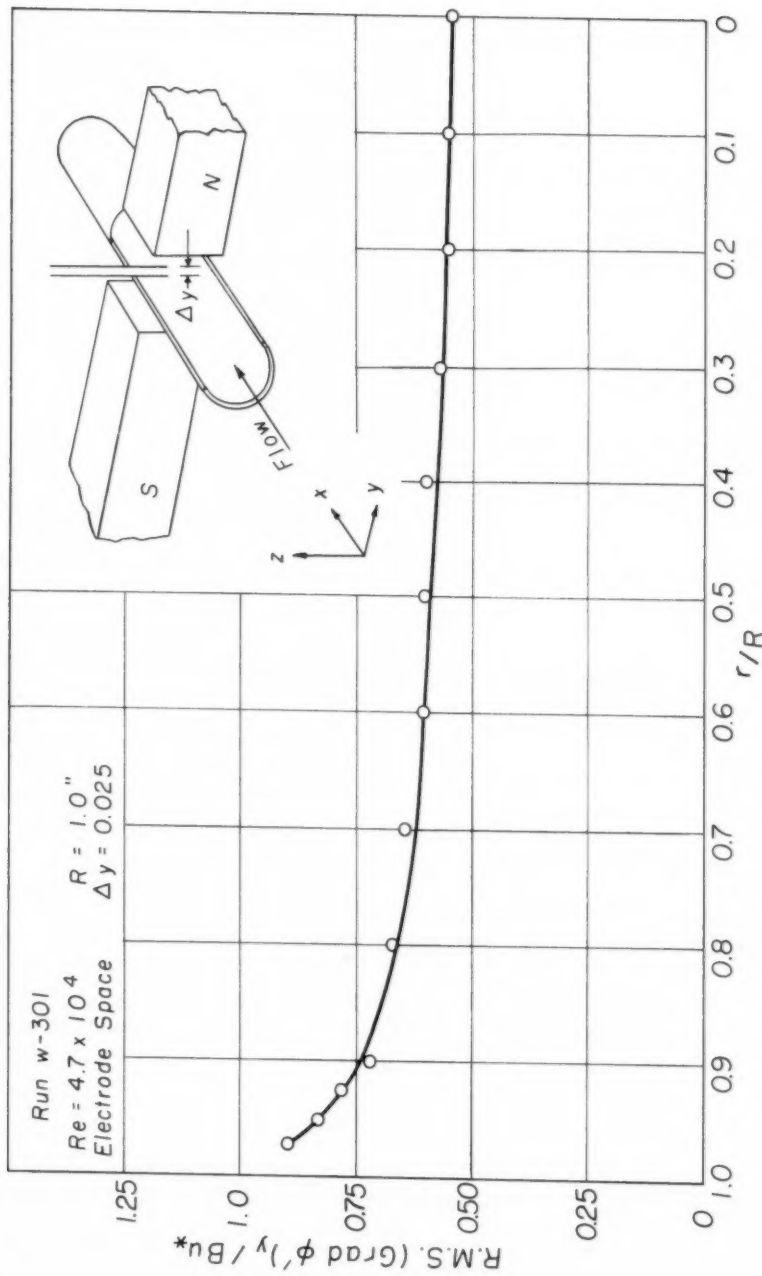
Fig.6 Measurement of R.M.S. Potential Gradient in the Direction of the
Magnetic Field as a Function of Radial Position in the Pipe
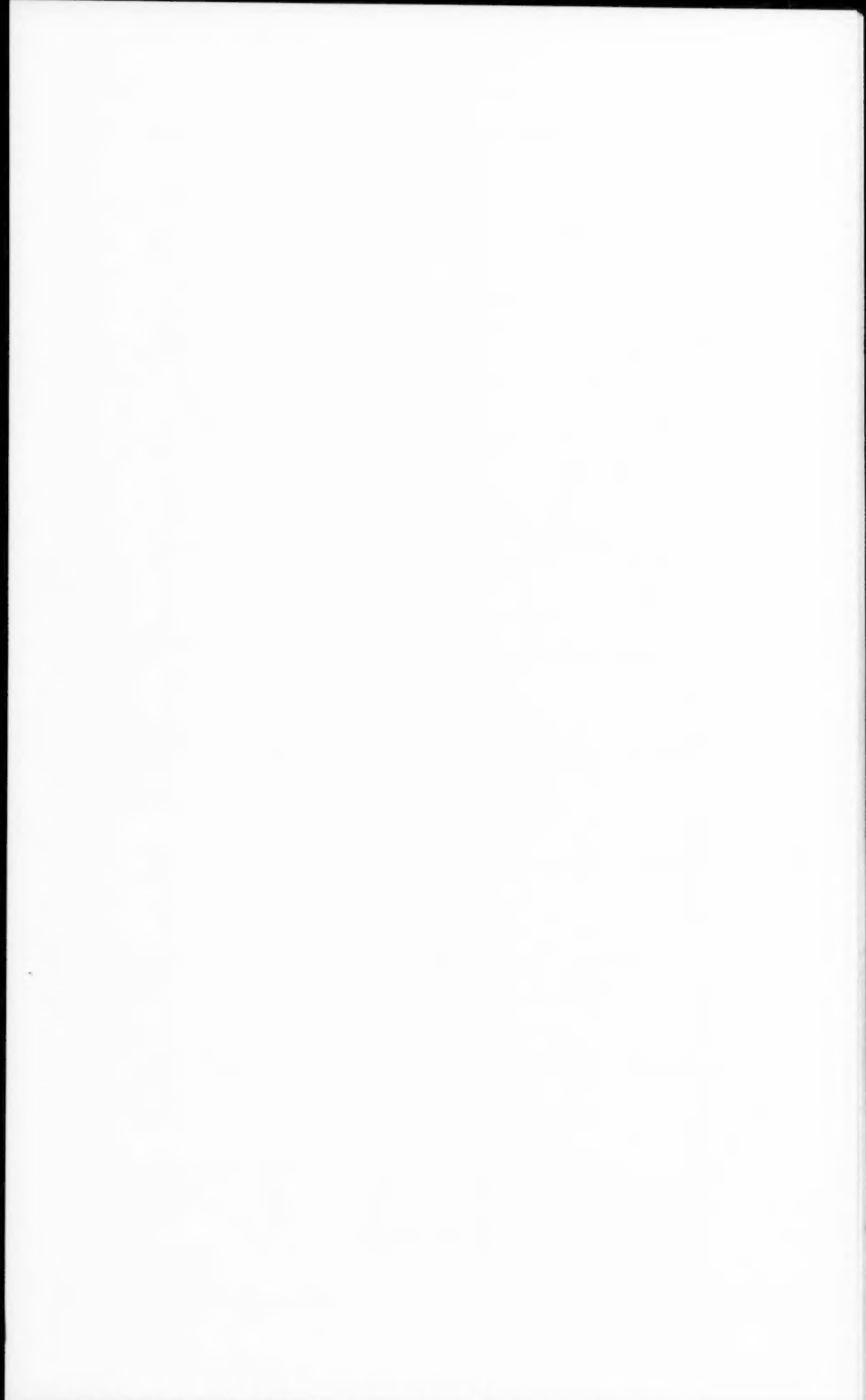
# Journal of the
# HYDRAULICS DIVISION
## Proceedings of the American Society of Civil Engineers

## 100 FREQUENCY CURVES OF NORTH AMERICAN RIVERS

### E. Kuiper,* M. ASCE
### (Proc. Paper 1395)

This paper presents frequency curves of maximum annual flood flows on important rivers in North America. The frequency curves are drawn as straight lines. It was found that the inclination of the lines is a function of drainage area, climate and soil conditions.

## SYNOPSIS

The present study was undertaken in the belief that the frequency curves of maximum annual flood peaks for one particular river station can be drawn with greater accuracy when due attention is paid to other frequency curves on the same or comparable streams.

After having investigated one hundred frequency curves of major streams on the North American Continent, it was concluded:

1. That frequency curves can generally be drawn as straight lines;
2. That topography and lakes have little bearing on the inclination of a frequency line;
3. That a dry climate and porous soils tend to steepen the frequency line;
4. That an increase in size of drainage area tends to flatten the frequency line.

It is believed that the results of this study can be of help in drawing frequency curves of flood flows of rivers that resemble the ones that are analysed in this study.

## INTRODUCTION

In most cases a frequency curve of maximum annual flood peaks at a given river station is based on the flood peaks recorded at that particular river

station. Little or no attention is paid to frequency curves at river stations upstream or downstream, or in similar drainage basins; however, it would seem reasonable that some relationship exists between such frequency curves. In order to investigate this possibility, a study was made of the frequency curves of maximum annual flood flows at one hundred river stations on the more important rivers in North America.

In order to facilitate the comparison between the different frequency curves, every series of flood peaks was converted into ratio-to-the-mean values. For plotting position and graph paper, the Hazen method and the Hazen log-probability paper were chosen. After the points were plotted, a method of drawing the frequency curves had to be selected. It was desirable to adopt the straight-line-by-eye method since this would facilitate the comparison of the different frequency curves. In order to determine if this would be justified, special attention was given to the plotted points of river stations with the longest period of record, and also some experiments were carried out that will be discussed in the following paragraphs. It was concluded that for the present study the use of the straight-line method was permissable.

The main part of the study was then devoted to the questions "if" and "how" the inclination of the straight frequency line is related to various drainage basin characteristics. Plain reasoning suggested that certain characteristics would have a certain bearing upon the inclination of the lines. These suppositions were then checked with the available data.

### Frequency Curves as Straight Lines

While studying the one hundred frequency curves that are presented in this paper, it appeared that the flood peaks from the longest periods of record had a tendency to fall on a straight line, when plotted on logarithmic probability paper. In Table 1 are assembled the stations with a period of record of sixty years and longer. In the last column is shown to what extent the plotted points fall on a straight line. It can be seen from the Table, and the corresponding Figures, that twelve out of twenty-two series of records can be represented by a straight line. Nine out of the remaining ten series approach a straight line fairly well. In only one case, at St. Paul on the Mississippi River, would a straight line fit poorly, and then, only with respect to the lower third of the points.

Demonstration of the misleading appearance of a number of points on a seemingly curved line is provided by the following experiment. A straight line was drawn on log-probability paper. From this line, one thousand discharge values were read at the frequency values: 0.05, 0.15, 0.25, 0.35, etc., up to 99.95. The one thousand items that were thus obtained represented a true straight frequency line. From this group of one thousand items, fifty items were selected, one by one, and by pure chance. This was repeated until twenty groups of fifty items each were obtained. These twenty series were plotted on frequency paper. Five series fitted the original straight line well; nine series fitted the line fairly well; six series fitted the line poorly; two of them would not fit a straight line at all!

It is recognized that such an experiment is no conclusive proof that frequency lines have to be straight. The basic series in this example had a straight-line distribution to start with, which is an unknown quantity in an actual case. However, it is demonstrated that a curved appearance of the

## TABLE 1

Stations with a period of record of 60 years and longer

| Fig.* | No.** | River | Station | Dr. Area in Sq.Mi. | Period of Record | Plotted Points on Str. Line |
|-------|-------|-------|---------|--------------------|------------------|------------------------------|
| 15 | 61 | Cumberland | Nashville | 12,900 | 112 | good |
| 22 | 81B | Connecticut | Hartford | 10,500 | 107 | good |
| 23 | 90B | Columbia | The Dalles | 237,000 | 92 | fair |
| 19 | 72 | Arkansas | Little Rock | 157,900 | 80 | good |
|    | 74 | Mississippi | St. Louis | 701,000 | 80 | good |
|    | 75 | Mississippi | Memphis | 932,800 | 80 | good |
| 20 | 76 | Mississippi | Vicksburg | 1,444,500 | 80 | good |
|    | 63 | Tennessee | Knoxville | 8,900 | 76 | fair |
|    | 64 | Tennessee | Chattanooga | 21,400 | 76 | fair |
| 16 | 65 | Tennessee | Florence | 30,800 | 76 | fair |
|    | 56 | Ohio | Pittsburgh | 19,100 | 75 | fair |
|    | 57 | Ohio | Cincinnati | 76,600 | 75 | good |
| 13 | 58 | Ohio | Metropolis | 203,000 | 75 | good |
| 7 | 25 | Mississippi | St. Paul | 36,800 | 74 | poor |
| 8 | 26 | Mississippi | Le Claire | 88,600 | 74 | fair |
|    | 27 | Mississippi | Keokuk | 119,000 | 74 | fair |
|    | 79 | Savannah | Augusta | 7,200 | 74 | good |
| 14 | 59 | Kanawah | Kanuchin Falls | 8,400 | 73 | good |
|    | 40 | Missouri | Fort Benton | 24,600 | 71 | fair |
| 11 | 42 | Missouri | Kansas City | 489,200 | 71 | good |
| 10 | 32 | Chippewa | Chippewa Falls | 5,600 | 63 | good |
|    | 82 | Hudson | Mechanicville | 4,500 | 62 | fair |

\*   Figure refers to Figure number. See Figure 1 for meaning of symbols.
\*\*  Number refers to number in Table 7.

plotted points can easily be a chance deviation from a true straight line
distribution.

From the observations presented in Table 1, and from the above experi-
ment it is tentatively concluded for the present studies that frequency curves
can be drawn as straight lines unless there is conclusive evidence that this
would not be justified.

In about twenty-five out of the one hundred cases, mostly containing the
stations with a short period of record, it was necessary to give some special
thought to the drawing of a straight line through the plotted points. Difficul-
ties were caused mostly by irregular scattered points from low to high, or by
a break in the general alignment of the points, or by one or a few of the high-
est points that were out of the general direction. In these cases, the follow-
ing considerations were made before the line was drawn.

Widely scattered points are usually caused by a short period of record
that is not representative for the real distribution of the flood peaks. In such
a case, it is difficult to draw a line in which confidence can be placed. The
only thing to do is to draw a line through the general direction of the points.
In the final appraisal of frequency curves, not too much weight should be
given to the curves that have to be derived in this way.

A break in the general alignment of the points is either caused by a non-
representative period of record or by special circumstances. The last pos-
sibility was investigated first and if no abnormalities were found, the line
was drawn by giving most of the weight to the upper part of the points, since
in this study, most of the interest in the frequency curves was focussed on
the region with the low frequencies.

One or a few of the highest points that were either too low or much too
high with respect to the general direction of the other points caused some
trouble. There were cases where the highest point was so much higher than
the other points that there could be no question as to this point not belonging
in the series. There were other cases, however, where the highest point was
rather high but where it was difficult, if not impossible, to determine whether
or not this point properly belonged in the records.

There are some considerations that were kept in mind when dealing with
these troublesome high points. First of all, the total number of station years
that was available for the present study amounts to about five thousand. They
are not all independent items because the stations are sometimes close to-
gether, or on one river, so that correlation is inevitable. However, it can be
assumed that they are equivalent to at least, say, a few thousand independent
streamflow data. In such an extensive series, it can be expected that some of
the relatively highest peak flows would fit nicely in a, say, 2,000-year period
of record. However, these high flows are bound to fall out of place in a 50-
year period of record.

Furthermore, there is the fact that in the present collection of streamflow
data, a few river stations have been especially selected because of the exces-
sive high floods that they contained; for instance, seven stations on the Kansas
River and tributaries and one on the Neosha River, all affected by the 1951
floods; four stations on the Arkansas River, affected by the 1921 flood; and the
Miami River at Dayton, affected by the 1913 flood. These extremes may not
even belong in a record period of a few thousand years and would have to be
studied separately.

Finally, there is the probability which is almost a certainty, that due to
chance, some periods contain records that are relatively too high and that

other periods contain records that are relatively too low.  Even if it is as-
sumed that all the records together represent a period of a few thousand
years, then it must still be expected that in the breakdown into one hundred
small periods, some of these periods receive more and others less than their
proper share of large floods.

As a result of the above considerations, the frequency curves in this study
are drawn by giving more weight to the general direction, indicated by the
majority of the plotted points, than to the position of one or a few of the high-
est points.

## The Influence of Drainage Basin Characteristics

The peak flow of a flood depends upon many variables.  First of all, there
is the factor of chance.  In one year, the flood peak may be large; in the next
year, it may be small.  This factor of chance is the principal cause of the
variability of peak flows that can be found at any stream gauging station.
However, chance is not the only factor that determines the variation between
the extreme low and high peaks.  The characteristics of the drainage basin
also play a role.

In the following paragraphs, the various factors that influence the magni-
tude of the peak flow will be discussed.  The purpose of the discussion is to
find out to what extent these factors have a bearing on the inclination of the
frequency curves of the flood peaks.  This discussion will be in general terms
only.  The following section will deal with specific cases, and it will be seen
how the findings of this section can be applied to the frequency curves of one
hundred river stations on the North American Continent.

### Effect of the Size of the Drainage Area

Consider two river stations a and b.  The respective drainage areas of a
and b, and also the climatological conditions, are identical.  Hence, the fre-
quency curve of flood flows at a must be the same as the one at b.  What type
of frequency curve can be expected at c, just below the confluence of the two
rivers?  If there was complete correlation in magnitude and complete co-
incidence in time between the flood peaks at a and b, the peaks at c would be
the sum of the peaks at a and b.  When expressed in ratio to the mean, the
curve c will coincide with curves a and b.

However, it is very seldom that complete correlation and complete co-
incidence occur in nature.  For practical purposes, it can be assumed that
they exist only partly or not at all.  In order to determine the effect of cor-
relation and co-incidence separately, it will be assumed that first of all there
is a complete correlation and no co-incidence.  This means that the peak
flows in one year are the same at a and b, but that they occur at different
dates.  When the peaks at a and b are far enough apart, the peaks at c will be
practically the same as the ones at a or at b.  When the peaks are fairly close
together, that is, when there is part-coincidence, the peaks at c will consist
of the peaks at a (or b), plus a part of the peaks at b (or a).  When a long
enough period of time is considered, the years with some co-incidence will
cancel the years with almost complete co-incidence and the practical result
is a certain degree of co-incidence.  The curve c can then be obtained by add-
ing to the peak flows of a, a certain percentage of the peak flows at b.  When
expressed in ratio to the mean flood, curve c again coincides with the curves
a and b.

Secondly, it will be assumed that there is no correlation at all, and complete co-incidence. This means that the peak flows at a and b occur every year on the same date but that there is no relationship between the magnitudes. The one may be extremely large while the other is average or even extremely small. This condition results in a curve c, obtained by combining items of curve a with arbitrary items of curve b, after representative series have been taken from each curve. When expressed in ratio to the mean flood, curve c is flatter than curves a and b.

From the above discussion, it follows that frequency curves have a tendency to become flatter when the drainage area increases, provided that the drainage basin characteristics remain the same. This tendency towards a decrease in ratio between the extreme floods and the mean flood is caused by the non-existence of complete correlation between the peak flows on the tributaries and main stem of a river system. One part of a drainage basin may produce a large flood but that does not necessarily imply that the other parts produce large floods also. The larger the drainage basin, the less correlation there is between the production of floods in the various sub-basins, and the smaller the ratio between the extreme floods and the mean.

### Effect of Topography

Consider two drainage basins, identical except for the fact that one has a topography that is twice as steep as the other. What effect will this have upon the frequency curve of the flood flows? Steep slopes mean a quick runoff of the precipitation and therefore, a unit-hydrograph with a relatively sharp peak. On account of the principle of the unit-hydrograph, it can be expected that a change in its shape will affect all floods to the same extent. Hence, all flood peaks in the drainage basin with the steeper topography are a certain ratio larger than the flood peaks in the other basin, provided that the runoff co-efficient remains the same. In other words, topography has no direct bearing on the steepness of the frequency curve. It was assumed in the above that the runoff co-efficient remained the same in both cases and at all flows. However, it can be expected that for low flows, the runoff coefficient is smaller than for high flows, and that the difference is smaller with steeper topography. This secondary effect of a changing runoff co-efficient will be discussed and included under the section "Effect of Soils."

### Effect of Climate

Consider two drainage basins, identical except for the fact that one is located in a region with a wet climate, like the Atlantic Coast of the United States; and the other in a region with a dry climate, like the Canadian Prairies. The wet climate will result in a relatively large figure of average annual rainfall and it can be expected that the magnitude of the mean flood is also relatively large. However, it has been learned from experience that the extreme rainstorms, and therefore, the extreme floods, may very well be of the same order of magnitude in both places. There are even dry regions where the extreme rainfalls are larger than in wet regions. In terms of flood magnitudes, this means that the dry regions can be expected to produce a relatively large ratio between extreme floods and the mean flood. In terms of the frequency curve, it means that the drainage basin in the dry region will show a relatively steep curve.

Effect of Soils

Consider two drainage basins, identical except for the fact that one has an impervious soil, resulting in a high runoff coefficient, and the other has a loose porous soil, resulting in a low runoff coefficient. What effect will this have upon the inclination of the frequency curve? In the case of the impervious soil, the runoff coefficient may range from a low of, say, sixty per cent during moderate rainfalls to a high of ninety per cent during heavy rainfalls of short duration. This means that the peak flows of the floods are approximately proportional to the size of the rainstorm.

In the drainage basin with the pervious soils, it can be expected that during moderate rainfalls, the infiltration capacity of the ground is so large that most or all of the precipitation will be absorbed in the soil and hence, that very little water will reach the streams. The runoff coefficient may be as low as a few per cent. During heavy rainfalls, however, especially if they are of a short duration, the water that infiltrates in the ground constitutes only a fraction of the total amount of precipitation and as a result, a relatively large proportion will reach the streams. The runoff coefficient may become as high as, say, fifty per cent. This means that in the case of the pervious soils, the peak flows increase much more rapidly than the size of the rainstorm and as a result, the ratio between the extreme floods and the mean flood is larger than in the case of the impervious soils. In other words, impervious soils tend to produce flatter frequency curves.

Effect of Natural Storage

Natural lakes have a tendency to reduce small and large flood peaks in approximately the same proportions. Consider, for instance, two river stations —a and b, one just upstream and one just downstream of a natural lake. It will be interesting to determine the frequency curve at b. For that purpose various surface areas of the lake were assumed and different types of floods were routed through the lake in order to determine the peaks at b. In each case, it was found that the ratio of the original peak to the reduced peak was almost independent of the size of the flood. In other words, natural lakes have little bearing on the inclination of a frequency curve. This conclusion does not hold for situations where the natural storage is carried over from one flood to another. In that case small flood peaks may be increased by a carry-over from preceding large peaks, with the result that the frequency curve will tend to flatten. In the extreme case of infinite storage the frequency line becomes horizontal.

Analysis of 100 Frequency Curves

It will be shown in this section that the effect of various drainage basin characteristics, as discussed in the previous section, can be found in the frequency curves of actual river flows. The purpose of this part of the study is to find out if relationship between drainage basin characteristics and frequency curve inclination is so well-defined that it can be used as guidance in determining the frequency curve of flood peaks of a particular river station.

In order to facilitate the analysis, it would be desirable if the inclination of the frequency line could be expressed in some numerical parameter. One of the simplest ways of doing this would be to quote the point where the frequency

line intersects the vertical line, representing the frequency value of one per cent. This parameter will be called R, which is then equivalent to the ratio of the one per cent flood to the mean flood. The problem is now to determine how R is influenced by the size of drainage basin, the climate, and the soils. It would be desirable if these independent variables could also be expressed in numerical parameters.

The first variable, the size of the drainage basin, can be expressed easily in numerical terms; namely, in square miles. The second and third variables are more difficult to express. Fortunately, they both produce similar results with regard to R and the mean flood. When the climate is dry, the mean flood is bound to be low and R can be expected to be high. When the soils are porous, the mean flood will also be low and R also be high. Therefore, it would seem logical to relate R to the mean flood instead of taking the climate and the soils both into consideration. The mean flood in itself is not a desirable indication because it also depends upon the size of the drainage basin. In order to overcome that difficulty the mean flood will be divided by the area of the drainage basin to the 0.8 power. Thus, a parameter F: "Flood Coefficient" is obtained that has from experience proven to be fairly constant when the characteristics of the drainage basin are constant, and when only the size of the basin varies. It can then be expected that, other variables being constant, R will be low when F is high, and vice versa.

Thus, there are two independent variables: size of drainage are D. A. and flood coefficient F; and the one dependent variable: the ratio of the one per cent flood to the mean flood R. Since there are two independent variables, it can be expected that the effect of one variable may obscure or even dominate the effect of the other one. For this reason the analysis will first of all be concerned with examples where either F or D. A. is kept more or less constant, and afterwards with examples where both vary at the same time.

The first example concerns the Tennessee Basin, where F is fairly constant and where the effect of D. A. upon R can be observed. It can be seen that R decreases when D. A. increases. The data are assembled in Table 2.

The second example concerns the Red River of the North Basin where F is also fairly constant. It can again be seen from Table 3 that R decreases when D. A. increases.

The third example concerns a variety of river stations, all with approximately the same D. A., but with different values of F. It can be seen from Table 4 that R decreases with an increase of F.

The fourth example shown in Table 5 concerns the Arkansas Basin, where F decreases with increasing drainage area. Although R is supposed to decrease with increasing drainage area, the variable F apparently dominates to such an extent that R increases instead of decreases.

The last example shown in Table 6 concerns the Mississippi Basin, where F increases with increasing drainage area. Here, a rapid decrease of R with increasing D. A. can be noted because the increasing F and the increasing D. A. have the same effect upon R.

In order to demonstrate the variation of R as a function of F and D. A. for all 100 frequency curves, Table 7 and Figure 25 have been prepared. In Table 7 all pertinent data of the 100 frequency curves have been listed. Although it was decided to determine R by drawing a straight frequency line by eye, the values of $C_V$, $C_S$, and $R_C$ (the computed one per cent ratio, by means of the Foster III table) have nevertheless been listed, in case they may prove to be of interest for future investigations. In Figure 25 the data have been

TABLE 2

| Fig. | No. | River | Station | D.A. | F. | R |
|------|-----|-------|---------|------|-----|-----|
|      | 62  | French Broad | Ashville | 950 | 72.6 | 2.6 |
|      | 63  | Tennessee | Knoxville | 8,900 | 65.7 | 2.4 |
|      | 64  | Tennessee | Chattanooga | 21,400 | 69.0 | 1.8 |
| 16   | 65  | Tennessee | Florence | 30,800 | 64.4 | 1.7 |

TABLE 3

| Fig. | No. | River | Station | D.A. | F. | R |
|------|-----|-------|---------|------|-----|-----|
| 4 | 6 | Pembina | Neche, N. D. | 3,200 | 3.0 | 5.0 |
|   | 1 | R.R. of the N. | Fargo, N.D. | 6,800 | 2.9 | 4.4 |
| 2 | 2 | "        "        " | Grand Forks, N.D. | 15,600 | 4.6 | 3.7 |
|   | 3 | "        "        " | Emerson, Man. | 36,200 | 4.7 | 3.6 |
| 3 | 5 | "        "        " | Winnipeg, Man. | 104,500 | 3.3 | 3.0 |

TABLE 4

| Fig. | No. | River | Station | D.A. | F. | R |
|------|-----|-------|---------|------|-----|-----|
| 5 | 11 | Qu'Appelle | Tantallon, Sask. | 17,500 | 0.4 | 5.8 |
|   | 69 | Arkansas | La Junta, Colo. | 12,200 | 4.7 | 4.3 |
|   | 29 | Minnesota | Mankato, Minn. | 14,900 | 6.2 | 3.6 |
|   | 95 | Snake | Neeley, Idaho | 14,100 | 10.9 | 2.8 |
|   | 39 | Des Moines | Keosanqua, Iowa | 13,900 | 20.0 | 2.5 |
| 15 | 61 | Cumberland | Nashville, Tenn | 12,900 | 63.0 | 1.7 |

TABLE 5

| Fig. | No. | River | Station | D.A. | F. | R |
|------|-----|-------|---------|------|-----|-----|
|    | 66 | Arkansas | Salida | 1,200 | 10.7 | 2.0 |
| 17 | 67 | "        | Canon City | 3,100 | 7.7 | 2.8 |
|    | 68 | "        | Pueblo | 4,700 | 7.1 | 3.2 |
|    | 69 | "        | La Junta | 12,200 | 4.7 | 4.3 |
| 18 | 70 | "        | Holly | 25,100 | 2.9 | 4.5 |
|    | 71 | "        | Wichita | 40,200 | 1.9 | 5.0 |

TABLE 6

| Fig. | No. | River | Station | D.A. | F. | R |
|------|-----|-------|---------|------|-----|-----|
| 9  | 28 | Minnesota | Montevideo | 6,200 | 3.1 | 5.4 |
|    | 29 | "         | Mankato | 14,900 | 6.2 | 3.6 |
| 7  | 25 | Mississippi | St. Paul | 36,800 | 8.3 | 2.5 |
| 8  | 26 | "           | Le Claire | 88,600 | 15.1 | 2.1 |
|    | 27 | "           | Keokuk | 119,000 | 15.4 | 2.0 |
| 20 | 76 | "           | Vicksburg | 1,144,500 | 18.1 | 1.7 |

TABLE 7

FLOOD FREQUENCY DATA

| Fig. No. | River | Station | Records | Dr. Area in sq.mi. | Mean flood in cfs | F | R | $C_v$ | $C_s$ | $R_c$ |
|---|---|---|---|---|---|---|---|---|---|---|
| | **RED RIVER BASIN** | | | | | | | | | |
| 1 | Red River of the North | Fargo, N. D. | 1902-51 | 6,800 | 3,350 | 2.9 | 4.4 | .91 | 2.40 | 4.6 |
| 2 | Red River of the North | Grand Forks, N. D. | 1902-51 | 26,100 | 15,600 | 4.6 | 3.7 | .68 | 1.36 | 3.3 |
| 3 | Red River of the North | Emerson, Man. | 1913-51 | 36,200 | 21,000 | 4.7 | 3.6 | .77 | 3.07 | 4.3 |
| 4 | Red River of the North | Winnipeg, Man. | 1913-51 | 45,500 | 27,900 | 5.2 | 3.2 | .60 | 2.08 | 3.3 |
| 5 | Red River of the North | Winnipeg, Man. | 1902-51 | 104,500 | 34,100 | 3.3 | 3.0 | .54 | 1.46 | 2.9 |
| 6 | Pembina | Neche, N. D. | 1913-51 | 3,200 | 1,910 | 3.0 | 5.0 | 1.00 | 3.15 | 5.3 |
| 7 | Red Lake | Crookston, Minn. | 1901-50 | 5,300 | 6,890 | 7.3 | 3.2 | .67 | 2.18 | 3.6 |
| 8 | Assiniboine | Millwood, Man. | 1913-51 | 7,700 | 4,150 | 3.2 | 5.0 | .98 | 2.26 | 4.9 |
| 9 | Assiniboine | Brandon, Man. | 1913-51 | 32,000 | 6,640 | 1.7 | 4.8 | .81 | 1.86 | 4.0 |
| 10 | Assiniboine | Headingley, Man. | 1913-51 | 59,000 | 9,200 | 1.4 | 3.9 | .60 | .79 | 2.8 |
| 11 | Qu'Appelle | Tantallon, Sask. | 1913-51 | 17,500 | 850 | .4 | 5.8 | .76 | 1.28 | 3.6 |
| 12 | Souris | Wawanesa, Man. | 1913-51 | 24,200 | 2,100 | .7 | 4.5 | .83 | 1.97 | 4.1 |
| | **SASKATCHEWAN RIVER BASIN** | | | | | | | | | |
| 13 | North Saskatchewan | Rocky Mt. Hse., Alta. | 1911-51 | 4,200 | 29,000 | 36.6 | 2.1 | .62 | 5.21 | 4.0 |
| 14 | North Saskatchewan | Edmonton, Alta. | 1911-51 | 10,500 | 48,700 | 29.6 | 2.6 | .62 | 3.32 | 3.7 |
| 15 | North Saskatchewan | Prince Albert, Sask. | 1911-51 | 46,100 | 47,600 | 8.8 | 2.7 | .59 | 3.64 | 3.6 |
| 16 | St. Mary | Kimball, Alta. | 1903-50 | 500 | 4,400 | 30.5 | 2.6 | .61 | 3.33 | 3.6 |
| 17 | St. Mary | Lethbridge, Alta. | 1911-51 | 6,700 | 22,400 | 19.5 | 4.1 | .82 | 2.12 | 4.2 |
| 18 | South Saskatchewan | Medicine Hat, Alta. | 1911-51 | 20,600 | 45,300 | 16.0 | 3.2 | .60 | 1.60 | 3.1 |
| 19 | South Saskatchewan | Saskatoon, Sask. | 1911-51 | 50,900 | 54,000 | 9.3 | 3.1 | .50 | 1.28 | 2.7 |
| 20 | Red Deer | Red Deer, Alta. | 1911-51 | 4,500 | 15,600 | 18.6 | 4.3 | .73 | 1.75 | 3.7 |
| 21 | Bow | Calgary, Alta. | 1911-51 | 3,100 | 16,000 | 25.8 | 2.5 | .47 | 2.31 | 2.9 |
| 22 | Saskatchewan | Nipawin, Sask. | 1911-51 | 97,000 | 90,000 | 9.6 | 2.5 | .50 | 2.00 | 2.9 |
| 23 | Saskatchewan | The Pas, Man. | 1911-51 | 149,500 | 63,000 | 4.6 | 1.9 | .27 | .86 | 1.8 |

R = ratio of 1 per cent flood to mean flood, determined by drawing straight frequency lines.

$R_c$ = ratio of 1 per cent flood to mean flood, computed from $C_v$, $C_s$, and Foster III table.

NOTE: F = flood coefficient = $\dfrac{\text{Mean Flood}}{[\text{Drainage Area}]^{0.8}}$

$C_v$ = coefficient of variation

$C_s$ = coefficient of skew.

TABLE 7 [continued]
FLOOD FREQUENCY DATA

| Fig. | No. | River | Station | Records | Dr. Area in sq.mi. | Mean Flood in cfs | $F$ | $R$ | $C_v$ | $C_s$ | $R_c$ |
|---|---|---|---|---|---|---|---|---|---|---|---|
| | | **UPPER MISSISSIPPI RIVER BASIN** | | | | | | | | | |
| 7 | 24 | Mississippi | Elk River, Minn. | 1915-50 | 14,500 | 18,500 | 8.7 | 2.6 | .48 | .47 | 2.3 |
| | 25 | Mississippi | St. Paul, Minn. | 1878-1950 | 36,800 | 37,100 | 8.3 | 2.5 | .51 | .61 | 2.4 |
| 8 | 26 | Mississippi | Le Claire, Iowa | 1878-1950 | 88,600 | 136,600 | 15.1 | 2.1 | .33 | .54 | 1.9 |
| | 27 | Mississippi | Keokuk, Iowa | 1878-1950 | 119,000 | 176,800 | 15.4 | 2.0 | .31 | .22 | 1.8 |
| 9 | 28 | Minnesota | Montevideo, Minn. | 1909-50 | 6,200 | 3,400 | 3.1 | 5.4 | 1.18 | 3.20 | 6.1 |
| | 29 | Minnesota | Mankato, Minn. | 1909-50 | 14,900 | 13,600 | 6.2 | 3.6 | .67 | .72 | 3.0 |
| | 30 | St. Croix | Swiss, Wis. | 1914-50 | 1,600 | 4,600 | 12.6 | 3.0 | .44 | 1.36 | 2.5 |
| | 31 | St. Croix | St. Croix, Wis. | 1914-50 | 5,900 | 21,400 | 20.5 | 2.8 | .52 | 1.12 | 2.7 |
| 10 | 32 | Chippewa River | Chippewa Falls, Wis. | 1888-1950 | 5,600 | 39,400 | 40.0 | 2.4 | .44 | 1.20 | 2.4 |
| | 33 | Wisconsin River | Merill, Wis. | 1909-50 | 2,600 | 15,300 | 28.4 | 2.4 | .57 | 2.78 | 3.4 |
| | 34 | Wisconsin | Muskoda, Wis. | 1909-50 | 10,300 | 41,500 | 25.6 | 2.1 | .37 | .20 | 1.9 |
| | 35 | Rock | Afton, Wis. | 1915-50 | 3,300 | 7,100 | 10.9 | 2.5 | .40 | .07 | 2.0 |
| | 36 | Rock | Lyndon, Ill. | 1915-50 | 9,000 | 27,100 | 18.7 | 2.4 | .42 | .18 | 2.1 |
| | 37 | Iowa | Iowa City, Iowa | 1915-50 | 3,200 | 13,100 | 20.0 | 3.1 | .63 | 1.43 | 3.2 |
| | 38 | Iowa | Wapello, Iowa | 1915-50 | 12,500 | 39,400 | 20.8 | 2.4 | .47 | .44 | 2.3 |
| | 39 | Des Moines | Keosauqua, Iowa | 1903-1950 | 13,900 | 41,100 | 20.0 | 2.5 | .54 | 1.77 | 3.0 |
| | | **MISSOURI RIVER BASIN** | | | | | | | | | |
| 11 | 40 | Missouri | Fort Benton, Mont. | 1881-1951 | 24,600 | 32,800 | 10.1 | 2.5 | .55 | 3.52 | 3.4 |
| | 41 | Missouri | Pierre, S. D. | 1892-1950 | 246,700 | 118,000 | 5.9 | 2.5 | .45 | 1.34 | 2.5 |
| | 42 | Missouri | Kansas City, Mo. | 1881-1951 | 489,200 | 193,500 | 5.4 | 2.4 | .44 | 2.00 | 2.6 |
| | 43 | Marias River | Shelby, Mont. | 1902-49 | 2,600 | 7,900 | 14.7 | 4.0 | .95 | 3.05 | 5.0 |
| | 44 | Beaverhead River | Barratts, Mont. | 1908-49 | 2,900 | 1,500 | 2.5 | 2.8 | .49 | 1.04 | 2.6 |
| | 45 | Big Horn | Thermopolis, Wyo. | 1900-49 | 8,100 | 13,100 | 9.8 | 2.3 | .36 | 1.12 | 2.2 |
| | 46 | Yellowstone | Sidney, Mont. | 1903-49 | 69,500 | 78,600 | 10.5 | 2.3 | .37 | .49 | 2.0 |

TABLE 7 [continued]
FLOOD FREQUENCY DATA

| Fig. No. | River | Station | Records | Dr. Area in sq.mi. | Mean Flood in cfs | F | R | Cv | Cs | Rc |
|---|---|---|---|---|---|---|---|---|---|---|
| **KANSAS RIVER BASIN** | | | | | | | | | | |
| 47 | Solomon River | Niles, Kans. | 1897-1951 | 6,700 | 8,700 | 7.5 | 4.8 | .87 | 2.97 | 4.7 |
| 48 | Smoky Hill | Enterprise, Kans. | 1903-51 | 19,200 | 13,500 | 5.1 | 4.1 | 1.00 | 4.79 | 5.7 |
| 49 | Big Blue | Randolph, Kans. | 1918-51 | 9,100 | 27,600 | 18.8 | 3.5 | .75 | 2.00 | 3.9 |
| 50 | Republican | Scandia, Kans. | 1895-1951 | 22,900 | 18,900 | 6.1 | 4.6 | .98 | 2.93 | 5.1 |
| 51 | Kansas | Ogden, Kans. | 1917-51 | 45,200 | 29,100 | 5.5 | 3.9 | 1.02 | 4.00 | 5.6 |
| 12 52 | Kansas | Topeka, Kans. | 1905-51 | 56,700 | 52,000 | 8.2 | 3.5 | .64 | 1.24 | 3.1 |
| 53 | Kansas | Bonner Springs, Kans. | 1918-51 | 59,900 | 67,700 | 10.2 | 3.1 | .59 | .48 | 2.6 |
| **OHIO RIVER BASIN** | | | | | | | | | | |
| 54 | Allegheny River | Red House, N. Y. | 1904-49 | 1,700 | 24,500 | 63.6 | 2.3 | .35 | .51 | 2.0 |
| 55 | Allegheny | Franklin, Pa. | 1904-49 | 6,000 | 79,400 | 75.2 | 2.2 | .34 | .58 | 2.0 |
| 56 | Ohio | Pittsburgh, Pa. | 1875-1949 | 19,100 | 246,600 | 92.5 | 1.7 | .28 | 1.68 | 2.0 |
| 57 | Ohio | Cincinnati, Ohio | 1875-1949 | 76,600 | 443,700 | 54.8 | 1.8 | .28 | .89 | 1.8 |
| 13 58 | Ohio | Metropolis, Ill. | 1875-1949 | 203,000 | 882,000 | 50.1 | 1.7 | .26 | .79 | 1.8 |
| 14 59 | Kanawha | Kanawha Falls, W. Va. | 1877-1949 | 8,400 | 125,600 | 91.0 | 2.2 | .38 | .90 | 1.2 |
| 60 | Miami | Dayton, Ohio | 1893-1919 | 2,200 | 35,900 | 74.0 | 3.0 | .46 | .27 | 2.2 |
| 15 61 | Cumberland River | Nashville, Tenn. | 1838-1949 | 12,900 | 122,200 | 63.0 | 1.7 | .23 | .40 | 1.6 |
| 62 | French Broad | Asheville, N. C. | 1896-1949 | 950 | 17,500 | 72.6 | 2.6 | .84 | 5.46 | 5.0 |
| 63 | Tennessee | Knoxville, Tenn. | 1874-1949 | 8,900 | 94,700 | 65.7 | 2.4 | .44 | .89 | 2.3 |
| 16 64 | Tennessee | Chattanooga, Tenn. | 1874-1949 | 21,400 | 201,000 | 69.0 | 1.8 | .31 | .30 | 1.8 |
| 65 | Tennessee | Florence, Ala. | 1874-1949 | 30,800 | 251,000 | 64.4 | 1.7 | .28 | .25 | 1.7 |

TABLE 7 [continued]
FLOOD FREQUENCY DATA

| Fig. No. | | River | Station | Records | Dr. Area in sq.mi. | Mean Flood in cfs | F | R | $C_v$ | $C_s$ | $R_c$ |
|---|---|---|---|---|---|---|---|---|---|---|---|
| | | **ARKANSAS RIVER BASIN** | | | | | | | | | |
| 17 | 66 | Arkansas | Salida, Colo. | 1895-1950 | 1,200 | 3,100 | 10.7 | 2.0 | .31 | .17 | 1.8 |
| | 67 | Arkansas | Canon City, Colo. | 1895-1950 | 3,100 | 4,800 | 7.7 | 2.8 | .60 | 2.71 | 3.4 |
| | 68 | Arkansas | Pueblo, Colo. | 1895-1950 | 4,700 | 6,200 | 7.1 | 3.2 | .64 | 2.67 | 3.6 |
| | 69 | Arkansas | La Junta, Colo. | 1913-50 | 12,200 | 8,900 | 4.7 | 4.3 | .85 | 1.53 | 4.0 |
| 18 | 70 | Arkansas | Holly, Colo. | 1913-50 | 25,100 | 9,500 | 2.9 | 4.5 | .90 | 1.40 | 4.1 |
| | 71 | Arkansas | Wichita, Kans. | 1922-51 | 40,200 | 9,200 | 1.9 | 5.0 | .80 | 1.33 | 3.8 |
| 19 | 72 | Arkansas | Little Rock, Ark. | 1872-1951 | 157,900 | 291,300 | 20.2 | 2.3 | .43 | 1.32 | 2.4 |
| | 73 | Neosha | Iola, Kans. | 1896-1951 | 3,800 | 28,300 | 38.7 | 3.7 | .63 | 1.37 | 3.1 |
| | | **MISSISSIPPI RIVER BASIN** | | | | | | | | | |
| 20 | 74 | Mississippi | St. Louis, Mo. | 1872-1951 | 701,000 | 560,100 | 11.8 | 2.1 | .39 | .78 | 2.1 |
| | 75 | Mississippi | Memphis, Tenn. | 1872-1951 | 932,800 | 1,249,000 | 20.9 | 1.7 | .25 | .82 | 1.7 |
| | 76 | Mississippi | Vicksburg, Miss. | 1872-1951 | 1,144,500 | 1,271,200 | 18.1 | 1.7 | .23 | .68 | 1.7 |
| | | **ST. LAWRENCE RIVER BASIN** | | | | | | | | | |
| 21 | 77 | Niagara | Buffalo, N. Y. | 1905-1950 | 263,000 | 208,600 | 9.6 | 1.2 | .09 | .72 | 1.3 |
| | | **ATLANTIC COAST** | | | | | | | | | |
| 22 | 78 | Chattahoochee | Alaga, Ala. | 1905-1949 | 8,300 | 78,500 | 57.0 | 2.7 | .50 | 1.34 | 2.7 |
| | 79 | Savannah | Augusta, La. | 1876-1949 | 7,200 | 112,900 | 94.0 | 3.1 | .60 | 1.64 | 3.1 |
| | 80 | Connecticut | White River Junc., Vt. | 1903-1949 | 4,100 | 53,100 | 68.5 | 2.3 | .42 | 2.02 | 2.6 |
| | 81[a] | Connecticut | Hartford, Conn. | 1903-1949 | 10,500 | 113,000 | 68.5 | 2.1 | .38 | 2.25 | 2.5 |
| | 81[b] | Connecticut | Hartford, Conn. | 1843-1949 | 10,500 | 112,600 | 68.2 | 2.0 | .35 | 1.38 | 2.2 |

TABLE 7 [continued]
FLOOD FREQUENCY DATA

| Fig. No. | River | Station | Records | Dr. Area in sq.mi. | Mean Flood in cfs | F | R | $C_v$ | $C_s$ | $R_c$ |
|---|---|---|---|---|---|---|---|---|---|---|
| | ATLANTIC COAST [continued] | | | | | | | | | |
| 82 | Hudson | Mechanicville, N. Y. | 1888-1949 | 4,500 | 42,500 | 50.8 | 2.1 | .40 | 2.46 | 2.6 |
| 83 | Susquehanna | Towanda, Pa. | 1894-1949 | 7,800 | 107,200 | 82.1 | 2.2 | .39 | 1.09 | 2.2 |
| 84 | West Br. Susquehanna | Williamsport, Pa. | 1894-1949 | 5,700 | 104,100 | 104.1 | 2.5 | .47 | 1.72 | 2.7 |
| 85 | Susquehanna | Harrisburg, Pa. | 1894-1949 | 24,100 | 232,600 | 88.0 | 2.1 | .37 | 2.31 | 2.4 |
| | COLUMBIA RIVER BASIN | | | | | | | | | |
| 86 | Columbia | Nicholson, B. C. | 1913-49 | 2,500 | 14,400 | 27.8 | 2.0 | .27 | .53 | 1.8 |
| 87 | Columbia | Revelstoke, B. C. | 1913-49 | 9,000 | 126,400 | 86.5 | 1.6 | .19 | .28 | 1.5 |
| 88 | Columbia | Birchbank, B. C. | 1913-49 | 34,000 | 234,400 | 55.5 | 1.7 | .22 | .30 | 1.6 |
| 89 | Columbia | Internat. Boundary | 1913-49 | 59,700 | 330,200 | 50.0 | 1.7 | .26 | .30 | 1.7 |
| 90[a] | Columbia | The Dalles, Oreg. | 1913-49 | 237,000 | 535,900 | 26.8 | 1.9 | .31 | .57 | 1.9 |
| 90[b] | Columbia | The Dalles, Oreg. | 1858-1949 | 237,000 | 609,900 | 30.5 | 1.8 | .29 | .38 | 1.8 |
| 91 | Flathead | Polson, Mont. | 1913-49 | 7,000 | 51,400 | 43.2 | 1.8 | .30 | .03 | 1.7 |
| 92 | Clark Fork | Plains, Mont. | 1913-49 | 19,900 | 82,170 | 30.3 | 1.8 | .33 | .07 | 1.8 |
| 93 | Pend Oreille | Internat. Boundary | 1913-49 | 25,200 | 90,700 | 27.4 | 2.1 | .35 | .33 | 1.9 |
| 94 | Snake | Moran, Wyo. | 1912-49 | 800 | 9,100 | 43.4 | 1.7 | .22 | .90 | 1.7 |
| 95 | Snake | Neeley, Idaho | 1912-49 | 14,100 | 22,600 | 10.9 | 2.8 | .43 | .56 | 2.2 |
| 96 | Snake | Weiser, Idaho | 1912-49 | 63,000 | 47,000 | 6.9 | 2.6 | .35 | .09 | 1.8 |
| 97 | Snake | Clarkston, Wash. | 1916-49 | 103,200 | 186,800 | 18.2 | 2.1 | .34 | .87 | 2.0 |
| | PACIFIC COAST | | | | | | | | | |
| 98 | Colorado | Glenwood Spr., Colo. | 1902-34 | 4,600 | 19,200 | 22.6 | 2.2 | .34 | .24 | 1.9 |
| 99[a] | Colorado | Yuma, Ariz. | 1902-34 | 244,800 | 97,100 | 4.8 | 2.8 | .48 | 1.38 | 2.7 |
| 99[b] | Colorado | Yuma, Ariz. | 1902-50 | 244,800 | 72,400 | 3.5 | 3.7 | .73 | 1.19 | 3.4 |
| 100 | Fraser | Hope, B. C. | 1912-50 | 85,600 | 307,500 | 34.0 | 1.5 | .22 | 1.14 | 1.7 |

23]

24]

Figure 1
LEGEND OF SYMBOLS:
Records:   Period of record used.
Max.    :  5 highest items in
           descending order.
D. A.   =  Drainage Area,
M. F.   =  Mean of annual peak flows
$C_v$   =  Coefficient of Variation
$C_s$   =  Coefficient of Skew
F       =  $\frac{M.F.}{D.A.^{0.8}}$
R       =  Ratio of 1% flood to M.F.
Hist.   =  Greatest historical flood
           known.

STRAIGHT LINE
DRAWN BY EYE    R

POINTS PLOTTED
ACCORDING TO
$p = \frac{n - 0.5}{m}$

M.F.

FREQUENCY IN PERCENT

RATIO TO MEAN FLOOD
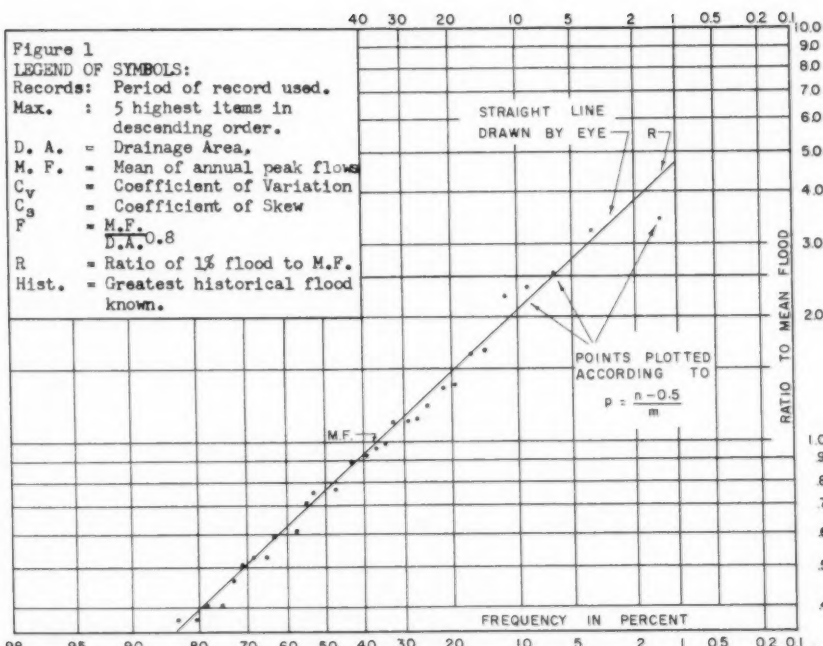
Figure 2 [No. 2 in Table 7]
RED RIVER OF THE NORTH
Grand Forks, N. D.

Records 1902 - 1951
Max. 1950, 1947, 1948, 1904, 1907
D. A.  26,100 sq. mi.
M. F.  15,600 cfs.
$C_v$ = 0.68        $C_s$ = 1.36
F = 4.6        R = 3.7
Hist. 1897:  80,000 cfs. = 5.1 M.F.

FREQUENCY IN PERCENT

RATIO TO MEAN FLOOD
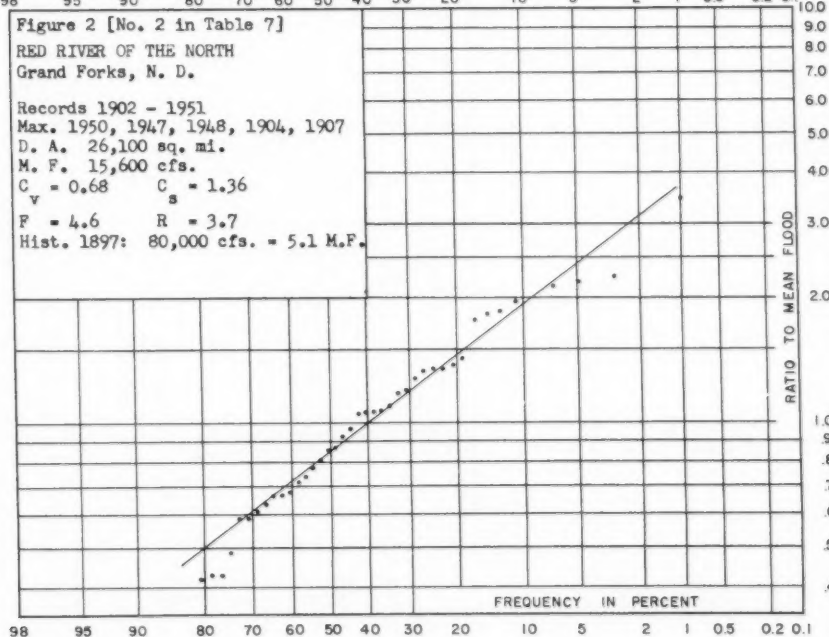
Figure 3 [No. 5 in Table 7]

RED RIVER OF THE NORTH
Winnipeg – Redwood, Man.

Records 1902-1951
Max. 1950, 1916, 1948, 1904, 1923
D. A. 104,500 sq. mi.
M. F. 34,100 cfs.
$C_v$ = 0.54          $C_s$ = 1.46
F  = 3.3          R  = 3.0
Hist. 1826:   225,000 cfs = 6.6 M.F.

FREQUENCY  IN  PERCENT

RATIO  TO  MEAN  FLOOD
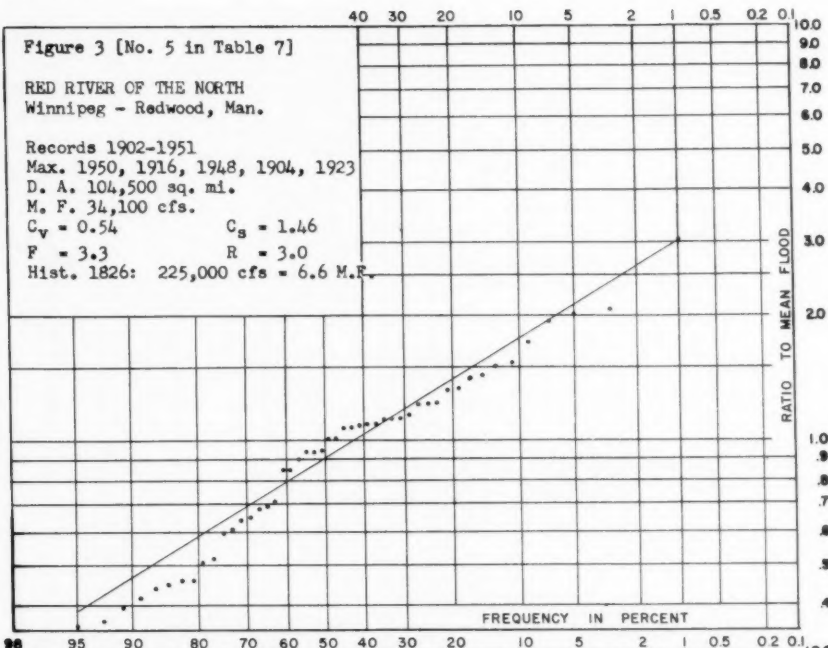


Figure 4 [No. 6 in Table 7]

PEMBINA RIVER,
Neche, N. D.

Records 1913 – 1951
Max. 1950, 1949, 1913, 1948, 1942
D. A. 3,200 sq. mi.
M. F. 1,910 cfs.
$C_v$ = 1.00          $C_s$  = 3.15
F  = 3.0          R  = 5.0

FREQUENCY  IN  PERCENT

RATIO  TO  MEAN  FLOOD
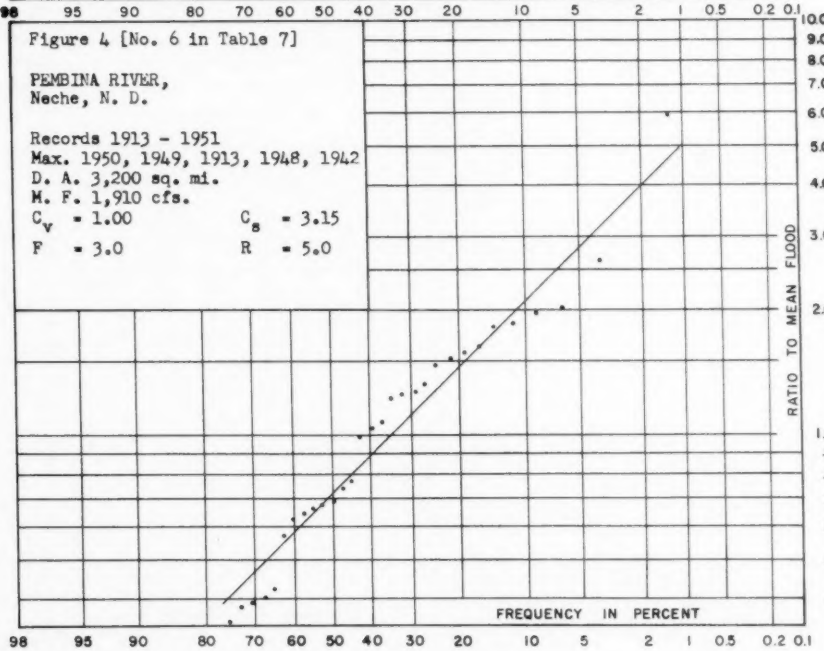
Figure 5 [No. 11 in Table 7]

QU'APPELLE RIVER,
Tantallon, Sask.

Records 1913-1951
Max. 1925, 1948, 1927, 1923, 1922
D. A. = 17,500 sq. mi.
M. F. = 850 cfs.
$C_v$ = 0.76      $C_s$ = 1.28
F = 0.4      R = 5.8
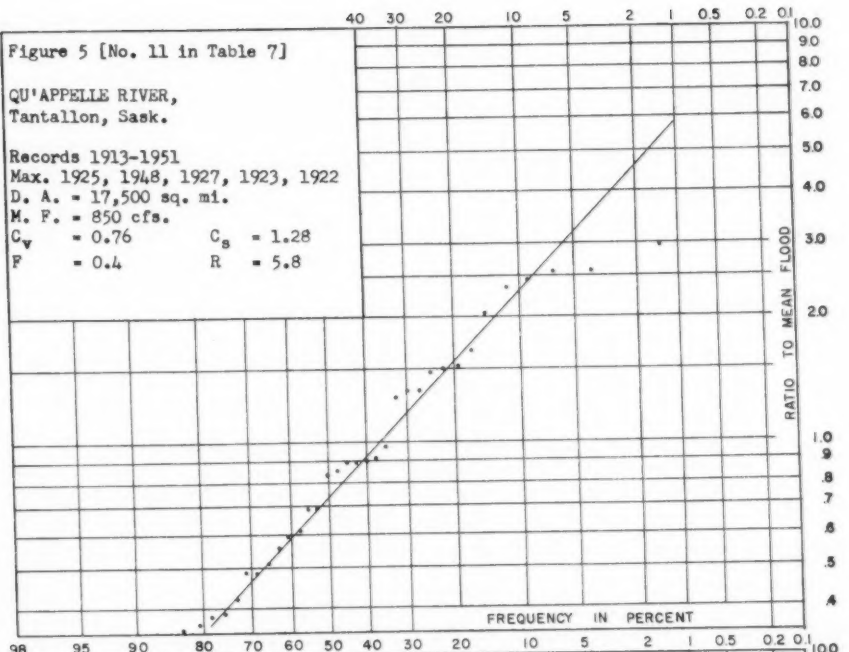


Figure 6 [No. 22 in Table 7]

SASKATCHEWAN RIVER,
Nipawin, Sask.

Records 1911-1951
Max. 1915, 1932, 1948, 1929, 1923
D. A. = 97,000 sq. mi.
M. F. = 90,000 cfs.
$C_v$ = 0.50      $C_s$ = 2.00
F = 9.6      R = 2.5
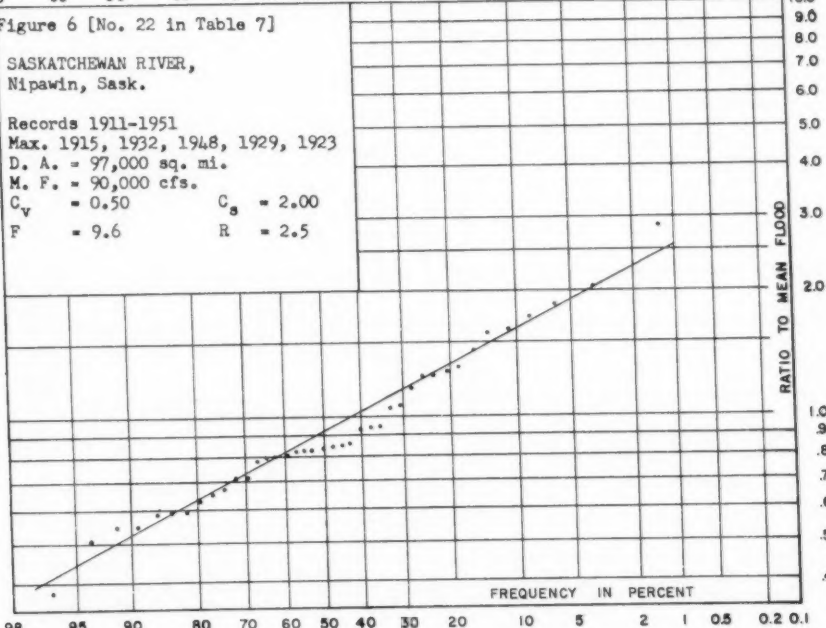
Figure 7 [No. 25 in Table 7]

MISSISSIPPI RIVER,
St. Paul, Minn.

Records 1878–1950
Max. 1881, 1897, 1916, 1908, 1917
D. A. 36,800 sq. mi.
M. F. 37,100 cfs.
$C_v$ = 0.51      $C_s$ = 0.61
F = 8.3      R = 2.5

FREQUENCY IN PERCENT

RATIO TO MEAN FLOOD
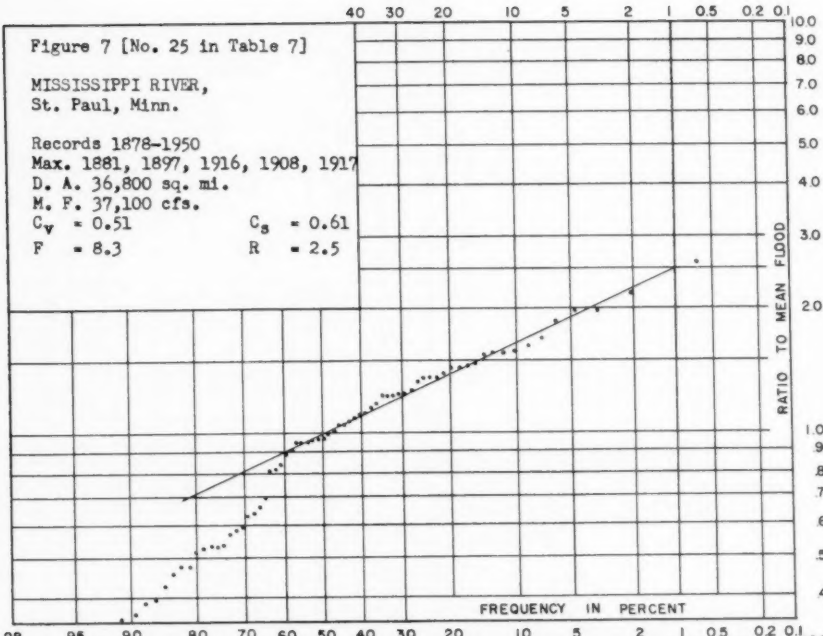
Figure 8 [No. 26 in Table 7]

MISSISSIPPI RIVER,
Le Claire, Iowa.

Records 1878–1950
Max. 1880, 1888, 1892, 1882, 1920
D. A. 88,600 sq. mi.
M. F. 136,600 cfs.
$C_v$ = 0.33      $C_s$ = 0.54
F = 15.1      R = 2.1

FREQUENCY IN PERCENT

RATIO TO MEAN FLOOD
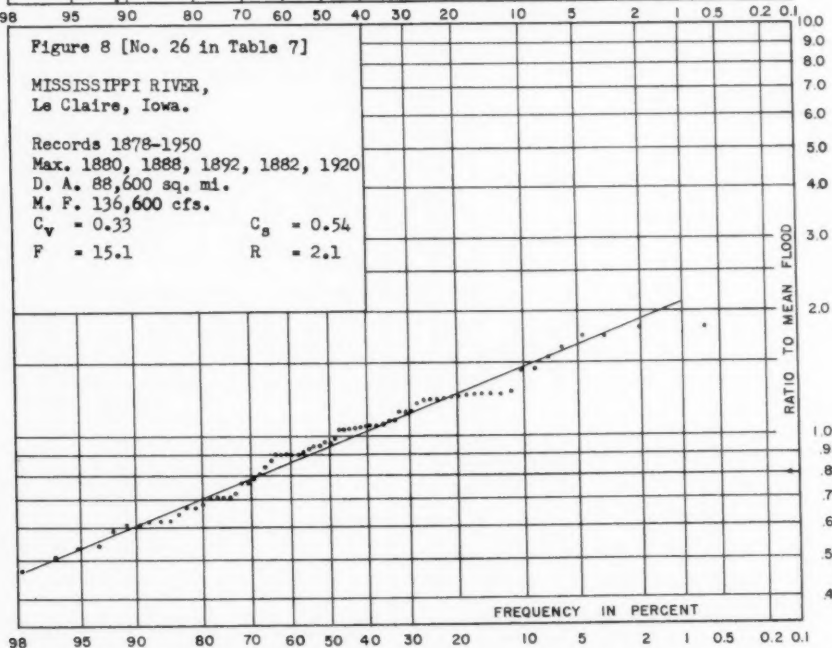
Figure 9 [No. 28 in Table 7]

MINNESOTA RIVER,
Montevideo, Minn.

Records 1909-1950
Max. 1919, 1917, 1943, 1920, 1947
D. A. 6,200 sq. mi.
M. F. 3,400 cfs
$C_v$ = 1.18        $C_s$ = 3.20
F   = 3.1          R   = 5.4

FREQUENCY   IN   PERCENT

RATIO   TO   MEAN   FLOOD
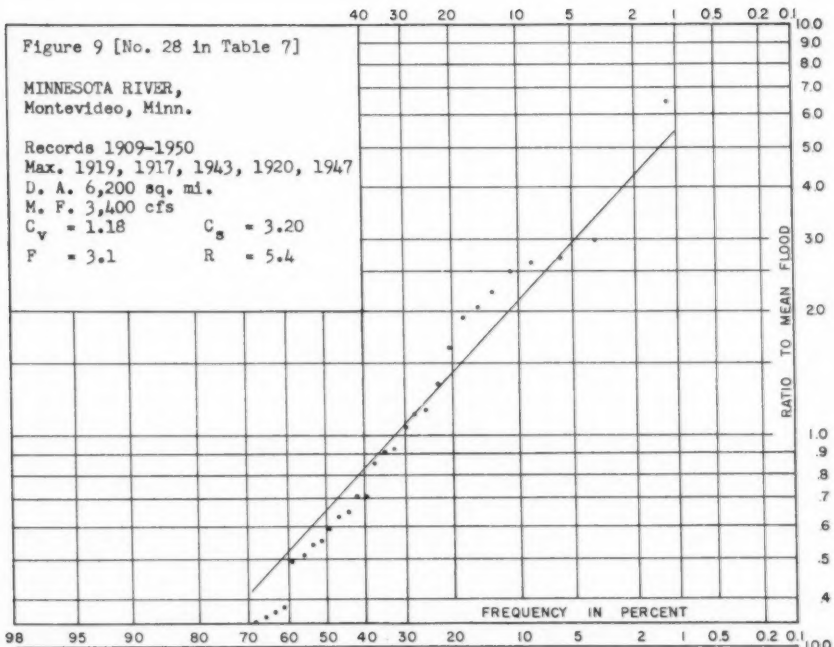


Figure 10 [No. 32 in Table 7]

CHIPPEWA RIVER,
Chippewa Falls, Wis.

Records 1888-1950
Max. 1941, 1943, 1920, 1938, 1905
D. A. 5,600 sq. mi.
M. F. 39,400 cfs.
$C_v$ = 0.44        $C_s$ = 1.20
F   = 40.0        R   = 2.4

FREQUENCY   IN   PERCENT

RATIO   TO   MEAN   FLOOD
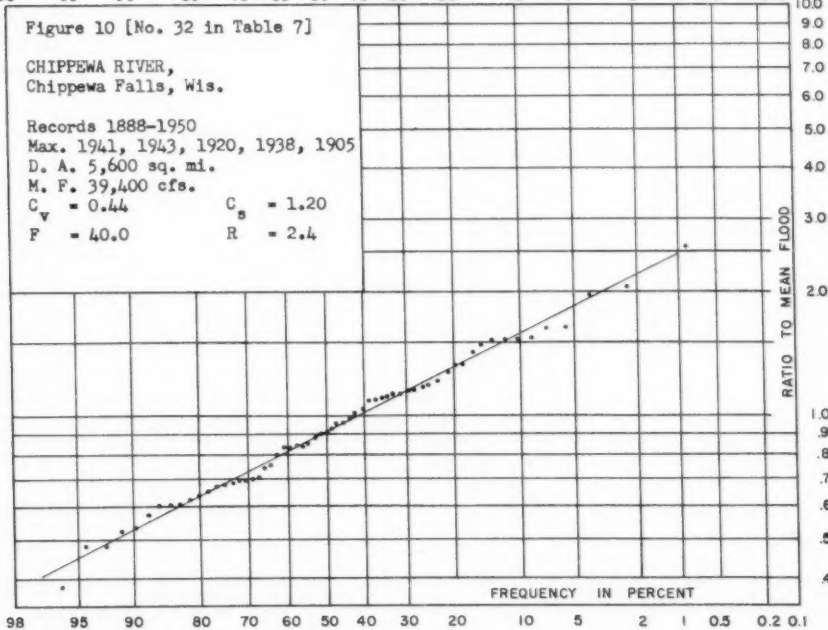
Figure 11 [No. 42 in Table 7]

MISSOURI RIVER,
Kansas City, Mo.

Records 1881-1951
Max. 1951, 1903, 1908, 1943, 1915
D. A. 489,200 sq. mi.
M. F. 193,500 cfs.
$C_v$ = 0.44　　　$C_s$ = 2.00
F = 5.4　　　　　R = 2.4
Hist. 1844: 625,000 cfs = 3.2 M.F.
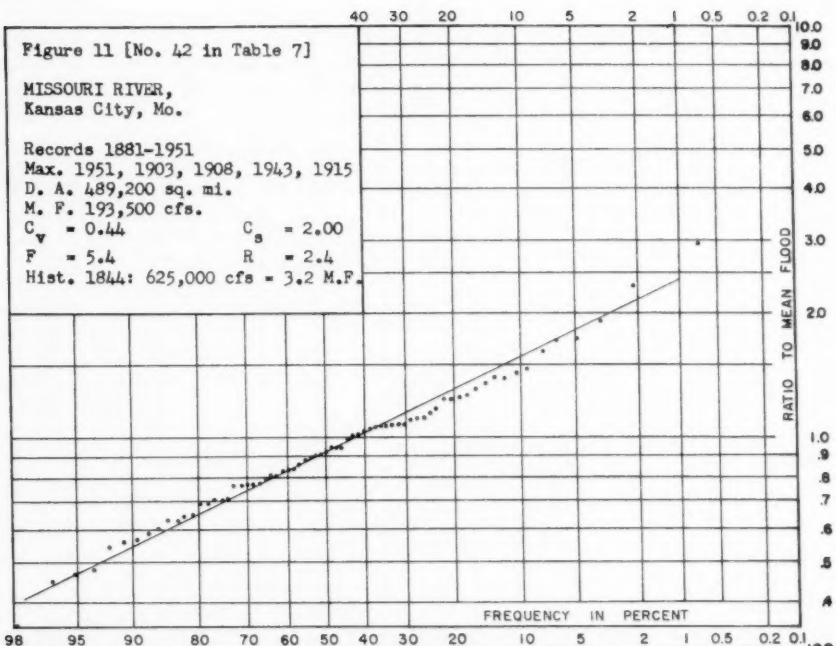


Figure 12 [No. 52 in Table 7]

KANSAS RIVER,
Topeka, Kans.

Records 1905-1951
Max. 1951, 1935, 1908, 1941, 1943
D. A. 56,700 sq. mi.
M. F. 60,700 cfs.
$C_v$ = 0.64　　　$C_s$ = 1.24
F = 8.2　　　　　R = 3.5
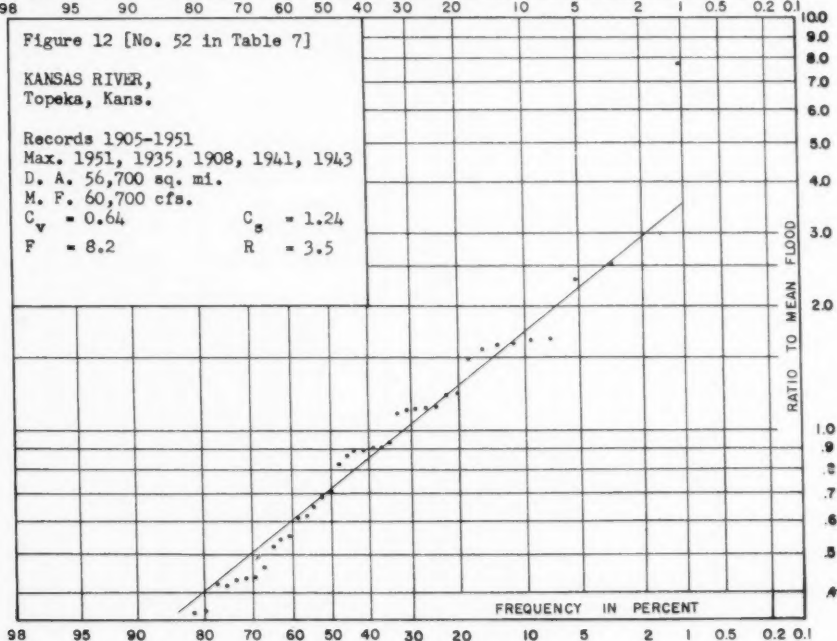
Figure 13 [No. 58 in Table 7]

OHIO RIVER,
Metropolis, Ill.

Records 1875-1949
Max. 1937, 1884, 1913, 1883, 1897
D. A. 203,000 sq. mi.
M. F. 882,000 cfs.
$C_v$ = 0.26        $C_s$ = 0.79
F    = 50.1        R    = 1.7
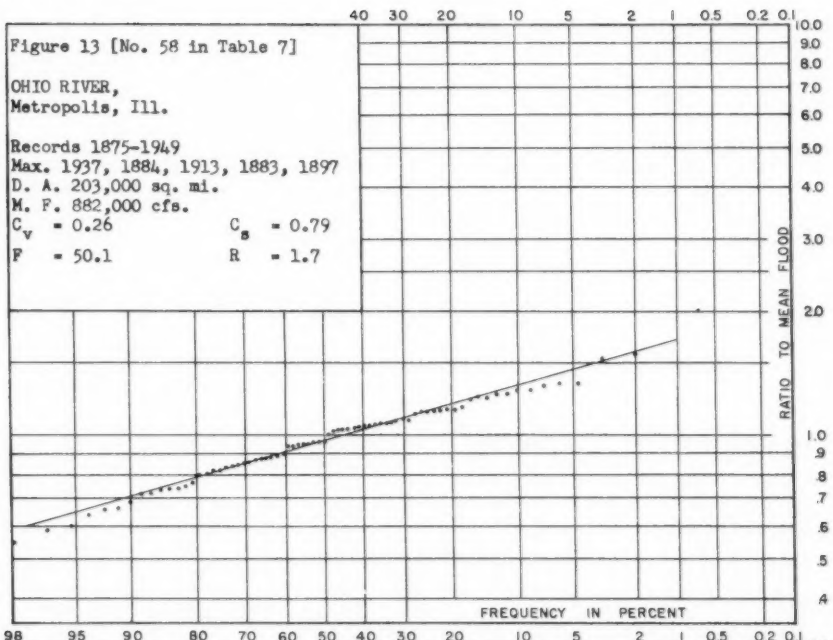


Figure 14 [No. 59 in Table 7]

KANAWHA RIVER,
Kanawha Falls, W. Va.

Records 1877-1949
Max. 1878, 1940, 1901, 1916, 1899
D. A. 8,400 sq. mi.
M. F. 125,600 cfs.
$C_v$ = 0.38        $C_s$ = 0.90
F    = 91.0        R    = 2.2
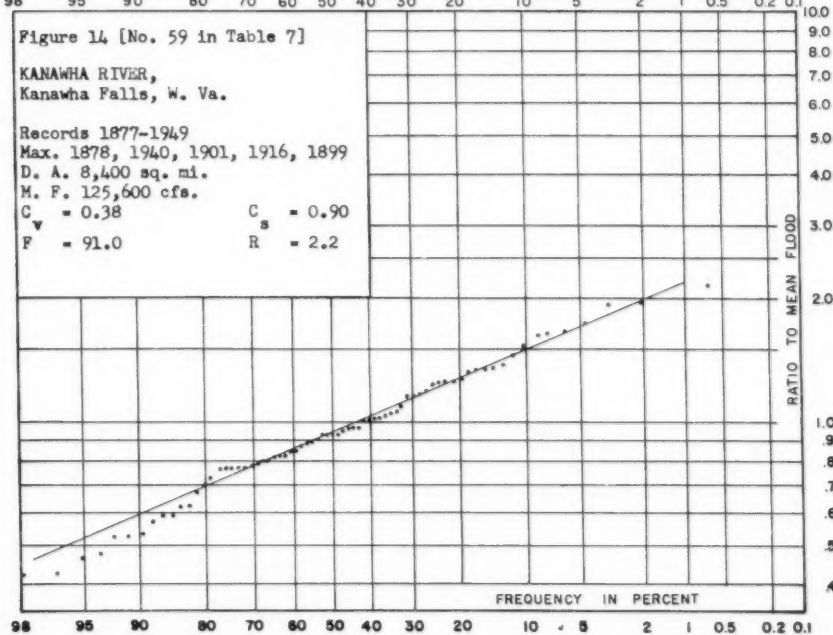
Figure 15 [No. 61 in Table 7]

CUMBERLAND RIVER,
Nashville, Tenn.

Records 1838-1949
Max. 1927, 1882, 1848, 1937, 1862
D. A. 12,900 sq. mi.
M. F. 122,200 cfs.
$C_v = 0.23$    $C_s = 0.40$
F   = 63.0    R   = 1.7
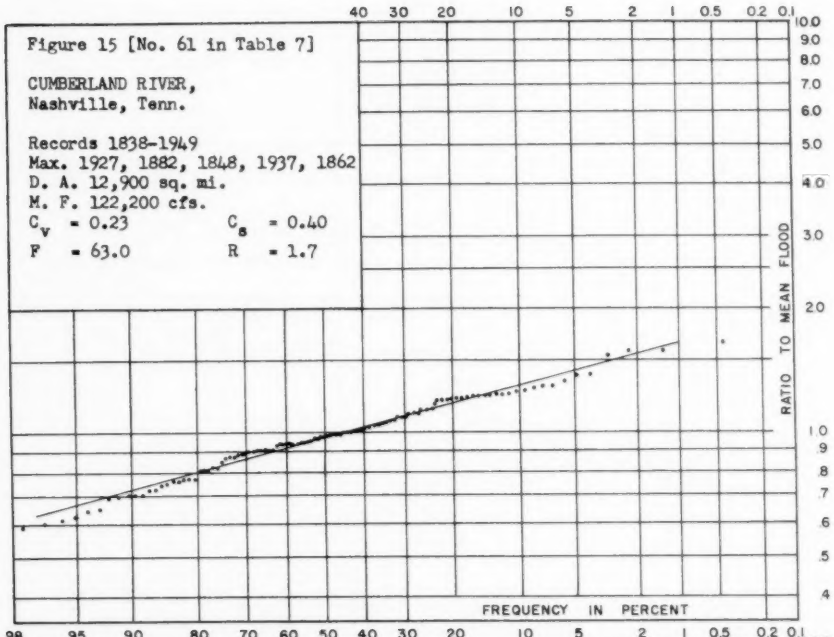
Figure 16 [No. 65 in Table 7]

TENNESSEE RIVER,
Florence, Ala.

Records 1874-1949
Max. 1897, 1882, 1875, 1948, 1886
D. A. 30,800 sq. mi.
M. F. 251,000 cfs.
$C_v = 0.28$    $C_s = 0.25$
F   = 64.4    R   = 1.7
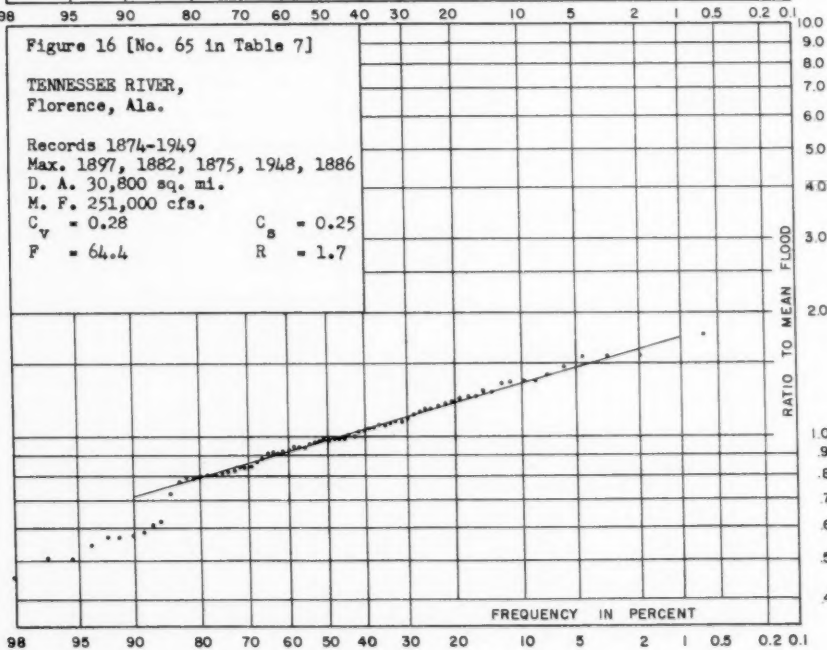
Figure 17 [No. 67 in Table 7]

ARKANSAS RIVER,
Canon City, Colo.

Records 1895-1950
Max. 1921, 1941, 1937, 1944, 1942
D. A. 3,100 sq. mi.
M. F. 4,800 cfs.
$C_v$ = 0.60           $C_s$ = 2.71
F = 7.7           R = 2.8
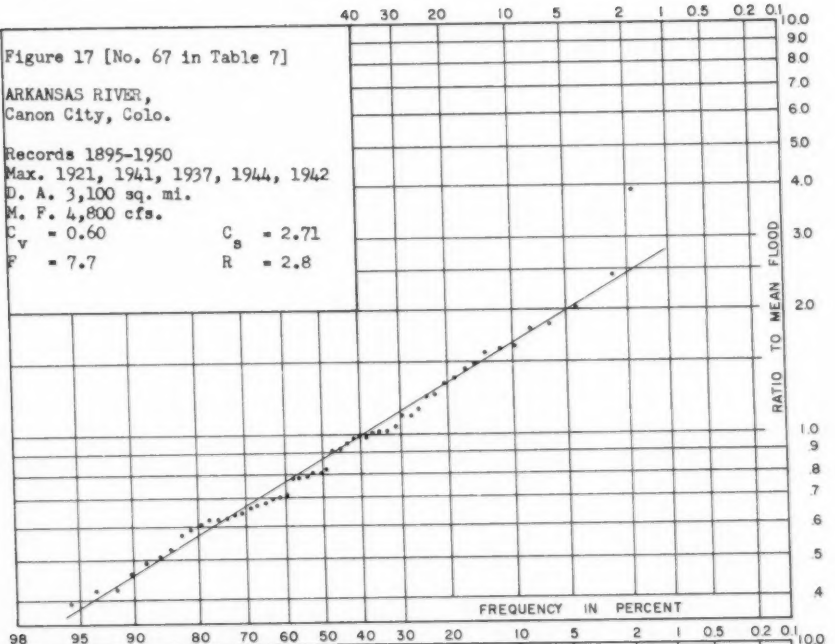
Figure 18 [No. 70 in Table 7]

ARKANSAS RIVER,
Holly, Colo.

Records 1913-1950
Max. 1921, 1942, 1927, 1925, 1936
D. A. 25,100 sq. mi.
M. F. 10,900 cfs.
$C_v$ = 0.90           $C_s$ = 1.40
F = 2.9           R = 4.5
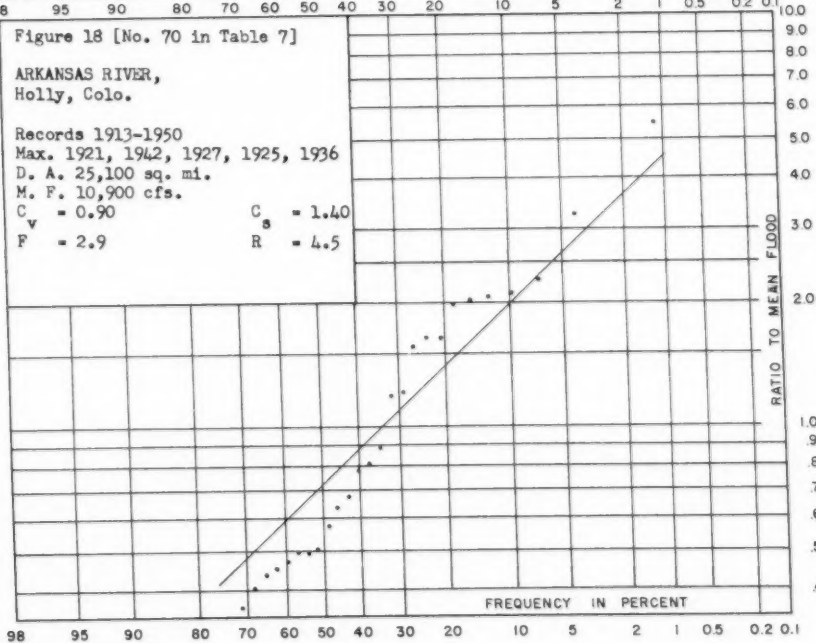
Figure 19 [No. 72 in Table 7]

ARKANSAS RIVER,
Little Rock, Ark.

Records 1872-1951
Max. 1927, 1892, 1943, 1877, 1884
D. A. 157,900 sq. mi.
M. F. 291,300 cfs.
$C_v$ = 0.43　　　　$C_s$ = 1.32
F = 20.2　　　　R = 2.3
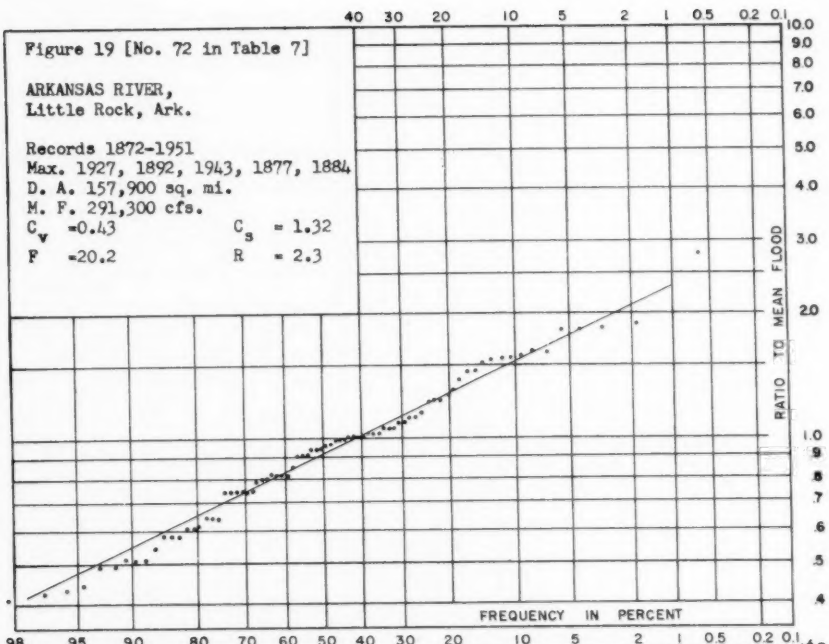


Figure 20 [No. 76 in Table 7]

MISSISSIPPI RIVER,
Vicksburg, Miss.

Records 1872-1951
Max. 1937, 1945, 1950, 1922, 1927
D. A. 1,144,500 sq. mi.
M. F. 1,271,200 cfs.
$C_v$ = 0.23　　　　$C_s$ = 0.68
F = 18.1　　　　R = 1.7
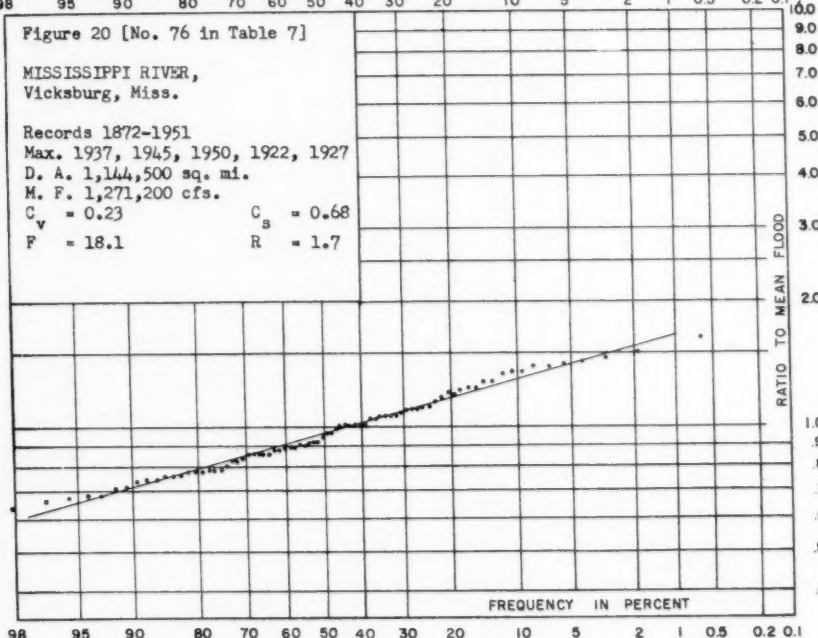
Figure 21 [No. 77 in Table 7]

NIAGARA RIVER,
Buffalo, N. Y.

Records 1905-1950
Max. 1929, 1947, 1943, 1913, 1917
D. A. 263,000 sq. mi.
M. F. 208,600 cfs.
$C_v$ = 0.09          $C_s$ = 0.72
F  = 9.6              R  = 1.2

FREQUENCY  IN  PERCENT

RATIO  TO  MEAN  FLOOD
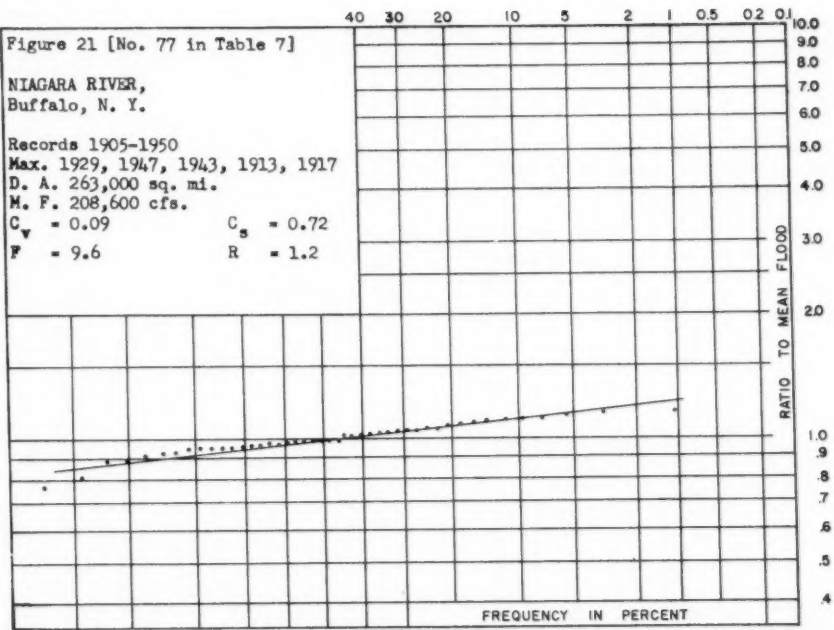


Figure 22 [No. 81B in Table 7]

CONNECTICUT RIVER,
Hartford, Conn.

Records 1843 - 1949
Max. 1936, 1938, 1854, 1928, 1862
D. A. 10,500 sq. mi.
M. F. 112,600 cfs
$C_v$ = 0.35          $C_s$ = 1.38
F  = 68.2             R  = 2.0

FREQUENCY  IN  PERCENT

RATIO  TO  MEAN  FLOOD

Figure 23 [No. 90B in Table 7]

COLUMBIA RIVER,
The Dalles, Oreg.

Records 1858-1949
Max. 1894, 1876, 1948, 1862, 1880
D. A. 237,000 sq. mi.
M. F. 609,900 cfs.
$C_v$ =0.29        $C_s$ = 0.38
$F$ =30.5          $R$ = 1.8

Figure 24 [No. 100 in Table 7]

FRASER RIVER,
Hope, B. C.

Records 1912-1950
Max. 1948, 1950, 1921, 1920, 1936
D. A. 85,600 sq. mi.
M. F. 307,500 cfs.
$C_v$ = 0.22        $C_s$ = 1.14
$F$ = 34.0          $R$ = 1.5
Hist. 1894: 618,000 cfs = 2.0 M.F.
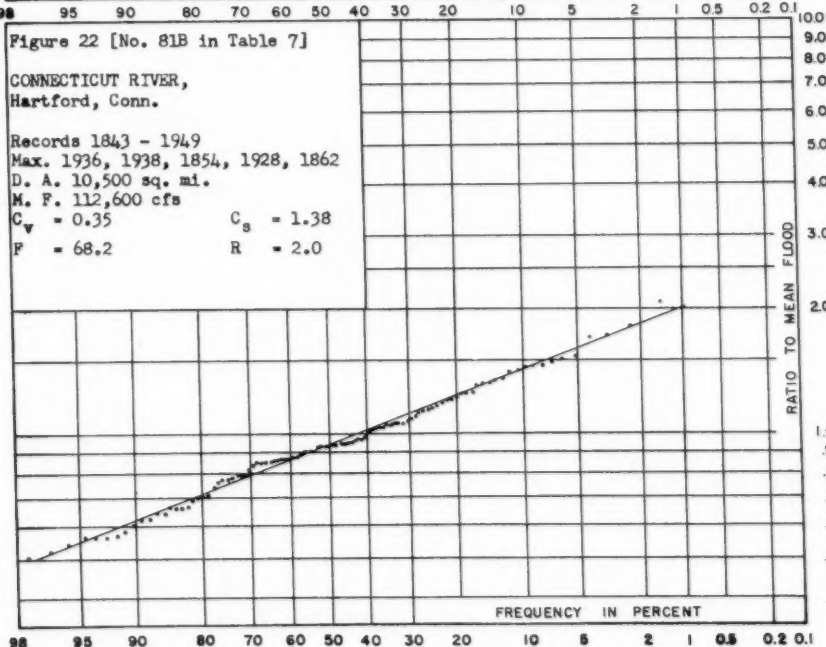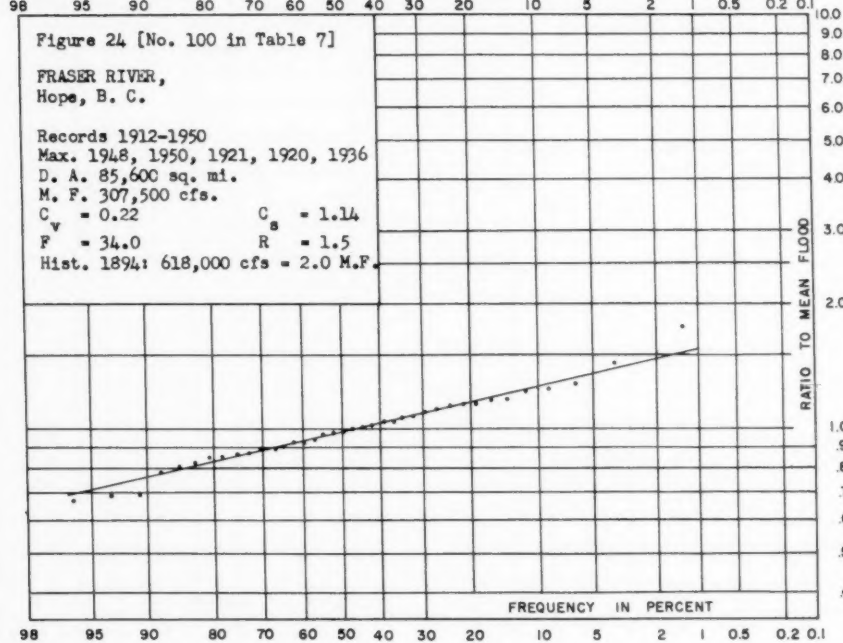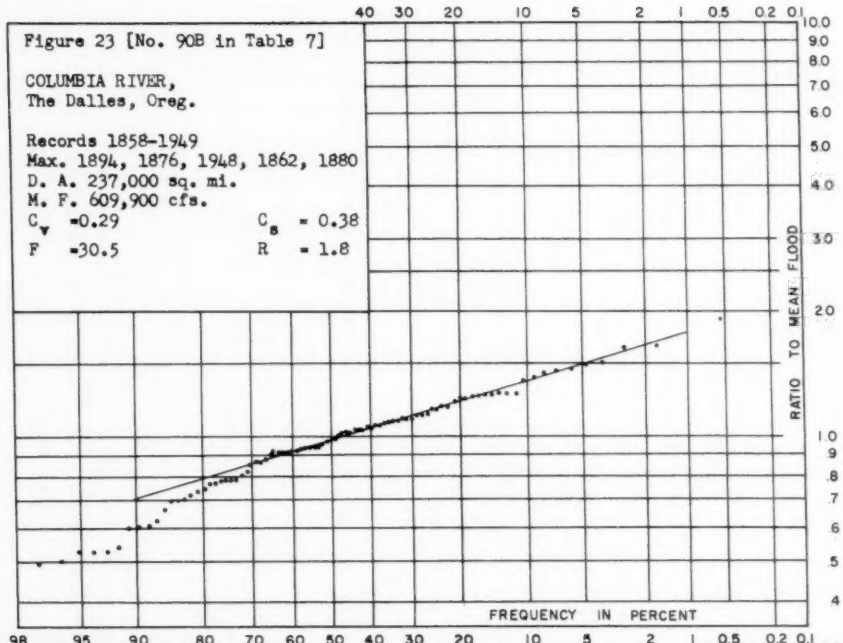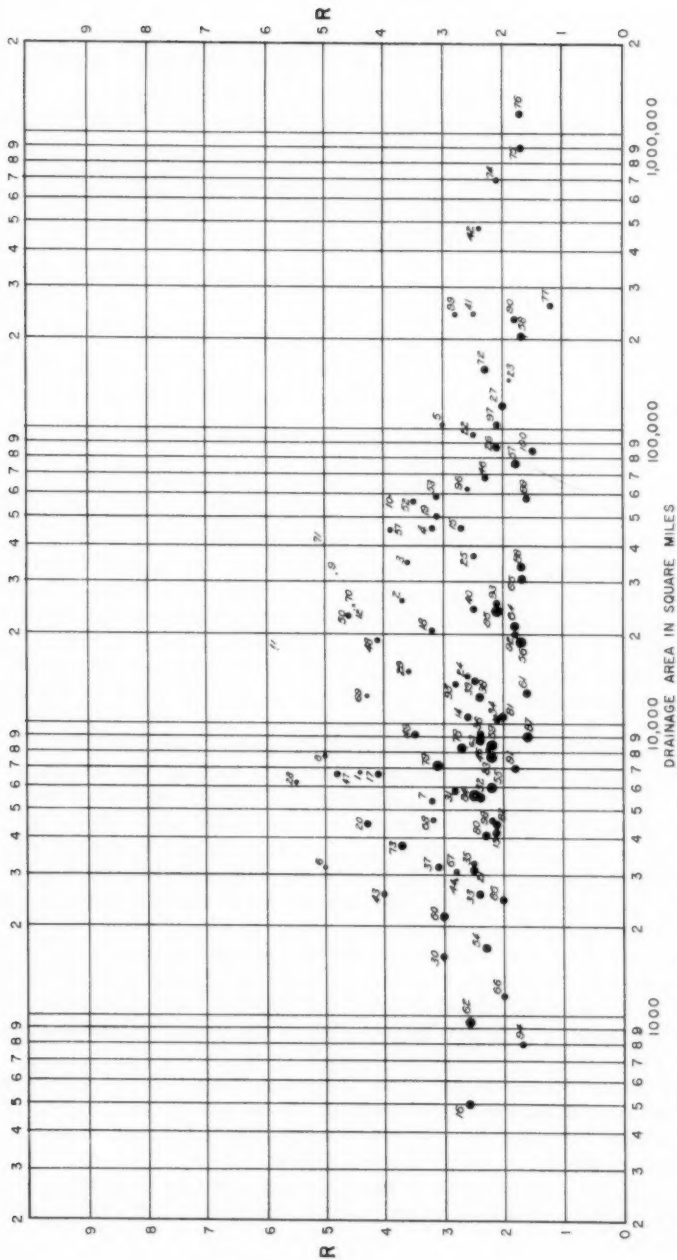
FIGURE 25 : RELATIONSHIP
BETWEEN D.A., R AND F.
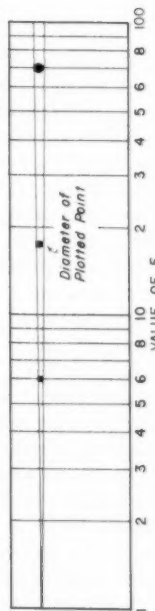
plotted. The size of the drainage area is plotted on the horizontal scale; the magnitude of F is expressed in the size of the plotted points; and the value of R is plotted on the vertical scale. It can be seen that R tends to decrease with an increase in drainage area and an increase in flood coefficient.

However, there is still an appreciable amount of scatter left in the diagram. There are several possible reasons for this.

1. It is likely that not all variable factors that affect the inclination of a frequency line are properly expressed in D.A. and F.
2. It is likely that a certain amount of scatter is due to non-representative records.
3. A certain amount of error is involved in drawing the straight frequency line.
4. It could be that a straight line is not the proper representation of the true frequency curve.

In view of the considerable amount of work involved, a further analysis has not been pursued.


### Possible Application

If an engineer is faced with the problem of drawing a frequency curve of maximum annual flood flows for a river station, and if he has decided that the frequency curve can be drawn as a straight line, and if he has access to flood frequency data at other places in the drainage basin or in similar drainage basins, he would be well advised to study all these available flood frequency data. There is a good possibility that he will find definite trends in the inclication of the frequency lines under consideration, in which case he could use these trends as guidance for his estimates.

For instance, suppose that a frequency curve has to be drawn for the annual peak flows at Saskatoon, Saskatchewan (Figure 25, Number 19) and let it be assumed that records were only available from 1932-1951, instead of the actual available period of 1911-51. It can be seen from Figure 27, where the twenty year period is plotted, that without further information the frequency line would probably be drawn as shown by the dashed line, corresponding to an R value of 2.5. However, in view of the short period of record, some further guidance in drawing the line would be desirable. In order to provide this guidance, all available F, R and D.A. values for stations in the Nelson River Drainage Basin have been plotted in Figure 28. Moreover, lines of equal F values have been estimated and drawn in the same figure. These lines are based not only on the points in Figure 28, but also on the general trend of F values in Figure 25.

From an appraisal of Figure 28 and using the computed F value of 8.4 from Figure 27 the R value of Saskatoon is selected at 3.1 and the frequency line in Figure 27 is corrected accordingly. From a comparison of Figures 26 and 27, it can be seen that the corrected frequency line in Figure 27 is now in close agreement with the originally established line in Figure 26. It should be noted that a discrepancy remains in the value of the mean flood, due to the short period of record.

Figure 26 [No. 19 in Table 7]

SOUTH SASKATCHEWAN RIVER,
Saskatoon, Sask.

Records 1911-1951
Max. 1923, 1915, 1932, 1929, 1948
D.A. 50,900 sq. mi.
M.F. 54,000 cfs.
$C_v$ = 0.50          $C_s$ = 1.28

F = 9.3          R = 3.1

FREQUENCY IN PERCENT

RATIO TO MEAN FLOOD
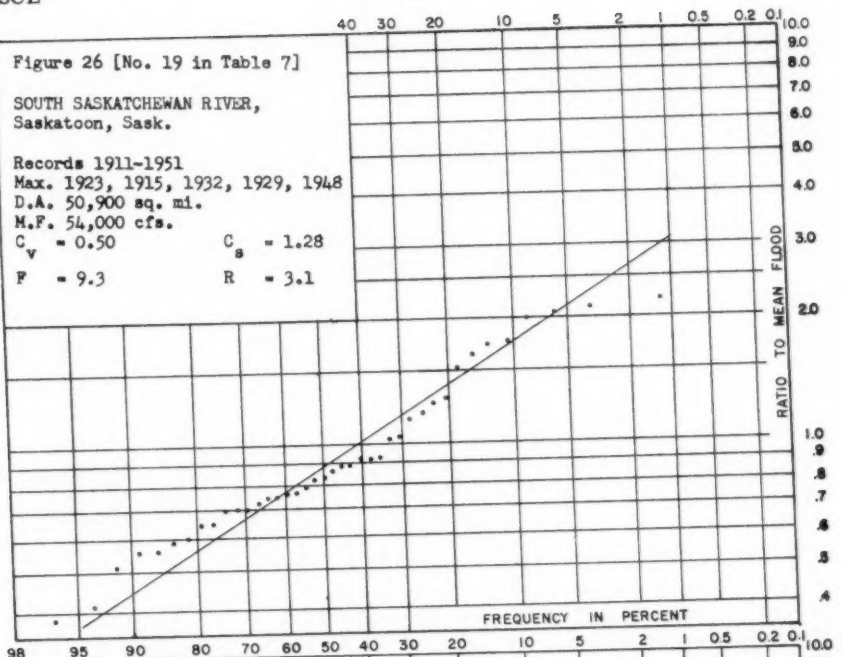
Figure 27

SOUTH SASKATCHEWAN RIVER,
Saskatoon, Sask.

Records 1932-1951
Max. 1932, 1948, 1947, 1942, 1951
D. A. 50,900 sq. mi.
M. F. 48,400 cfs.

F = 8.4          R = 3.1

FREQUENCY IN PERCENT

RATIO TO MEAN FLOOD
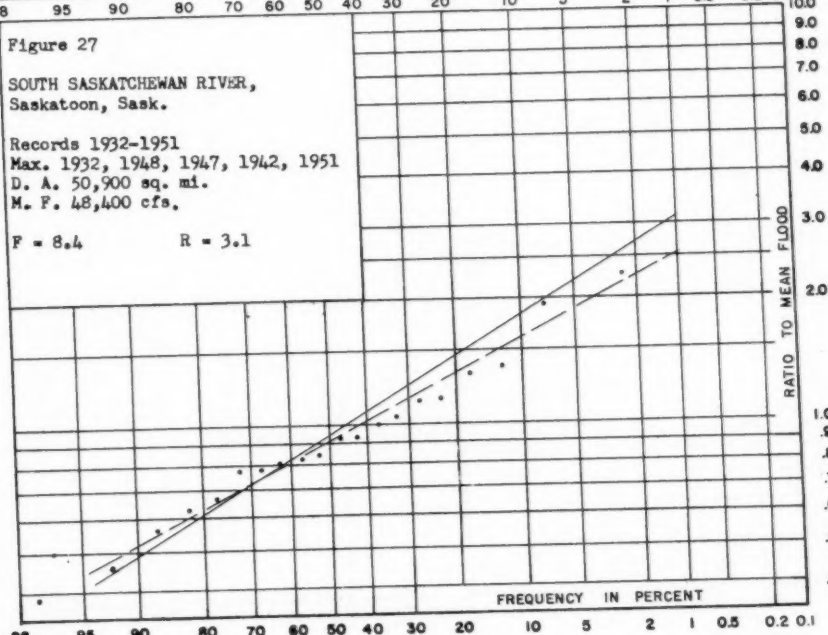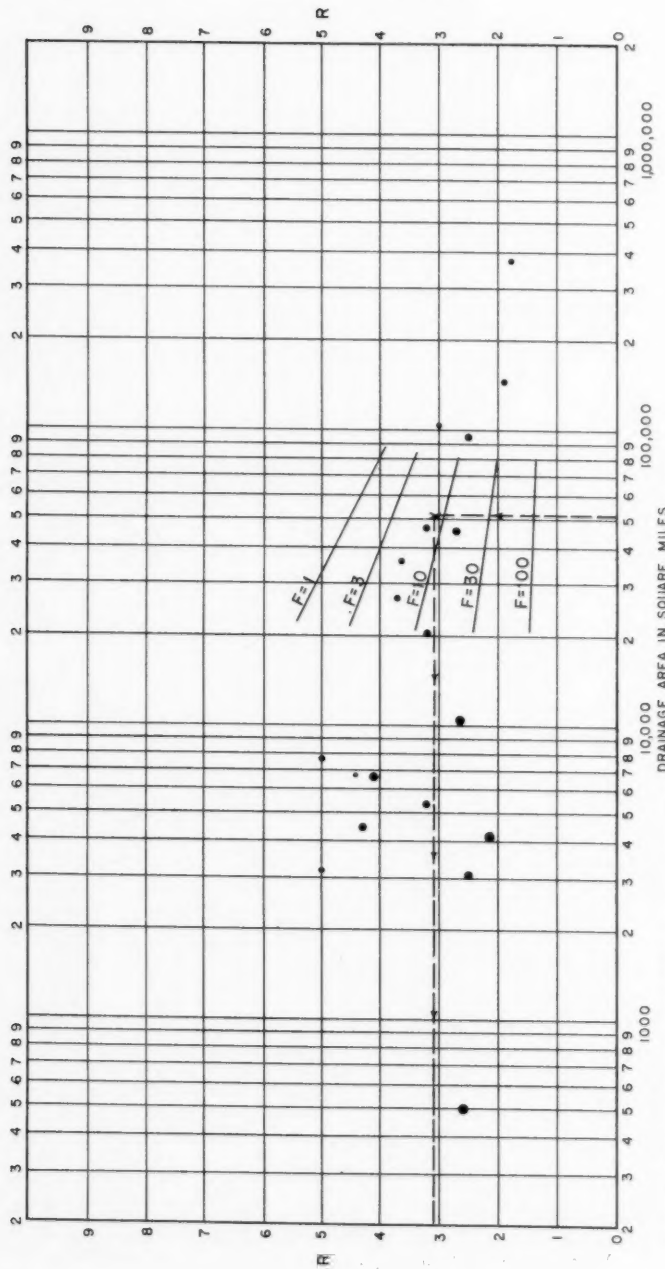
FIGURE 28 : D. A., R AND F.
NELSON RIVER DRAINAGE BASIN
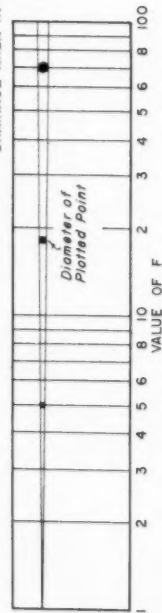
## CONCLUSIONS

1. When maximum annual flood flows, expressed in ratio to the mean, are plotted on logarithmic probability paper, they tend to fall on a straight line.

2. The inclination of the frequency line tends to decrease with an increase of drainage area, all other drainage basin characteristics remaining the same.

3. The inclination of the frequency line tends to decrease with an increase of the flood coefficient F (equal to the mean of the annual peak flows in cfs, divided by the drainage area in square miles, to the 0.8 power), all other drainage basin characteristics remaining the same.

4. The personal judgment that is involved in drawing or extending the frequency line of one particular river station can be improved by appraising frequency lines in the same or in similar drainage basins.
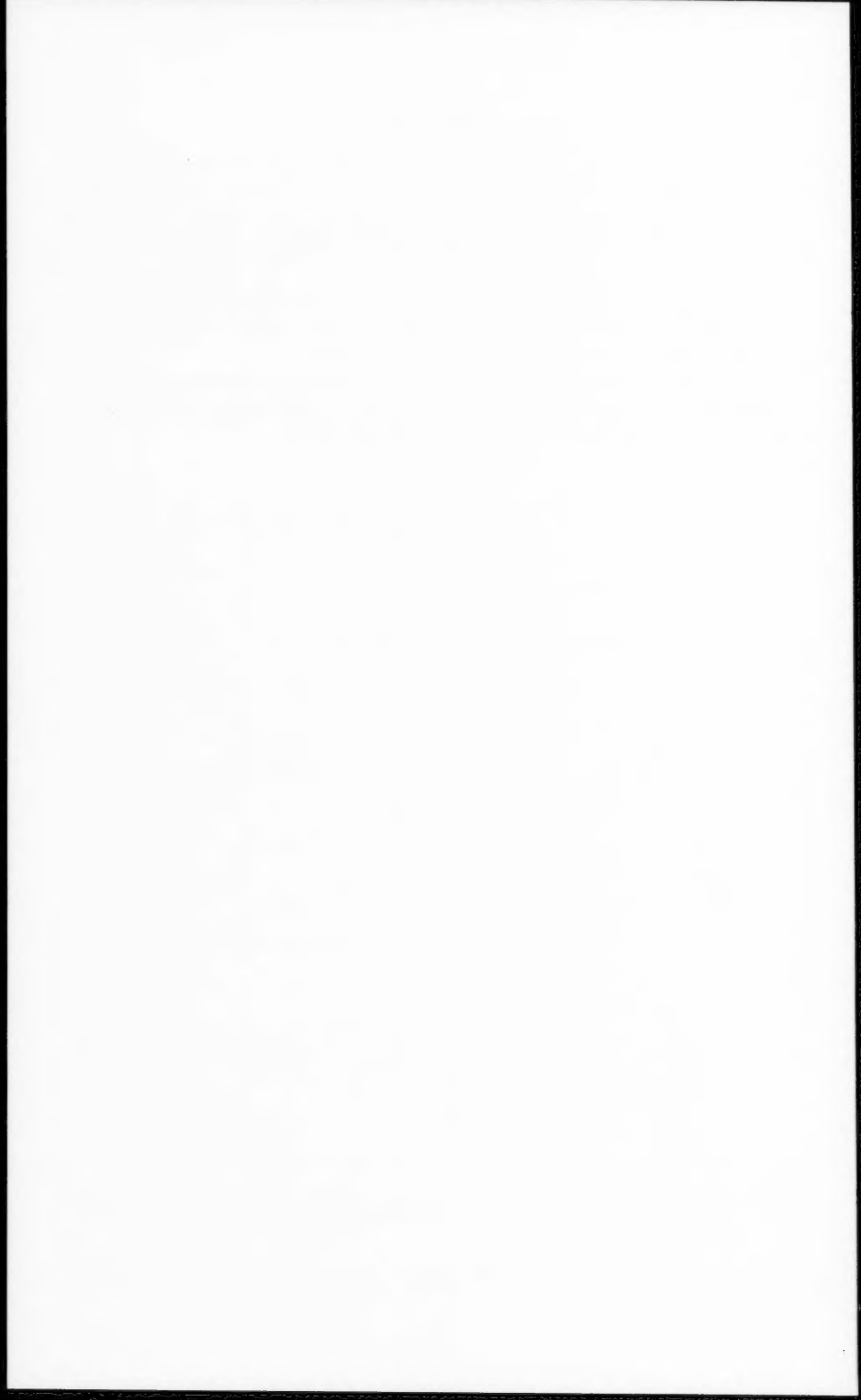
Journal of the
# HYDRAULICS DIVISION
Proceedings of the American Society of Civil Engineers

THE HYDRAULIC DESIGN OF STILLING BASINS:
HYDRAULIC JUMPS ON A HORIZONTAL APRON (BASIN I)

J. N. Bradley[1] M. ASCE and A. J. Peterka[2] M. ASCE
(Proc. Paper 1401)

### FOREWORD

This is one of a group of six papers on the hydraulic design of stilling basins and their associated appurtenances. Although original data from hydraulic models are presented in tabular form, the papers emphasize practical design procedures. Basin sizes and dimensions are given in easy-to-use dimensionless forms so that dependable stilling basins may be designed without the need for exceptional judgment or extensive experience. Sample problems are included.

The "Introduction" and "Experimental Equipment" are included in Paper 1401 but apply to all papers in this group. Paper 1401 is an academic study of the hydraulic jump on a flat floor. Useful information is presented concerning energy losses, applicability of the hydraulic jump formula, length of jump, and a new classification of the various types of jumps.

Paper 1402 covers the design of a short hydraulic jump stilling basin having an end sill and chute blocks. Paper 1403 describes a shorter stilling basin which utilizes baffle piers. In both papers information is given to determine the critical dimensions of the stilling basin, the tail water range, and the water surface profile in the basin.

Paper 1404 describes a special type of hydraulic jump basin for use when the Froude number of the incoming flow is low, and the jump produces waves in the downstream channel. An alternate design and two types of wave suppressors are also developed.

Paper 1405 describes the design of a stilling basin having a sloping apron. The extra tail water depth required and the merits of a sloping apron are evaluated, as is the basin length for a range of apron slopes.

Paper 1406 develops the design of impact basins for discharges up to 340 second feet and incoming velocities up to 30 feet per second. No tail water is required. The bibliography in this paper applies to all papers in this group.

1. Hydr. Engr., U. S. Bureau of Public Roads, Washington, D. C., formerly of U. S. Bureau of Reclamation, Denver, Colo.
2. Hydr. Engr., U. S. Bureau of Reclamation, Denver, Colo.

## ABSTRACT

A study of the hydraulic jump from a practical viewpoint is presented and the results obtained are correlated with those of others. Included in the study are the applicability of the hydraulic jump formula, the length of jump over the entire practical range, and a new classification for the various forms of the hydraulic jump.

---

## INTRODUCTION

Although hundreds of stilling basins and energy dissipating devices have been designed in conjunction with spillways, outlet works, and canal structures, it is still necessary in many cases to make model studies of individual structures to be certain that these will operate as anticipated. The reason for these repetitive tests, in many cases, is that a factor of uncertainty exists, which in retrospect is related to an incomplete understanding of the overall characteristics of energy dissipators.

Many laboratory studies have been made on individual structures over a period of years, by different personnel, for different groups of designers, with each structure having different allowable design limitations. Attempts to analyze the assembled data resulted in sketchy and, at times, inconsistent results having only vague connecting links. Extensive library research into the works of others revealed the fact that the necessary correlation factors are non-existent.

To fill the need for up-to-date hydraulic design information on stilling basins and energy dissipators, a research program on this general subject was begun with a rather academic study of the hydraulic jump, observing all phases as it occurs in open channel flow. With a broader understanding of this phenomenon it was then possible to proceed to the more practical aspects of stilling basin design.

Existing knowledge, including laboratory and field tests collected from Bureau of Reclamation records and experiences over a 23-year period, was used to establish a direct approach to the practical problems encountered in hydraulic design. Hundreds of tests were also performed on both available and specially constructed equipment to obtain a fuller understanding of the data at hand and to close the many loopholes. Testing and analysis were synchronized to establish valid curves in critical regimes, providing sufficient understanding of energy dissipators in their many forms to establish workable design criteria. Since all the test points were obtained by the same personnel, using standards established before testing began, and since results and conclusions were evaluated from the same datum, the data presented are believed to be consistent and reliable.

These papers, therefore, are the result of an integrated attempt to generalize the design of stilling basins, energy dissipators, and associated appurtenances. In most instances design rules and procedures are clearly stated in simple terms with limits fixed in a definite range. In other cases, however, it is necessary to state procedures and limits in broader terms, making it necessary to carefully read the accompanying text.

Proper use of the material in these papers will eliminate the need for hydraulic model tests on many individual structures, particularly the smaller

ones.  Structures obtained by following the recommendations in this report will be conservative in that they will contain a desirable factor of safety. However, to further reduce structure sizes, to account for unsymmetrical conditions of approach or getaway, or to evaluate other unusual conditions not covered in this discussion, model studies will still prove beneficial.

## Experimental Equipment

Five test flumes were used at one time or another to obtain the experimental data required on the hydraulic jump basins, Flumes A and B, Figure 1; Flumes C and D, Figure 2; and Flume F, Figure 3.  The arrangement shown as Flume E, Figure 3, actually occupied a portion of Flume D during one stage of the testing, but it will be designated as a separate flume for ease of reference.  Each flume served a useful purpose either in verifying similarity or extending the range of the experiments.  Flumes A, B, C, D, and E contained overflow sections so that the jet entered the stilling basin at an angle to the horizontal.  The degree of the angle varied in each case.  In Flume F, the entering jet was horizontal since it emerged from under a vertical slide gate.

The experiments were started in an existing model of a flat-chute spillway, Figure 1A, having a small discharge and low velocity.  This was not an ideal piece of equipment for general experiments as the training walls on the chute were diverging.  The rapid expansion caused the distribution of flow entering the stilling basin to shift with each change in discharge; nonetheless, this piece of equipment served a purpose in that it aided in getting the research program underway.

Tests were then continued in a glass-sided laboratory flume 2 feet wide and 40 feet long in which an overflow section was installed, Flume B, Figure 1. The crest of the overflow section was 5.5 feet above the floor, while the downstream face was on a slope of 0.7:1.  The capacity was about 10 cfs.

Later, the work was carried on at the base of a chute 18 inches wide having a slope of 2 horizontal to 1 vertical and a drop of approximately 10 feet, Flume C, Figure 2.  The stilling basin had a glass wall on one side.  The discharge capacity was 5 cfs.

The largest scale experiments were made on a glass-sided laboratory flume 4 feet wide and 80 feet long, in which an overfall crest with a slope of 0.8:1 was installed, Flume D, Figure 2.  The drop from headwater to tail water in this case was approximately 12 feet, and the maximum discharge was 28 cfs.

The downstream end of the above flume was also utilized for testing small overflow sections 0.5 to 1.5 feet in height.  The maximum discharge used was 10 cfs.  As stated above, this piece of equipment will be designated as Flume E, and is shown on Figure 3.

The sixth piece of equipment was a tilting flume which could be adjusted for slopes up to 12°, Flume F, Figure 3.  This flume was 1 foot wide by 20 feet long; the head available was 2.5 feet, and the flow was controlled by a slide gate.  The discharge capacity was about 3 cfs.

Each flume contained a head gage, a tail gage, a scale for measuring the length of the jump, a point gage for measuring the average depth of flow entering the jump, and a means of regulating the tail water depth.  The discharge in all cases was measured through the laboratory venturi meters or portable

FIGURE 1
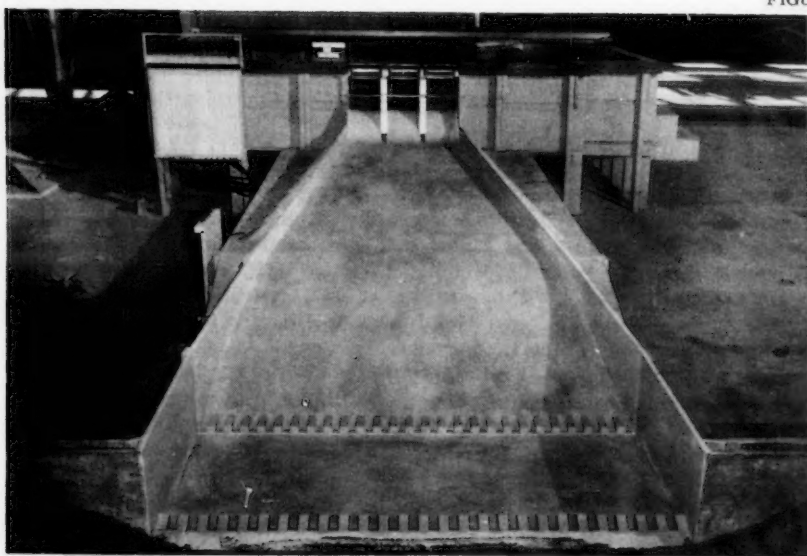


TEST FLUME A
Width of basin 5 feet, drop 3 feet, discharge 6 cfs
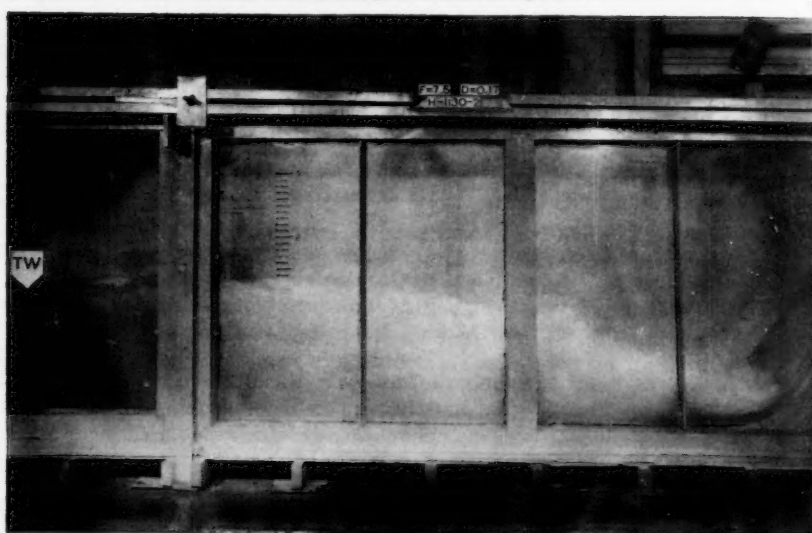


TEST FLUME B
Width 2 feet, drop 5.5 feet, discharge 10 cfs
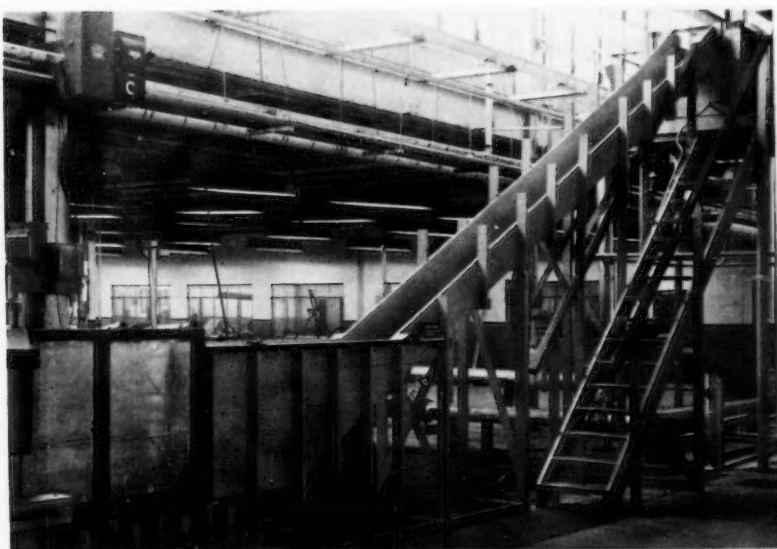
TEST FLUME C
Width 1.5 feet, drop 10 feet, discharge 5 cfs, slope 2:1
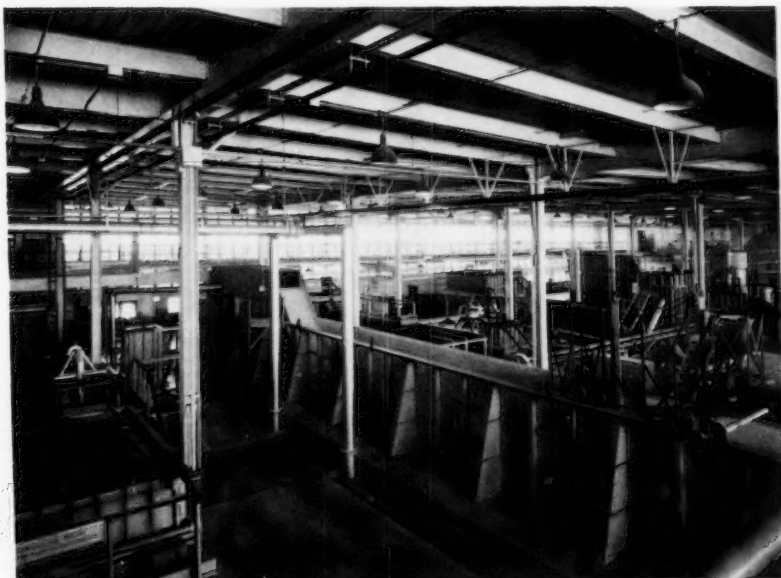


TEST FLUME D
Width 4 feet, drop 12 feet, discharge 28 cfs, slope 0.8:1

FIGURE 3



TEST FLUME (E)
Width 4 feet, Drop 0.5-1.5 feet, Discharge 10 cfs
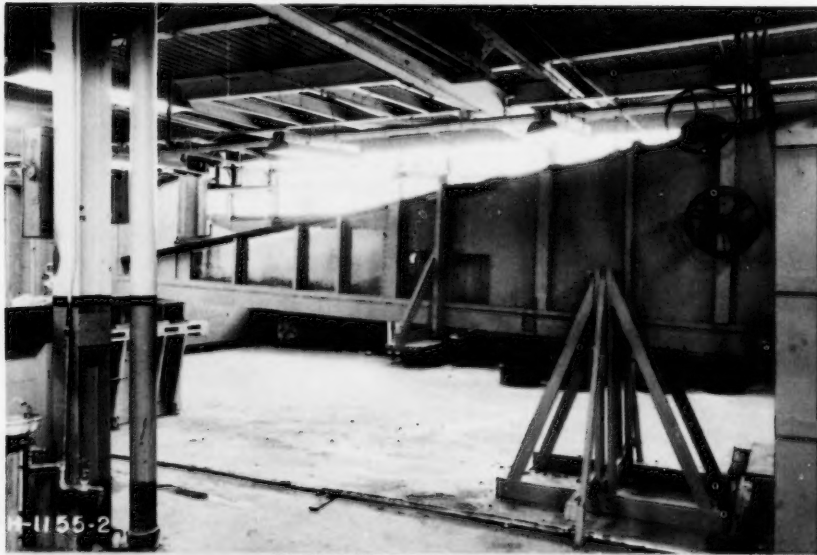


TEST FLUME (F)
Adjustable tilting type, maximum slope 12 degrees,
width one foot, discharge 5 cfs

venturi-orifice meters. The tail water depth was measured by a point gage
operating in a stilling well. The tail water depth was regulated by an adjust-
able weir at the end of each flume.

Other test setups were used to develop the impact basin, wave suppressor,
etc. These are described in the appropriate sections.

## General Investigation of the Hydraulic Jump on Horizontal Apron (Basin I)

### Introduction

A tremendous amount of experimental, as well as theoretical, work has
been performed in connection with the hydraulic jump on a horizontal apron.
To mention a few of the experimenters who contributed basic information,
there are: Bahkmeteff and Matske,[1] [9] Safranez,[3] Woycicki,[4] Chertonosov,[10]
Einwachter,[11] Elms,[12] Hinds,[14] Forcheimer,[21] Kennison,[22] Kozeny,[23]
Rehbock,[24] Schoklitsch,[25] Woodward,[26] and others. There is probably no
phase of hydraulics that has received more attention, yet, from a practical
viewpoint, there is still much to be learned.

The first phase of the present study (Section 1) was academic in nature
consisting of observing the hydraulic jump in its various forms and correlat-
ing the results with those of others; the primary purpose being to become bet-
ter acquainted with the overall jump phenomenon. The objectives were: (1) to
determine the applicability of the hydraulic jump formula for the entire range
of conditions experienced in design; (2) to determine the length of the jump
over the entire practical range and to correlate the findings with results of
other experimenters where possible; and (3) observe, catalog, and evaluate
the various forms of the jump.

### Current Experimentation

To satisfactorily observe the hydraulic jump throughout its entire range
required tests in all six test flumes. This involved about 125 tests, Table 1,
for discharges of 1 to 28 cfs. The number of flumes used enhanced the value
of the results in that it was possible to observe the degree of similitude ob-
tained for the various sizes of jumps. Greatest reliance was naturally placed
on the results from the larger flumes, since the action in small jumps is too
rapid for the eye to follow. Friction and viscosity also become a measurable
factor. This was demonstrated by the fact that the length of jump obtained
from the two smaller flumes, A and F, was consistently shorter than that ob-
served for the larger flumes. Out-of-scale frictional resistance on the floor
and side walls produced a short jump. As testing advanced and this deficiency
became better understood, some allowance was made for this effect in the
observations.

### Experimental Results

Definitions of the symbols used in connection with the hydraulic jump on a
horizontal floor are shown on Figure 4. The procedure followed in each test
of this series was to first establish a flow. The tail water depth was then
gradually increased until the front of the jump moved upstream to Section 1,
indicated on Figure 4. The tail water depth was then measured, the length of
the jump recorded, and the depth of flow entering the jump, $D_1$, was obtained
by averaging a generous number of point gage measurements taken

## Table 1

### NATURAL STILLING BASIN WITH HORIZONTAL FLOOR
### (Stilling Basin I)

| (1) S = tan Slope of flume of floor | (2) | (3) Q cfs | (4) W = Width of stilling basin ft | (5) q per ft of W | (6) :W = $D_2$ ft | (7) $V_1$ ft/sec | (8) $D_1$ ft | (9) $\frac{D_2}{D_1}$ | (10) $F_1 = \frac{V_1}{\sqrt{gD_1}}$ | (11) L Length of Jump ft | (12) $\frac{L}{D_2}$ | (13) $\frac{L}{D_1}$ | (14) $E_1 = d_1 + \frac{V_1^2}{2g}$ ft | (15) $E_2 = d_2 + \frac{V_2^2}{2g}$ ft | (16) $E_L = E_1 - E_2$ ft | (17) $\frac{E_L}{D_1}$ | (18) $\frac{E_L}{E_1}$ % | (19) Gate opening ft |
|---|---|---|---|---|---|---|---|---|---|---|---|---|---|---|---|---|---|---|
| A | 0 | 3.000 | 4.915 | 0.610 | 0.564 | 8.47 | 0.072 | 7.83 | 5.56 | 3.0 | 5.32 | 42 | 1.187 | 0.582 | 0.605 | 8.40 | 51.0 | |
| | | 3.500 | | 0.712 | 0.612 | 8.79 | .081 | 7.56 | 5.44 | 3.3 | 5.39 | 41 | 1.282 | 0.633 | 0.649 | 8.01 | 50.6 | |
| | | 4.000 | | 0.814 | 0.651 | 8.95 | .091 | 7.15 | 5.23 | 3.5 | 5.38 | 38 | 1.336 | 0.675 | 0.661 | 7.26 | 49.5 | |
| | | 4.500 | | 0.916 | 0.694 | 8.98 | .102 | 6.80 | 4.96 | 3.8 | 5.48 | 37 | 1.354 | 0.721 | 0.633 | 6.21 | 46.8 | |
| | | 5.000 | | 1.017 | 0.730 | 9.08 | .112 | 6.52 | 4.78 | 4.1 | 5.62 | 37 | 1.392 | 0.760 | 0.632 | 5.64 | 45.4 | |
| B | 0 | 4.300 | 2.000 | 2.150 | 1.480 | 17.48 | .123 | 12.03 | 8.78 | 9.0 | 6.08 | 73 | 4.868 | 1.513 | 3.355 | 27.28 | 68.9 | |
| | | 5.000 | | 2.500 | 1.600 | 17.48 | .143 | 11.19 | 8.15 | 10.1 | 6.31 | 71 | 4.888 | 1.638 | 3.250 | 22.73 | 66.5 | |
| | | 3.000 | | 1.500 | 1.235 | 17.24 | .087 | 14.20 | 10.30 | 7.5 | 6.07 | 66 | 4.702 | 1.259 | 3.443 | 39.57 | 73.2 | |
| | | 6.000 | | 3.000 | 1.754 | 17.54 | .171 | 10.26 | 7.47 | 10.6 | 6.04 | 62 | 4.948 | 1.799 | 3.149 | 18.42 | 63.6 | |
| | | 7.000 | | 3.500 | 1.908 | 17.59 | .199 | 9.59 | 6.95 | 11.5 | 6.03 | 58 | 5.003 | 1.960 | 3.043 | 15.29 | 60.8 | |
| | | 8.000 | | 4.000 | 2.016 | 17.47 | .229 | 8.80 | 6.43 | 12.3 | 6.10 | 54 | 4.968 | 2.077 | 2.891 | 12.62 | 58.2 | |
| | | 7.000 | | 3.500 | 1.900 | 17.41 | .201 | 9.45 | 6.84 | 11.5 | 6.05 | 57 | 4.908 | 1.953 | 2.955 | 14.70 | 60.2 | |
| | | 3.110 | | 1.550 | 1.240 | 17.61 | .088 | 14.09 | 10.46 | 7.9 | 6.37 | 90 | 4.903 | 1.264 | 3.639 | 41.35 | 74.2 | |
| | | 4.100 | | 2.050 | 1.440 | 17.52 | .117 | 12.31 | 9.03 | 8.7 | 6.04 | 74 | 4.883 | 1.471 | 3.412 | 29.16 | 69.9 | |
| | | 5.975 | | 2.988 | 1.760 | 17.58 | .170 | 10.35 | 7.51 | 10.2 | 5.80 | 60 | 4.969 | 1.605 | 3.164 | 18.61 | 63.7 | |
| | | 7.010 | | 3.505 | 1.900 | 17.52 | .200 | 9.50 | 6.90 | 11.3 | 5.95 | 56 | 4.957 | 1.953 | 3.014 | 15.07 | 60.7 | |
| | | 8.000 | | 4.000 | 2.030 | 17.54 | .228 | 8.90 | 6.48 | 12.6 | 6.21 | 55 | 5.006 | 2.090 | 2.916 | 12.79 | 58.3 | |
| | | 4.150 | | 2.075 | 1.450 | 17.44 | .119 | 12.18 | 8.91 | 8.8 | 6.07 | 74 | 4.842 | 1.482 | 3.360 | 28.24 | 69.4 | |
| | | 5.500 | | 2.750 | 1.691 | 17.40 | .158 | 10.70 | 7.72 | 10.7 | 6.33 | 68 | 4.860 | 1.732 | 3.128 | 19.80 | 64.4 | |
| | | 6.000 | | 3.000 | 1.764 | 17.44 | .172 | 10.26 | 7.41 | 11.0 | 6.24 | 64 | 4.895 | 1.809 | 3.086 | 17.94 | 63.0 | |
| | | 6.500 | | 3.250 | 1.827 | 17.38 | .187 | 9.77 | 7.08 | 11.3 | 6.18 | 60 | 4.878 | 1.876 | 3.002 | 16.05 | 61.5 | |
| | | 2.000 | | 1.000 | 1.000 | 17.24 | .058 | 17.24 | 12.62 | 6.4 | 6.40 | 110 | 4.674 | 1.016 | 3.658 | 63.07 | 78.3 | |
| | | 2.500 | | 1.250 | 1.104 | 17.36 | .072 | 15.33 | 11.40 | 6.7 | 6.07 | 93 | 4.752 | 1.124 | 3.628 | 50.39 | 76.3 | |
| | | 3.000 | | 1.500 | 1.235 | 17.44 | .086 | 14.36 | 10.48 | 7.4 | 5.99 | 86 | 4.809 | 1.258 | 3.551 | 41.29 | 73.8 | |

Table 1—Continued

| (1) | (2) | (3) | (4) | (5) | (6) | (7) | (8) | (9) | (10) | (11) | (12) | (13) | (14) | (15) | (16) | (17) | (18) | (19) |
|---|---|---|---|---|---|---|---|---|---|---|---|---|---|---|---|---|---|---|
| B | 0 | 3.500 | 2.000 | 1.750 | 1.325 | 17.50 | 0.100 | | 13.25 | 9.75 | 7.8 | 5.89 | 78 | 4.856 | 1.352 | 3.504 | 35.04 | 72.2 |
| | | 4.000 | | 2.000 | 1.433 | 17.39 | .115 | | 12.46 | 9.04 | 8.5 | 5.93 | 74 | 4.811 | 1.463 | 3.348 | 29.11 | 69.6 |
| | | 4.500 | | 2.250 | 1.517 | 17.44 | .129 | | 11.76 | 8.56 | 9.4 | 6.20 | 73 | 4.852 | 1.551 | 3.301 | 25.59 | 68.0 |
| | | 5.000 | | 2.500 | 1.599 | 17.24 | .145 | | 11.03 | 7.98 | 10.0 | 6.25 | 69 | 4.761 | 1.637 | 3.124 | 21.54 | 65.6 |
| | | 5.500 | | 2.750 | 1.691 | 17.40 | .158 | | 10.70 | 7.72 | 10.7 | 6.33 | 68 | 4.860 | 1.732 | 3.128 | 19.50 | 64.4 |
| C | 0 | 1.000 | 1.500 | 0.667 | 0.910 | 20.21 | .033 | 27.58 | 19.55 | 9.55 | 5.0 | 5.49 | 152 | 6.375 | 0.918 | 5.457 | 165.36 | 85.6 |
| | | 1.500 | | 1.000 | 1.125 | 20.43 | .048 | 23.44 | 16.76 | 16.76 | 6.4 | 5.69 | 133 | 6.785 | 1.137 | 5.648 | 117.07 | 83.2 |
| | | 2.000 | | 1.333 | 1.300 | 21.16 | .063 | 20.63 | 14.86 | 14.86 | 7.7 | 5.92 | 122 | 7.016 | 1.316 | 5.700 | 90.48 | 81.2 |
| | | 2.500 | | 1.667 | 1.465 | 21.39 | .078 | 18.78 | 13.48 | 13.48 | 8.9 | 6.08 | 114 | 7.169 | 1.485 | 5.684 | 72.87 | 79.3 |
| | | 3.000 | | 2.000 | 1.615 | 21.74 | .092 | 17.55 | 12.63 | 12.63 | 9.7 | 6.01 | 105 | 7.431 | 1.639 | 5.792 | 62.96 | 77.9 |
| | | 3.380 | | 2.253 | 1.730 | 22.09 | .102 | 16.96 | 12.19 | 12.19 | 10.8 | 6.24 | 106 | 7.679 | 1.756 | 5.923 | 58.07 | 77.1 |
| | | 3.750 | | 2.667 | 1.890 | 22.79 | .117 | 16.15 | 11.74 | 11.74 | 11.1 | 5.87 | 95 | 8.152 | 1.921 | 6.261 | 53.51 | 76.5 |
| | | 4.440 | | 2.960 | 2.010 | 23.13 | .128 | 15.70 | 11.39 | 11.39 | 12.3 | 6.11 | 96 | 8.435 | 2.044 | 6.391 | 49.93 | 75.8 |
| | | 1.250 | | 0.833 | 0.914 | 17.35 | .048 | 19.04 | 13.96 | 13.96 | 5.4 | 5.91 | 112 | 4.723 | 0.927 | 3.796 | 79.08 | 80.4 |
| | | 1.750 | | 1.167 | 1.135 | 18.82 | .062 | 18.30 | 13.32 | 13.32 | 6.5 | 5.73 | 105 | 5.563 | 1.151 | 4.412 | 71.16 | 79.3 |
| | | 2.250 | | 1.500 | 1.320 | 19.48 | .077 | 17.14 | 12.37 | 12.37 | 7.8 | 5.91 | 101 | 5.969 | 1.340 | 4.629 | 60.12 | 77.6 |
| | | 2.750 | | 1.833 | 1.468 | 20.37 | .090 | 16.31 | 11.97 | 11.97 | 9.1 | 6.20 | 101 | 6.533 | 1.492 | 5.041 | 56.01 | 77.1 |
| | | 3.250 | | 2.167 | 1.616 | 20.84 | .104 | 15.54 | 11.39 | 11.39 | 10.0 | 6.19 | 96 | 6.849 | 1.644 | 5.205 | 50.05 | 76.0 |
| | | 3.750 | | 2.500 | 1.736 | 21.19 | .118 | 14.71 | 10.87 | 10.87 | 11.0 | 6.34 | 93 | 7.091 | 1.760 | 5.323 | 45.11 | 75.1 |
| | | 4.250 | | 2.833 | 1.870 | 21.14 | .134 | 13.96 | 10.18 | 10.18 | 11.6 | 6.20 | 87 | 7.074 | 1.905 | 5.169 | 38.57 | 73.1 |
| D | 0 | 4.000 | 3.970 | 1.008 | 1.110 | 20.16 | .050 | 22.20 | 15.89 | 15.89 | 6.5 | 5.86 | 130 | 6.361 | 1.123 | 5.238 | 104.76 | 82.3 |
| | | 5.000 | | 1.259 | 1.220 | 20.31 | .062 | 19.68 | 14.37 | 14.37 | 7.5 | 6.15 | 121 | 6.467 | 1.236 | 5.231 | 84.37 | 80.9 |
| | | 6.000 | | 1.511 | 1.376 | 20.43 | .074 | 18.19 | 13.23 | 13.23 | 8.4 | 6.24 | 114 | 6.549 | 1.365 | 5.184 | 70.05 | 79.2 |
| | | 7.000 | | 1.763 | 1.460 | 20.50 | .086 | 16.98 | 12.32 | 12.32 | 9.0 | 6.16 | 105 | 6.612 | 1.483 | 5.129 | 59.64 | 77.6 |
| | | 8.000 | | 2.015 | 1.570 | 20.56 | .098 | 16.02 | 11.55 | 11.55 | 9.7 | 6.18 | 99 | 6.662 | 1.595 | 5.067 | 51.70 | 76.1 |
| | | 9.000 | | 2.267 | 1.670 | 20.80 | .109 | 15.32 | 11.11 | 11.11 | 10.0 | 5.99 | 92 | 6.827 | 1.699 | 5.128 | 47.05 | 75.1 |
| | | 8.080 | | 2.035 | 1.600 | 20.56 | .099 | 16.16 | 11.52 | 11.52 | 9.5 | 5.94 | 96 | 6.663 | 1.625 | 5.038 | 50.89 | 75.6 |
| | | 11.730 | | 2.955 | 1.962 | 21.41 | .138 | 14.22 | 10.16 | 10.16 | 12.4 | 6.32 | 90 | 7.256 | 1.997 | 5.259 | 38.11 | 72.5 |
| | | 10.000 | | 2.519 | 1.752 | 20.99 | .120 | 14.60 | 10.68 | 10.68 | 10.4 | 5.94 | 87 | 6.961 | 1.784 | 5.177 | 43.14 | 74.4 |
| | | 3.000 | | 0.756 | 0.994 | 19.69 | .038 | 25.11 | 12.98 | 12.98 | 5.4 | 5.66 | 142 | 6.181 | 0.964 | 5.217 | 137.29 | 84.4 |
| | | 5.000 | | 1.259 | 1.250 | 20.31 | .062 | 20.16 | 14.37 | 14.37 | 7.4 | 5.92 | 119 | 6.467 | 1.266 | 5.201 | 83.89 | 80.4 |
| | | 7.000 | | 1.763 | 1.452 | 20.50 | .086 | 16.88 | 12.12 | 12.12 | 8.7 | 5.99 | 101 | 6.612 | 1.475 | 5.137 | 59.73 | 77.7 |

Table 1--Continued

| (1) | (2) | (3) | (4) | (5) | (6) | (7) | (8) | (9) | (10) | (11) | (12) | (13) | (14) | (15) | (16) | (17) | (18) | (19) |
|---|---|---|---|---|---|---|---|---|---|---|---|---|---|---|---|---|---|---|
| D | 0 | 9.000 | 3.970 | 2.267 | 1.693 | 20.80 | 0.109 | 15.53 | 11.11 | 10.5 | 6.20 | 96 | 6.827 | 1.721 | 5.106 | 46.84 | 74.8 | |
| | | 11.720 | | 2.952 | 1.922 | 21.39 | .138 | 13.93 | 10.15 | 11.4 | 5.93 | 83 | 7.243 | 1.959 | 5.284 | 38.29 | 73.0 | |
| | | 10.000 | | 2.519 | 1.780 | 20.99 | .120 | 14.83 | 10.68 | 11.2 | 6.29 | 93 | 6.961 | 1.811 | 5.150 | 42.92 | 74.0 | |
| | | 12.000 | | 3.023 | 1.953 | 21.29 | .142 | 13.75 | 9.96 | 12.3 | 6.30 | 87 | 7.180 | 1.990 | 5.190 | 36.55 | 72.3 | |
| | | 14.000 | | 3.526 | 2.163 | 21.63 | .163 | 13.27 | 9.44 | 13.0 | 6.01 | 80 | 7.428 | 2.204 | 5.224 | 32.05 | 70.3 | |
| | | 16.000 | | 4.030 | 2.330 | 22.02 | .183 | 12.73 | 9.07 | 13.8 | 5.92 | 75 | 7.712 | 2.376 | 5.336 | 29.16 | 69.2 | |
| | | 18.000 | | 4.534 | 2.495 | 22.56 | .201 | 12.41 | 8.87 | 15.4 | 6.17 | 77 | 8.104 | 2.546 | 5.558 | 27.65 | 68.6 | |
| | | 4.980 | | 1.254 | 1.220 | 20.23 | .062 | 19.68 | 14.32 | 7.0 | 5.74 | 113 | 6.417 | 1.236 | 5.181 | 83.56 | 80.7 | |
| | | 10.000 | | 2.519 | 1.792 | 20.99 | .120 | 14.93 | 10.68 | 11.0 | 6.14 | 92 | 6.961 | 1.823 | 5.138 | 42.82 | 73.8 | |
| | | 11.000 | | 2.771 | 1.867 | 21.15 | .131 | 14.25 | 10.30 | 11.3 | 6.05 | 86 | 7.077 | 1.901 | 5.176 | 39.51 | 73.1 | |
| | | 13.000 | | 3.275 | 2.009 | 21.55 | .152 | 13.22 | 9.74 | 12.4 | 6.17 | 82 | 7.363 | 2.050 | 5.313 | 34.95 | 72.2 | |
| | | 15.000 | | 3.778 | 2.180 | 21.84 | .173 | 12.60 | 9.25 | 13.3 | 6.10 | 77 | 7.580 | 2.226 | 5.354 | 30.95 | 70.6 | |
| | | 6.500 | | 1.637 | 1.412 | 20.46 | .080 | 17.65 | 12.75 | 8.9 | 6.30 | 111 | 6.580 | 1.433 | 5.147 | 64.34 | 78.2 | |
| | | 4.980 | | 1.254 | 1.220 | 20.23 | .062 | 19.68 | 14.32 | 7.0 | 5.74 | 113 | 6.417 | 1.236 | 5.181 | 83.56 | 80.7 | |
| | | 17.000 | | 4.282 | 2.410 | 22.30 | .192 | 12.56 | 8.77 | 14.6 | 6.05 | 76 | 7.914 | 2.461 | 5.453 | 28.40 | 68.9 | |
| | | 19.000 | | 4.786 | 2.560 | 22.79 | .210 | 12.19 | 8.56 | 15.3 | 5.98 | 73 | 8.275 | 2.614 | 5.661 | 26.96 | 68.4 | |
| | | 21.000 | | 5.290 | 2.656 | 23.20 | .228 | 11.65 | 8.56 | 16.0 | 6.02 | 70 | 8.586 | 2.717 | 5.869 | 25.74 | 68.4 | |
| | | 26.160 | | 6.589 | 3.060 | 24.22 | .272 | 11.25 | 8.19 | 19.4 | 6.34 | 71 | 9.381 | 3.132 | 6.249 | 22.97 | 66.6 | |
| | | 22.980 | | 5.788 | 2.842 | 24.12 | .240 | 11.84 | 8.68 | 18.7 | 6.58 | 78 | 9.274 | 2.907 | 6.367 | 26.53 | 68.7 | |
| | | 23.930 | | 6.028 | 2.845 | 23.73 | .254 | 11.20 | 8.30 | 18.3 | 6.43 | 72 | 8.998 | 2.915 | 6.083 | 23.95 | 67.6 | |
| | | 28.370 | | 7.147 | 3.202 | 24.56 | .291 | 11.00 | 8.02 | 21.0 | 6.56 | 72 | 9.657 | 3.279 | 6.378 | 21.92 | 66.0 | |
| | 0 | 0.960 | 1.000 | 0.960 | 0.792 | 12.15 | .079 | 10.03 | 7.62 | 4.0 | 5.05 | 51 | 2.371 | 0.815 | 1.556 | 19.70 | 65.6 | 0.125 |
| | | 0.815 | | 0.815 | 0.653 | 9.59 | .085 | 7.68 | 5.80 | 3.0 | 4.59 | 35 | 1.513 | 0.677 | 0.836 | 9.84 | 55.3 | |
| | | 0.680 | | 0.680 | 0.540 | 8.61 | .079 | 6.84 | 5.40 | 2.4 | 4.44 | 30 | 1.230 | 0.565 | 0.665 | 8.42 | 54.1 | |
| | | 1.580 | | 1.580 | 0.992 | 11.70 | .135 | 7.35 | 5.61 | 6.2 | 6.25 | 46 | 2.261 | 1.031 | 1.230 | 9.11 | 54.4 | .208 |
| | | 1.200 | | 1.200 | 0.740 | 8.89 | .135 | 5.48 | 4.26 | 4.3 | 5.81 | 32 | 1.362 | 0.781 | 0.581 | 4.30 | 42.7 | |
| | | 1.400 | | 1.400 | 0.880 | 10.37 | .135 | 6.52 | 4.97 | 5.4 | 6.14 | 40 | 1.805 | 0.919 | 0.886 | 6.56 | 49.1 | |
| | | 2.230 | | 2.230 | 1.220 | 12.89 | .173 | 7.05 | 5.46 | 7.3 | 5.98 | 42 | 2.753 | 1.272 | 1.481 | 8.56 | 53.8 | .281 |
| | | 1.730 | | 1.730 | 0.992 | 10.00 | .173 | 5.36 | 4.24 | 5.2 | 5.61 | 30 | 1.726 | 0.981 | 0.745 | 4.31 | 43.2 | |
| | | 1.250 | | 1.250 | 0.644 | 7.23 | .173 | 3.72 | 3.06 | 3.4 | 5.28 | 20 | 0.985 | 0.702 | 0.283 | 1.64 | 28.7 | |
| | | 1.150 | | 1.150 | 0.581 | 6.65 | .173 | 3.36 | 2.82 | 3.1 | 5.34 | 18 | 0.860 | 0.642 | 0.218 | 1.26 | 25.3 | |
| | | 1.400 | | 1.400 | 0.638 | 6.69 | .210 | 3.04 | 2.57 | 3.3 | 5.17 | 16 | 0.901 | 0.712 | 0.189 | 0.90 | 21.0 | .333 |
| | | 1.850 | | 1.850 | 0.882 | 8.81 | .210 | 4.20 | 3.39 | 5.0 | 5.67 | 24 | 1.415 | 0.950 | 0.465 | 2.21 | 32.9 | |

Table 1—Continued

| (1) | (2) | (3) | (4) | (5) | (6) | (7) | (8) | (9) | (10) | (11) | (12) | (13) | (14) | (15) | (16) | (17) | (18) | (19) |
|---|---|---|---|---|---|---|---|---|---|---|---|---|---|---|---|---|---|---|
| F | 0 | 2.200 | 1.000 | 2.200 | 1.075 | 10.48 | 0.210 | 5.12 | 4.03 | 6.2 | 5.77 | 30 | 1.915 | 1.140 | 0.775 | 3.69 | 40.5 | |
| | | 2.740 | | 2.740 | 1.345 | 13.05 | .210 | 6.40 | 5.02 | 8.2 | 6.10 | 39 | 2.854 | 1.410 | 1.444 | 6.88 | 50.6 | |
| | | 1.830 | | 1.830 | 0.753 | 7.29 | .251 | 3.00 | 2.56 | 3.5 | 4.65 | 14 | 1.076 | 0.845 | 0.231 | 0.92 | 21.5 | 0.396 |
| | | 2.350 | | 2.350 | 1.023 | 9.36 | .251 | 4.08 | 3.29 | 5.6 | 5.47 | 22 | 1.611 | 1.105 | 0.506 | 2.02 | 31.4 | |
| | | 2.780 | | 2.780 | 1.235 | 11.08 | .251 | 4.92 | 3.90 | 7.2 | 5.83 | 29 | 2.157 | 1.314 | 0.843 | 3.36 | 39.1 | |
| | | 3.165 | | 3.165 | 1.427 | 12.61 | .251 | 5.69 | 3.44 | 8.4 | 5.89 | 33 | 2.720 | 1.504 | 1.216 | 4.84 | 44.7 | |
| | | 1.900 | | 1.900 | 0.704 | 6.67 | .285 | 2.47 | 2.20 | 3.2 | 4.55 | 11 | 0.976 | 0.847 | 0.159 | 0.56 | 16.3 | .458 |
| | | 2.540 | | 2.540 | 1.016 | 8.91 | .285 | 3.56 | 2.94 | 5.3 | 5.22 | 19 | 1.518 | 1.113 | 0.405 | 1.42 | 26.7 | |
| | | 3.000 | | 3.000 | 1.219 | 10.53 | .285 | 4.28 | 3.48 | 7.0 | 5.74 | 25 | 2.007 | 1.313 | 0.694 | 2.44 | 34.6 | |
| | | 3.460 | | 3.460 | 1.435 | 12.14 | .285 | 5.04 | 4.01 | 8.3 | 5.78 | 29 | 2.574 | 1.525 | 1.049 | 3.68 | 40.8 | |
| E | 0 | 5.000 | 3.970 | 1.259 | 0.840 | 10.49 | .120 | 7.00 | 5.34 | 5.0 | 5.95 | 42 | 1.831 | 0.875 | 0.956 | 7.97 | 52.2 | Dam 1.5' high |
| | | 6.000 | | 1.511 | 0.940 | 10.57 | .143 | 6.57 | 4.92 | 5.6 | 5.96 | 39 | 1.880 | 0.980 | 0.900 | 6.29 | 47.9 | |
| | | 7.000 | | 1.763 | 0.990 | 10.75 | .164 | 6.04 | 4.67 | 5.9 | 5.96 | 36 | 1.960 | 1.039 | 0.921 | 5.62 | 47.0 | |
| | | 8.000 | | 2.014 | 1.080 | 10.69 | .185 | 5.84 | 4.46 | 6.3 | 5.83 | 34 | 2.029 | 1.134 | 0.895 | 4.84 | 44.1 | |
| | | 9.000 | | 2.266 | 1.160 | 11.05 | .205 | 5.66 | 4.30 | 6.6 | 5.69 | 28 | 2.104 | 1.219 | 0.885 | 4.32 | 42.1 | |
| | | 11.000 | | 2.770 | 1.260 | 11.17 | .248 | 5.08 | 3.95 | 7.1 | 5.63 | 32 | 2.188 | 1.335 | 0.853 | 3.44 | 39.0 | |
| | | 4.000 | | 1.008 | 0.770 | 10.28 | .098 | 7.86 | 5.79 | 4.7 | 6.10 | 48 | 1.742 | 0.796 | 0.946 | 9.65 | 54.3 | |
| | | 10.000 | | 2.518 | 1.220 | 11.09 | .227 | 5.37 | 4.10 | 6.9 | 5.66 | 30 | 2.139 | 1.286 | 0.853 | 3.76 | 39.9 | |
| | 0 | 10.00 | 3.970 | 2.518 | 1.080 | 8.99 | .280 | 3.66 | 3.00 | 6.0 | 5.56 | 21 | 1.536 | 1.164 | 0.372 | 1.33 | 24.2 | Dam 10" high |
| | | 9.000 | | 2.266 | 1.000 | 8.78 | .258 | 3.88 | 3.05 | 5.5 | 5.50 | 21 | 1.457 | 1.080 | 0.377 | 1.46 | 25.9 | |
| | | 8.000 | | 2.014 | 0.960 | 8.76 | .230 | 4.17 | 3.22 | 5.0 | 5.21 | 22 | 1.413 | 1.029 | 0.384 | 1.67 | 27.2 | |
| | | 7.000 | | 1.763 | 0.900 | 8.24 | .214 | 4.21 | 3.13 | 4.7 | 5.22 | 24 | 1.269 | 0.961 | 0.308 | 1.44 | 24.3 | |
| | | 6.000 | | 1.511 | 0.820 | 8.39 | .180 | 4.56 | 3.48 | 4.3 | 5.24 | 24 | 1.274 | 0.873 | 0.401 | 2.23 | 31.5 | |
| | | 5.000 | | 1.259 | 0.760 | 7.77 | .162 | 4.69 | 3.40 | 4.1 | 5.39 | 25 | 1.102 | 0.803 | 0.299 | 1.85 | 27.2 | |
| | | 4.000 | | 1.007 | 0.660 | 7.75 | .130 | 5.08 | 3.79 | 3.7 | 5.61 | 28 | 1.064 | 0.697 | 0.367 | 2.82 | 34.5 | |
| | | 3.000 | | 0.755 | 0.570 | 7.95 | .100 | 5.70 | 4.21 | 3.3 | 5.79 | 33 | 1.082 | 0.597 | 0.485 | 4.85 | 44.8 | |
| | 0 | 5.084 | 3.970 | 1.281 | 0.620 | 5.80 | .221 | 2.81 | 2.17 | 2.6 | 4.19 | 12 | 0.744 | 0.686 | 0.058 | 0.26 | 7.80 | Dam 6" high |
| | | 3.675 | | 0.926 | 0.510 | 5.12 | .168 | 3.04 | 2.20 | 2.5 | 4.90 | 15 | 0.576 | 0.561 | 0.015 | 0.09 | 2.60 | |
| | | 2.440 | | 0.615 | 0.410 | 5.44 | .113 | 3.63 | 2.85 | 2.2 | 5.36 | 19 | 0.573 | 0.445 | 0.128 | 1.13 | 22.30 | |
| | | 7.680 | | 1.93 | 0.770 | 5.69 | .340 | 2.26 | 1.72 | 3.0 | 3.90 | 9 | 0.874 | 0.866 | 0.008 | 0.02 | 0.92 | |
| | | 6.000 | | 1.511 | 0.690 | 5.68 | .266 | 2.59 | 1.93 | 2.8 | 4.06 | 10 | 0.768 | 0.765 | 0.003 | 0.01 | 0.39 | |

FIGURE 4



Q = Total discharge in c.f.s.
W = Width of flume in feet.
q = Discharge in c.f.s. per foot of width.
$E_1$ = Energy entering jump.
$E_2$ = Energy leaving jump.
$F_1$ = Froude number $-\frac{V_1}{\sqrt{gd_1}}$.
$D_j$ = $D_2 - D_1$ - Height of jump.

$E_1 - E_2$ = Energy loss in jump.

$E_2 = D_2 + \frac{V_2^2}{2g}$

$E_1 = D_1 + \frac{V_1^2}{2g}$

RELATION OF SPECIFIC ENERGY
TO DEPTH OF FLOW

HYDRAULIC JUMP - ON HORIZONTAL FLOOR
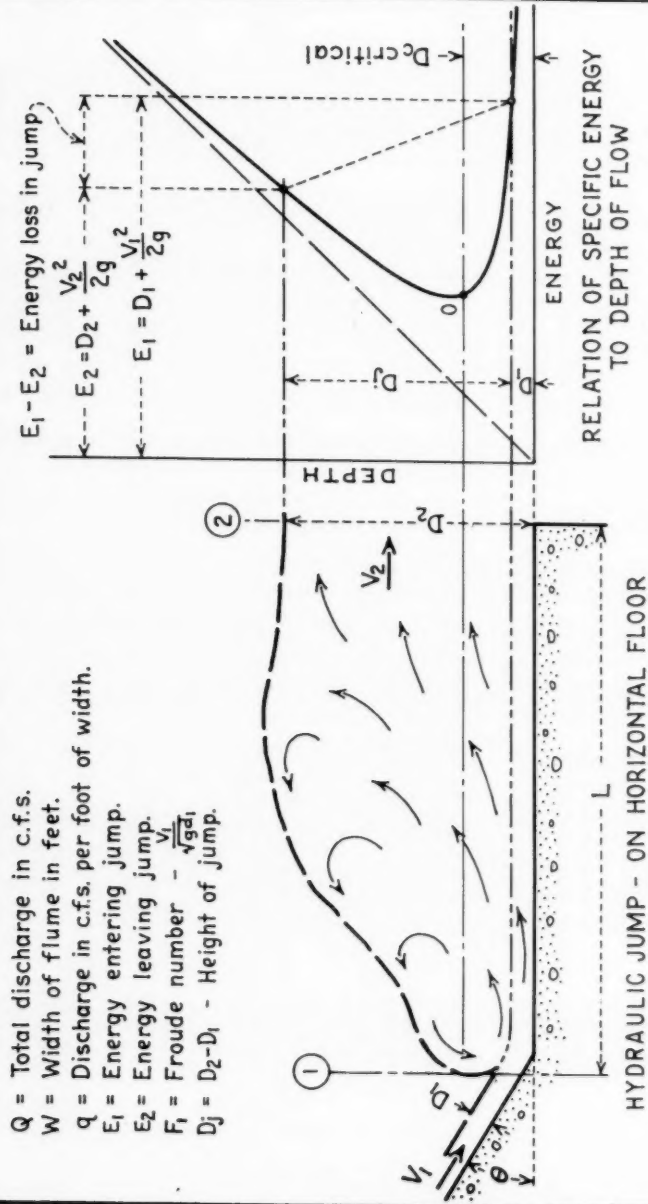
HYDRAULIC JUMP STUDIES
STILLING BASIN I
DEFINITION OF SYMBOLS

437

immediately upstream from Section 1. The results of the measurements and succeeding computations are tabulated in Table 1. The measured quantities are tabulated as follows: total discharge, (Column 3); tail water depth, (Column 6); length of jump, (Column 11), and depth of flow entering jump, (Column 8).

Column 1 indicates the test flumes in which the experiments were performed, and Column 4 shows the width of each flume. All computations are based on discharge per foot width of flume; unit discharges (q) are shown in Column 5.

The velocity entering the jump $V_1$, Column 7, was computed by dividing q (Column 5) by $D_1$ (Column 8).

The Froude Number

The Froude number, Column 10, Table 1, is:

$$F_1 = \frac{V_1}{\sqrt{gD_1}} \tag{1}$$

where $F_1$ is a dimensionless parameter, $V_1$ and $D_1$ are velocity and depth of flow, respectively, entering the jump, and g is the acceleration of gravity. The law of similitude states that where gravitational forces predominate, as they do in open channel phenomena, the Froude number should have the same value in model and prototype. Therefore, a model-shaped jump in a test flume will have the identical characteristics of a prototype jump in a stilling basin, if the Froude numbers of the incoming flows are the same. Although energy conversions in a hydraulic jump bear some relation to the Reynolds number, gravity forces predominate, and the Froude number becomes most useful in plotting stilling basin characteristics. Bakhmeteff and Matzke[1] demonstrated this application in 1936 when they related stilling basin characteristics to the square of the Froude number, $\frac{V^2}{gD_1}$, which they termed the kinetic flow factor.

The Froude number (1) will be used throughout this presentation. As the acceleration of gravity is a constant, the term g could be omitted. Its inclusion makes the expression dimensionless, however, and the form shown as (1) is preferred.

Applicability of Hydraulic Jump Formula

The theory of the hydraulic jump in horizontal channels has been treated thoroughly by others (see Bibliography), and will not be repeated here. The expression for the hydraulic jump, based on pressure-momentum may be written:[15]

$$D_2 = -\frac{D_1}{2} + \sqrt{\frac{D_1^2}{4} + \frac{2V_1^2 D_1}{g}} \tag{2}$$

or

$$D_2 = -\frac{D_1}{2} + \sqrt{\frac{D_1^2}{4} + \frac{2V_1^2 D_1^2}{gD_1}}$$

Transposing $D_1$ to the left side of the equation and substituting $F_1{}^2$ for $\dfrac{V_1{}^2}{gD_1}$,

$$\frac{D_2}{D_1} = -1/2 + \sqrt{1/4 + 2F_1{}^2}$$

or

$$\frac{D_2}{D_1} = 1/2 \left( \sqrt{1 + 8F_1{}^2} - 1 \right) \tag{3}$$

Expression (3) shows that the ratio of conjugate depths is strictly a function of the Froude number. The ratio $\dfrac{D_2}{D_1}$ is plotted with respect to the Froude number on Figure 5. The line, which is virtually straight except for the lower end, represents the above expression for the hydraulic jump; while the points, which are experimental, are from Columns 9 and 10, Table 1. The agreement is quite good for the entire range.

There is an unsuspected characteristic in the curve, however, which is mentioned here but will be enlarged on later. Although the tail water depth, recorded in Column 6 of Table 1, was sufficient to bring the front of the jump to Section 1 (Figure 4) in each test, the ability of the jump to remain at Section 1 for a slight lowering of tail water depth became more difficult for the higher and lower values of the Froude number. The jump was least sensitive to variation in tail water depth in the middle range, or values of $F_1$ from 4.5 to 9.

Length of Jump

The length of the jump measurement, Column 11, Table 1, was the most difficult to determine. Special care was therefore given to this measurement. Where chutes or overfalls were used, the front of the jump was held at the intersection of the chute and the horizontal floor, as shown on Figure 4. The length of jump was measured from this point to a point downstream where either the high-velocity jet began to leave the floor or to a point on the surface immediately downstream from the roller, whichever was the longer. In the case of Flume F, where the flow discharged from a gate onto a horizontal floor, the front of the jump was maintained just downstream from the completed contraction of the entering jet. In both cases the point at which the high-velocity jet begins to rise from the floor is not fixed, but tends to shift upstream and downstream. This is also true of the roller on the surface. It was at first difficult to repeat length observations within 5 percent by either criterion, but with practice satisfactory measurements became possible. It was the intention to judge the length of the jump from a practical standpoint; in other words, the end of the jump, as chosen, would represent the end of the concrete floor and side walls of a conventional stilling basin.

A system devised to measure velocities on the bottom, to aid in determining the length of jump, proved inadequate and too laborious to allow completion of the program planned. Visual observations, therefore, proved to be the most satisfactory as well as the most rapid method for determining the length measurement.

FIGURE 5

HYDRAULIC JUMP STUDIES
RATIO OF TW DEPTH
TO $D_1$
STILLING BASIN I
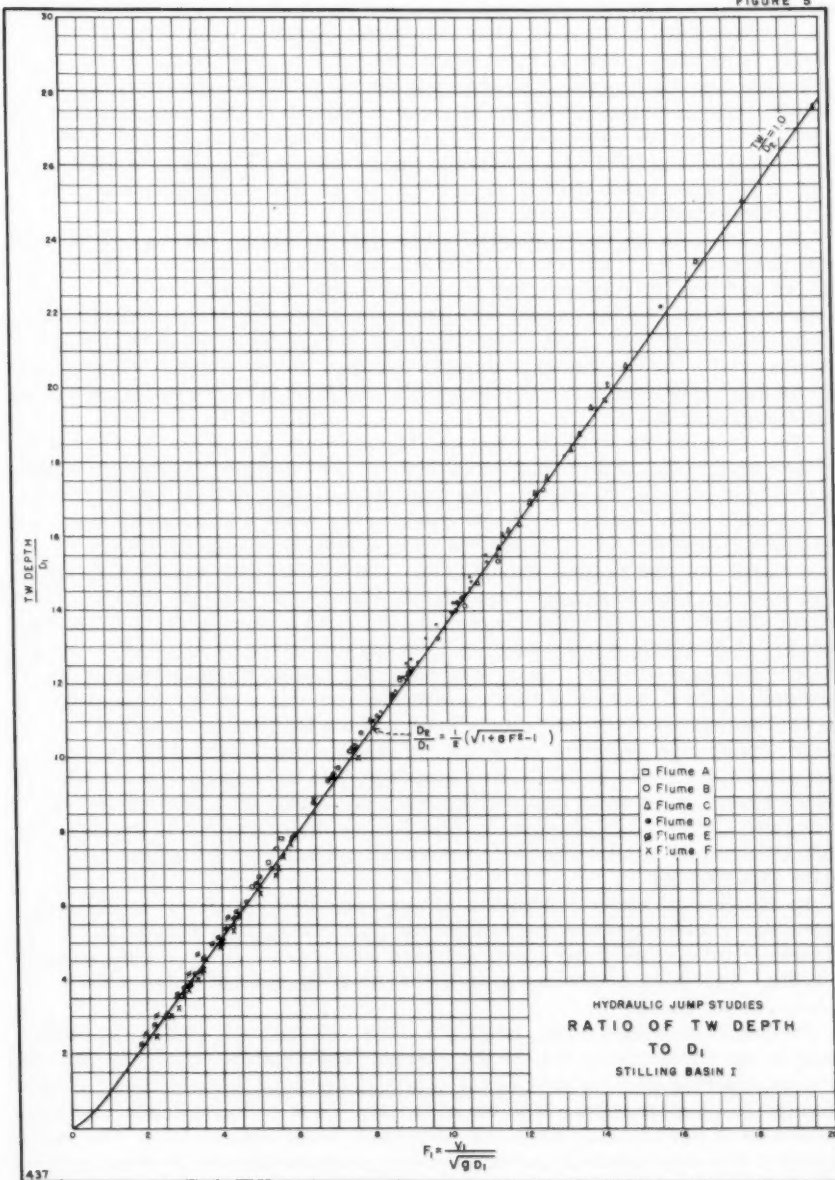
The length of jump has been plotted in two ways. The first is perhaps the better method while the second is the more common and useful. The first method is shown in Figure 6 where the ratio, length of jump to $D_1$ (Column 13, Table 1), is plotted with respect to the Froude number (Column 10) for results from the six test flumes. The resulting curve is of fairly uniform curvature, which is the principal advantage of these coordinates. The second method of plotting, where the ratio, length of jump to the conjugate tail water depth $D_2$ (Column 12) is plotted with respect to the Froude number, is presented on Figure 7. This latter method of plotting will be used throughout the study. The points represent the experimental values.

In addition to the curve established by the test points, curves representing the results of three other experimenters are shown on Figure 7. The best known and most widely accepted curve for length of jump is that of Bakhmeteff and Matzke[1] which was determined from experiments made at Columbia University. The greater portion of this curve, labeled 1, is at variance with the present experimental results. Because of the wide use this curve has experienced, a rather complete explanation is presented regarding the disagreement.

The experiments of Bakhmeteff and Matzke were performed in a flume 6 inches wide, with limited head. The depth of flow entering the jump was adjusted by a vertical slide gate. The maximum discharge was approximately 0.7 cfs, and the thickness of the jet entering the jump, $D_1$, was 0.25 foot for a Froude number of 1.94. The results up to a Froude number of 2.5 are in agreement with the present experiments. To increase the Froude number, it was necessary for Bakhmeteff and Matzke to decrease the gate opening. The extreme case involved a discharge of 0.14 cfs and a value of $D_1$ of 0.032 foot, for $F_1 = 8.9$, which is much smaller than any discharge or value of $D_1$ used in the present experiments. Thus, it is reasoned that as the gate opening decreased, in the 6-inch-wide flume, frictional resistance in the channel downstream increased out of proportion to that which would have occurred in a larger flume or a prototype structure. Thus, the jump formed in a shorter length than it should. In laboratory language, this is known as "scale effect," and is construed to mean that prototype action is not faithfully reproduced. It is quite certain that this was the case for the major portion of curve 1. In fact, Bahkmeteff and Matzke were somewhat dubious concerning the small scale experiments.

To confirm the above conclusion, it was found that results from Flume F, which was 1 foot wide, became erratic when the value of $D_1$ approached 0.10. Figures 6 and 7 show three points obtained with a value of $D_1$ of approximately 0.085. The three points are given the symbol ⊠ and fall short of the recommended curve.

The two remaining curves, labeled 3 and 4, on Figure 7, portray the same trend as the curve obtained from the current experiments. The criterion used by each experimenter for judging the length of the jump is undoubtedly responsible for the displacement. The curve labeled 3 was obtained at the Technical University of Berlin on a flume 1/2 meter wide by 10 meters long. The curve labeled 4 was determined from experiments performed at the Federal Institute of Technology, Zurich, Switzerland, on a flume 0.6 of a meter wide and 7 meters long. The curve numbers are the same as the reference numbers in the Bibliography which refer to the work.

As can be observed from Figure 7, the test results from Flumes B, C, D, E, and F plot sufficiently well to establish a single curve. The five points

FIGURE 6

HYDRAULIC JUMP STUDIES
LENGTH OF JUMP IN TERMS OF $D_1$
STILLING BASIN I

SYMBOLS
■ Flume A
○ Flume B
△ Flume C
• Flume D
▲ Flume E
* Flume F

$F_1 = \dfrac{V_1}{\sqrt{gD_1}}$

$\dfrac{L}{D_2}$

FIGURE 7



HYDRAULIC JUMP STUDIES

LENGTH OF JUMP
IN TERMS OF $D_2$

STILLING BASIN I
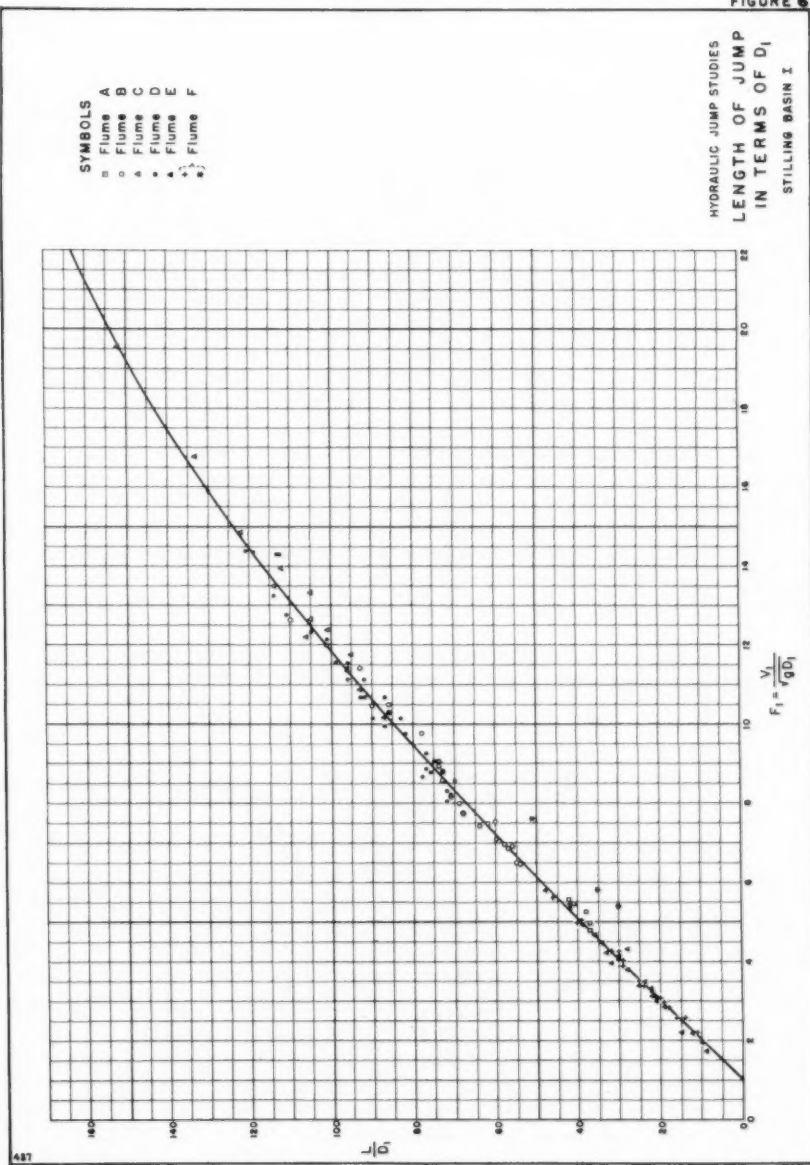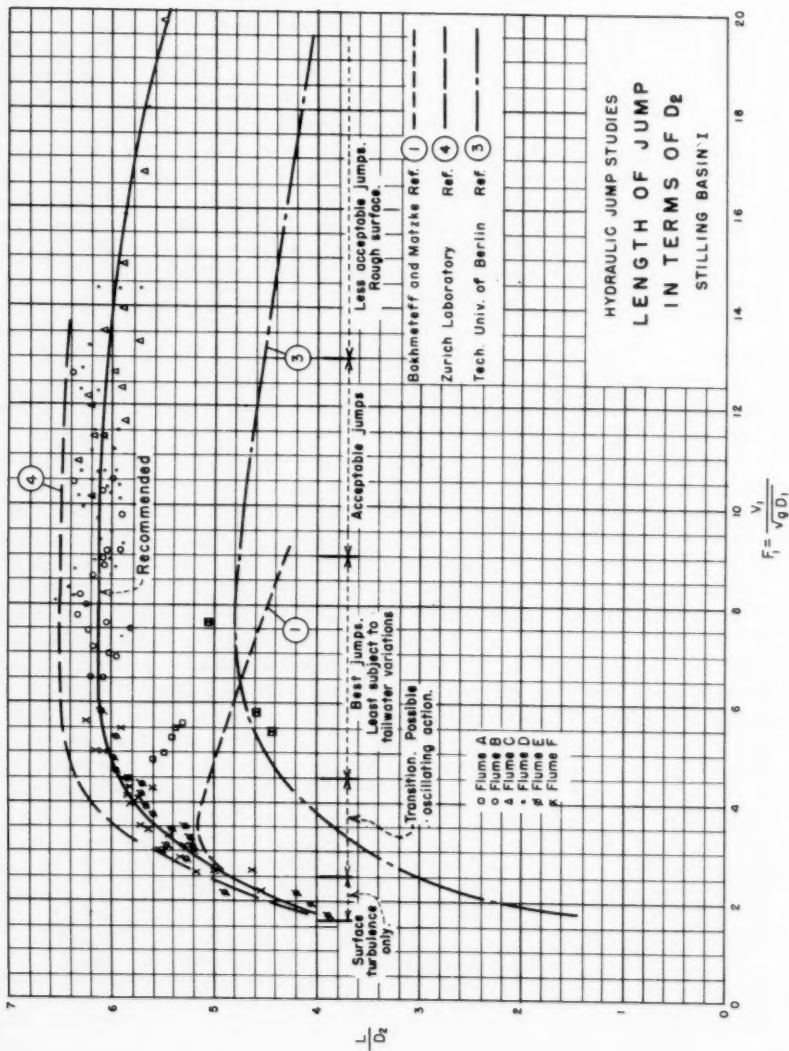
from Flume A, denoted by squares, appear somewhat erratic and plot to the right of the general curve. Henceforth, reference to Figure 7 will concern only the recommended curve which is considered applicable for general use.

## Energy Absorption in Jump

With the experimental information available the energy absorbed in the jump may be computed. Columns 14 through 18, Table 1, list the computations, and the symbols may be defined by consulting the specific energy diagram in Figure 4. Column 14 lists the total energy, $E_1$, entering the jump at Section 1 for each test. This is simply the depth of flow, $D_1$, plus the velocity head computed at the point of measurement. The energy leaving the jump, which is the depth of flow plus the velocity head at Section 2, is tabulated in Column 15. The differences in the values of Columns 14 and 15 constitute the loss of energy, in feet of water, attributed to the conversion, Column 16. Column 18 lists the percentage of energy lost in the jump, $E_L$, to the total energy entering the jump, $E_1$. This percentage is plotted with respect to the Froude number and is shown as the curve to the left on Figure 8. For a Froude number of 2.0, which would correspond to a relatively thick jet entering the jump at low velocity, the curve shows the energy absorbed in the jump to be about 7 percent of the total energy entering. Considering the other extreme, for a Froude number of 19, which would be produced by a relatively thin jet entering the jump at very high velocity, the absorption by the jump would amount to 85 percent of the energy entering. Thus, the hydraulic jump can perform over a wide range of conditions. There are poor jumps and good jumps, with the most satisfactory occurring over the center portion of the curve.

Another method of expressing the energy absorption in a jump is to express the loss, $E_L$, in terms of $D_1$. The curve to the right on Figure 8 shows the ratio $\dfrac{E_L}{D_1}$ (Column 17, Table 1) plotted against the Froude number. Losses in feet of head are obtained from this method.

## Forms of the Hydraulic Jump

The hydraulic jump may occur in at least four different distinct forms on a horizontal apron, as shown on Figure 9. All of these forms are encountered in practice. The internal characteristics of the jump and the energy absorption in the jump vary with each form. Fortunately these forms, some of which are desirable and some undesirable, can be cataloged conveniently with respect to the Froude number, as shown in Figure 9.

When the Froude number is unity, the water is flowing at critical depth; thus a jump cannot form. This corresponds to Point 0 on the specific energy diagram of Figure 4. For values of the Froude number between 1.0 and 1.7 there is only a slight difference in the conjugate depths $D_1$ and $D_2$. A slight ruffle on the water surface is the only apparent feature that differentiates this flow from flow at critical depth. As the Froude number approaches 1.7, a series of small rollers develop on the surface as indicated in Figure 9, and this action remains much the same but with further intensification up to a value of about 2.5. In this range there is no particular stilling basin problem involved; the water surface is quite smooth, the velocity throughout is fairly uniform, and the energy loss is low.

FIGURE 8



HYDRAULIC JUMP STUDIES

LOSS OF ENERGY IN JUMP ON HORIZONTAL FLOOR
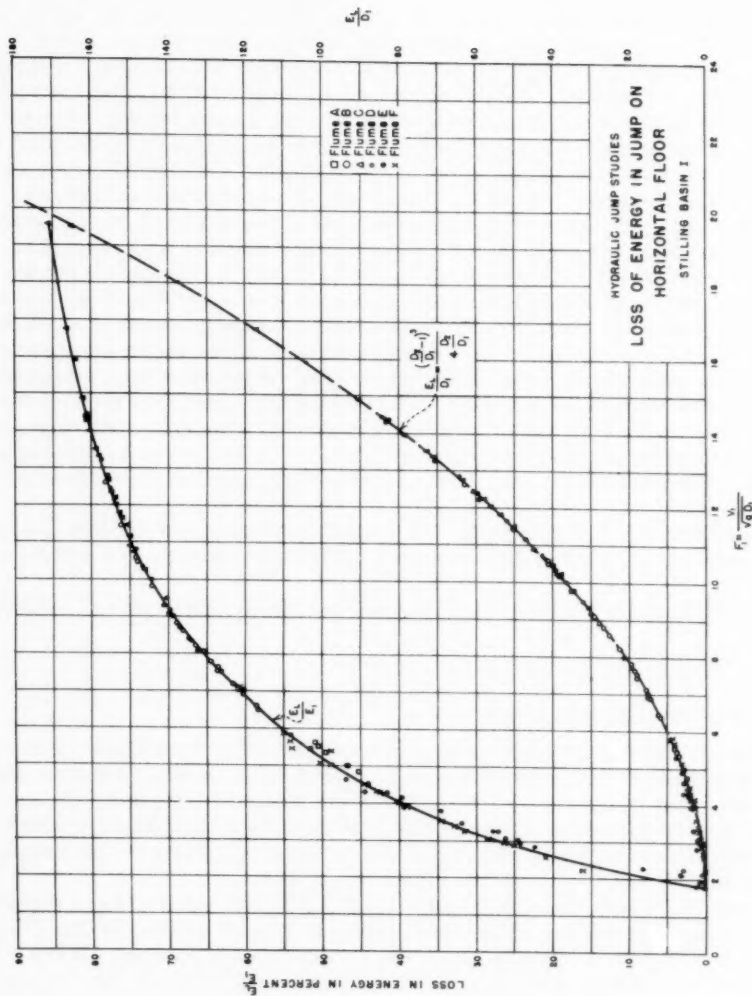
STILLING BASIN I
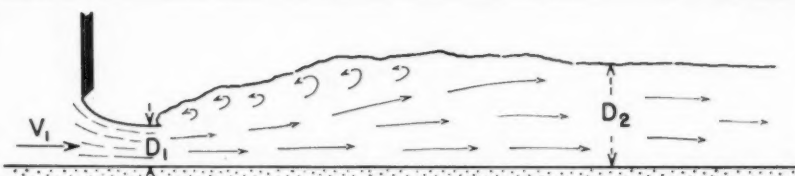
FIGURE 9



$F_1 = 1.7 - 2.5$

PRE JUMP - VERY LOW ENERGY LOSS

Oscillating jet

Roller
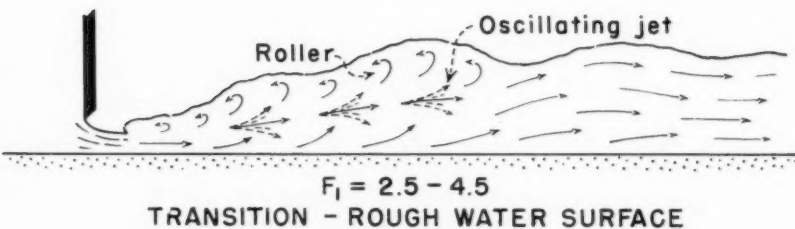
$F_1 = 2.5 - 4.5$

TRANSITION - ROUGH WATER SURFACE

$F_1 = 4.5 - 9.0$
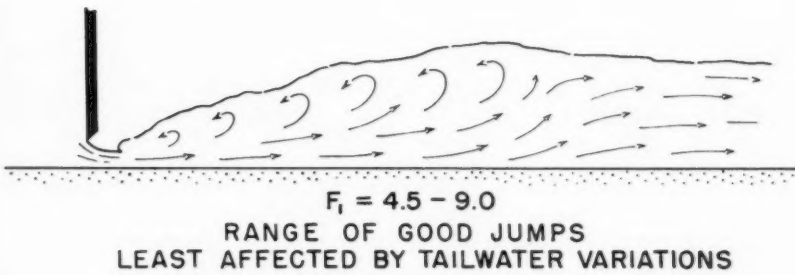
RANGE OF GOOD JUMPS
LEAST AFFECTED BY TAILWATER VARIATIONS
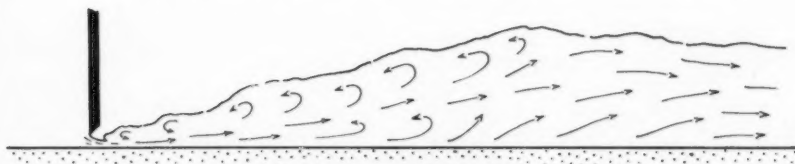
$F = 9.0 - $ UPWARD
EFFECTIVE BUT ROUGH

HYDRAULIC JUMP STUDIES
STILLING BASIN I
JUMP FORMS

Figure 9 indicates the type of jump that may be encountered at values of the Froude number from 2.5 to 4.5. This type has a pulsating action and is usually seen in low head structures. The entering jet oscillates from bottom to surface with no regular period. Turbulence occurs near the bottom at one instant and entirely on the surface the next. Each oscillation produces a large wave of irregular period which in prototype structures has been observed to travel for miles causing damage to earth banks and riprap. This case is of sufficient importance *that a separate section, Section 4, has been devoted to the practical aspects of design.

A well stabilized jump can be expected for the range of Froude numbers between 4.5 and 9, Figure 9. In this range, the downstream extremity of the surface roller and the point at which the high-velocity jet tends to leave the floor occur in practically the same vertical plane. The jump is well balanced and the action is thus at its best. The energy absorption in the jump for Froude numbers from 4.5 to 9 ranges from 45 to 70 percent, Figure 8.

As the Froude number increases above 9, the form of the jump gradually changes to that shown in Figure 9. This is the case where $V_1$ is very high, $D_1$ is comparatively small, and the difference in conjugate depths is large. The high-velocity jet no longer carries through for the full length of the jump. In other words, the downstream extremity of the surface roller now becomes the determining factor in judging the length of the jump. Slugs of water rolling down the front face of the jump intermittently fall into the high-velocity jet generating additional waves downstream, and a rough surface can prevail. Figure 8 shows that the energy dissipation for this case is high and may reach 85 percent.

The limits of the Froude number given above for the various forms of jump are not definite values, but overlap somewhat depending on local factors. Returning to Figure 7, it is found that the length curve catalogs the various phases of the jump quite well. The flat portion of the curve indicates the range of best operation. The steep portion of the curve to the left definitely indicates an internal change in the form of the jump. In fact, two changes are manifest, the form shown in Figure 9A and the form, which might better be called a transition stage, shown in Figure 9B. The right end of the curve on Figure 7 also indicates a change in form, but to less extent.

## Practical Consideration

Although it was the intention to stress the academic rather than the practical viewpoint in this paper, this is the logical place to point out a few of the practical aspects of stilling basin design using horizontal aprons. Considering the four forms of jump just discussed, the following are pertinent:

1. All jump forms are encountered in stilling basin design.

2. The form in Figure 9A requires no baffles or special devices in the basin. The only requirement is to provide the proper length of pool, which is relatively short. This can be obtained from Figure 7.

3. The form in Figure 9B is one of the most difficult to handle and is frequently encountered in the design of canal structures, diversion or low dam spillways, and even outlet works. Baffle piers or appurtenances in the basin are of little value. Waves are the main source of difficulty and methods for coping with them are discussed in Paper 1404. The present information may prove valuable in that it will help to restrict the use of jumps in the 2.5 to 4.5 Froude number range. In many cases the critical range cannot be avoided,

but in others the jump may be brought into the desirable range by altering the dimensions of the structure.

4. No particular difficulty is encountered in the form valuable as a means of shortening the length of basin. This is discussed in Papers 1402 and 1403.

5. As the Froude number increases, the jump becomes more sensitive to tail water depth. For numbers as low as 8, a tail water depth greater than the conjugate depth is advisable to be certain that the jump will stay on the apron. This phase will be discussed in more detail in following Papers.

6. When the Froude number is greater than 10 the difference in conjugate depths is great, and, generally speaking, a very deep basin with high training walls is required. On high spillways the cost of the stilling basin may not be commensurate with the results obtained. A bucket type dissipator may give comparable results at less cost. On lower head structures the action in the basin will be rugged in appearance with surface disturbances being of greatest concern.

7. High Froude numbers will always occur for flow through extremely small gate openings on even the smallest structures. Unless the discharge for these conditions represents an appreciable percentage of the design flow, the high Froude numbers have no significance.

Water-surface Profiles and Pressures

Water-surface profiles for the jump on a horizontal floor were not measured as these have already been determined by Bakhmeteff and Matzke,[1] Newman and LaBoon,[19] and Moore.[27,18] It has been shown by several experimenters that the vertical pressures on the floor of the stilling basin are virtually the same as the static head indicated by the water-surface profile.

Conclusions

The foregoing experiments and discussion serve to associate the Froude number with the hydraulic jump and stilling basin design. The ratio of conjugate depths, the length of jump, the type of jump to be expected, and the losses involved have all been related to this number. The principal advantage of this form of presentation is that one may see the entire picture at a glance with a minimum of calculation.

Application of Results (Example 1)

Water flowing under a sluice gate discharges into a rectangular stilling basin the same width as the gate. The average velocity and the depth of flow after contraction of the jet is complete are: $V_1$ = 85 ft/sec and $D_1$ = 5.6 feet. Determine the conjugate tail water depth, the length of basin required to confine the jump, the effectiveness of the basin to dissipate energy, and the type of jump to be expected.

$$F_1 = \frac{V_1}{\sqrt{gD_1}} = \frac{85}{\sqrt{32.2 \times 5.6}} = 6.34$$

Entering Figure 5 with this value

$$\frac{D_2}{D_1} = 8.5$$

The conjugate tail water depth

$$D_2 = 8.5 \times 5.6 = 47.6 \text{ feet}$$

Entering the recommended curve on Figure 7 with a Froude number of 6.34

$$\frac{L}{D_2} = 6.13$$

Length of basin necessary to confine the jump

$$L = 6.13 \times 47.6 = 292 \text{ feet}$$

Entering Figure 8 with the above value of the Froude number, it is found that the energy absorbed in the jump is 58 percent of the energy entering.

By consulting Figure 9 it is apparent that a very satisfactory jump can be expected.

The following Papers deal with the more practical aspects of stilling basin design, such as modifying the jump by baffles and sills to increase stability and shorten the length.

# Journal of the
# HYDRAULICS DIVISION

## Proceedings of the American Society of Civil Engineers

HYDRAULIC DESIGN OF STILLING BASINS:
HIGH DAMS, EARTH DAMS, AND LARGE CANAL STRUCTURES
(BASIN II)

J. N. Bradley[1] M. ASCE and A. J. Peterka[2] M. ASCE
(Proc. Paper 1402)

## FOREWORD

This is one of a group of six papers on the hydraulic design of stilling basins and their associated appurtenances. Although original data from hydraulic models are presented in tabular form, the papers emphasize practical design procedures. Basin sizes and dimensions are given in easy-to-use dimensionless forms so that dependable stilling basins may be designed without the need for exceptional judgment or extensive experience. Sample problems are included.

The "Introduction" and "Experimental Equipment" are included in Paper 1401 but apply to all papers in this group. Paper 1401 is an academic study of the hydraulic jump on a flat floor. Useful information is presented concerning energy losses, applicability of the hydraulic jump formula, length of jump, and a new classification of the various types of jumps.

Paper 1402 covers the design of a short hydraulic jump stilling basin having an end sill and chute blocks. Paper 1403 describes a shorter stilling basin which utilizes baffle piers. In both papers information is given to determine the critical dimensions of the stilling basin, the tail water range, and the water surface profile in the basin.

Paper 1404 describes a special type of hydraulic jump basin for use when the Froude number of the incoming flow is low, and the jump produces waves in the downstream channel. An alternate design and two types of wave suppressors are also developed.

Paper 1405 describes the design of a stilling basin having a sloping apron. The extra tail water depth required and the merits of a sloping apron are evaluated, as is the basin length for a range of apron slopes.

Paper 1406 develops the design of impact basins for discharges up to 340 second feet and incoming velocities up to 30 feet per second. No tail water is

required.  The bibliography in this paper applies to all papers in this group.

---

## ABSTRACT

An analysis of the critical dimensions of 36 existing hydraulic jump still-
ing basins and hydraulic model verification tests are used to generalize the
design of a stilling basin, utilizing chute blocks and an end sill.  Tail water
ranges, jump lengths, water surface profiles, etc., values are provided in
dimensionless forms.

---

## INTRODUCTION

Stilling basins are seldom designed to confine the entire length of the
hydraulic jump on the paved apron as was assumed in Paper 1401; first, for
economic reasons and secondly, because there are means for modifying the
jump characteristics to obtain comparable or better performance in shorter
lengths.  It is possible to reduce the jump length by the installation of acces-
sories such as blocks, baffles, and sills in the stilling basin.  In addition to
shortening the jump, the accessories exert a stabilizing effect and in some
cases increase the factor of safety.

This study concerns stilling basins of the type which have been used on
high dam and earth dam spillways, and large canal structures, and will be
denoted as Basin II, Figure 10.  The basin contains chute blocks at the up-
stream end and a dentated sill near the downstream end.  No baffle piers are
used in Basin II because of the relatively high velocities entering the jump.
The principal aim in these tests was to (1) generalize the design, and (2) de-
termine the range of operating conditions for which this basin is best suited.
Since many of these basins have been designed, constructed, and operated,
some of which were checked with models, the principal task in accomplishing
the first objective was to tabulate and analyze the dimensions of existing
structures.  Only structures on which firsthand information was available
were used.

### Results of Compilation

With the aid of Figure 10, most of the symbols used in Table 2 are self-
explanatory.  The use of baffle piers is limited to Basin III.  Column 1 lists
the reference material used in compiling the table.  Column 2 lists the maxi-
mum reservoir elevation, Column 3 the maximum tail water elevation,
Column 5 the elevation of the stilling basin floor, and Column 6 the maximum
discharge for each spillway.  Column 4 indicates the height of the structure
studied, showing a maximum fall from headwater to tail water of 179 feet, a
minimum of 14 feet, and an average of 85 feet.  Column 7 shows that the width
of the stilling basins varied from 1,197.5 to 20 feet.  The discharge per foot
of basin width, Column 8, varied from 760 to 52 cfs, with 265 as an average.
The computed velocity, $V_1$ (hydraulic losses estimated in some cases), enter-
ing the stilling basin (Column 9) varied from 108 to 38 feet per second, and
the depth of flow, $D_1$, entering the basin (Column 10) varied from 8.80 to 0.60

feet. The value of the Froude number (Column 11) varied from 22.00 to 4.31. Column 12 shows the actual depth of tail water above the stilling basin floor, which varied from 60 to 12 feet, while Column 14 lists the computed, or conjugate, tail water depth for each stilling basin. The conjugate depths, $D_2$, were obtained from Figure 5, (paper 1401). The ratio of the actual tail water depth to the conjugate depth is listed for each basin in Column 15.

### Tail Water Depth

The ratio of actual tail water depth to conjugate depth shows a maximum of 1.67, a minimum of 0.73, and an average of 0.99. In other words, on the average, the basin floor was set to provide a tail water depth equal to the conjugate or necessary depth.

### Chute Blocks

The chute blocks used at the entrance to the stilling basin varied in size and spacing. Some basins contained nothing at this point, others a solid step, but in the majority of cases a serrated device, known as chute blocks, was utilized. The chute blocks at the upstream end of the basin tend to corrugate the jet, lifting a portion of it from the floor, resulting in a shorter length of jump than would be possible without them. These blocks also tend to improve the action in the jump. The proportioning of chute blocks has been the subject of much discussion. The tabulation in Columns 19 through 24 of Table 2 shows the sizes which have been used. Column 20 shows the height of the chute blocks, while Column 21 gives the ratio of height of block to the depth, $D_1$. The ratios of height of block to $D_1$ indicate a maximum of 2.72, a minimum of 0.81, and an average of 1.35. This is somewhat higher than was shown to be necessary by the verification tests discussed later; a block equal to $D_1$ in height is sufficient.

The width of the blocks is shown in Column 22. Column 23 gives the ratio of width of the block to height, with a maximum of 1.67, a minimum of 0.44, and an average of 0.97. The ratio of width of block to spacing, tabulated in Column 24, shows a maximum of 1.91, a minimum of 0.95, and an average of 1.15. The three ratios indicate that the proportion: height equals width, equals spacing, equals $D_1$ should be a satisfactory standard for chute block design. The wide variation shows that these dimensions are not critical.

### Dentated Sill

The sill in or at the end of the basin was either solid or had some form of dentated arrangement, as designated in Column 25. A dentated sill located at the end of the apron is recommended. The shape of the dentates and the angle of the sills varied considerably in the spillways tested, Columns 26 through 31. The position of the dentated sill also varied and this is indicated by the ratio $\dfrac{X}{L_{II}}$ in Column 26. The distance, X, is measured to the downstream edge of the sill, as illustrated in Figure 10. The ratio $\dfrac{X}{L_{II}}$ varied from 1 to 0.65, with an average of 0.97.

The heights of the dentates are given in Column 27. The ratio of height of block to the conjugate tail water depth is shown in Column 28. These ratios show a maximum of 0.37, a minimum of 0.08, and an average of 0.20. The width to height ratio, Column 30, shows a maximum of 1.25, a minimum of 0.33, and average of 0.76. The ratio of width of block to spacing, Column 31, shows a maximum of 1.91, a minimum of 1.0, and an average of 1.13. For the

purpose of generalization, the following proportions are recommended:
(1) height of dentated sill = $0.2D_2$, (2) width of blocks = $0.15D_2$, and (3) spacing
of blocks = $0.15D_2$, where $D_2$ is the conjugate tail water depth. It is recom-
mended that the dentated sill be placed at the downstream end of the apron.

Columns 32 through 38 show the proportions of additional baffle blocks
used on three of the stilling basins. These are not necessary and are not
recommended for this type of basin.

### Additional Details

Column 18 indicates the angle, with the horizontal, at which the high-
velocity jet enters the stilling basin for each of the spillways. The maximum
angle was $34^O$ and the minimum $14^O$. The effect of the vertical angle of the
chute on the action of the hydraulic jump could not be evaluated from the in-
formation available. This factor will be considered, however, in Section 5 in
connection with sloping apron design.

Column 39 designates the cross section of the basin. In all but three cases
the basins were rectangular. The three cross sections that were trapezoidal
had side slopes varying from 1/4:1 to 1/2:1. The generalized designs present-
ed in this report are for stilling basins with rectangular cross sections.
Where trapezoidal basins are contemplated a model study is strongly
recommended.

Column 40, Table 2, indicates that in the majority of basins constructed for
earth dam spillways the wing walls were normal to the training walls. Five
basins were constructed without wing walls using a rock blanket for protec-
tion. The remainder utilized angling wing walls or warped transitions down-
stream from the basin. The latter are common on canal structures. The ob-
ject, of course, is to build the cheapest wing wall that will afford the
necessary protection. The type of wing wall is usually dictated by local con-
ditions such as width of the channel downstream, depth to foundation rock,
degree of protection needed, etc., thus wing walls are not amenable to
generalization.

### Verification Tests

An inspection of the data shows that the structures listed in Table 2 do not
cover the desired range of operating conditions. There is insufficient infor-
mation to determine the length of basin for the larger values of the Froude
number, there is little or no information on the tail water depth at which
sweepout occurs, and the information available is of little value for generaliz-
ing the problem of water-surface profiles. Laboratory tests were therefore
performed to extend the range and to supply the missing data. The experi-
ments were made on 17 Type II basins, proportioned according to the above
rules, and installed in Flumes B, C, D, and E (see Columns 1 and 2, Table 3).
Each basin was judged at the discharge for which it was designed, the length
was adjusted to the minimum that would produce satisfactory operation, and
the absolute minimum tail water depth for acceptable operation was measured.
The basin operation was also observed for flows less than the designed dis-
charge and found to be satisfactory in each case.

Table 3 is quite similar to Table 2 with the exception that the length of
basin $L_{II}$ (Column 11) was determined by experiment, and the tail water depth
at which the jump just began to sweep out of the basin was recorded (Column
13).

Tail Water Depth

The solid line on Figure 11 was obtained from the hydraulic jump formula $\frac{D_2}{D_1} = 1/2 \, (\sqrt{1 + 8F^2} - 1)$ and represents conjugate tail water depth. It is the same as the line shown on Figure 5, (paper 1401). The dashed lines on Figure 11 are merely guides drawn for tail water depths other than conjugate depth. The points shown as dots were obtained from Column 13 of Table 2 and constitute the ratio of actual tail water depth to $D_1$ for each basin listed. It can be observed that the majority of the basins were designed for conjugate tail water depth or less. The minimum tail water depth for Basin II, obtained from Column 14 of Table 3, is shown on Figure 11. The curve labeled "Minimum TW Depth Basin II" indicates the point at which the front of the jump moves away from the chute blocks. In other words, any additional lowering of the tail water would cause the jump to leave the basin. Consulting Figure 11 it can be observed that the margin of safety for a Froude number of 2 is 0 percent; while for a number of 6 it increases to 6 percent, for a number of 10 it diminishes to 4 percent, and for a number of 16 it is 2.5 percent. To be certain that this is understood, it will be stated another way. The jump will no longer operate properly when the tail water depth approaches $0.98D_2$ for a Froude number of 2 or $0.94D_2$ for a number of 6 or $0.96D_2$ for a number of 10, or $0.975D_2$ for a number of 16. The margin of safety is largest in the middle range. For the two extremes of the curve it is advisable to provide a tail water greater than conjugate depth to be safe. For these reasons the Type II basin should never be designed for less than conjugate depth and a minimum safety factor of 5 percent of $D_2$ is recommended.

Several precautions should be taken when determining tail water elevations. First, tail water curves are usually extrapolated for the discharges encountered in design, so they can be in error. Secondly, the actual tail water depth usually lags, in a temporal sense, that of the tail water curve for rising flow and leads the curve for a falling discharge. Extra tail water should therefore be provided if reasonable increasing increments of discharge limit the performance of the structure because of a lag in building up tail water depth. Thirdly, a tail water curve may be such that the most adverse condition occurs at less than the maximum designed discharge; and fourthly, temporary or permanent retrogression of the riverbed downstream may be a factor needing consideration. These factors, some of which are difficult to evaluate, are all important in stilling basin design, and suggest that an adequate factor of safety is essential. It is advisable to construct a jump height curve, superimposed on the tail water curve, for each basin to determine the most adverse operating condition. This procedure will be illustrated later.

The verification tests repeatedly demonstrated that there is no simple remedy for a deficiency in tail water depth. Increasing the length of basin, which is the remedy often attempted in the field, will not compensate for deficiency in tail water depth. For these reasons, care should be taken to consider all factors that may affect the tail water at a future date.

Length of Basin

The necessary length of Basin II, determined by the verification tests, is shown as the intermediate curve on Figure 12. The squares indicate the test points (Columns 10 and 12 of Table 3). The black dots represent existing

basins (Columns 11 and 17, Table 2). Conjugate depth was used in the ordinate ratio rather than actual tail water depth since it could be computed for each case.

The dots scatter considerably but an average curve drawn through these points would be lower than the Basin II curve. In Figure 12, therefore, it appears that in practice a basin about 3 times the conjugate depth is actually used when a basin about 4 times the conjugate is recommended from the verification tests. It should be remembered, however, that the shorter basins were all model tested and every opportunity was taken to reduce the basin length. The extent and depth of bed erosion, wave heights, favorable flood frequencies, flood duration and other factors were all used to justify reducing the basin length. Lacking definite knowledge of this type in designing a basin for field construction without model tests, the longer basins indicated by the verification tests curve are recommended.

The Type II basin curve has been arbitrarily terminated at Froude number 4, as the jump may be unstable at lower numbers. The chute blocks have a tendency to stabilize the jump and reduce the 4.5 limit discussed for Basin I. For basins having Froude numbers below 4.5 see Paper 1404.

## Water-surface Profiles

Water-surface profiles were measured during the tests to aid in computing uplift pressures under the basin apron. As the water surface in the stilling basin tests fluctuated rapidly it was felt that a high degree of accuracy in measurement was not necessary. This was found to be true when the approximate water-surface profiles obtained were plotted, then generalized. It was found that the profile in the basin could be closely approximated by a straight line making an angle $\alpha$ with the horizontal. This line can also be considered to be a pressure profile.

The angle $\alpha$ (Column 24, Table 3) observed in each of the verification tests has been plotted with respect to the Froude number on Figure 13. The slope increases with the Froude number. To use the curve in Figure 13, a horizontal line is drawn at conjugate depth on a scale drawing of the basin. A vertical line is also drawn from the upstream face of the dentated sill. Beginning at the point of intersection, a sloping line is constructed as shown. The above procedure gives the approximate water surface and pressure profile for conjugate tail water depth. Should the tail water depth be greater than $D_2$, the profile will resemble the uppermost line on Figure 13; the angle remains unchanged. This information applies only for the Type II basin, constructed as recommended in this section.

## CONCLUSIONS

The following rules are recommended for generalization of Basin II, Figure 14:

1. Set apron elevation to utilize full conjugate tail water depth, plus an added factor of safety if needed. An additional factor of safety is advisable for both low and high values of the Froude number (see Figure 11). A minimum margin of safety of 5 percent of $D_2$ is recommended.

2. Basin II may be effective down to a Froude number of 4 but the lower values should not be taken for granted (see Paper 1404 for values less than 4.5).

3. The length of basin can be obtained from the intermediate curve on Figure 12.

4. The height of chute blocks is equal to the depth of flow entering the basin, or $D_1$, Figure 14. The width and spacing should be equal to approximately $D_1$; however, this may be varied to eliminate fractional blocks. A space equal to $\dfrac{D_1}{2}$ is preferable along each wall to reduce spray and maintain desirable pressures.

5. The height of the dentated sill is equal to $0.2D_2$, while the maximum width and spacing recommended is approximately $0.15D_2$. In this case a block is recommended adjacent to each side wall, Figure 14. The slope of the continuous portion of the end sill is 2:1. In the case of narrow basins, which would involve only a few dentates according to the above rule, it is advisable to reduce the width and the spacing so long as this is done proportionately. Reducing the width and spacing actually improves the performance in narrow basins, thus, the minimum width and spacing of the dentates is governed only by structural considerations.

6. It is not necessary to stagger the chute blocks and the sill dentates. In fact this practice is usually inadvisable from a construction standpoint.

7. The verification tests on Basin II indicated no perceptible change in the stilling basin action with respect to the slope of the chute preceding the basin. The slope of chute varied from 0.6:1 to 2:1 in these tests, Column 25, Table 3. Actually, the slope of the chute does have an effect on the hydraulic jump in some cases. This subject will be discussed in more detail in Paper 1405 with regard to sloping aprons. It is recommended that the sharp intersection between chute and basin apron, Figure 14, be replaced with a curve of reasonable radius $(R \gtreqless 4D_1)$ when the slope of the chute is 1:1 or greater. Chute blocks can be incorporated on the curved face as readily as on the plane surfaces. On steep chutes the length of top surface on the chute blocks should be made sufficiently long to deflect the jet.

Following the above rules will result in a safe, conservative stilling basin for spillways with fall up to 200 feet and for flows up to 500 cfs per foot of basin width, provided the jet entering the basin is reasonably uniform both as to velocity and depth. For greater falls, larger unit discharges, or possible asymmetry, a model study of the specific design is recommended.

## Aids in Computation

Before presenting an example illustrating the method of proportioning Basin II, a chart will be presented which should be of special value for preliminary computations. The chart makes it possible to determine $V_1$ and $D_1$ with a fair degree of accuracy, for chutes having slopes of 0.8:1 or steeper, where computation is a difficult and arduous procedure. The chart presented as Figure 15 represents a composite of experience, computation, and a limited amount of experimental information obtained from prototype tests on Shasta and Grand Coulee Dams. There is much to be desired in the way of experimental confirmation; however, it is felt that this chart is sufficiently accurate for preliminary design.

The ordinate on Figure 15 is the fall from reservoir level to stilling basin floor, while the abscissa is the ratio of actual to theoretical velocity at

entrance to the stilling basin. The theoretical velocity $V_T = \sqrt{2g(Z-H/2)}$ (see Figure 15). The actual velocity is the term desired. The curves represent different heads, H, on the crest of the spillway. As is reasonable, the larger the head on the crest, the more nearly the actual velocity a⁺ the base of the spillway will approach the theoretical. For example, with H = 40 feet and Z = 230 feet, the actual velocity at the base of the dam would be 0.95 of the computed theoretical velocity; while with a head of 10 feet on the crest, the actual velocity would be 0.75 $V_T$. The value of $D_1$ may then be computed by dividing the unit discharge by the actual velocity obtained from Figure 15.

The chart is not applicable for chutes flatter than 9.6:1 as frictional resistance assumes added importance in this range. Therefore, it will be necessary to compute the hydraulic losses starting at the gate section where critical depth is known.

Insufflation, produced by air from the atmosphere mixing with the sheet of water during the fall, need not be considered in the hydraulic jump computations. Insufflation need be considered principally in determining the height of chute and stilling basin walls. It is usually not possible to construct walls sufficiently high to confine all spray and splash; thus, the best that can be hoped for is a height that is reasonable and commensurate with the material and terrain to be protected.

## Application of Results (Example 2)

The crest of an overfall dam, having a downstream slope of 0.7:1, is 200 feet above the horizontal floor of the stilling basin. The head on the crest is 30 feet and the maximum discharge is 480 cfs per foot of stilling basin width. Proportion a Type II stilling basin for these conditions.

Entering Figure 15 with a head of 30 feet over the crest and a total fall of 230 feet,

$$\frac{V_A}{V_T} = 0.92$$

The theoretical velocity $V_T = \sqrt{2g(230-\frac{30}{2})} = 117.6$ ft/sec

The actual velocity $V_A = V_1 = 117.6 \times 0.92 = 108.2$ ft/sec

$$D_1 = \frac{q}{V_1} = \frac{480}{108.2} = 4.44 \text{ feet}$$

The Froude number

$$F_1 = \frac{V_1}{\sqrt{gD_1}} = \frac{108.2}{\sqrt{32.2 \times 4.44}} = 9.04$$

Entering Figure 11 with a Froude number of 9.04, the solid line gives

$$\frac{TW}{D_1} = 12.3$$

As TW and $D_2$ are synonomous in this case, the conjugate tail water depth

$$D_2 = 12.3 \text{ x } 4.44 = 54.6 \text{ feet}$$

The minimum tail water line for the Type II basin on Figure 11 shows that a factor of safety of about 4 percent can be expected for the above Froude number.

Should it be desired to provide a margin of safety of 7 percent, the following procedure may be followed: Consulting the line for minimum TW depth for the Type II basin, Figure 11,

$$\frac{TW}{D_1} = 11.85 \text{ for a Froude number of } 9.04$$

The tail water depth at which sweepout is incipient:

$$T_{so} = 11.85 \text{ x } 4.44 = 52.6 \text{ feet}$$

Adding 7 percent to this figure, the stilling basin apron should be positioned for a tail water depth of

$$52.6 + 3.7 = 56.3 \text{ feet or } 1.03D_2$$

The length of basin can be obtained by entering the intermediate curve on Figure 12 with the Froude number of 9.04

$$\frac{L_{II}}{D_2} = 4.28$$

$$L_{II} = 4.28 \text{ x } 54.6 = 234 \text{ feet (see Figure 14)}$$

The height, width, and spacing of the chute blocks as recommended is $D_1$, thus the dimension can be 4 feet 6 inches.

The height of the dentated sill is $0.2D_2$ or 11 feet, while the width and spacing of the dentates can be $0.15D_2$ or 8 feet 3 inches.
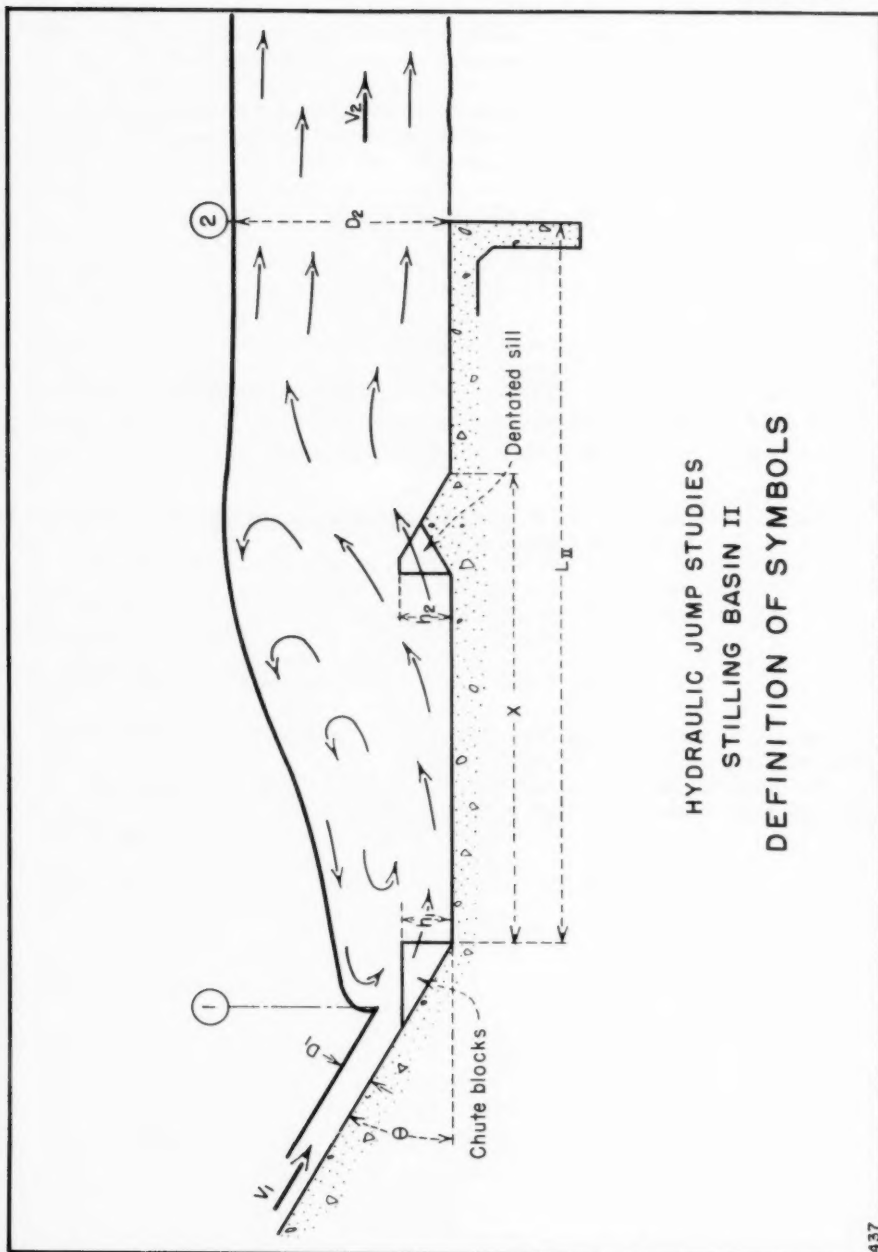
HYDRAULIC JUMP STUDIES
STILLING BASIN II
DEFINITION OF SYMBOLS

FIGURE 11



HYDRAULIC JUMP STUDIES
STILLING BASINS I, II AND III
MINIMUM TAILWATER DEPTHS
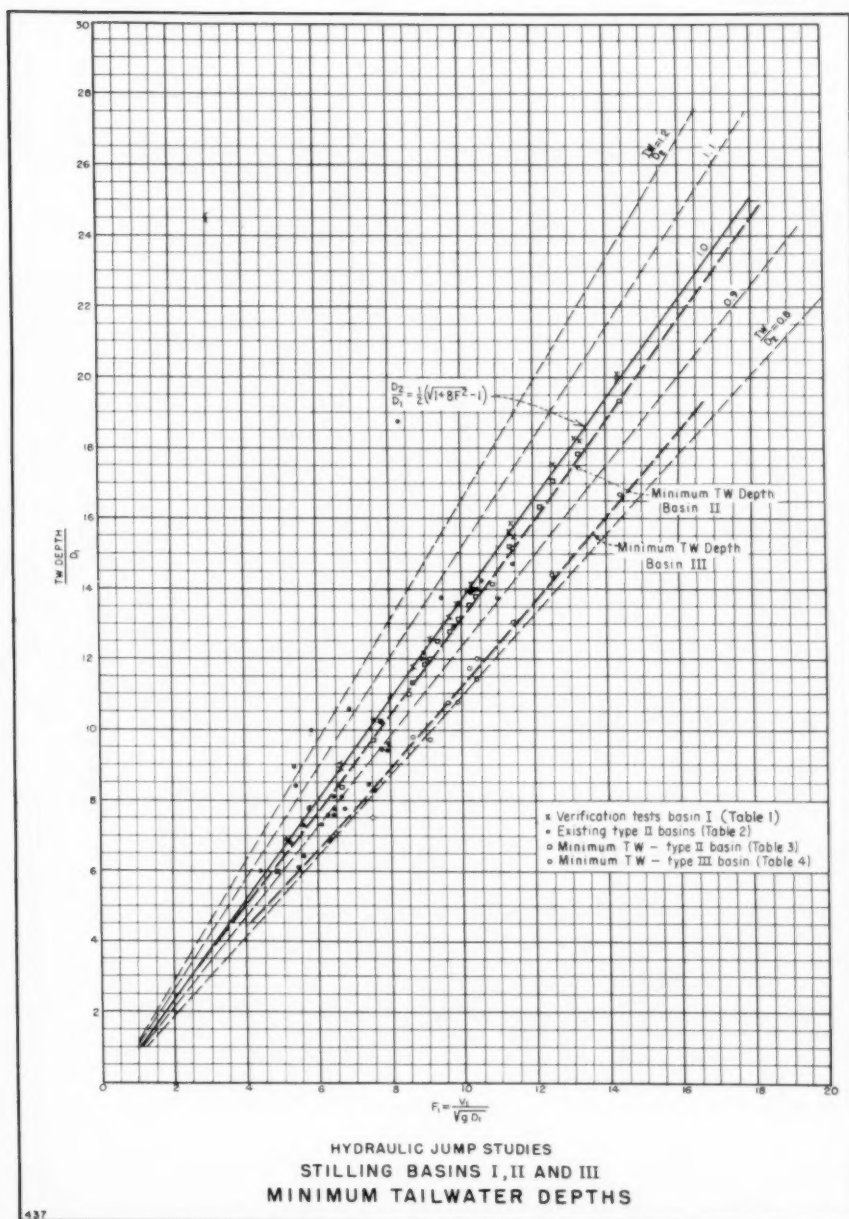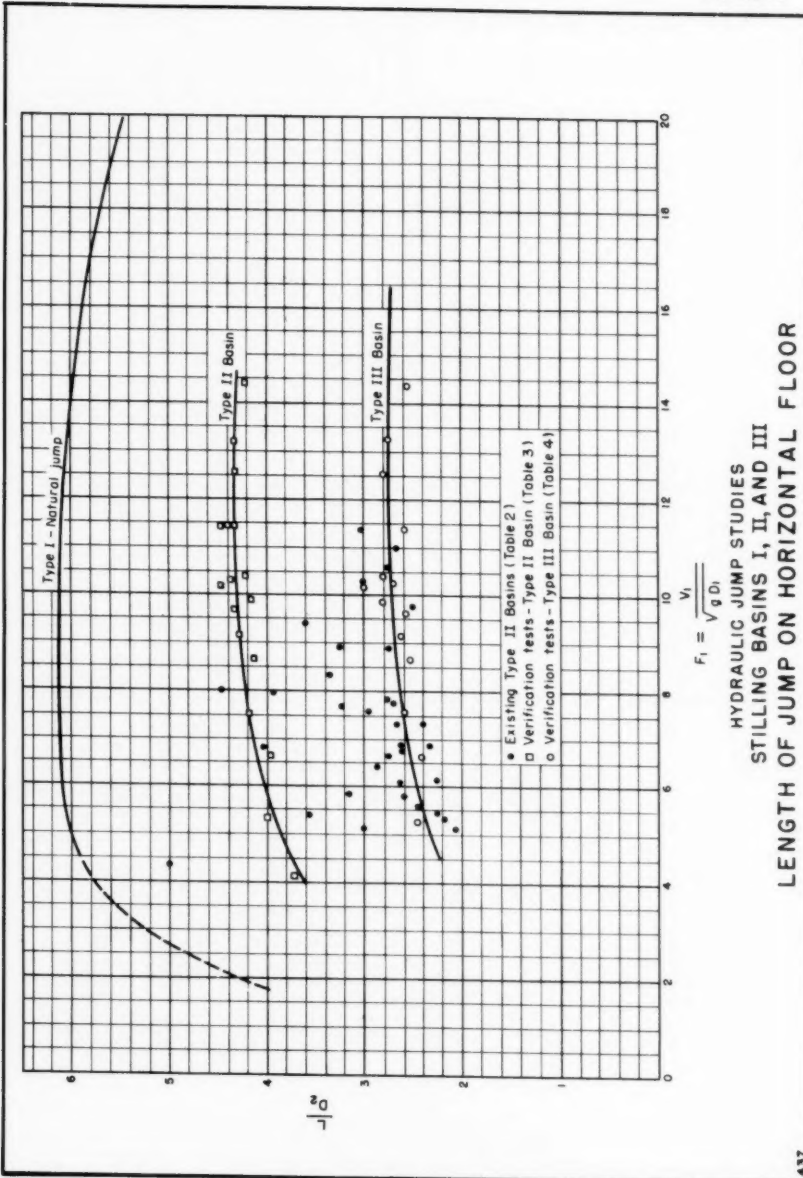
FIGURE 12



HYDRAULIC JUMP STUDIES
STILLING BASINS I, II, AND III
LENGTH OF JUMP ON HORIZONTAL FLOOR

FIGURE 13
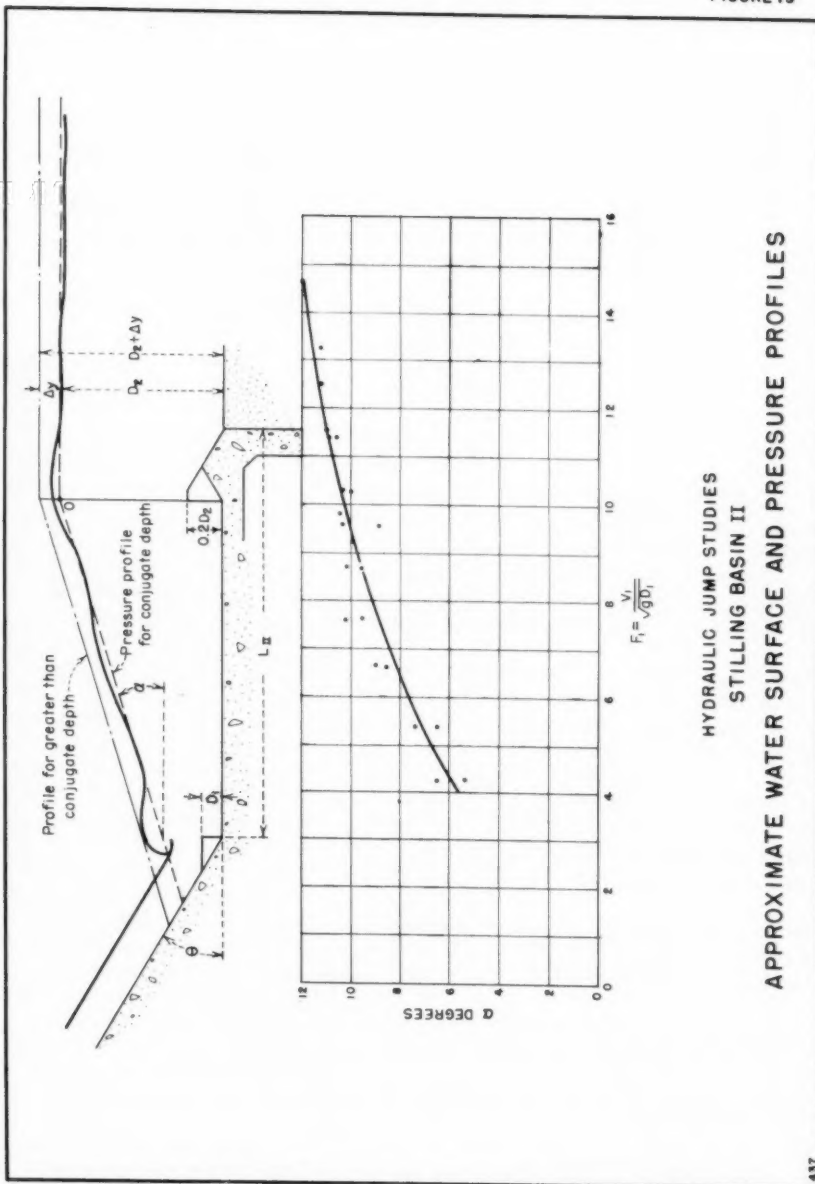


HYDRAULIC JUMP STUDIES
STILLING BASIN II

APPROXIMATE WATER SURFACE AND PRESSURE PROFILES

FIGURE 14
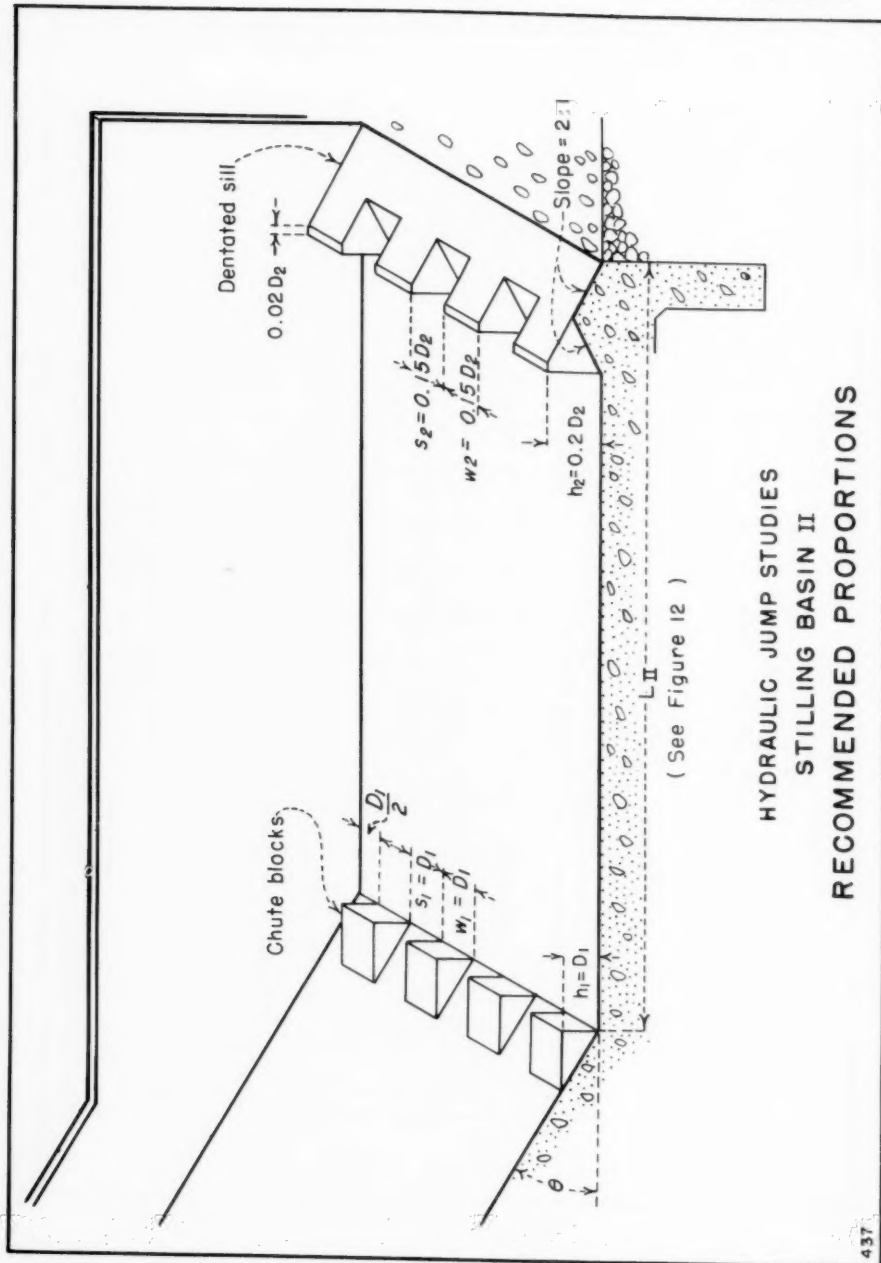


HYDRAULIC JUMP STUDIES

STILLING BASIN II

RECOMMENDED PROPORTIONS

Journal of the

# HYDRAULICS DIVISION

Proceedings of the American Society of Civil Engineers

## HYDRAULIC DESIGN OF STILLING BASINS: SHORT STILLING BASIN FOR CANAL STRUCTURES, SMALL OUTLET WORKS, AND SMALL SPILLWAYS (BASIN III)

J. N. Bradley[1] M. ASCE, and A. J. Peterka[2] M. ASCE
(Proc. Paper 1403)

### FOREWORD

This is one of a group of six papers on the hydraulic design of stilling basins and their associated appurtenances. Although original data from hydraulic models are presented in tabular form, the papers emphasize practical design procedures. Basin sizes and dimensions are given in easy-to-use dimensionless forms so that dependable stilling basins may be designed without the need for exceptional judgment or extensive experience. Sample problems are included.

The "Introduction" and "Experimental Equipment" are included in Paper 1401 but apply to all papers in this group. Paper 1401 is an academic study of the hydraulic jump on a flat floor. Useful information is presented concerning energy losses, applicability of the hydraulic jump formula, length of jump, and a new classification of the various types of jumps.

Paper 1402 covers the design of a short hydraulic jump stilling basin having an end sill and chute blocks. Paper 1403 describes a shorter stilling basin which utilizes baffle piers. In both papers information is given to determine the critical dimensions of the stilling basin, the tail water range, and the water surface profile in the basin.

Paper 1404 describes a special type of hydraulic jump basin for use when the Froude number of the incoming flow is low, and the jump produces waves in the downstream channel. An alternate design and two types of wave suppressors are also developed.

Paper 1405 describes the design of a stilling basin having a sloping apron. The extra tail water depth required and the merits of a sloping apron are evaluated, as is the basin length for a range of apron slopes.

Paper 1406 develops the design of impact basins for discharges up to 340

second feet and incoming velocities up to 30 feet per second. No tail water is
required. The bibliography in this paper applies to all papers in this group.

---

## ABSTRACT

Continuing the development in Paper 1402, this paper describes tests to
generalize the design of a shorter stilling basin containing chute blocks, end
sill, and one row of baffle piers. General design rules and sample problems
are included. Critical basin dimensions, water surface profiles, and tail
water ranges are presented in dimensionless forms.

---

## INTRODUCTION

Basin II (paper 1402) often is considered too conservative and consequently
overcostly for structures carrying relatively small discharges at moderate
velocities. In this Paper a minimum basin is developed for a class of smaller
structures in which the velocity at the entrance to the basin is moderate or
low (5 to 60 feet per second, corresponding to an overall head of about 100
feet). Further economies in basin length are accomplished with baffle piers.
Verification test results are used to determine the range over which Basin III
will operate satisfactorily, and to obtain data necessary to generalize the
design.

### Development

The most effective way to shorten a stilling basin is to modify the jump by
the addition of appurtenances in the basin. One restriction imposed on these
appurtenances, however, is that they must be self-cleaning or nonclogging.
This restriction thus limits the appurtenances to blocks or sills which can be
incorporated on the stilling basin apron.

Numerous experiments were therefore performed using various types and
arrangements of baffle piers and sills on the apron in an effort to obtain the
best possible solution. Some of the arrangements tested are shown on
Figure 16. The blocks were positioned in both single and double rows with
the second row staggered with respect to the first. Arrangement "a" on
Figure 16 consisted of a solid curved sill which was tried in several positions
on the apron. This sill required an excessive tail water depth to be effective.
The solid sill was then replaced with baffle piers. For certain heights,
widths, and spacing, block "b" performed quite well, resulting in a water sur-
face similar to that shown on Figure 19. Block "c" was ineffective for any
height. The velocity passed over the block at about a 45° angle, thus was not
impeded, and the water surface downstream was very turbulent with waves.
Stepped block "d," both for single and double rows, was much the same as
"c." The cube "e" was effective when the best height, width, spacing, and
position on the apron were found. The front of the jump was almost vertical
and the water surface downstream was quite flat and smooth, much like the
water surface shown on Figure 19. Block "f" performed identically with the

FIGURE 15

HYDRAULIC JUMP STUDIES
CURVES FOR DETERMINATION OF
VELOCITY ENTERING STILLING
BASIN FOR STEEP SLOPES
0.8:1 TO 0.6:1

PROTOTYPE TESTS
X Shasta Dam
O Grand Coulee Dam
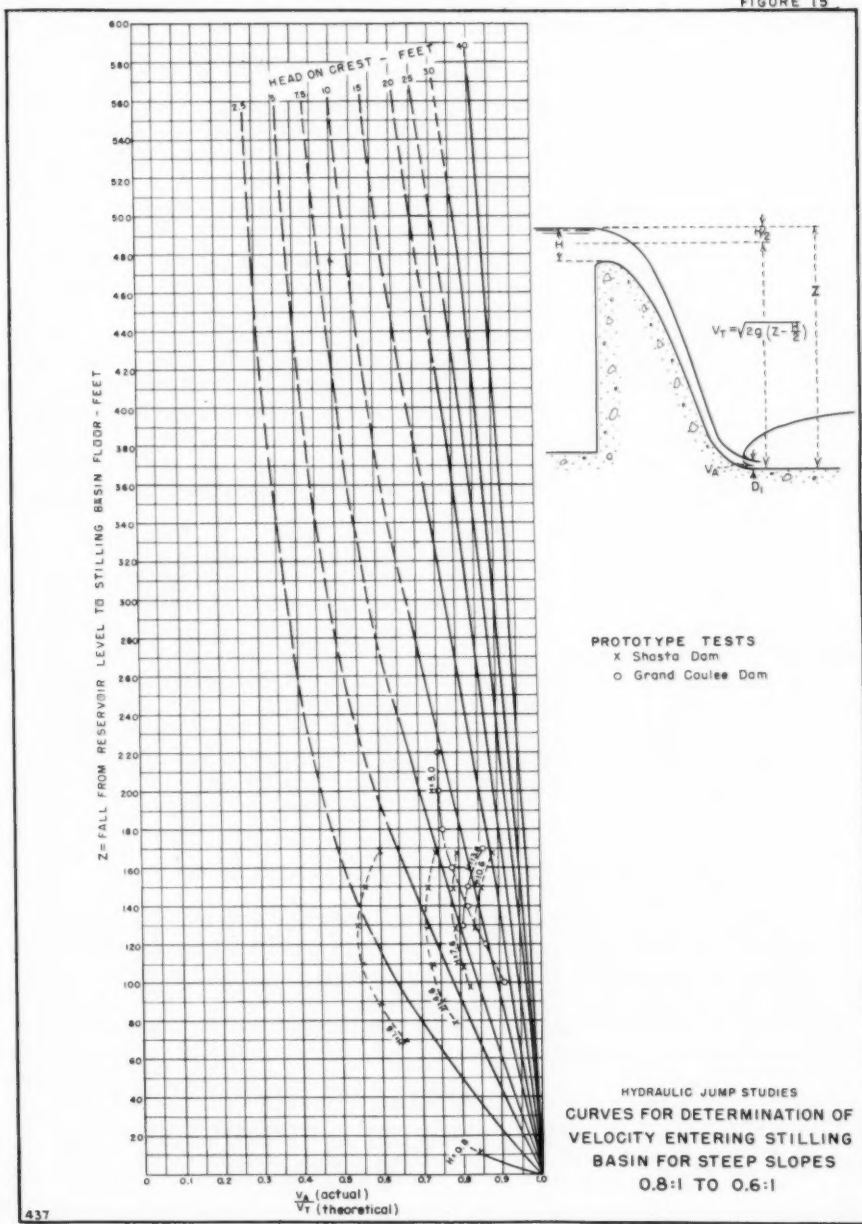
FIGURE 16
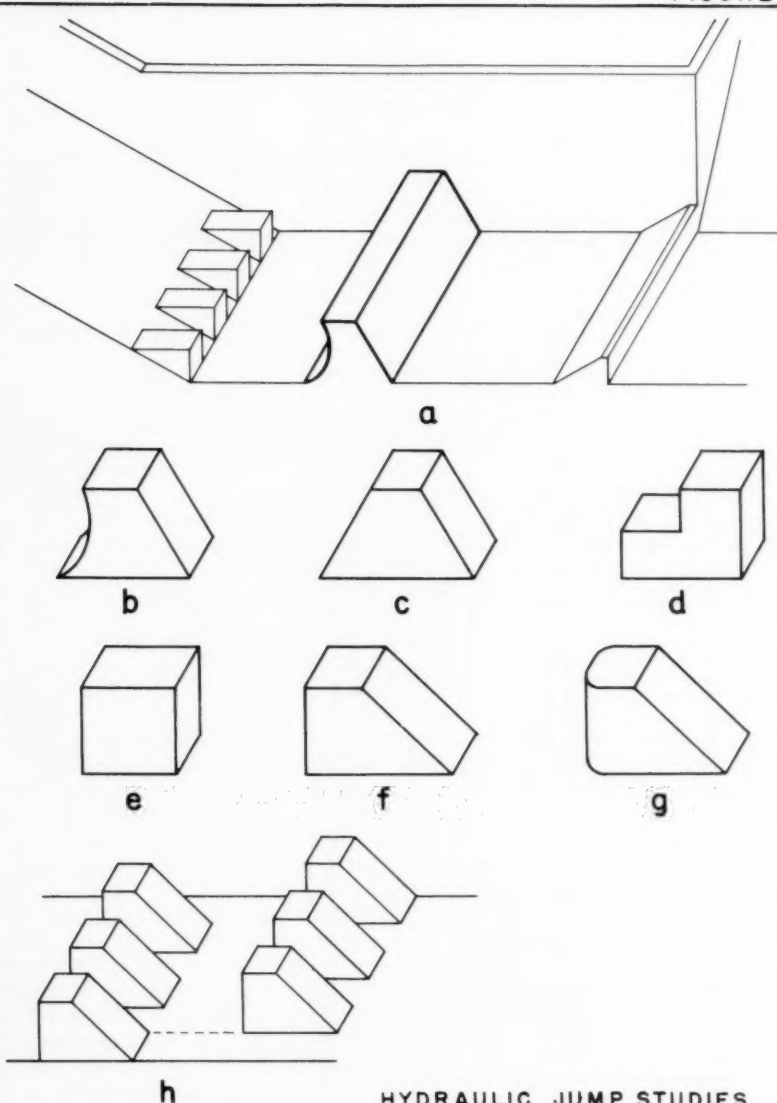


HYDRAULIC JUMP STUDIES

RECORD OF APPURTENANCES

BASIN III

cubical block "e." The important feature as to shape appeared to be the vertical upstream face. The foregoing blocks and others not mentioned here were all tested in single and double rows. The second row in each case was of little value, sketch "h," Figure 16.

Block "g" is the same as block "f" with the corners rounded. It was found that rounding the corners greatly reduced the effectiveness of the blocks. In fact a double row of blocks with rounded corners did not perform as well as a single row of blocks "b," "e," or "f." As block "f" is usually preferable from a construction standpoint, it was used throughout the remaining tests to determine a general design with respect to height, width, spacing, and position on the apron.

In addition to experimenting with the baffle piers, variations in the size and shape of the chute blocks and the end sill were also tested. It was found that the chute blocks should be kept small, no larger than $D_1$ if possible, to prevent the chute blocks from directing the flow over the baffle piers. The end sill had little or no effect on the jump proper when baffle piers are placed as recommended. Thus, there is no need for a dentated end sill and most any type of solid end sill will suffice. The basin as finally developed is shown on Figure 17. This basin is principally an impact dissipation device whereby the baffle piers are called upon to do most of the work. The chute blocks aid in stabilizing the jump and the solid type end sill is for scour control.

## Verification Tests

At the conclusion of the development work, a set of verification tests was made to examine and record the performance of this basin, which will be designated as Basin III, over the entire range of operating conditions that may be met in practice. The tests were made on a total of 14 basins constructed in Flumes B, C, D, and E. The conditions under which the tests were run, the dimensions of the basin, and the results are recorded in Table 4. The headings are identical with those of Table 3 except for the dimensions of the baffle piers and end sills. The additional symbols can be identified from Figure 18.

## Stilling Basin Performance and Design

Stilling basin action was quite stable for this design; in fact, more so than for either Basins I (paper 1401) or II (paper 1402), The front of the jump was steep and there was less wave action to contend with downstream than in either of the former basins. In addition, Basin III has a large factor of safety against jump sweepout and operates equally well for all values of the Froude number above 4.0. The verification tests served to show that Basin III was very satisfactory.

Basin III should not be used where baffle piers will be exposed to velocities above the 50 to 60 feet per second range without the full realization that cavitation and resulting damage may occur. For velocities above 50 feet per second Basin II or hydraulic model studies are recommended.

### Chute Blocks

The recommended proportions for Basin III are shown on Figure 18. The

FIGURE 17

HYDRAULIC JUMP STUDIES
STILLING BASIN III
RECOMMENDED PROPORTIONS
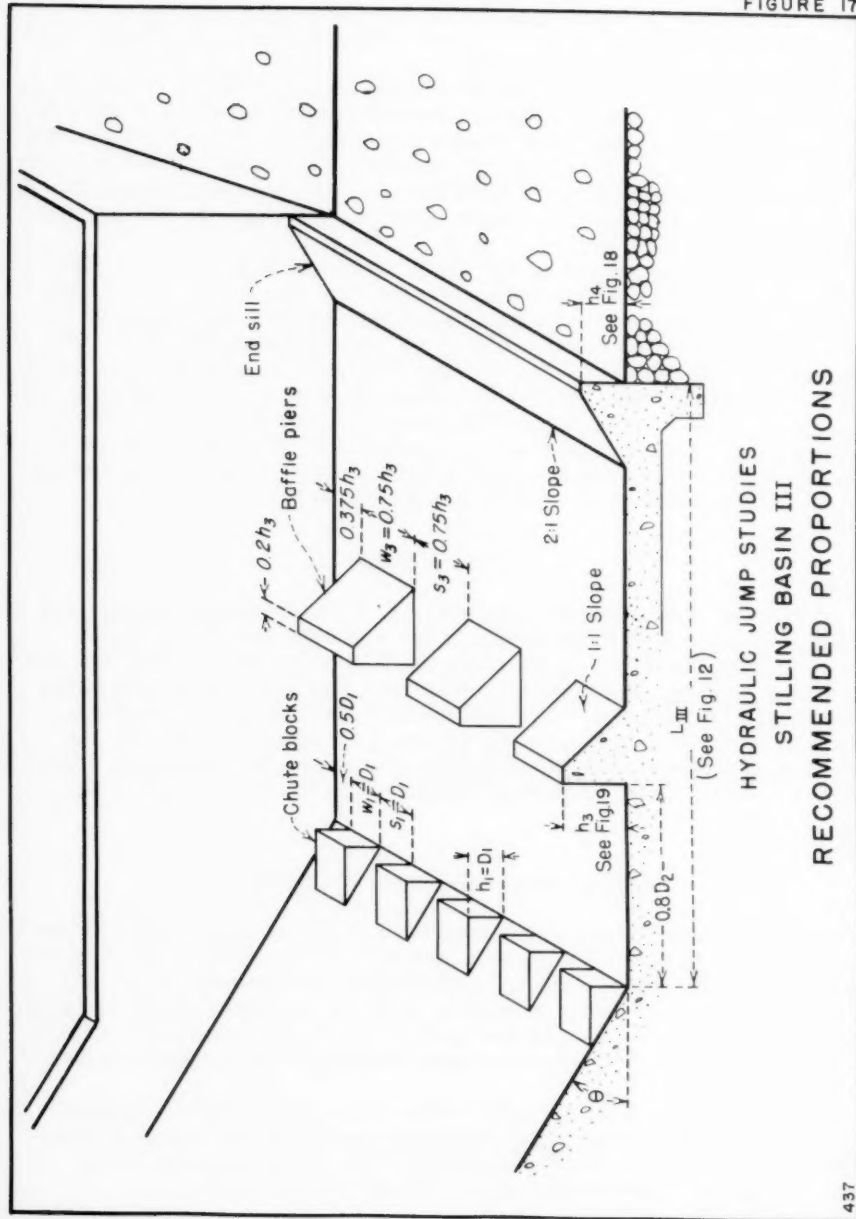
FIGURE 18
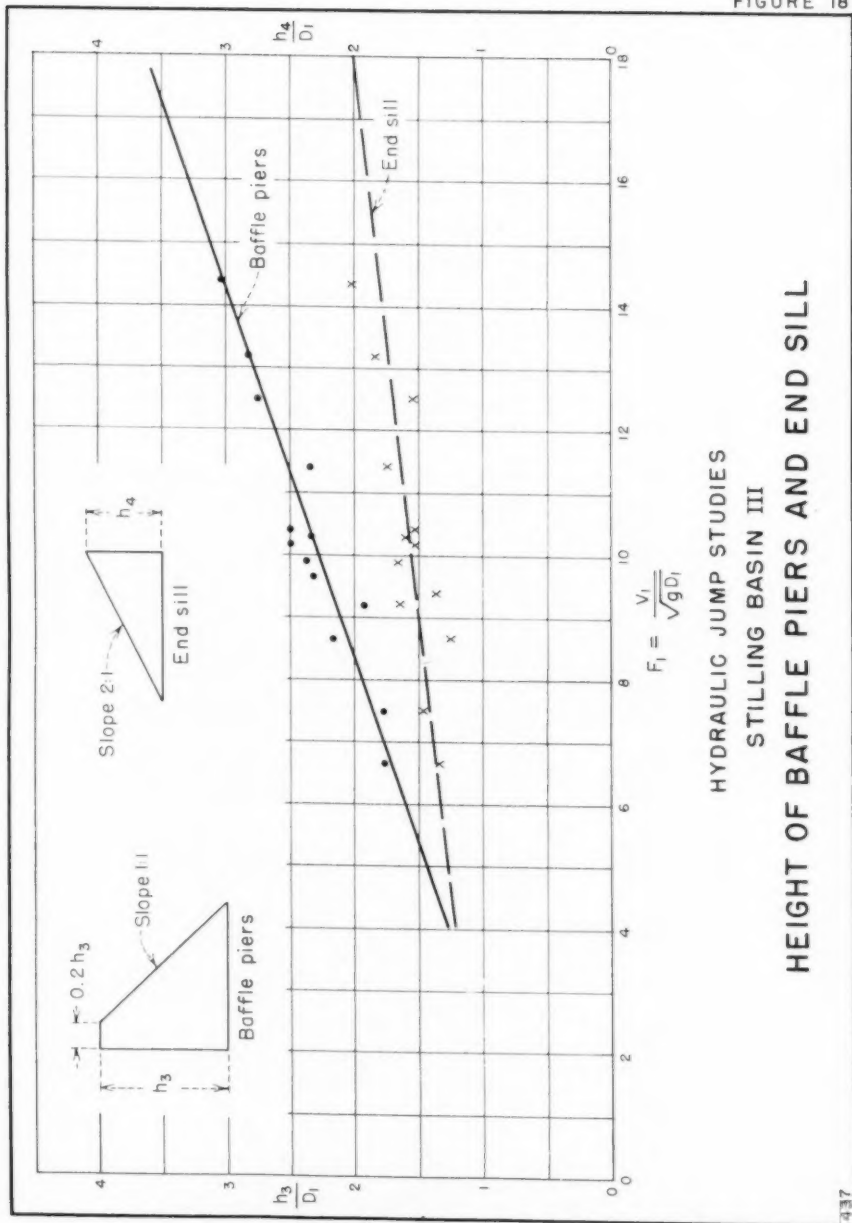


HYDRAULIC JUMP STUDIES
STILLING BASIN III
HEIGHT OF BAFFLE PIERS AND END SILL

$$F_1 = \frac{V_1}{\sqrt{g D_1}}$$

Table 2

MODEL RESULTS ON EXISTING TYPE II STILLING BASINS

| Dam | Max res el | TW el | Fall HW to TW ft | Basin floor el | Max Q cfs | W Width of basin, ft | q cfs/ft | $V_1$, ft/sec | $D_1$ ft | $F_1 = \dfrac{V_1}{\sqrt{gD_1}}$ | TW depth ft | $\dfrac{D_1}{\text{TW depth}}$ | $D_2$ (conj) ft | $\dfrac{\text{TW depth}}{D_2(\text{conj})}$ | L Basin length, ft | $\dfrac{L}{D_2(\text{conj})}$ | Slope of entry, ° | Chute blks Type | $h_1$ Ht ft |
|---|---|---|---|---|---|---|---|---|---|---|---|---|---|---|---|---|---|---|---|
| (1) | (2) | (3) | (4) | (5) | (6) | (7) | (8) | (9) | (10) | (11) | (12) | (13) | (14) | (15) | (16) | (17) | (18) | (19) | (20) |
| Rye Patch | 4123 | 4085.5 | 37.5 | 4062 | 20,000 | 110 | 182 | *53 | 3.40 | 5.15 | 23.5 | 6.81 | 22.5 | 1.04 | 46 | 2.04 | 33 | Solid | 4.0 |
| Unity | 3820 | 3771 | 49 | 3749 | 10,000 | 55.5 | 180 | 62 | 2.90 | 6.42 | 22 | 7.59 | 25.0 | 0.88 | 59 | 2.36 | 26.7 | Teeth | 3.5 |
| Alcova | 5500 | 5354 | 146 | 5309 | 55,000 | 150 | 367 | 98 | 3.75 | 8.88 | 45 | 12.00 | 45.5 | 0.97 | 125 | 2.75 | 25.0 | Solid | 4.3 |
| Shadow Mt | 8367 | 8332 | 35 | 8313 | 10,000 | 70 | 143 | 55 | 2.60 | 6.09 | 19 | 7.31 | 21.0 | 0.91 | 56 | 2.67 | 28 | T | 3.0 |
| Boysen (Final) | 4752 | 4628 | 124 | 4594 | 20,000 | 66 | 303 | 85 | 3.55 | 7.98 | 34 | 9.58 | 38.2 | 0.89 | 151 | 3.95 | 34 | T | 4.0 |
| Boysen (Prelm) | 4752 | 4646.5 | 105.5 | 4600 | 62,000 | 125 | 496 | 90 | 5.70 | 6.63 | 46.5 | 8.16 | 50.7 | 0.92 | 140 | 2.76 | 33.7 | T | 6.0 |
| Scofield | 7630 | 7583.6 | 46.4 | 7564 | 6,200 | 40 | 155 | 61 | 2.54 | 6.74 | 19.6 | 7.72 | 23.0 | 0.85 | 60 | 2.61 | 33.7 | T | 3.5 |
| Boca | 5605 | 5508 | 97 | 5487 | 8,000 | 75 | 107 | 73 | 1.47 | 10.53 | 21 | 14.28 | 21.2 | 0.99 | 58.6 | 2.66 | 26.7 | T | 4.0 |
| Fresno | 2591 | 2528 | 63 | 2499.5 | 51,000 | 190 | 268 | 70 | 3.85 | 7.40 | 28.5 | 7.40 | 32.0 | 0.89 | 85 | 2.66 | 33.7 | T | 4.0 |
| Bull Lake | 5805 | 5743.5 | 61.5 | 5725 | 33,000 | 100 | 100 | 59 | 1.70 | 7.97 | 18.5 | 10.88 | 18.3 | 1.01 | 75 | 4.10 | 14 | None | 4.5 |
| Caballo | 4182 | 4118 | 64 | 4086 | 33,000 | 108 | 306 | 72 | 4.22 | 6.29 | 32 | 7.58 | 35.0 | 0.92 | 78.2 | 2.23 | 26.7 | T | 2.6 |
| Moon Lake | 8137 | 8028.2 | 108.8 | 8005 | 10,000 | 75 | 133 | 74 | 1.80 | 9.74 | 23.2 | 12.90 | 23.8 | 0.98 | 60 | 2.52 | 26.7 | T | 3.0 |
| Deer Creek | 5417 | 5285 | 132 | 5260 | 12,000 | 75 | 160 | 86 | 1.87 | 11.00 | 25 | 13.37 | 28.0 | 0.89 | 75 | 2.68 | 26.7 | T | 8.0 |
| Alamogordo | 4275 | 4163 | 112 | 4118 | 56,000 | 110 | 509 | 96 | 5.30 | 7.33 | 45 | 8.49 | 52.0 | 0.87 | 125 | 2.40 | 26.7 | T | 8.0 |
| Enders | 3129.5 | 3057 | 73 | 3016 | 200,000 | 400 | 500 | 79 | 6.33 | 5.54 | 41 | 6.38 | 46.5 | 0.88 | 115 | 2.47 | 26.7 | T | 6.0 |
| Medicine Creek | 2408.9 | 2328 | 81 | 2287 | 97,800 | 262 | 373 | 80 | 6.32 | 5.55 | 41 | 7.31 | 47.0 | 0.87 | 125 | 2.66 | 26.7 | T | 6.75 |
| Cedar Bluff | 2192 | 2074.3 | 118 | 2035.5 | 87,400 | 200 | 437 | 93 | 4.68 | 7.60 | 39 | 8.33 | 48.0 | 0.81 | 141 | 2.94 | 18.5 | T | 7.0 |
| Falcon | 314.2 | 235 | 79 | 175 | 456,000 | 600 | 760 | 56 | 8.80 | 5.13 | 60 | 6.82 | 60.0 | 1.00 | 180 | 3.00 | 26.7 | T | 8.0 |
| Trenton | 2785 | 2700.6 | 84 | 2653 | 133,000 | 266 | 500 | 81 | 6.20 | 5.76 | 48 | 7.74 | 47.6 | 1.01 | 125 | 2.63 | 18.5 | T | 5.0 |
| Cachuma | 757.6 | 578.8 | 179 | 523 | 161,000 | 322 | 500 | 108 | 4.63 | 8.84 | 56 | 12.09 | 55.8 | 1.00 | 153 | 2.74 | 26.7 | T | 5.5 |

*Estimated hydraulic losses.

Table 2--Continued

| | (21) | (22) | (23) | (24) | (25) | (26) | (27) | (28) | (29) | (30) | (31) | (32) | (33) | (34) | (35) | (36) | (37) | (38) | (39) | (40) |
|---|---|---|---|---|---|---|---|---|---|---|---|---|---|---|---|---|---|---|---|---|
| Tiber | 2.51 | 5.0 | 0.71 | 1.0 | T | 1.0 | 8.0 | 0.21 | 5.0 | 0.62 | 1.0 | -- | -- | -- | -- | -- | -- | -- | R | Normal |
| Imperial Splwy | 0.90 | 2.49 | 1.02 | 1.03 | T | 1.0 | 3.75 | 0.20 | 3.27 | 1.01 | 1.0 | -- | -- | -- | -- | -- | -- | -- | R | 20° warp |
| Imperial Slcwy | 1.33 | 3.0 | 0.90 | 0.95 | T | 0.65 | 5.0 | 0.36 | 5.67 | 1.13 | 1.1 | -- | -- | -- | -- | -- | -- | -- | R | 20° warp |
| Grassy Lake | 1.05 | 1.67 | 1.67 | 1.0 | T | 1.0 | 2.0 | 0.14 | 1.33 | 0.66 | 1.0 | -- | -- | -- | -- | -- | -- | -- | R | Normal |
| Box Butte | 2.06 | 3.0 | 0.91 | 1.0 | T | 1.0 | 3.0 | 0.18 | 3.0 | 1.0 | 1.0 | -- | -- | -- | -- | -- | -- | -- | R | Normal |
| Siphon Drop | 1.50 | 2.25 | 1.0 | 1.0 | T | 1.0 | 3.25 | 0.29 | 2.25 | 0.69 | 1.0 | T | 0.72 | 3.25 | 0.28 | 2.25 | 1.44 | 1.0 | R | 45° warp |
| Pilot Knob | 1.56 | 2.5 | 1.0 | 1.0 | T | 1.0 | 5.0 | 0.28 | 5.0 | 1.0 | 1.0 | -- | -- | -- | -- | -- | -- | -- | R | 45° warp |
| AA Canal Drp[1] | 0.97 | 1.75 | 1.0 | 1.0 | Solid | 1.0 | 2.0 | 0.08 | -- | -- | -- | -- | -- | -- | -- | -- | -- | -- | R | 30° warp |
| Wasteway #2 | -- | -- | -- | -- | Solid | 1.0 | 2.0 | 0.12 | -- | -- | -- | T | 0.71 | 2.41 | 0.15 | 2.41 | 1.0 | 1.0 | R | 30° warp |
| Big Sandy #2 | 1.12 | 3.25 | 1.30 | 1.0 | T | 1.0 | 3.0 | 0.12 | 3.25 | 1.08 | 1.0 | T | 0.73 | 5.0 | 0.12 | 3.75 | 0.75 | 1.0 | T | Normal |
| Cherry Creek | -- | -- | -- | -- | Solid | 1.0 | 5.0 | 0.12 | -- | -- | -- | -- | -- | -- | -- | -- | -- | -- | R | None |
| Pine View | -- | -- | -- | -- | T | 0.91 | 10.0 | 0.19 | 6.0 | 1.20 | 1.0 | -- | -- | -- | -- | -- | -- | -- | T | Warp curv |
| Agency Valley | 0.83 | -- | -- | -- | T | 1.0 | 5.0 | 0.37 | 3.33 | 0.33 | 1.0 | -- | -- | -- | -- | -- | -- | -- | T | 50° warp |
| Davis | 1.96 | 13.0 | 0.91 | 1.86 | T | 1.0 | 14.3 | 0.23 | 13.0 | 0.91 | 1.86 | -- | -- | -- | -- | -- | -- | -- | R | Normal |
| Bonny | 1.94 | 5.0 | 0.72 | 1.0 | T | 1.0 | 8.0 | 0.21 | 5.0 | 0.62 | 1.0 | -- | -- | -- | -- | -- | -- | -- | R | Normal |
| Cle Elum | -- | -- | -- | -- | T | 1.0 | 10.0 | 0.33 | 10.0 | 1.0 | 1.0 | -- | -- | -- | -- | -- | -- | -- | R | None |
| Maximum | 2.72 | | 1.67 | 1.91 | | 1.0 | | 0.37 | | 1.25 | 1.91 | | 0.73 | | 0.28 | | 1.44 | 1.0 | | |
| Minimum | 0.81 | | 0.44 | 0.95 | | 0.65 | | 0.08 | | 0.33 | 1.00 | | 0.71 | | 0.12 | | 0.75 | 1.0 | | |
| Average | 1.35 | | 0.97 | 1.15 | | 0.97 | | 0.20 | | 0.76 | 1.13 | | 0.71 | | 0.12 | | | 1.0 | | |

R = Rectangular
T = Trapezoidal

Table 2--Continued

| Dam | $h_1/D_1$ (21) | $W_1$ Width ft (22) | $W_1/h_1$ (23) | $W_1/s_1$ (24) | Type (25) | Pos on apron $x_1/L_1$ (26) | $h_2$ Ht ft (27) | $h_2/D_2$ (28) | $W_2$ Width ft (29) | $W_2/h_2$ (30) | $W_2/s_2$ (31) | Type (32) | Pos on apron $x_1/L_1$ (33) | Ht ft (34) | $Ht/D_2$ (35) | Width ft (36) | Ht/Width (37) | Width/Spacing (38) | Type of basin (39) | Wing walls at end of basin (40) |
|---|---|---|---|---|---|---|---|---|---|---|---|---|---|---|---|---|---|---|---|---|
| | | Chute blks | | | | | End sill | | | | | | | Intermediate baffle blocks | | | | | | |
| Rye Patch | 1.18 | -- | -- | -- | Solid | 1.0 | 2.0 | 0.09 | -- | -- | -- | -- | -- | -- | -- | -- | -- | -- | R | 45° warp |
| Unity | 1.21 | 1.83 | 0.52 | 1.0 | Teeth | 0.93 | 5.5 | 0.22 | 2.17 | 0.39 | 1.0 | -- | -- | -- | -- | -- | -- | -- | R | Normal |
| Alcova | 1.15 | -- | -- | -- | T | 1.0 | 10.0 | 0.22 | 5.0 | 0.50 | 1.0 | -- | -- | -- | -- | -- | -- | -- | R | None |
| Shadow Mt | 1.16 | 4.0 | 1.33 | 1.78 | T | 1.0 | 3.5 | 0.17 | 4.0 | 1.14 | 1.78 | -- | -- | -- | -- | -- | -- | -- | R | Normal |
| Boysen (Final) | 1.13 | 5.25 | 1.31 | 1.75 | T | 0.68 | 8.75 | 0.23 | 5.25 | 0.60 | 1.75 | -- | -- | -- | -- | -- | -- | -- | R | None |
| Boysen (Prelm) | 1.05 | 7.5 | 1.25 | 1.8 | T | 1.0 | 8.0 | 0.16 | 7.5 | 0.94 | 1.8 | -- | -- | -- | -- | -- | -- | -- | R | None |
| Scofield | 1.38 | 3.5 | 1.0 | 1.91 | T | 1.0 | 4.0 | 0.17 | 3.5 | 0.88 | 1.91 | -- | -- | -- | -- | -- | -- | -- | R | Normal |
| Boca | 2.72 | 3.0 | 0.75 | 1.0 | T | 1.0 | 4.0 | 0.19 | 3.0 | 0.75 | 1.0 | -- | -- | -- | -- | -- | -- | -- | R | Normal |
| Fresno | 1.04 | 4.0 | 1.0 | 1.0 | T | 1.0 | 6.0 | 0.19 | 4.0 | 0.67 | 1.0 | -- | -- | -- | -- | -- | -- | -- | R | 45° warp |
| Bull Lake | -- | -- | -- | -- | T | 1.0 | 4.0 | 0.22 | 5.0 | 1.25 | 1.0 | -- | -- | -- | -- | -- | -- | -- | R | Normal |
| Caballo | 1.07 | 4.0 | 0.89 | 1.0 | T | 0.90 | 6.5 | 0.19 | 4.0 | 0.62 | 1.0 | -- | -- | -- | -- | -- | -- | -- | R | Normal |
| Moon Lake | 1.44 | 1.875 | 0.72 | 1.0 | T | 0.85 | 5.0 | 0.21 | 3.75 | 0.75 | 1.0 | -- | -- | -- | -- | -- | -- | -- | R | Normal |
| Deer Creek | 1.60 | 3.0 | 1.0 | 1.0 | T | 1.0 | 5.0 | 0.18 | 3.0 | 0.60 | 1.0 | -- | -- | -- | -- | -- | -- | -- | R | Normal |
| Alamogordo | 1.51 | 3.5 | 0.44 | 1.0 | T | 1.0 | 9.0 | 0.17 | 4.0 | 0.44 | 1.0 | -- | -- | -- | -- | -- | -- | -- | R | Normal |
| Enders | 0.95 | 5.0 | 0.83 | 1.0 | T | 1.0 | 12.0 | 0.26 | 5.0 | 0.42 | 1.0 | -- | -- | -- | -- | -- | -- | -- | R | Normal |
| Medicine Creek | 1.07 | 6.0 | 0.89 | 1.0 | T | 1.0 | 8.0 | 0.17 | 6.0 | 0.75 | 1.0 | -- | -- | -- | -- | -- | -- | -- | R | Normal |
| Cedar Bluff | 1.49 | 6.0 | 0.86 | 1.0 | T | 1.0 | 9.0 | 0.19 | 6.0 | 0.67 | 1.0 | -- | -- | -- | -- | -- | -- | -- | R | Normal |
| Falcon | 0.91 | 10.0 | 1.25 | 1.0 | T | 1.0 | 12.0 | 0.20 | 10.0 | 0.83 | 1.0 | -- | -- | -- | -- | -- | -- | -- | R | 45° vert |
| Trenton | 0.81 | 5.0 | 1.0 | 1.0 | T | 1.0 | 9.0 | 0.19 | 5.0 | 0.56 | 1.0 | -- | -- | -- | -- | -- | -- | -- | R | Normal |
| Cachuma | 1.19 | 5.08 | 0.92 | 1.0 | T | 1.0 | 12.0 | 0.21 | 5.08 | 0.42 | 1.0 | -- | -- | -- | -- | -- | -- | -- | R | Normal |

R = Rectangular

Table 2--Continued

| (1) | (2) | (3) | (4) | (5) | (6) | (7) | (8) | (9) | (10) | (11) | (12) | (13) | (14) | (15) | (16) | (17) | (18) | (19) | (20) |
|---|---|---|---|---|---|---|---|---|---|---|---|---|---|---|---|---|---|---|---|
| Tiber | 3014.9 | 2835.8 | 179 | 2797 | 54,250 | 200 | 271 | 97 | 2.79 | 10.26 | 39 | 13.98 | 39.0 | 1.00 | 117 | 3.25 | 18 | T | 7.0 |
| Imperial Splwy | 191 | 168 | 23 | 150 | 150,000 | 1197.5 | 125 | 49 | 2.60 | 5.44 | 16 | 6.16 | 18.5 | 0.87 | 41 | 2.22 | 14 | T | 2.33 |
| Imperial Slcvy | 181 | 155 | 26 | 140 | 24,000 | 248.3 | 97 | 38 | 2.50 | 4.31 | 15 | 6.00 | 14.0 | 1.07 | 69 | 4.93 | 14 | T | 3.33 |
| Grassy Lake | 7220 | 7100 | 110 | 7066 | 1,200 | 20 | 60 | 63 | 0.95 | 11.41 | 14 | 14.73 | 14.8 | 0.95 | 45 | 3.04 | 26.7 | T | 1.0 |
| Box Butte | 4014 | 3961 | 53 | 3946.5 | 2,500 | 40 | 62 | 56 | 1.60 | 7.84 | 15 | 9.37 | 16.9 | 0.89 | 50 | 2.96 | 22 | T | 3.3 |
| Siphon Drop | 169.7 | 150.7 | 19 | 136 | 2,000 | 33.5 | 60 | 40 | 1.50 | 5.80 | 15 | 10.0 | 11.5 | 1.30 | 36 | 3.13 | 22 | T | 2.25 |
| Pilot Knob | 170.26 | 124 | 46 | 94.5 | 13,155 | 140 | 94 | 59 | 1.60 | 8.34 | 30 | 18.7 | 18.0 | 1.67 | 60 | 3.33 | 18.5 | T | 2.5 |
| AA Canal Drp 1 | 43.6 | 29.2 | 14 | 13.3 | 8,700 | 118 | 74 | 40 | 1.80 | 5.32 | 16 | 8.89 | 12.5 | 1.28 | 27 | 2.16 | 22 | T | 1.75 |
| Wasteway #2 | 1185.75 | 1027.4 | 159 | 1014.9 | 2,100 | 40 | 52 | 92 | 0.60 | 22.00 | 12 | 21.4 | 16.5 | 0.73 | 45 | 2.73 | 24.7 | Vanes: | -- |
| Big Sandy #2 | 6761.3 | 6702 | 59 | 6679 | 7,500 | 50 | 150 | 66 | 2.24 | 7.70 | 23 | 10.26 | 23.3 | 0.99 | 75 | 3.57 | 33.7 | T | 2.5 |
| Cherry Creek | 5632.4 | 5558 | 74 | 5518 | 45,000 | 116 | 388 | 80 | 4.90 | 6.46 | 40 | 8.16 | 42.0 | 0.95 | 120 | 2.86 | 25 | None | -- |
| Pine View | 4870 | 4817 | 53 | 4785 | 9,000 | 40 | 225 | 59 | 3.80 | 5.42 | 32 | 8.42 | 27.0 | 1.19 | 96 | 3.55 | 33.7 | None | -- |
| Agency Valley | 3340 | 3266.5 | 74 | 3234 | 10,000 | 50 | 200 | 66 | 3.00 | 6.82 | 32 | 10.68 | 27.0 | 1.19 | 110 | 4.07 | 33.7 | Solid | 2.5 |
| Davis | 647 | 515.5 | 131 | 460 | 175,000 | 246 | 711 | 97 | 7.30 | 6.41 | 56 | 7.64 | 62.0 | 0.90 | 100 | 1.61 | 14 | T | 14.3 |
| Bonny | 3737.6 | 3623 | 114.6 | 3589 | 64,700 | 215 | 301 | 84 | 3.60 | 7.76 | 34 | 9.44 | 38.0 | 0.89 | 102 | 2.68 | 20 | T | 7.0 |
| Cle Elum | 2240 | 2130 | 110 | 2097 | 40,000 | 200 | 200 | 82 | 2.40 | 9.46 | | 13.74 | 30.0 | 1.10 | 108 | 3.60 | 33.7 | None | -- |
| Maximum | | | 179 | | | 1197.5 | 760 | 108 | 8.80 | 22.00 | 60 | 21.40 | 62.0 | 1.67 | 180 | 4.93 | 34 | | |
| Minimum | | | 14 | | | 20 | 52 | 38 | 0.60 | 4.31 | 12 | 6.00 | 11.5 | 0.73 | 27 | 1.61 | 14 | | |
| Average | | | 85 | | | | 265 | | | | | | | 0.99 | | 2.90 | | | |

### Table 3

#### VERIFICATION TESTS ON TYPE II STILLING BASIN

| Flume | Test | $Q$ cfs | $W$ Width of basin ft | $q$ per ft of W cfs | TW depth of W ft | $V_1$ ft/ sec | $D_1$ ft | $\dfrac{D_2}{D_1}$ | $F_1 = \dfrac{V_1}{\sqrt{gD_1}}$ | $L_{II}$ ft | $\dfrac{L_{II}}{D_2}$ | $T_{so}$ TW at sweep out ft |
|---|---|---|---|---|---|---|---|---|---|---|---|---|
| (1) | (2) | (3) | (4) | (5) | (6) | (7) | (8) | (9) | (10) | (11) | (12) | (13) |
| B | 1 | 2.50 | 2.00 | 1.25 | 1.120 | 17.36 | 0.072 | 15.60 | 11.39 | 4.95 | 4.42 | 1.09 |
|   | 2 | 4.00 |   | 2.00 | 1.430 | 17.54 | .114 | 12.54 | 9.16 | 6.10 | 4.27 | 1.37 |
|   | 3 | 6.00 |   | 3.00 | 1.750 | 17.65 | .170 | 10.29 | 7.54 | 7.30 | 4.17 | 1.65 |
|   | 4 | 8.00 |   | 4.00 | 2.030 | 17.86 | .224 | 9.06 | 6.64 | 8.00 | 3.94 | 1.88 |
| C | 5 | 1.60 | 1.50 | 1.07 | 1.070 | 17.49 | .061 | 17.54 | 12.48 | 4.60 | 4.30 | 1.04 |
|   | 6 | 2.10 |   | 1.40 | 1.240 | 17.94 | .078 | 15.89 | 11.32 | 5.40 | 4.35 | 1.18 |
|   | 7 | 2.63 |   | 1.75 | 1.355 | 18.26 | .096 | 14.11 | 10.39 | 5.70 | 4.21 | 1.32 |
|   | 8 | 2.75 |   | 1.83 | 1.400 | 18.33 | .100 | 14.00 | 10.21 | 6.23 | 4.45 | 1.36 |
|   | 9 | 4.00 |   | 2.67 | 1.785 | 20.36 | .131 | 13.62 | 9.91 | 7.40 | 4.15 | 1.73 |
| D | 10 | 5.00 | 3.97 | 1.26 | 1.235 | 20.30 | .062 | 19.91 | 14.38 | 5.10 | 4.13 | 1.20 |
|   | 11 | 6.00 |   | 1.51 | 1.350 | 20.41 | .074 | 18.24 | 13.21 | 5.80 | 4.30 | 1.32 |
|   | 12 | 9.80 |   | 2.47 | 1.750 | 21.84 | .113 | 15.50 | 11.45 | 7.80 | 4.46 | 1.73 |
|   | 13 | 11.00 |   | 2.77 | 1.855 | 21.15 | .131 | 14.16 | 10.29 | 8.10 | 4.37 | 1.82 |
|   | 14 | 13.00 |   | 3.27 | 2.020 | 21.39 | .153 | 13.20 | 9.64 | 8.70 | 4.31 | 1.95 |
|   | 15 | 20.00 |   | 5.04 | 2.585 | 23.00 | .319 | 11.80 | 8.66 | 10.60 | 4.10 | 2.48 |
| E | 16 | 5.00 | 3.97 | 1.26 | 0.840 | 10.49 | .120 | 7.00 | 5.33 | 3.36 | 4.00 | 0.79 |
|   | 17 | 10.00 |   | 2.52 | 1.220 | 11.09 | .227 | 5.37 | 4.10 | 4.51 | 3.70 | 1.10 |

Table 3--Continued

| Flume | Test | $\dfrac{T_{so}}{D_1}$ | $\dfrac{T_{so}}{D_2}$ | $\dfrac{h_1}{Ht}$ ft | $\dfrac{h_1}{D_1}$ | $\dfrac{W_1}{h_1}$ | $\dfrac{s_1}{h_1}$ | $h_2$ Ht den-tated sill ft | $\dfrac{h_2}{D_2}$ | $\dfrac{W_2}{h_2}$ | $\dfrac{s_2}{h_2}$ | Slope: water sur-face ° | Slope of Chute |
|---|---|---|---|---|---|---|---|---|---|---|---|---|---|
| | | (14) | (15) | (16) | (17) | (18) | (19) | (20) | (21) | (22) | (23) | (24) | (25) |
| 3 | 1 | 15.13 | 0.97 | 0.073 | 1.01 | 1.0 | 1.0 | 0.219 | 0.196 | 0.75 | 0.75 | 10.5 | 0.7:1 |
| | 2 | 12.02 | .96 | .114 | 1.00 | 1.0 | 1.0 | .286 | .200 | 0.75 | 0.75 | 10.0 | |
| | 3 | 9.70 | .94 | .170 | 1.00 | 1.0 | 1.0 | .352 | .201 | 0.75 | 0.75 | 9.6 | |
| | 4 | 8.39 | .93 | .229 | 1.02 | 1.0 | 1.0 | .406 | .200 | 0.75 | 0.75 | 9.0 | |
| C | 5 | 17.04 | .97 | .062 | 1.02 | 1.0 | 1.0 | .320 | .300 | 0.75 | 0.75 | 11.3 | 2:1 |
| | 6 | 15.12 | .95 | .078 | 1.00 | 1.0 | 1.0 | .260 | .210 | 0.75 | 0.75 | 10.8 | |
| | 7 | 13.75 | .97 | .105 | 1.09 | 1.0 | 1.0 | .250 | .185 | 0.75 | 0.75 | 10.5 | |
| | 8 | 13.60 | .97 | .100 | 1.00 | 1.0 | 1.0 | .310 | .221 | 0.75 | 0.75 | 10.0 | |
| | 9 | 13.21 | .97 | .131 | 1.00 | 1.0 | 1.0 | .446 | .250 | 0.75 | 0.75 | 10.4 | |
| D | 10 | 19.35 | .97 | .062 | 1.00 | 1.0 | 1.0 | .250 | .203 | 1.00 | 1.00 | 12.0 | 0.6:1 |
| | 11 | 17.83 | .98 | .074 | 1.00 | 1.0 | 1.0 | .270 | .200 | 1.00 | 1.00 | 11.2 | |
| | 12 | 15.31 | .99 | .153 | 1.35 | 1.0 | 1.0 | .400 | .229 | 1.00 | 1.00 | 10.0 | |
| | 13 | 13.89 | .98 | .131 | 1.00 | 1.0 | 1.0 | .396 | .214 | 0.75 | 0.75 | 10.2 | |
| | 14 | 12.75 | .97 | .153 | 1.00 | 1.0 | 1.0 | .400 | .198 | 0.75 | 0.75 | 8.3 | |
| | 15 | 11.32 | .96 | .219 | 1.00 | 1.0 | 1.0 | .517 | .200 | 0.75 | 0.75 | 9.5 | |
| E | 16 | 6.58 | .94 | .122 | 1.02 | 1.0 | 1.0 | .200 | .238 | 0.75 | 0.75 | 6.5 | Varied |
| | 17 | 9.02 | .90 | .235 | 1.04 | 1.0 | 1.0 | .270 | .221 | 0.75 | 0.75 | 5.3 | |

## Table 4

## VERIFICATION TESTS ON TYPE III STILLING BASIN

| Flume | Test | $Q$ cfs | $W$ | $q$ per ft of $W$ | $TW$ ft | $V_1$ ft/sec | $D_1$ ft | $\frac{D_2}{D_1}$ | $F_1 = \frac{V_1}{\sqrt{gD_1}}$ | $L_{III}$ ft | $\frac{L_{III}}{D_2}$ | $T_{so}$: TW at sweep out ft | $\frac{T_{so}}{D_1}$ | $\frac{T_{so}}{D_2}$ | Slope of Chute |
|---|---|---|---|---|---|---|---|---|---|---|---|---|---|---|---|
| (1) | (2) | (3) | (4) | (5) | (6) | (7) | (8) | (9) | (10) | (11) | (12) | (13) | (14) | (15) | (16) |
| B | 1 | 2.500 | 2.000 | 1.250 | 1.120 | 17.36 | 0.072 | 15.56 | 11.41 | 2.90 | 2.59 | 0.94 | 13.05 | 0.84 | 0.7:1 |
|   | 2 | 4.000 |       | 2.000 | 1.430 | 17.54 | .114  | 12.54 | 9.16  | 3.70 | 2.59 | 1.11 | 9.73  | .78  |       |
|   | 3 | 6.000 |       | 3.000 | 1.750 | 17.65 | .170  | 10.29 | 7.54  | 4.50 | 2.57 | 1.29 | 7.58  | .74  |       |
|   | 4 | 8.000 |       | 4.000 | 2.030 | 17.86 | .224  | 9.06  | 6.64  | 4.90 | 2.41 | 1.57 | 7.00  | .77  |       |
| C | 5 | 1.600 | 1.500 | 1.067 | 1.070 | 17.49 | .061  | 17.54 | 12.48 | 3.00 | 2.80 | 0.88 | 14.42 | .82  | 2:1 |
|   | 6 | 2.630 |       | 1.753 | 1.350 | 18.26 | .096  | 14.06 | 10.39 | 3.80 | 2.81 | 1.16 | 12.08 | .86  |       |
|   | 7 | 2.750 |       | 1.833 | 1.400 | 18.33 | .100  | 14.00 | 10.21 | 4.20 | 3.00 | 1.17 | 11.70 | .84  |       |
|   | 8 | 4.000 |       | 2.667 | 1.785 | 20.36 | .131  | 13.62 | 9.91  | 5.00 | 2.80 | 1.42 | 10.84 | .8C  |       |
| D | 9 | 5.000 | 3.970 | 1.259 | 1.250 | 20.30 | .062  | 20.16 | 14.38 | 3.20 | 2.56 | 1.04 | 16.77 | .83  | 0.6:1 |
|   | 10| 6.000 |       | 1.511 | 1.350 | 20.41 | .074  | 18.24 | 13.21 | 3.70 | 2.74 | 1.12 | 15.13 | .83  |       |
|   | 11| 11.00 |       | 2.771 | 1.860 | 21.15 | .131  | 14.20 | 10.29 | 5.00 | 2.69 | 1.50 | 11.45 | .81  |       |
|   | 12| 13.00 |       | 3.274 | 2.020 | 21.40 | .153  | 13.20 | 9.64  | 5.20 | 2.57 | 1.65 | 10.78 | .82  |       |
|   | 13| 20.00 |       | 5.038 | 2.585 | 23.00 | .219  | 11.80 | 8.66  | 6.46 | 2.50 | 2.15 | 9.82  | .83  |       |
| E | 14| 5.000 | 3.970 | 1.259 | 0.840 | 10.49 | .120  | 7.00  | 5.33  | 2.10 | 2.50 | 0.70 | 5.83  | .83  | Varied |

Table 4--Continued

| Flume | Test | Ht of chute blks: h₃ ft (17) | h₁/D₁ (18) | W₁/h₁ (19) | s₁/h₁ (20) | Ht of baffle piers: h₃ ft (21) | h₃/D₁ (22) | W₃/h₃ (23) | s₃/h₃ (24) | Distance to baffles ft (25) | LIII/3D₂ (26) | Ht of end sill: h₄ ft (27) | h₄/D₁ (28) | Depth upstream from baffles ft (29) | Z/D₂ (30) |
|---|---|---|---|---|---|---|---|---|---|---|---|---|---|---|---|
| B | 1 | 0.073 | 1.01 | 1.0 | 1.0 | 0.167 | 2.32 | 1.0 | 1.0 | 0.800 | 0.714 | 0.125 | 1.74 | 0.50 | 0.54 |
|   | 2 | .114 | 1.00 | 1.0 | 1.0 | .218 | 1.91 | 1.0 | 1.0 | 0.920 | .643 | .187 | 1.64 | 0.80 | .56 |
|   | 3 | .333 | 1.96 | 0.6 | 0.6 | .302 | 1.78 | 1.0 | 1.0 | 1.200 | .686 | .250 | 1.47 | 0.95 | .54 |
|   | 4 | .229 | 1.02 | 1.0 | 1.0 | .396 | 1.77 | 1.0 | 1.0 | 1.340 | .660 | .302 | 1.35 | 1.20 | .59 |
| C | 5 | .062 | 1.02 | 1.0 | 1.0 | .167 | 2.74 | 0.75 | 0.75 | 0.850 | .794 | .092 | 1.51 | 0.60 | .56 |
|   | 6 | .100 | 1.04 | 1.0 | 1.0 | .240 | 2.50 | 0.75 | 0.75 | 1.000 | .741 | .146 | 1.52 | 0.65 | .48 |
|   | 7 | .146 | 1.46 | 1.0 | 1.0 | .250 | 2.50 | 0.75 | 0.75 | 1.210 | .864 | .156 | 1.56 | 0.70 | .50 |
|   | 8 | .187 | 1.43 | 0.75 | 0.75 | .312 | 2.38 | 0.75 | 0.75 | 1.430 | .801 | .219 | 1.67 | 0.90 | .50 |
| D | 9 | .062 | 1.00 | 1.0 | 1.0 | .188 | 3.03 | 1.0 | 1.0 | 1.000 | .800 | .125 | 2.02 | 0.60 | .48 |
|   | 10 | .083 | 1.12 | 1.0 | 1.0 | .208 | 2.81 | 1.0 | 1.0 | 1.120 | .830 | .135 | 1.82 | 0.65 | .48 |
|   | 11 | .135 | 1.03 | 1.0 | 1.0 | .302 | 2.31 | 1.0 | 1.0 | 1.250 | .672 | .208 | 1.59 | 0.95 | .51 |
|   | 12 | .156 | 1.02 | 1.0 | 1.0 | .354 | 2.31 | 1.0 | 1.0 | 1.680 | .832 | .208 | 1.36 | 1.05 | .52 |
|   | 13 | .219 | 1.00 | 1.0 | 1.0 | .479 | 2.19 | 0.75 | 0.75 | 2.153 | .833 | .271 | 1.24 | 1.30 | .50 |
| E | 14 | .122 | 1.02 | 1.0 | 1.0 | .215 | 1.79 | 0.75 | 0.75 | 0.672 | .833 | .150 | 1.25 | 0.55 | .65 |

height, width, and spacing of the chute blocks are equal to $D_1$, the same as was recommended for Basin II (paper 1402). Larger heights were tried, as can be observed from Column 18, Table 4, but are not recommended. The larger chute blocks tend to throw a portion of the high-velocity jet over the baffle piers. Some cases will be encountered in design, however, where $D_1$ is less than 8 inches. In such cases the blocks may be made 8 inches high, which is considered by some designers to be the minimum size possible from a construction standpoint. The width and spacing are the same as the height, but this may be varied so long as the aggregate width of spaces approximately equals the total width of the blocks.

## Baffle Piers

The height of the baffle piers increases with the Froude number as can be observed from Columns 22 and 10, Table 4. The height, in terms of $D_1$, can be obtained from the upper line on Figure 18. The width and spacing may be varied but the total of the spaces should equal the total width of blocks. The most satisfactory width and spacing was found to be three-fourths of the height. It is not necessary to stagger the baffle piers with the chute blocks as this is often difficult and there is little to be gained from a hydraulic standpoint.

The most effective position of the baffle piers is $0.8D_2$ downstream from the chute blocks as shown in Figure 17. The actual positions used in the verification tests are shown in Column 25, Table 4. The recommended position, height and spacing of the baffle piers on the apron should be adhered to carefully, as these dimensions are important. For example, if the blocks are set appreciably upstream from the position shown they will produce a cascade with resulting wave action. On the other hand, if the baffles are set farther downstream than shown, a longer basin will be required. Likewise, if the baffles are too high they can produce a cascade, while if too low a rough water surface will result. It is not the intention to give the impression that the position or height of the baffle blocks are critical. Their position or height are not critical so long as the above proportions are followed. There exists a reasonable amount of leeway in all directions; however, one cannot place the baffle piers on the pool floor at random and expect anything like the excellent action associated with the Type III basin.

The baffle piers may be in the form shown on Figure 17, or they may be cubes; either shape is effective. The corners of the baffle blocks should not be rounded, as the sharp edges are effective in producing eddies which in turn aid in the dissipation of energy. Small chambers on the pier edges are permissible.

## End Sill

The height of the solid end sill is also shown to vary with the Froude number although there is nothing critical about this dimension. The heights of the sills used in the verification tests are shown in Columns 27 and 28 of Table 4. The height of the end sill in terms of $D_1$ is plotted with respect to the Froude number and shown as the lower line on Figure 18. A slope of 2:1 was used throughout the tests since previous sill experiments had showed that minimum wave heights and erosion could be expected with this slope.

Tail Water Depth

As in the case of Basin II (paper 1402), full conjugate depth, measured above the apron, is also recommended for Basin III. There are several reasons for this: First, the best operation for this stilling basin occurs at full conjugate tail water depth; secondly, if less than the conjugate depth is used, the surface velocities leaving the pool are high, the jump action is impaired, and there is a greater chance for scour downstream; and thirdly, if the baffle blocks erode with time, the additional tail water depth will serve to lengthen the interval between repairs. On the other hand, there is no hydraulic advantage in using greater than the conjugate depth, as the action in the pool will show little or no improvement. The same precautions should be considered when determining the tail water for Basin III that were discussed for Basin II, (paper 1402).

The margin of safety for Basin III varies from 15 to 18 percent depending on the value of the Froude number, as can be observed by the dashed line labeled "Minimum Tail Water Depth—Basin III," on Figure 11. The points, from which the line was drawn, were obtained from the verification tests, Columns 10 and 14, Table 4. Again, this line does not represent complete sweepout, but the point at which the front of the jump moves away from the chute blocks and the basin no longer functions properly. In special cases it may be necessary to encroach on this wide margin of safety, however, it is not advisable as a general rule for the reasons stated above.

Length of Basin

The length of Basin III, which is related to the Froude number, can be obtained by consulting the lower curve of Figure 12, (paper 1402). The points, indicated by circles, were obtained from Columns 10 and 12, Table 4, and indicate the extent of the verification tests. The length is measured from the downstream end of the chute blocks to the downstream end of the end sill, Figure 17. Although this curve was determined conservatively, it will be found that the length of Basin III is less than one-half the length needed for a basin without appurtenances. Basin III, as was true of Basin II, may be effective for values of the Froude number as low as 4.5, thus the length curve was terminated at this value.

Water Surface and Pressure Profiles

Approximate water-surface profiles were obtained for Basin III during the verification tests. The front of the jump was so steep, Figure 19, that only two measurements were necessary; the tail water depth and the depth upstream from the baffle piers. The tail water depth is shown in Column 6 and the upstream depth is recorded in Column 29 of Table 4. The ratio of the upstream depth to conjugate depth is shown in Column 30. As can be observed, the ratio is much the same regardless of the value of the Froude number. The average of the ratios in Column 30 is 0.52. Thus it will be assumed that the depth upstream from the baffle blocks is one-half the tail water depth.

The profile represented by the crosshatched area, Figure 19, is for conjugate tail water depth. For a greater tail water depth, $D_z$, the upstream depth would be $\frac{D_z}{2}$. For a tail water depth less than conjugate, $D_y$, the upstream depth would be approximately $\frac{D_y}{2}$. There appears to be no particular

FIGURE 19
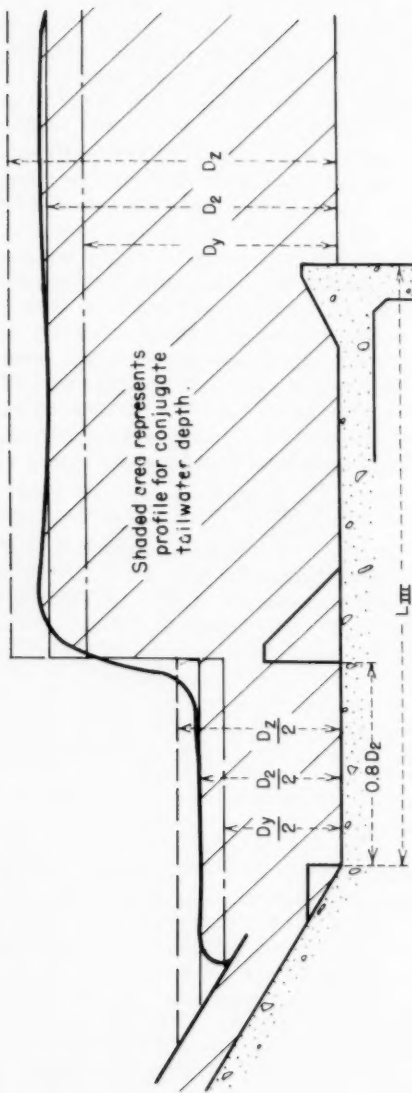


HYDRAULIC JUMP STUDIES
STILLING BASIN III
APPROXIMATE WATER SURFACE AND PRESSURE PROFILES

significance in the fact that this ratio is one-half.

The information on Figure 19 applies only to Basin III, proportioned according to the rules set forth. It can be assumed that for all practical purposes the pressure and water-surface profiles are the same. There will be a localized increase in pressure on the apron immediately upstream from each baffle block but this has been taken into account, more or less, by extending the diagram to full tail water depth beginning at the upstream face of the baffle blocks.

### Recommendations

The following rules pertain to the design of the Type III basin, Figure 17:

1. The stilling basin operates best at full conjugate tail water depth, $D_2$. A reasonable factor of safety is inherent in the conjugate depth for all values of the Froude number (Figure 11, paper 1402) and it is recommended that this margin of safety not be encroached upon.

2. The length of pool, which is less than one-half the length of the natural jump, can be obtained by consulting the curve for Basin III in Figure 12, (paper 1402). As a reminder, an excess of tail water depth does not substitute for pool length or vice versa.

3. Stilling Basin III may be effective for values of the Froude number as low as 4.0 but this cannot be stated for certain (consult Paper 1404 for values under 4.5).

4. Height, width, and spacing of chute blocks should equal the average depth of flow entering the basin, or $D_1$. Width of blocks may be decreased, provided spacing is reduced a like amount. Should $D_1$ prove to be less than 8 inches, make the blocks 8 inches high.

5. The height of the baffle piers varies with the Froude number and is given on Figure 18. The blocks may be cubes or they may be constructed as shown on Figure 17; the upstream face should be vertical and in one plane. The vertical face is important. The width and spacing of baffle piers are also shown on Figure 17. In narrow structures where the specified width and spacing of blocks do not appear practical, block width and spacing may be reduced, provided they are reduced a like amount. A half space is recommended adjacent to the walls.

6. The upstream face of the baffle piers should be set at a distance of $0.8D_2$ from the downstream face of the chute blocks (Figure 17). This dimension is also important.

7. The height of the solid sill at the end of the basin can be obtained from Figure 18. The slope is 2:1 upward in the direction of flow.

8. It is undesirable to round or streamline the edges of the chute blocks, end sill or baffle piers. Streamlining of baffle piers may result in loss of half of their effectiveness. Small chamfers to prevent chipping of the edges is permissible.

9. It is recommended that a radius of reasonable length $(R \gtrless 4D_1)$ be used at the intersection of the chute and basin apron for slopes of $45^\circ$ or greater.

10. As a general rule the slope of the chute has little effect on the jump unless long flat slopes are involved. This phase will be considered in Paper 1405 on sloping aprons.

Since Basin III is close-coupled, the above rules should be followed closely for its proportioning. If the proportioning is to be varied from that recommended, or if the limits given below are exceeded, a model study is advisable. Arbitrary limits for the Type III basin are set at 200 cfs per foot of basin width and 50 to 60 feet per second entrance velocity until experience demonstrates otherwise.

### Application of Results (Example 3)

Given the following computed values for a small overflow dam

| $Q$ cfs | $q$ cfs | $V_1$ ft/sec | $D_1$ ft |
|---|---|---|---|
| 3,900 | 78.0 | 69 | 1.130 |
| 3,090 | 61.8 | 66 | 0.936 |
| 2,022 | 40.45 | 63 | 0.642 |
| 662 | 13.25 | 51 | 0.260 |

and the tail water curve for the river, identified by the solid line on Figure 20, proportion Basin III for the most adverse condition utilizing full conjugate tail water depth. The flow is symmetrical and the width of the basin is 50 feet. (The purpose of this example is to demonstrate the use of the jump elevation curve.)

The first step is to compute the jump elevation curve which in this case is $D_2$ plus the elevation of the basin floor. As $V_1$ and $D_1$ are given, the Froude number is computed and tabulated in Column 2, Table 5, below:

Table 5

| $Q$ cfs (1) | $F_1$ (2) | $\dfrac{D_2}{D_1}$ (3) | $D_1$ ft (4) | $D_2$ ft (5) | Jump elevation | |
|---|---|---|---|---|---|---|
| | | | | | Curve a (6) | Curve a' (7) |
| 3,900 | 11.42 | 15.75 | 1.130 | 17.80 | 617.5 | 615.0 |
| 3,090 | 12.02 | 16.60 | 0.936 | 15.54 | 615.2 | 612.7 |
| 2,022 | 13.85 | 19.20 | 0.642 | 12.33 | 612.0 | 609.5 |
| 662 | 17.62 | 24.5 | 0.260 | 6.37 | 606.1 | 603.6 |

Entering Figure 11 (paper 1402) with these values of the Froude number values of $\dfrac{TW}{D_1}$ are obtained for conjugate tail water depth from the solid line. These values are also $\dfrac{D_2}{D_1}$ and are shown listed in Column 3. The conjugate tail water depths for the various discharges, Column 5, were obtained by multiplying the values in Column 3 by those in Column 4.

If it were assumed that the most adverse operating condition occurs at the maximum discharge of 3,900 cfs, the stilling basin apron should be placed at elevation 617.5 - 17.8 or elevation 599.7

FIGURE 20
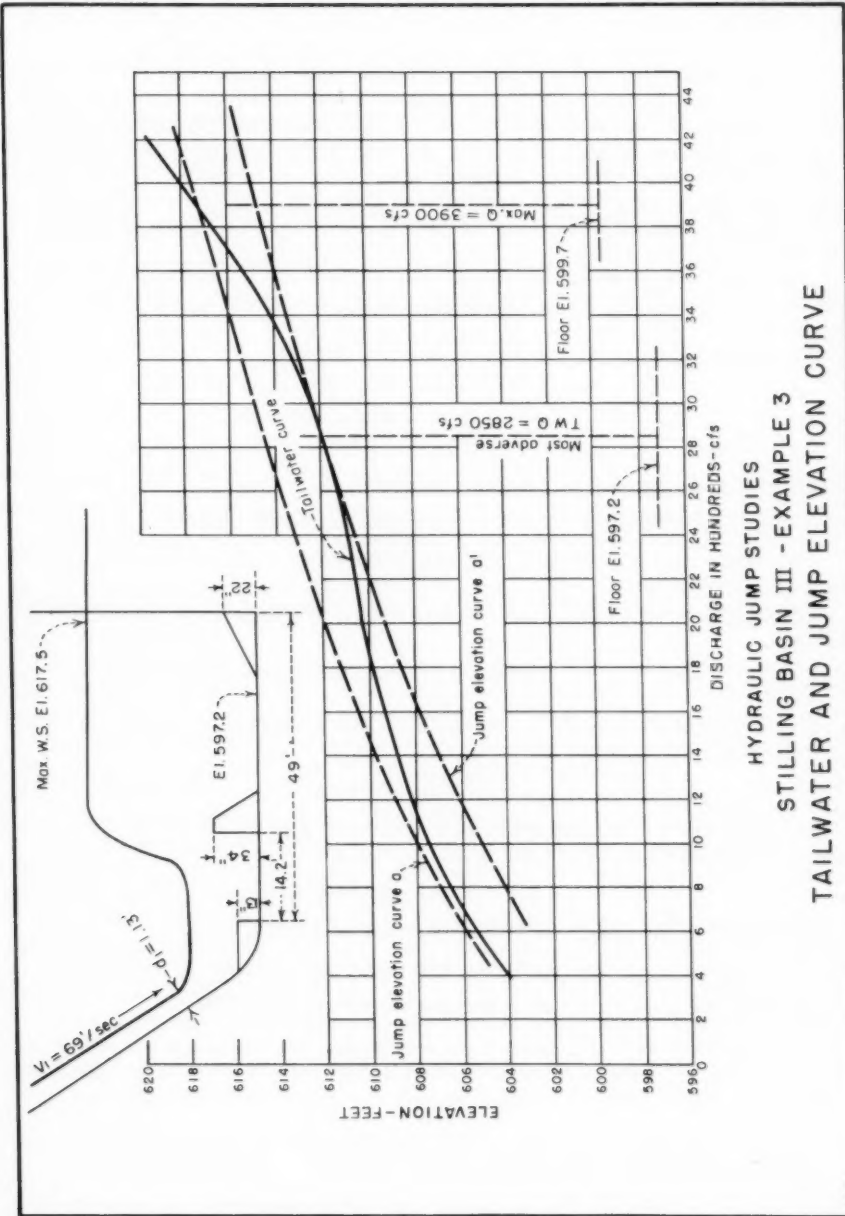


HYDRAULIC JUMP STUDIES
STILLING BASIN III - EXAMPLE 3
TAILWATER AND JUMP ELEVATION CURVE

With the apron at elevation 599.7 the tail water required for conjugate tail water depth for each discharge would follow the elevations listed in Column 6. Plotting Columns 1 and 6 on Figure 20 results in Curve a, which shows that the tail water depth is inadequate for all but the maximum discharge.

The tail water curve is unusual in that the most adverse tail water condition occurs at a discharge of approximately 2,850 cfs rather than maximum. As full conjugate tail water depth is desired for the most adverse tail water condition, it is necessary to shift the jump elevation curve downward to match the tail water curve for a discharge of 2,850 cfs (see Curve a' , Figure 20). The coordinates for Curve a' are given in Columns 1 and 7, Table 5. This will place the basin floor 2.5 feet lower, or elevation 597.2 feet, as shown in the sketch on Figure 20.

Although the position of the basin floor was set for a discharge of 2,850 cfs, the remaining details are proportioned for the maximum discharge 3,900 cfs.

Entering Figure 12 with a Froude number of 11.42,

$$\frac{L_{III}}{D_2} = 2.75, \text{ and the length of}$$

basin required $L_{III}$ = 2.75 x 17.80 = $\underline{48.95}$ feet.

(Notice that conjugate depth was used, not tail water depth.)

The height, width, and spacing of chute blocks are equal to $D_1$ or 1.130 feet (use $\underline{13}$ or $\underline{14}$ inches).

The height of the baffle piers for a Froude number of 11.42 (Figure 19) is $2.5D_1$.

$$h_3 = 2.5 \times 1.130 = 2.825 \text{ feet (use } \underline{34} \text{ inches).}$$

The width and spacing of the baffle piers are preferably three-fourths of the height or

$$0.75 \times 34 = \underline{25.5} \text{ inches.}$$

From Figure 17, the upstream face of the baffle piers should be $0.8D_2$ from the downstream face of the chute blocks, or

$$0.8 \times 17.80 = \underline{14.24} \text{ feet.}$$

The height of the solid end sill, Figure 18, is $1.60D_1$, or

$$h_4 = 1.60 \times 1.130 = 1.81 \text{ feet (use } \underline{22} \text{ inches).}$$

The final dimensions of the basin are shown on Figure 20.

Journal of the

# HYDRAULICS DIVISION

Proceedings of the American Society of Civil Engineers

HYDRAULIC DESIGN OF STILLING BASINS: STILLING BASIN AND
WAVE SUPPRESSORS FOR CANAL STRUCTURES, OUTLET WORKS,
AND DIVERSION DAMS (BASIN IV)

J. N. Bradley[1] M. ASCE and A. J. Peterka[2] M. ASCE
(Proc. Paper 1404)

### FOREWORD

This is one of a group of six papers on the hydraulic design of stilling basins and their associated appurtenances. Although original data from hydraulic models are presented in tabular form, the papers emphasize practical design procedures. Basin sizes and dimensions are given in easy-to-use dimensionless forms so that dependable stilling basins may be designed without the need for exceptional judgment or extensive experience. Sample problems are included.

The "Introduction" and "Experimental Equipment" are included in Paper 1401 but apply to all papers in this group. Paper 1401 is an academic study of the hydraulic jump on a flat floor. Useful information is presented concerning energy losses, applicability of the hydraulic jump formula, length of jump, and a new classification of the various types of jumps.

Paper 1402 covers the design of a short hydraulic jump stilling basin having an end sill and chute blocks. Paper 1403 describes a shorter stilling basin which utilizes baffle piers. In both papers information is given to determine the critical dimensions of the stilling basin, the tail water range, and the water surface profile in the basin.

Paper 1404 describes a special type of hydraulic jump basin for use when the Froude number of the incoming flow is low, and the jump produces waves in the downstream channel. An alternate design and two types of wave suppressors are also developed.

Paper 1405 describes the design of a stilling basin having a sloping apron. The extra tail water depth required and the merits of a sloping apron are evaluated, as is the basin length for a range of apron slopes.

Paper 1406 develops the design of impact basins for discharges up to 340

second feet and incoming velocities up to 30 feet per second. No tail water is required. The bibliography in this paper applies to all papers in this group.

---

## ABSTRACT

Where the Froude number of the incoming flow is low, the hydraulic jump produces objectionable waves downstream. This study generalizes the design of two stilling basins and two types of wave suppressors for stabilizing the water surface. Sample problems are used to illustrate the design procedures recommended.

---

## INTRODUCTION

In this Paper the characteristics of the hydraulic jump and the design of an adequate stilling basin for Froude numbers between 2.5 and 4.5 are discussed. This range is encountered principally in the design of canal structures, but occasionally low dams and outlet works fall in this category. In the 2.5 to 4.5 Froude number range, the jump is not fully developed and the previously discussed methods of design do not apply (papers 1401-1403). The main problem concerns the waves created in the hydraulic jump, making the design of a suitable wave suppressor a part of the stilling basin problem.

Four means of reducing wave heights are discussed. The first is an integral part of the stilling basin design and should be used only in the 2.5 to 4.5 Froude number range. The second may be considered to be an alternate design and may be used over a greater range of Froude numbers. These types are discussed as a part of the stilling basin design. The third and fourth devices are considered as appurtenances which may be included in an original design or added to an existing structure. Also, they may be used in any open channel flow-way without consideration of the Froude number. These latter devices are described under the heading Wave Suppressors.

### Jump Characteristics—Froude Number 2.5 to 4.5

For low values of the Froude number, 2.5 to 4.5, the entering jet oscillates intermittently from bottom to surface, as indicated in Figure 9B, (paper 1401) with no particular period. Each oscillation generates a wave which is difficult to dampen. In narrow structures, such as canals, waves may persist to some degree for miles. As they encounter obstructions in the canal, such as bridge piers, turnouts, checks, and transitions, reflected waves may be generated which tend to dampen, modify, or intensify the original wave. Waves are destructive to earth-lined canals and riprap and produce undesirable surges at gaging stations and in measuring devices. Structures in this range of Froude numbers are the ones which have been found to require the most maintenance.

On wide structures, such as diversion dams, wave action is not as pronounced when the waves can travel laterally as well as parallel to the direction of flow. The combined action produces some dampening effect but also

results in a choppy water surface.  These waves may or may not be dissipated in a short distance.  Where outlet works, operating under heads of 50 feet or greater, fall within the range of Froude numbers between 2.5 and 4.5, a model study of the stilling basin is imperative.  A model study is the only means of including preventive or corrective devices in the structure so that proper performance can be assured.

### Stilling Basin Design—Froude Number 2.5 to 4.5

Development Tests

The best way to combat a wave problem is to eliminate the wave at its source; in other words, concentrate on altering the condition which generates the wave.  In the case of the stilling basin preceded by an overfall or chute, two schemes were apparent for eliminating waves at their source.  The first was to break up the entering jet by opposing it with directional jets deflected from baffle piers or sills.  The second was to bolster or intensify the roller, shown in the upper portion of Figure 9B, (paper 1401) by directional jets deflected from large chute blocks.

The first method was unsuccessful in that the number and size of appurtenances necessary to break up the jet occupied so much volume that the devices themselves posed an obstruction to the flow.  This conclusion was based on tests in which various shaped baffle and guide blocks were systematically placed in a stilling basin in combination with numerous types of spreader teeth and deflectors in the chute.  The program involved dozens of tests, and not until all conceivable ideas were tried was this approach abandoned.  A few of the basic ideas tested are shown on Figure 21, a, b, c, f, g, and h.

Final Tests

Deflector Blocks

The second approach, that of attempting to intensify the roller, yielded better results.  In this case, large blocks were placed well up on the chute, while nothing was installed in the stilling basin proper.  The object was to direct a jet into the base of the roller in an attempt to strengthen it.  After a number of trials, the roller was actually intensified which did improve the stability of the jump.  Sketches d and e on Figure 21 indicate the only schemes that showed promise, although many variations were tried.  After finding an arrangement that was effective, approximations were tested to make the field construction as simple as possible.  The dimensions and proportions of the adopted deflector blocks are shown on Figure 22.

The object in the latter scheme was to place as few appurtenances as possible in the path of the flow, as volume occupied by appurtenances helps to create a backwater problem, thus requiring higher training walls.  The number of deflector blocks shown on Figure 22 is a minimum requirement to accomplish the purpose set forth.  The width of the blocks is shown equal to $D_1$ and this is the maximum width recommended.  From a hydraulic standpoint it is desirable that the blocks be constructed narrower than indicated, preferably $0.75D_1$.  The ratio of block width to spacing should be maintained as 1:2.5. The extreme tops of the blocks are $2D_1$ above the floor of the stilling basin. The blocks may appear to be rather high and, in some cases, extremely long, but this is essential as the jet must play at the base of the roller to be

effective. To accommodate the various slopes of chutes and ogee shapes en-
countered, a rule has been established that the horizontal length of the blocks
should be at least $2D_1$. The upper surface of each block is sloped at $5^0$ in a
downstream direction as it was found that this feature resulted in better oper-
ation, especially at the discharges lower than the design flow.

### Tail Water Depth

A tail water depth 5 to 10 percent greater than the conjugate depth is
strongly recommended for the above basin. Since the jump is very sensitive
to tail water depth at these low values of the Froude number, a slight de-
ficiency in tail water depth may allow the jump to sweep completely out of the
basin. The jump performs much better and wave action is diminished if the
tail water depth is increased to approximately $1.1D_2$.

### Basin Length and End Sill

The length of this basin, which is relatively short, can be obtained from
the upper curve on Figure 12 (paper 1402). No additional blocks or appur-
tenances are needed in the basin, as these will prove a greater detriment than
aid. The addition of a small triangular sill placed at the end of the apron for
scour control is desirable. A sill of the type used on Basin III may also be
used, Figure 18 (paper 1403).

### Performance

If designed for the maximum discharge, this stilling basin will perform
satisfactorily for all flows. Waves below the stilling basin will still be in
evidence but will be of the ordinary variety usually encountered with jumps of
a higher Froude number. This design is applicable to rectangular cross sec-
tions only.

### Alternate Stilling Basin Design—Small Drops

### Performance

An alternate basin for reducing wave action at the source, for values of the
Froude number between 2.5 and 4.5, is particularly applicable to small drops
in canals. The Froude number in this case is computed the same as though
the drop were an overflow crest. A series of steel rails, channel irons or
timbers in the form of a grizzly are installed at the drop, as shown in Figure
23. The overfalling jet is separated into a number of long, thin sheets of wa-
ter which fall nearly vertically into the canal below. Energy dissipation is
excellent and the usual wave problem is avoided. If the rails are tilted down-
ward at an angle of $3^0$ or more, the grid is self-cleaning.

The use of this device is particularly justified when the Froude number is
below 3.0. If use of a jump were possible the maximum energy loss would be
less than 27 percent at best, Figure 8, (paper 1401). The suggested device
accomplishes nearly as much energy loss and provides a smooth water sur-
face in addition.

### Design

Two spacing arrangements of the beams were tested in the laboratory: in
the first, the spacing was equal to the width of the beams, and in the second,
the spacing was two-thirds of the beam width. The latter was the more effec-
tive. In the first, the length of beams required was about 2.9 times the depth

of flow (y) in the canal upstream, while in the second, it was necessary to in-
crease the length to approximately 3.6y.  The following expression can be
used for computing the length of beams:

$$L = \frac{Q}{CSN \sqrt{2gy}}$$ (4)

where Q is the total discharge in cfs, C is an experimental coefficient, S is
the width of a space in feet, N is the number of spaces, g is the acceleration
of gravity and y is the depth of flow in the canal upstream (see Figure 23).
The value of C for the two arrangements tested was 0.245.

Should it be desired to maintain a certain level in the canal upstream, the
grid may be made adjustable and tilted upward to act as a check; however,
this arrangement may pose a cleaning problem.

## Wave Suppressors

The two stilling basins described above may be considered to be wave sup-
pressors, although the suppressor effect is obtained from the necessary fea-
tures of the stilling basin.  If greater wave reduction is required on a pro-
posed structure, or if a wave suppressor is required to be added to an existing
flow-way, the two types discussed below may prove useful.  Both are ap-
plicable to most open channel flow-ways having rectangular, trapezoidal, or
other cross-sectional shapes.  The first or raft type may prove more eco-
nomical than the second or underpass type, but rafts do not provide the degree
of wave reduction obtainable with the underpass type.  Both types may be used
without regard to the Froude number.

### Raft Type Wave Suppressor

In a structure of the type shown in Figure 24, there are no means for
eliminating waves at their source.  Tests showed that appurtenances in the
stilling basin merely produced severe splashing and created a backwater ef-
fect, resulting in submerged flow at the gate for the larger flows.  Submerged
flow reduced the effective head on the structure, and in turn, the capacity.
Tests on several suggested devices showed that rafts provided the best an-
swer to the wave problem when additional submergence could not be tolerated.
The general arrangement of the tested structure is shown in Figure 24.  The
Froude number varied from 3 to 7, depending on the head behind the gate and
the gate opening.  Velocities in the canal ranged from 5 to 10 feet per second.
Waves were 1.5 feet high, measured from trough to crest.

During the course of the experiments a number of rafts were tested; thick
rafts with longitudinal slots, thin rafts made of perforated steel plate, and
others, both floating and fixed.  Rigid and articulated rafts were tested in
various arrangements.

The most effective raft arrangement consisted of two rigid stationary rafts
20 feet long by 8 feet wide, made from 6- by 8-inch timbers, placed in the
canal downstream from the stilling basin (Figure 24).  A space was left be-
tween timbers and lighter cross pieces were placed on the rafts parallel to the
flow, giving the appearance of many rectangular holes.  Several essential re-
quirements for the raft were apparent:  (1) that the rafts be perforated in a

regular pattern; (2) that there be some depth to these holes; (3) that at least two rafts be used; and (4) that the rafts be rigid and held stationary.

It was found that the ratio of hole area to total area of raft could be from 1:6 to 1:8. The 8-foot width, W on Figure 24, is a minimum dimension. The rafts must have sufficient thickness so that the troughs of the waves do not break free from the underside. The top surfaces of the rafts are set at the mean water surface in a fixed position so that they cannot move. Spacing between rafts should be at least three times the raft dimension, measured parallel to the flow. The first raft decreases the wave height about 50 percent, while the second raft effects a similar reduction. Surges over the raft dissipate themselves by flow downward through the holes. For this specific case the waves were reduced from 18 to 3 inches in height.

Under certain conditions wave action is of concern only at the maximum discharge when freeboard is endangered, so the rafts can be a permanent installation. Should it be desired to suppress the waves at partial flows, the rafts may be made adjustable, or, in the case of trapezoidal channels, a second set of rafts may be placed under the first set for partial flows. The rafts should perform equally well in trapezoidal as well as rectangular channels.

The recommended raft arrangement is also applicable for suppressing waves with a regular period such as wind waves, waves produced by the starting and stopping of pumps, etc. In this case, the position of the downstream raft is important. The second raft should be positioned downstream at some fraction of the wave length. Placing it at a full wave length could cause both rafts to be ineffective. Thus, for narrow canals it may be advisable to make the second raft portable. However, if it becomes necessary to make the rafts adjustable or portable, or if a moderate increase in depth in the stilling basin can be tolerated, consideration should be given to the type of wave suppressor discussed below.

## Underpass Type Wave Suppressor

### General Description

By far the most effective wave dissipator is the short-tube type of underpass suppressor. The name "short-tube" is used because the structure has many of the characteristics of the short-tube discussed in hydraulic textbooks. This wave suppressor may be added to an existing structure or included in the original construction. In either case it provides a sightly structure, permanent in nature, which is economical to construct and effective in operation.

Essentially, the structure consists of a horizontal roof placed in the flow channel with a headwall sufficiently high to cause all flow to pass beneath the roof. The height of the roof above the channel floor may be set to effectively reduce wave heights for a considerable range of flows or channel stages. The length of the roof, however, determines the amount of wave suppression obtained for any particular roof setting.

The recommendations for this structure are based on three separate model investigations, each having different flow conditions and wave reduction requirements. The design is then generalized and design procedures given, including a sample problem.

### Performance

The effectiveness of the underpass wave suppressor is illustrated in Figures 25 and 26. Figure 25 shows one of the hydraulic models used to

develop the wave suppressor and the effect of the suppressor on the waves in
the canal. Figure 26 shows before and after photographs of the prototype in-
stallation, indicating that the prototype performance was as good as predicted
by the model. In this instance it was desired to reduce wave heights entering
a lined canal to prevent overtopping of the canal lining at near maximum dis-
charges. Below 3,000 second-feet, waves were in evidence but did not overtop
the lining. For larger discharges, however, the stilling basin produced
moderate waves which were actually intensified by the short transition be-
tween the basin and the canal. These intensified waves overtopped the lining
at 4,000 second-feet and became a real problem at 4,500 second-feet. Tests
were made with a suppressor 21 feet long using discharges from 2,000 to
5,000 second-feet. The suppressor was located downstream from the stilling
basin.

Figure 27, Test 1, shows the results of tests to determine the optimum
opening between the roof and the channel floor using the maximum discharge
5,000 second-feet. With a 14-foot opening, waves were reduced from about
8 feet to about 3 feet. Waves were reduced to less than 2 feet with an opening
of 11 feet. Smaller openings produced less wave height reductions, due to the
turbulence created at the underpass exit. Thus, it may be seen that an open-
ing of from 10 to 12 feet produced optimum results.

With the opening set at 11 feet the suppressor effect was then determined
for other discharges. These results are shown on Figure 27, Test 2. Wave
height reduction was about 78 percent at 5,000 second-feet, increasing to
about 84 percent at 2,000 second-feet. The device became ineffective at about
1,500 second-feet when the depth of flow became less than the height of the
roof.

To determine the effect of suppressor length on the wave reduction, other
factors were held constant while the length was varied. Tests were made on
suppressors 10, 21, 30, and 40 feet long for discharges of 2, 3, 4, and 5 thou-
sand second-feet, Figure 27, Test 3. Roof lengths in terms of the downstream
depth, $D_2$, for 5,000 second-feet were $0.62D_2$, $1.31D_2$, and $2.5D_2$, respectively.
In terms of a 20-foot-long underpass, halving the roof length almost doubled
the downstream wave height while doubling the 20-foot length almost halved
the resulting wave height.

The same type of wave suppressor was successfully used in an installation
where it was necessary to obtain optimum wave height reductions, since flow
from the underpass discharged directly into a measuring flume in which it
was desired to obtain accurate discharge measurements. The capacity of the
structure was 625 cubic feet per second but it was necessary for the under-
pass to function for low flows as well as for the maximum. With an underpass
$3.5D_2$ long and set as shown in Figure 28, the wave reductions were as shown
in Table 6.

Figure 28 shows actual wave traces recorded by an oscillograph. Here it
may be seen that the maximum wave height, measured from minimum trough
to maximum crest did not occur on successive waves. Thus, the water sur-
face will appear smoother to the eye than is indicated by the maximum wave
heights recorded in Table 6.

General Design Procedure

To design an underpass for a particular structure there are three main
considerations: (1) how deeply should the roof be submerged, (2) how long an
underpass should be constructed to accomplish the necessary wave reduction,

## Table 6

### WAVE HEIGHTS IN FEET--PROTOTYPE
#### Maximum Head

| Discharge in cfs | 625 | | 550 | | 400 | | 200 | | 100 | |
|---|---|---|---|---|---|---|---|---|---|---|
| | Upstream* | Downstream* | U | D | U | D | U | D | U | D |
| Wave heights in feet | **3.8 plus | 0.3 | 4.2 | 0.3 | 4.5 | 0.4 | 3.6 | 0.4 | 1.7 | 0.3 |

and (3) how much increase in flow depth will occur upstream from the underpass. These considerations are discussed in order.

Based on the two installations shown in Figures 27 and 28, and on other experiments, it has been found that maximum wave reduction occurs when the roof is submerged about 33 percent, i.e., when the under side of the underpass is set 33 percent of the flow depth below the water surface for maximum discharge, Figure 29C. Submergences greater than 33 percent (for the cases tested) produced undesirable turbulence at the underpass outlet resulting in less overall wave reduction. With the usual tail water curve, submergence and the percent reduction in wave height will become less, in general, for smaller than maximum discharges. This is illustrated by the upper curve in Figure 29C. The lower curve shows a near constant value for less submergence, but it is felt that this is a somewhat special case since the wave heights for less than maximum discharge were smaller and of shorter period than in the usual case.

It is known that the wave period greatly affects the performance of a given underpass, with the greatest wave reduction occurring for short period waves. Since the wave periods to be expected are usually not known in advance, it is desirable to eliminate this factor from consideration. Fortunately, wave action below a stilling basin usually has no measurable period but consists of a mixture of generated and reflected waves best described as a choppy water surface. This fact makes it possible to provide a practical solution from limited data and to eliminate the wave period from consideration except in this general way: waves must be of the variety ordinarily found downstream from hydraulic jumps or energy dissipators. These usually have a period of not more than about 5 seconds. Longer period waves may require special treatment not covered in this discussion. Fortunately, too, there generally is a tendency for the wave period to become less with decreasing discharge. Since the suppressor provides a greater percentage reduction on shorter period waves, this tends to offset the characteristics of the device to give less wave reduction for reduced submergence at lower discharges. It is therefore advisable in the usual case to submerge the underpass about 33 percent for the maximum discharge. For less submergence, the wave reduction can be estimated from Figure 29C.

The minimum length of underpass required depends on the amount of wave reduction considered necessary. If it is sufficient to obtain a nominal reduction to prevent overtopping of a canal lining at near maximum discharge or to prevent waves from attacking channel banks, a length $1D_2$ to $1.5D_2$ will

provide from 60 to 75 percent wave height reduction, provided the initial waves have periods up to about 5 seconds. The shorter the wave period the greater the reduction for a given underpass. For long period waves, little wave reduction may occur because of the possibility of the wave length being nearly as long or longer than the underpass, with the wave passing "untouched" beneath the underpass.

To obtain greater than 75 percent wave reductions, a longer underpass is necessary. Under ideal conditions an underpass $2D_2$ to $2.5D_2$ in length may provide up to 88 percent wave reduction for wave periods up to about 5 seconds. Ideal conditions include a velocity beneath the underpass of less than, say, 10 feet per second and a length of channel 3 to 4 times the length of the underpass downstream from the underpass which may be used as a quieting pool to still the small turbulence waves created at the underpass exit.

Wave height reduction up to about 93 percent may be obtained by using an underpass $3.5D_2$ to $4D_2$ long. Included in this length is a 4:1 sloping roof extending from the underpass roof elevation to the tail water surface. The sloping portion should not exceed about one-quarter of the total length of underpass. Since slopes greater than 4:1 do not provide the desired draft tube action they should not be used. Slopes flatter than 4:1 provide better draft tube action and are therefore desirable.

Since the greatest wave reduction occurs in the first $D_2$ of underpass length, it may appear advantageous to construct two short underpasses rather than one long one. In the one case tested, two underpasses each $1D_2$ long, with a length $5D_2$ between them, gave an added 10 percent wave reduction advantage over one underpass $2D_2$ long. The extra cost of another headwall should be considered, however.

Table 7 summarizes the amount of wave reduction obtainable for various underpass lengths.

To determine the backwater effect of placing the underpass in the channel, Figure 29B will prove helpful. Data from four different underpasses were

## Table 7

### EFFECT OF UNDERPASS LENGTH ON WAVE REDUCTION
For Underpass Submergence 33 Percent and
Maximum Velocity Beneath 14 ft/sec

| Underpass length | Percent wave reduction* |
|---|---|
| $1D_2$ to $1.5D_2$ | 60 to 75 |
| $2D_2$ to $2.5D_2$ | 80 to 88 |
| $3.5$ to $4.0D_2$ | 90 to 93** |

*For wave periods up to 5 seconds.
**Upper limit only with draft tube type outlet.

used to obtain the two curves shown. Although the test points from which the curves were drawn showed minor inconsistencies, probably because factors other than those considered also affected the depth of water upstream from the underpass, the submitted curves are sufficiently accurate for design purposes. Figure 29B shows two curves of the discharge coefficient "C" versus average velocity beneath the underpass, one for underpass lengths of $1D_2$ to $2D_2$ and the other for lengths $3D_2$ to $4D_2$. Intermediate values may be interpolated although accuracy of this order is not usually required.

Pressures on the underpass were measured by means of piezometers to determine the direction and magnitude of the forces acting. Average pressures on the headwall were found to be about static, with distribution in a straight line from zero at the water surface to static pressure at the bottom. Pressures along the underside of the roof were found to be 1 to 2 feet below atmospheric; for design purposes they may be considered to be atmospheric. Pressures on the downstream vertical wall were equal to static pressures. In other words there is only a slight tendency (except for the force of breaking waves which was not measured) to move the underpass downstream, and there is a slight resultant force tending to hold the underpass down.

## Sample Problem, Example 4

To illustrate the use of the preceding data in designing an underpass, a sample problem will be helpful.

A rectangular channel 30 feet wide and 14 feet deep flows 10 feet deep at maximum discharge, 2,400 cfs. It is estimated that waves will be 5 feet high and of the ordinary variety having a period less than 5 seconds. It is desired to reduce the height of the waves to approximately 1 foot at maximum discharge by installing an underpass-type wave suppressor without increasing the depth of water upstream from the underpass more than 15 inches.

To obtain maximum wave reduction at maximum discharge, the underpass should be submerged 33 percent. Therefore, the depth beneath the underpass is 6.67 feet with a corresponding velocity of 12 ft/sec, $(V = \dfrac{2,400}{30 \times 6.67})$. To reduce the height of the waves from 5 feet to 1 foot, an 80 percent reduction in wave height is indicated, and, from Table 7, requires an underpass approximately $2D_2$ in length.

From Figure 29B, C = 1.07 for $2D_2$ and a velocity of 12 ft/sec.

From the equation given on Figure 29B:

$$\text{Total head, } h + h_v = \left(\frac{Q}{CA\sqrt{2g}}\right)^2 = \left(\frac{2,400}{8.02 \times 1.07 \times 200}\right)^2 = 1.95 \text{ feet}$$

$h + h_v$ is the total head required to pass the flow and $h$ represents the backwater effect of increase in depth of water upstream from the underpass. The determination of values for $h$ and $h_v$ is done by trial and error. As a first determination, assume that $h + h_v$ represents the increase in head.

Then, channel approach velocity, $V_1 = \dfrac{Q}{A} =$

$$\frac{2,400}{(10 + 1.95)30} = 6.7 \text{ ft/sec}$$

$$h_v = \frac{(V_1)^2}{2g} = \frac{(6.7)^2}{64.4} = 0.70 \text{ foot}$$

$$\text{and } h = 1.95 - 0.70 = 1.25 \text{ feet}$$

To refine the calculation, the above computation is repeated using the new head

$$V_1 = \frac{2,400}{(10 + 1.25)30} = 7.1 \text{ ft/sec}$$

$$h_v = 0.72 \text{ foot}$$

$$\text{and } h = 1.17 \text{ feet}$$

Further refinement is unnecessary.

Thus, the average water surface upstream from the underpass is 1.2 feet higher than the tail water which satisfies the assumed design requirement of a maximum backwater of 15 inches. The length of the underpass is $2D_2$ or 20 feet, and the waves are reduced 80 percent to a maximum height of approximately 1 foot.

If it is desired to reduce the wave heights still further, a longer underpass is required. Using Table 7 and Figure 29B as in the above problem, an underpass 3.5 to $4.0D_2$ or 35 to 40 feet in length reduces the waves 90 to 93 percent, making the downstream waves approximately 0.5 foot high and creating a backwater, h, of 1.61 feet.

In providing freeboard for the computed backwater, h, allowance should be made for waves and surges which, in effect, are above the computed water surface. One-half the wave height or more, measured from crest to trough, should be allowed above the computed surface. Full wave height would provide a more conservative design for the usual short period waves encountered in flow channels.

The headwall of the underpass should be extended to this same height and a seawall overhang placed at the top to turn wave spray back into the basin. An alternate method would be to place a cover, say $2D_2$ long, upstream from the underpass headwall.

To insure obtaining the maximum wave reduction for a given length of underpass, a 4:1 sloping roof should be provided at the downstream end of the underpass, as indicated on Figure 28. This slope may be considered as part of the overall length. The sloping roof will help reduce the maximum wave height and will also reduce the frequency with which it occurs, providing in all respects a better appearing water surface. If the flow entering the underpass contains entrained air in the form of rising air bubbles, a few small vents in the underpass roof will relieve the possibility of air spurts and resulting surface turbulence at the underpass exit.

If the underpass is to be used downstream from a stilling basin the underpass must be placed sufficiently downstream to prevent turbulent flow, such as occurs at the end of a basin, from entering and passing through the wave suppressor. In highly turbulent flow the underpass is only partly effective.

A close inspection of the submitted data will reveal that slightly better results were obtained in the tests than are claimed in the example. This was done to illustrate the degree of conservatism required, since it should be understood that the problem of wave reduction can be very complex if unusual conditions prevail.

FIGURE 21



HYDRAULIC JUMP STUDIES
RECORD OF APPURTENANCES
BASIN IV.

FIGURE 22



HYDRAULIC JUMP STUDIES

STILLING BASIN IV
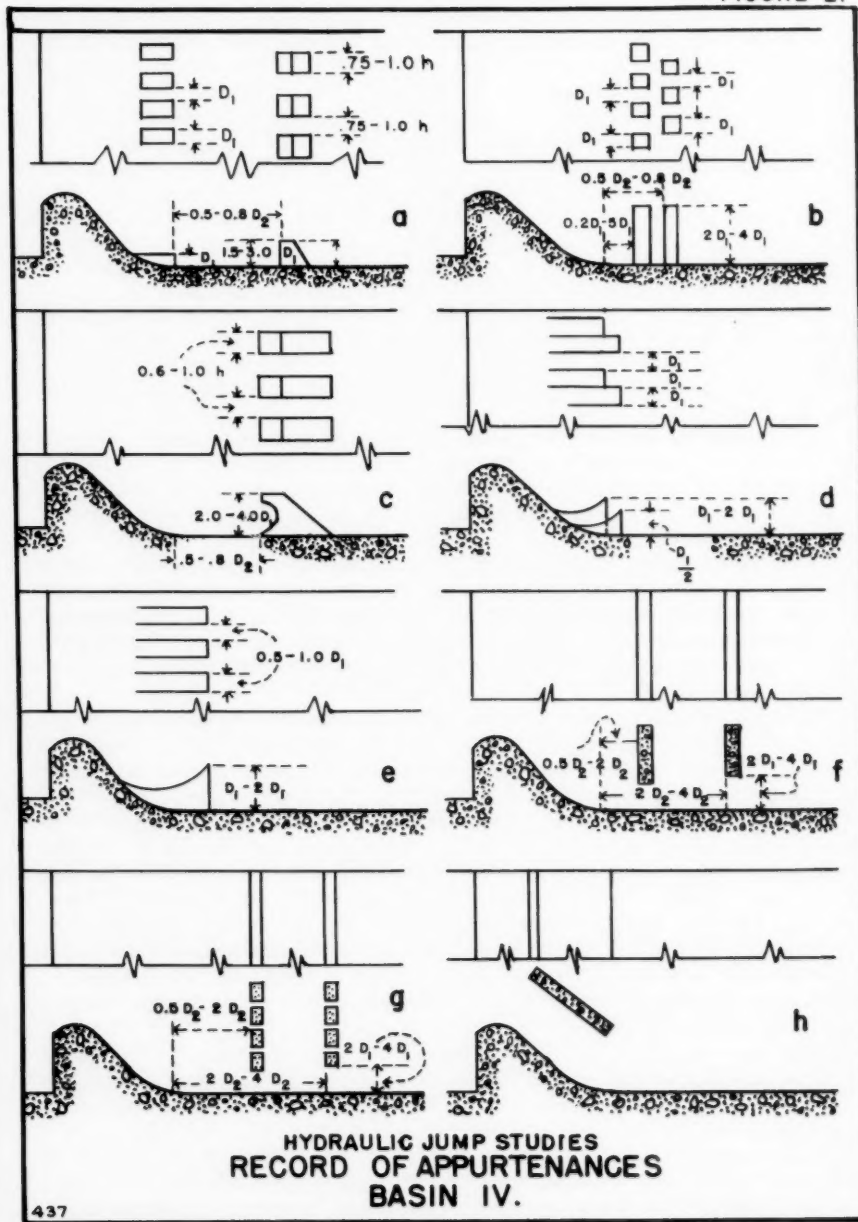
FOR FROUDE NUMBERS 2.5 – 4.5
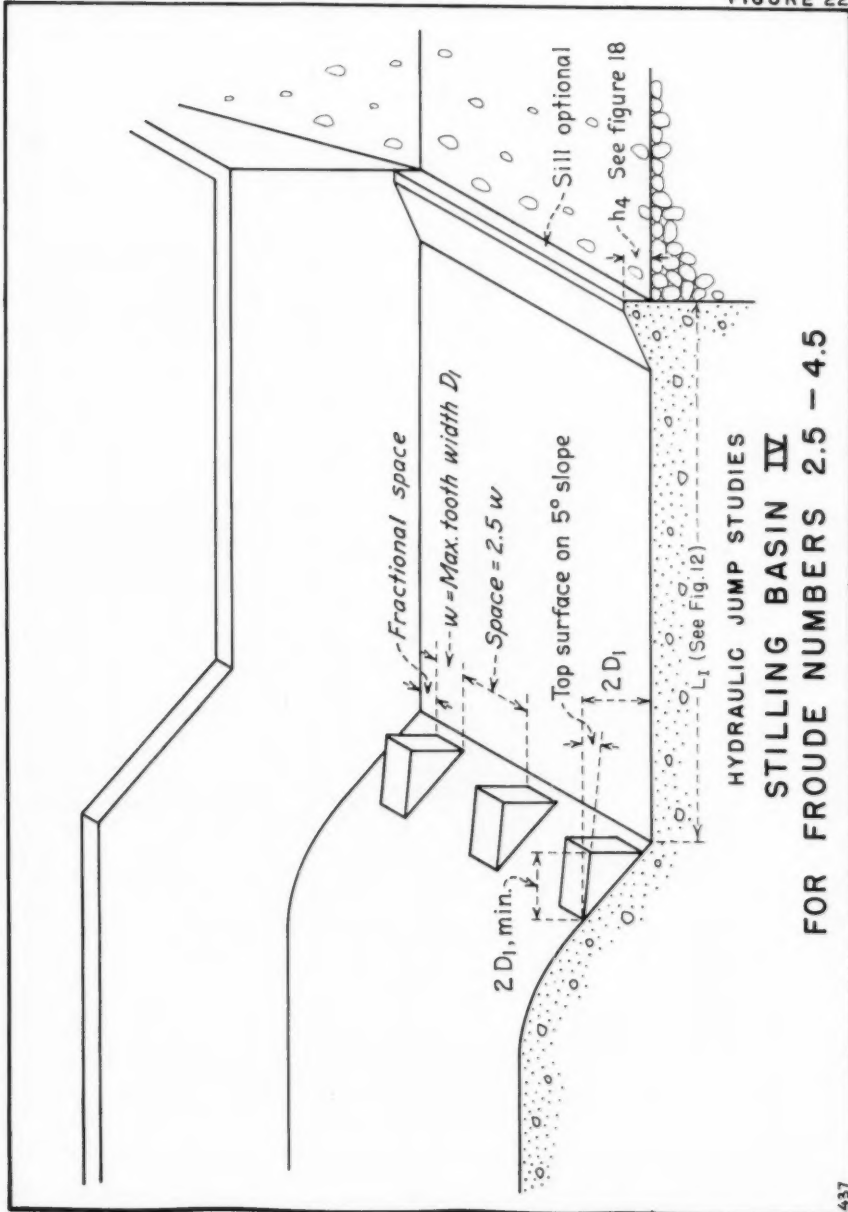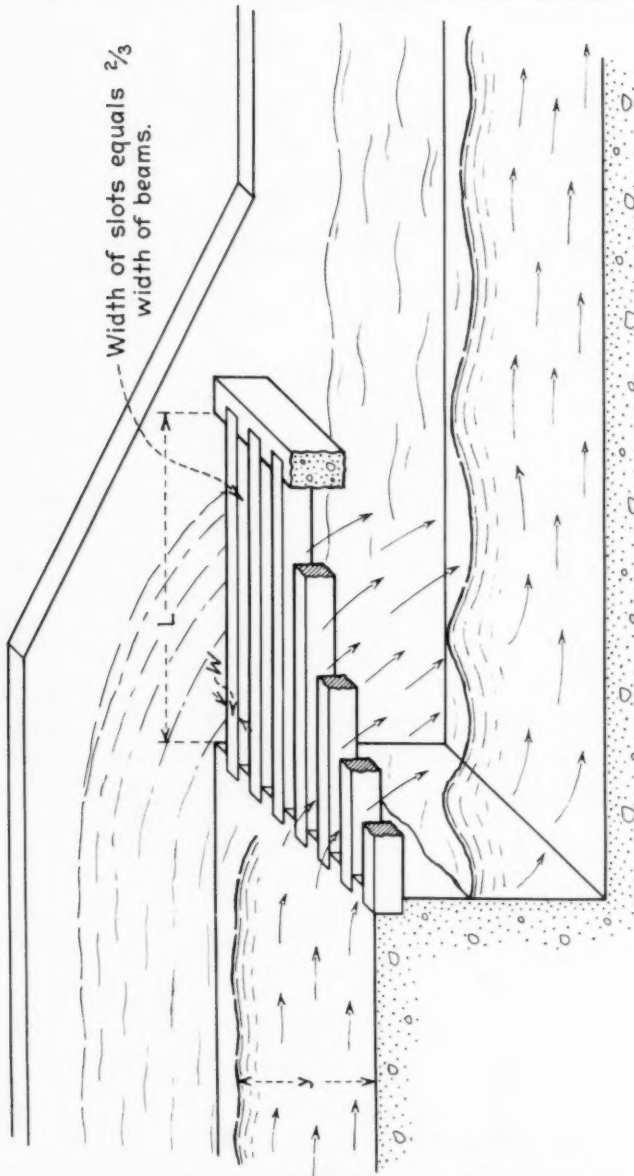
FIGURE 23



HYDRAULIC JUMP STUDIES

DROP-TYPE ENERGY DISSIPATOR (ALTERNATE BASIN IV)
FOR FROUDE NUMBERS 2.5 – 4.5

437

FIGURE 24

HYDRAULIC JUMP STUDIES
RAFT WAVE SUPPRESSOR (TYPE IV)
FOR FROUDE NUMBERS 2.5 - 4.5
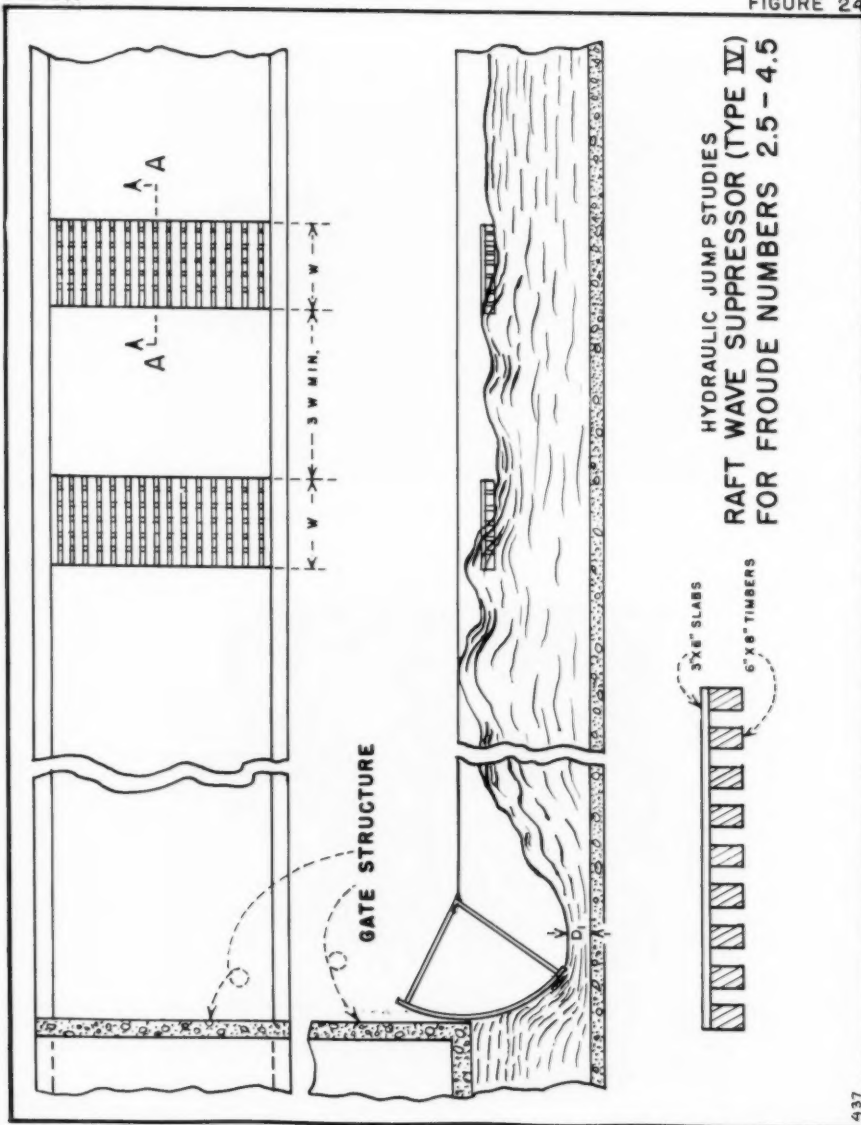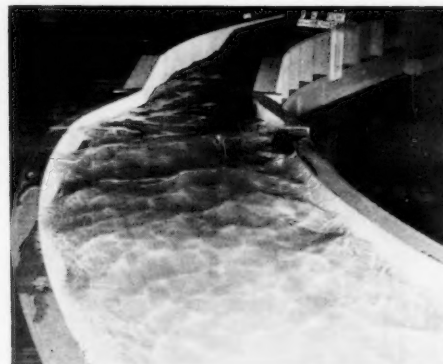
Figure 25



Without suppressor - waves overtop canal.



Suppressor in place - Length $1.3D_2$, submerged
30 percent

Performance of Underpass Wave Suppressor
1:32 Scale Model
Discharge 5,000 Second-feet

Figure 26
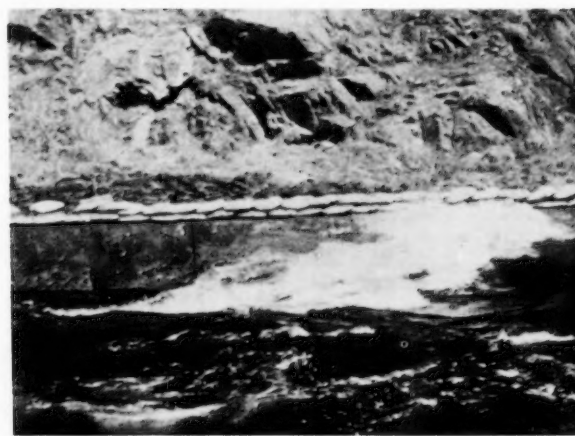


Friant-Kern Canal - Q = 3900 c.f.s.
Before wave suppressor was installed



Friant-Kern Canal - Q = 3900 c.f.s.
After wave suppressor was installed

FIGURE 27
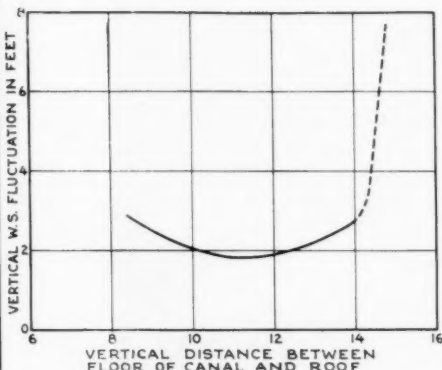
TEST NO. 1
TO DETERMINE MOST EFFECTIVE
ELEVATION FOR ROOF - Q = 5000 cfs.

VERTICAL DISTANCE BETWEEN
FLOOR OF CANAL AND ROOF

PLAN

SECTION

APPROX. WATER SURFACE
FLUCTUATION AT Q = 5000 cfs
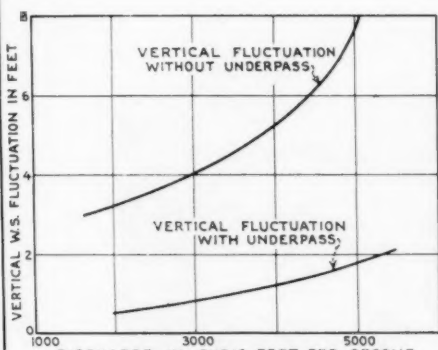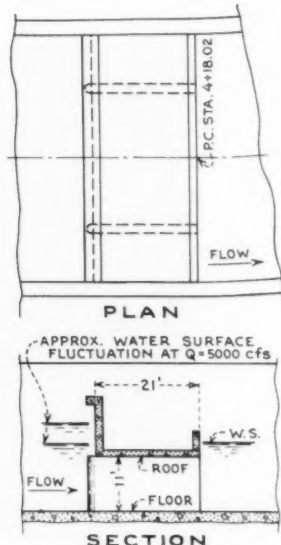
TEST NO. 2
TO DETERMINE EFFECTIVENESS OF
UNDERPASS AT VARIOUS DISCHARGES

VERTICAL FLUCTUATION
WITHOUT UNDERPASS

VERTICAL FLUCTUATION
WITH UNDERPASS

DISCHARGE IN CUBIC FEET PER SECOND
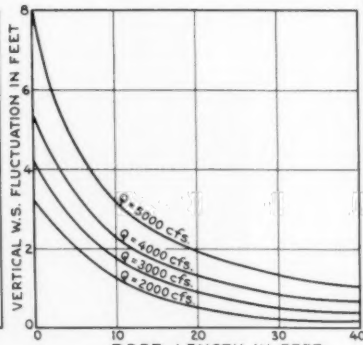
TEST NO. 3
EFFECT OF UNDERPASS LENGTH
ON WATER SURFACE FLUCTUATION

ROOF LENGTH IN FEET

Q = 5000 cfs.
Q = 4000 cfs.
Q = 3000 cfs.
Q = 2000 cfs.

WAVE SUPPRESSOR FOR
FRIANT - KERN CANAL
RESULTS OF HYDRAULIC MODEL TESTS

FIGURE 28

CARTER LAKE DAM NO.1 • OUTLET WORKS

WAVE HEIGHT RECORDS

(MODEL SCALE 1:16)

FIGURE 29



A = Flow area beneath underpass
h = Flow-producing head
$h_V$ = Velocity head in approach

$$H_V = \frac{V_1^2}{2g}$$

A

$l = 1D_2$ to $2D_2$

$l = 3D_2$ to $4D_2$

$C$ IN $Q = CA\sqrt{2g(h+h_V)}$

AVERAGE VELOCITY , V, IN UNDERPASS

B

CARTER

FRIANT

% REDUCTION IN WATER SURFACE FLUCTUATION

% SUBMERGENCE OF UNDERPASS $- \dfrac{h''}{D_2}$

C
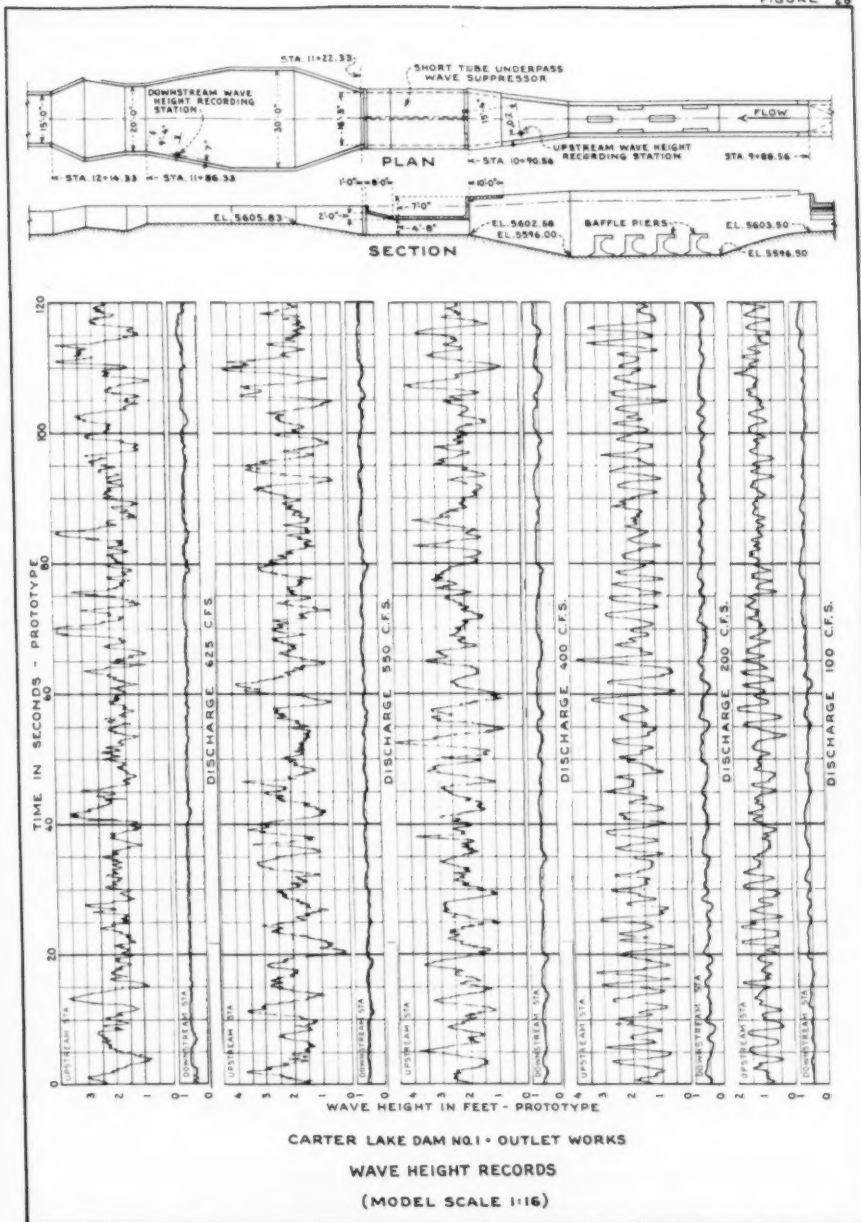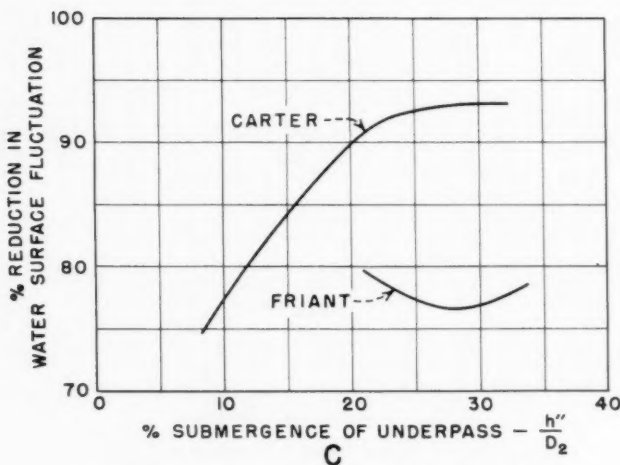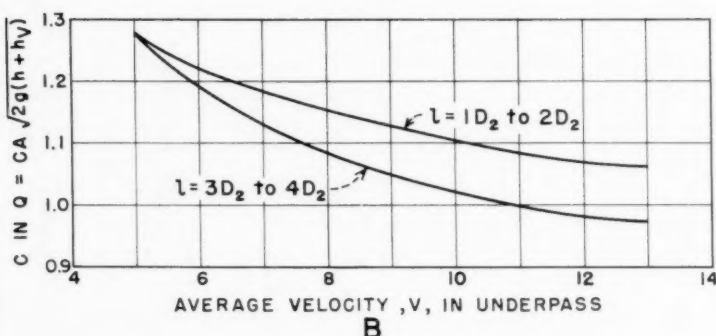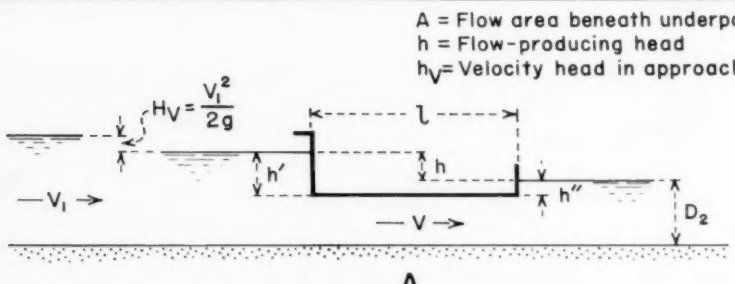
HYDRAULIC CHARACTERISTICS
UNDERPASS WAVE SUPPRESSOR

437

Journal of the

# HYDRAULICS DIVISION

Proceedings of the American Society of Civil Engineers

### HYDRAULIC DESIGN OF STILLING BASINS: STILLING BASIN WITH SLOPING APRON (BASIN V)

J. N. Bradley[1] M. ASCE and A. J. Peterka[2] M. ASCE
(Proc. Paper 1405)

### FOREWORD

This is one of a group of six papers on the hydraulic design of stilling basins and their associated appurtenances. Although original data from hydraulic models are presented in tabular form, the papers emphasize practical design procedures. Basin sizes and dimensions are given in easy-to-use dimensionless forms so that dependable stilling basins may be designed without the need for exceptional judgment or extensive experience. Sample problems are included.

The "Introduction" and "Experimental Equipment" are included in Paper 1401 but apply to all papers in this group. Paper 1401 is an academic study of the hydraulic jump on a flat floor. Useful information is presented concerning energy losses, applicability of the hydraulic jump formula, length of jump, and a new classification of the various types of jumps.

Paper 1402 covers the design of a short hydraulic jump stilling basin having an end sill and chute blocks. Paper 1403 describes a shorter stilling basin which utilizes baffle piers. In both papers information is given to determine the critical dimensions of the stilling basin, the tail water range, and the water surface profile in the basin.

Paper 1404 describes a special type of hydraulic jump basin for use when the Froude number of the incoming flow is low, and the jump produces waves in the downstream channel. An alternate design and two types of wave suppressors are also developed.

Paper 1405 describes the design of a stilling basin having a sloping apron. The extra tail water depth required and the merits of a sloping apron are evaluated, as is the basin length for a range of apron slopes.

Paper 1406 develops the design of impact basins for discharges up to 340

second feet and incoming velocities up to 30 feet per second. No tail water is required. The bibliography in this paper applies to all papers in this group.

---

## ABSTRACT

Procedures and rules for the design of a stilling basin with a sloping apron are presented along with a discussion of the relative merits of sloping and horizontal aprons. Critical basin dimensions and tail water requirements are presented in dimensionless form. Recommendations are verified from an analysis of 13 existing basins having sloping aprons.

---

## INTRODUCTION

Much has been said, pro and con, concerning the advantages and disadvantages of stilling basins with sloping aprons. Discussions have continued indefinitely because there were not sufficient supporting data available from which to draw conclusions. In this study, therefore, the sloping apron was investigated sufficiently to answer many of the debatable questions and also to provide more definite design data.

Four flumes, A, B, D, and F, Figures 1, 2, and 3, (paper 1401) were used to obtain the range of Froude numbers desired for the tests. In Flumes A, B, and D, floors were installed to the slope desired, while Flume F could be tilted to obtain slopes from $0^{0}$ to $12^{0}$. The slope in this discussion is the tangent of the angle between the floor and the horizontal and is designated as "$\tan \phi$." Five principal measurements were made in these tests, namely: the discharge, the average depth of flow entering the jump, the length of the jump, the tail water depth, and the slope of the apron. The tail water was adjusted so that the front of the jump formed either at the intersection of the spillway face and the sloping apron or, in the case of the tilting flume, at a selected point.

The jump on a sloping apron takes many forms depending on the slope and arrangement of the apron, the value of the Froude number, and the concentration of flow (discharge per foot of width), but the dissipation is as effective as occurs in the true hydraulic jump on a horizontal apron.

### Previous Experimental Work

Previous experimental work on the sloping apron has been carried on by several experimenters. In 1934, the late C. L. Yarnell of the United States Department of Agriculture supervised a series of experiments on the hydraulic jump on sloping aprons. Carl Kindsvater[5] later compiled these data and presented a rather complete picture, both experimentally and theoretically, for one slope, namely: 1:6 ($\tan \phi = 0.167$). G. H. Hickox[5] presented data for a series of experiments on a slope of 1:3 ($\tan \phi = 0.333$). Bakhmeteff[1] and Matzke[6] performed experiments on slopes of 0 to 0.07 in a flume 6 inches wide.

From an academic standpoint, the jump may occur in several ways on a

sloping apron, as outlined by Kinsdvater, presenting separate and distinct problems, Figure 30. Case A has the jump on a horizontal apron. In Case B, the toe of the jump forms on the slope, while the end occurs over the horizontal apron. In Case C, the toe of the jump is on the slope, and the end is at the junction of the slope and the horizontal apron; in Case D, the entire jump forms on the slope. With so many possibilities, it is easily understood why experimental data have been lacking on the sloping apron. Messrs. Yarnell, Kindsvater, Bakhmeteff, and Matzke limited their experiments to Case D. B. D. Rindlaub[7] of the University of California concentrated on the solution of Case B, but his experimental results are complete for only one slope, that of $12.33^{o}$ (tan $\phi = 0.217$).

## Sloping Apron Tests

From a practical standpoint, the scope of the present test program need not be so broad as outlined in Figure 30. For example, the action in Cases C and D is for all practical purposes the same, if it is assumed that a horizontal floor begins at the end of the jump for Case D. Sufficient tests were made on Case C to verify the above statement that Cases C and D can be considered as one. The first of the current experiments to be described in this chapter involves Case D. The second set of tests deals with Case B. Case B is virtually Case A operating with excessive tail water depth. As the tail water depth is further increased, Case B approaches Case C. The results of Case A have already been discussed in the preceding chapters, and Cases D and B will be considered here in order.

### Tail Water Depth (Case D)

Data obtained from the four flumes used in the sloping apron tests (Case D experiments) are tabulated in Table 8. The headings are much the same as those in previous tables, but need some explanation. Column 2 lists the tangents of the angles of the slopes tested. The depth of flow entering the jump, $D_1$, Column 8, was measured at the beginning of the jump in each case, corresponding to Section 1, Figure 30. It represents the average of a generous number of point gage measurements. The velocity at this same point, $V_1$, Column 7, was computed by dividing the unit discharge, q (Column 5), by $D_1$. The length of jump, Column 11, was measured in the flume, bearing in mind that the object of the test was to obtain practical data for stilling basin design. The end of the jump was chosen as the point where the high velocity jet began to lift from the floor, or a point on the level tail water surface immediately downstream from the surface roller, whichever occurred farthest downstream. The length of the jump, as tabulated in Column 11, is the horizontal distance from Sections 1 to 2, Figure 30. The tail water depth, tabulated in Column 6, is the depth measured at the end of the jump, corresponding to the depth at Section 2 on Figure 30.

The ratio $\frac{TW}{D_1}$ (Column 9, Table 8) is plotted with respect to the Froude number (Column 10) for sloping aprons having tangents 0.05 to 0.30 on Figure 31. The plot for the horizontal apron (tan $\phi = 0$) is the same as shown in Figure 5, (paper 1401). Superimposed on Figure 31 are data from Kindsvater,[5] Hickox,[5] Bahkmeteff,[1] and Matzke.[6] The agreement is within experimental error.
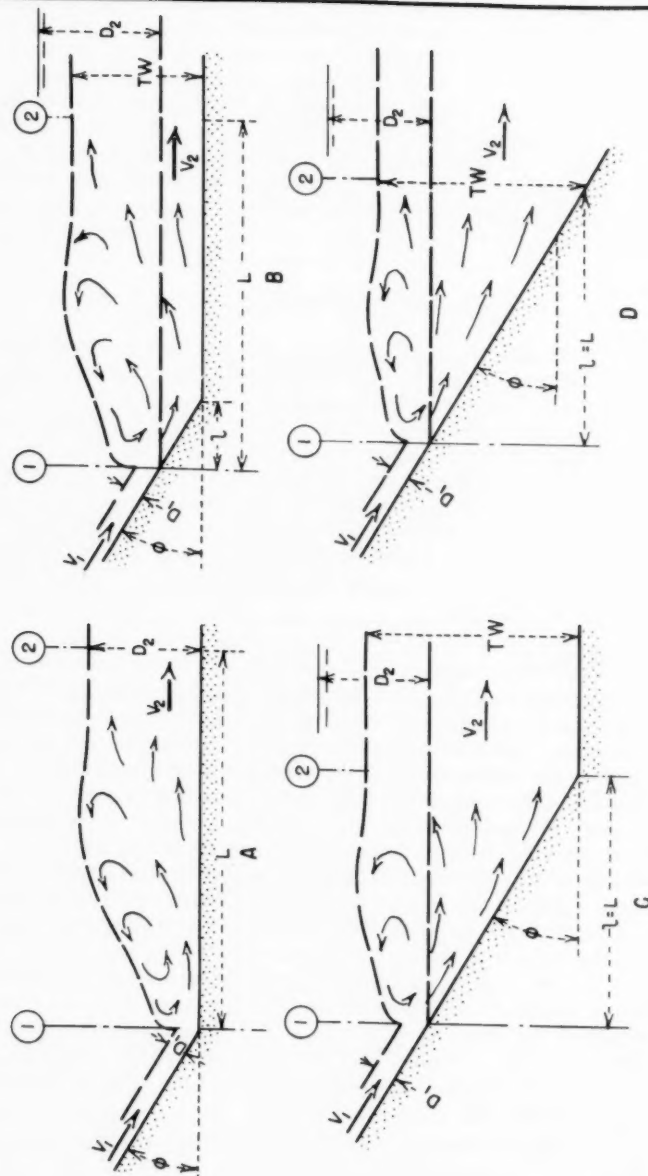
FIGURE 30



HYDRAULIC JUMP STUDIES
STILLING BASIN V
SLOPING APRONS

437

HYDRAULIC JUMP STUDIES
STILLING BASIN V (CASE D)
HYDRAULIC JUMP ON SLOPING APRON
RATIO OF TAILWATER DEPTH TO $D_1$
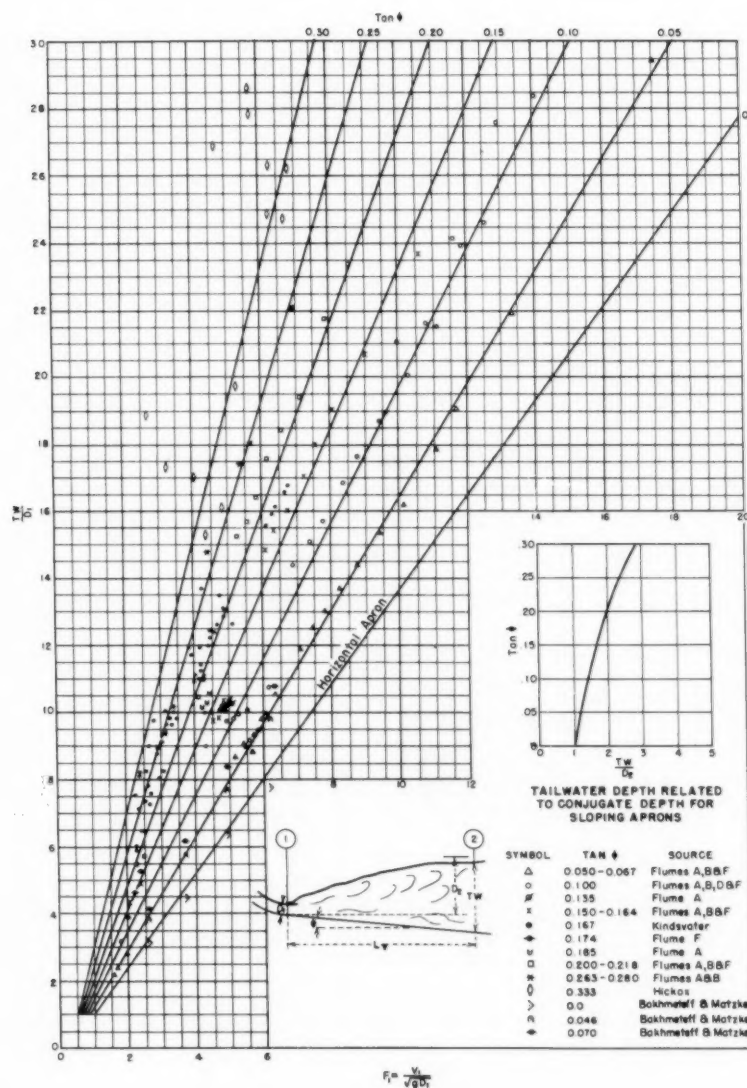
## Table 8

### STILLING BASINS WITH SLOPING APRON
### Case D, Basin V

| Test of flume (1) | Slope :tan ∅ (2) | Q of cfs (3) | W Total Width of basin ft (4) | q per ft of basin cfs (5) | TW ft (6) | V₁ ft/sec (7) | D₁ ft (8) | $\frac{TW}{D_1}$ (9) | $F_1 = \frac{V_1}{\sqrt{gD_1}}$ (10) | L Length of Jump ft (11) | $\frac{L}{TW}$ (12) | $\frac{D_2}{D_1}$ (13) | D₂ Conj TW ft (14) | $\frac{TW}{D_2}$ (15) | $\frac{L}{D_2}$ (16) | K Shape factor (17) |
|---|---|---|---|---|---|---|---|---|---|---|---|---|---|---|---|---|
| A | 0.067 | 2.000 | 4.880 | 0.410 | 0.520 | 7.88 | 0.052 | 10.00 | 6.09 | 2.60 | 5.00 | 8.20 | 0.426 | 1.22 | 6.11 | 2.50 |
| | | 2.250 | | 0.461 | 0.560 | 8.09 | .057 | 9.82 | 5.97 | 2.90 | 5.18 | 7.90 | 0.450 | 1.24 | 6.45 | 2.50 |
| | | 2.500 | | 0.512 | 0.589 | 8.26 | .062 | 9.50 | 5.85 | 3.10 | 5.26 | 7.85 | 0.466 | 1.21 | 6.38 | 2.40 |
| | | 2.750 | | 0.564 | 0.629 | 8.42 | .067 | 9.39 | 5.73 | 3.30 | 5.25 | 7.70 | 0.516 | 1.22 | 6.40 | 2.45 |
| | | 3.000 | | 0.615 | 0.660 | 8.54 | .072 | 9.17 | 5.61 | 3.40 | 5.15 | 7.55 | 0.544 | 1.21 | 6.25 | 2.45 |
| | | 3.250 | | 0.666 | 0.694 | 8.65 | .077 | 9.01 | 5.49 | 3.45 | 4.97 | 7.40 | 0.570 | 1.22 | 6.05 | 2.50 |
| | | 3.500 | | 0.717 | 0.744 | 8.74 | .082 | 9.07 | 5.38 | 3.60 | 4.84 | 7.20 | 0.590 | 1.26 | 6.10 | 2.80 |
| | | 1.500 | 4,350 | 0.345 | 0.474 | 7.67 | .045 | 10.53 | 6.37 | 2.40 | 5.06 | 8.60 | 0.387 | 1.22 | 6.20 | 2.50 |
| | | 2.500 | | 0.575 | 0.642 | 8.46 | .068 | 9.44 | 5.72 | 3.20 | 4.98 | 7.70 | 0.523 | 1.23 | 6.12 | 2.50 |
| | | 3.500 | | 0.805 | 0.792 | 8.85 | .091 | 8.70 | 5.17 | 4.00 | 5.05 | 6.90 | 0.628 | 1.26 | 6.37 | 2.75 |
| | 0.096 | 2.000 | 4,830 | 0.414 | 0.560 | 7.96 | .052 | 10.77 | 6.15 | 2.50 | 4.47 | 8.20 | 0.426 | 1.31 | 5.87 | 2.04 |
| | | 2.500 | | 0.518 | 0.652 | 7.97 | .065 | 10.03 | 5.51 | 3.60 | 5.52 | 7.45 | 0.484 | 1.35 | 7.44 | 2.28 |
| | | 3.000 | | 0.621 | 0.745 | 8.28 | .075 | 9.93 | 5.33 | 3.20 | 4.30 | 7.10 | 0.532 | 1.40 | 6.01 | 2.40 |
| | | 3.500 | | 0.725 | 0.835 | 8.53 | .085 | 9.82 | 5.15 | 3.60 | 4.31 | 6.90 | 0.586 | 1.42 | 6.15 | 2.50 |
| | | 4.000 | | 0.828 | 0.940 | 8.63 | .096 | 9.79 | 4.90 | 4.00 | 4.26 | 6.50 | 0.624 | 1.51 | 6.41 | 2.75 |
| | 0.135 | 2.000 | 4,810 | 0.416 | 0.620 | 6.93 | .060 | 10.33 | 4.99 | 2.50 | 4.06 | 6.60 | 0.396 | 1.56 | 6.32 | 2.15 |
| | | 2.500 | | 0.520 | 0.710 | 7.54 | .069 | 10.29 | 5.06 | 3.00 | 4.23 | 6.75 | 0.466 | 1.52 | 6.44 | 2.07 |
| | | 3.000 | | 0.624 | 0.895 | 7.80 | .080 | 10.06 | 4.66 | 3.20 | 3.97 | 6.40 | 0.512 | 1.57 | 6.25 | 2.15 |
| | | 3.500 | | 0.728 | 0.905 | 8.09 | .090 | 10.06 | 4.75 | 3.60 | 3.98 | 6.30 | 0.567 | 1.60 | 6.34 | 2.22 |
| | | 4.000 | | 0.832 | 0.985 | 8.58 | .097 | 10.15 | 4.85 | 3.90 | 3.96 | 6.40 | 0.621 | 1.59 | 6.28 | 2.19 |
| | 0.152 | 1.500 | 4,350 | 0.345 | 0.540 | 6.27 | .055 | 9.82 | 4.71 | 2.10 | 3.89 | 6.20 | 0.341 | 1.58 | 6.16 | 1.94 |
| | | 2.000 | | 0.460 | 0.663 | 6.76 | .068 | 9.75 | 4.57 | 2.55 | 3.85 | 6.10 | 0.415 | 1.60 | 6.15 | 2.00 |
| | | 2.500 | | 0.575 | 0.790 | 7.57 | .076 | 10.39 | 4.84 | 3.10 | 3.92 | 6.45 | 0.490 | 1.61 | 6.33 | 2.00 |
| | | 3.000 | | 0.690 | 0.900 | 7.67 | .090 | 10.00 | 4.50 | 3.40 | 3.78 | 6.00 | 0.540 | 1.67 | 6.30 | 2.10 |

Table 8--Continued

| (1) | (2) | (3) | (4) | (5) | (6) | (7) | (8) | (9) | (10) | (11) | (12) | (13) | (14) | (15) | (16) | (17) |
|---|---|---|---|---|---|---|---|---|---|---|---|---|---|---|---|---|
| A | 0.185 | 1.500 | 4.350 | 0.345 | 0.600 | 6.05 | 0.057 | 10.53 | 4.47 | 2.15 | 3.58 | 5.90 | 0.336 | 1.78 | 6.40 | 1.83 |
|  |  | 2.000 |  | 0.460 | 0.720 | 6.57 | .070 | 10.29 | 4.38 | 2.60 | 3.61 | 5.80 | 0.406 | 1.77 | 6.40 | 1.83 |
|  |  | 2.500 |  | 0.575 | 0.840 | 7.01 | .082 | 10.24 | 4.31 | 3.00 | 3.57 | 5.70 | 0.467 | 1.80 | 6.42 | 1.85 |
|  | 0.218 | 1.750 | 4.350 | 0.402 | 0.700 | 6.00 | .067 | 10.45 | 4.08 | 2.30 | 3.29 | 5.45 | 0.365 | 1.92 | 6.30 | 1.70 |
|  |  | 2.250 |  | 0.517 | 0.862 | 6.63 | .078 | 11.05 | 4.19 | 2.70 | 3.13 | 5.55 | 0.433 | 1.99 | 6.24 | 1.73 |
|  | 0.280 | 1.250 | 4.350 | 0.287 | 0.620 | 4.70 | .061 | 10.16 | 3.35 | 1.60 | 2.58 | 4.25 | 0.259 | 2.39 | 6.18 | 1.44 |
|  |  | 1.500 |  | 0.345 | 0.675 | 4.79 | .072 | 9.38 | 3.15 | 1.80 | 2.67 | 4.05 | 0.292 | 2.31 | 6.17 | 1.44 |
|  |  | 1.750 |  | 0.402 | 0.752 | 4.79 | .084 | 8.95 | 2.91 | 1.95 | 2.59 | 3.70 | 0.311 | 2.42 | 6.27 | 1.46 |
| B | 0.052 | 1.000 | 2.000 | 0.500 | 0.850 | 17.24 | .029 | 29.48 | 17.85 | 4.10 | 4.79 | 24.75 | 0.718 | 1.19 | 5.71 | 2.94 |
|  |  | 1.500 |  | 0.750 | 1.010 | 16.30 | .046 | 21.96 | 13.40 | 5.10 | 5.05 | 18.45 | 0.849 | 1.19 | 6.01 | 2.80 |
|  |  | 2.000 |  | 1.000 | 1.160 | 16.39 | .061 | 19.02 | 11.69 | 6.10 | 5.26 | 16.10 | 0.982 | 1.18 | 6.21 | 2.78 |
|  |  | 2.500 |  | 1.250 | 1.300 | 17.12 | .073 | 17.81 | 11.16 | 6.50 | 5.00 | 15.35 | 1.121 | 1.16 | 5.80 | 2.45 |
|  |  | 3.000 |  | 1.500 | 1.426 | 17.05 | .088 | 16.20 | 10.13 | 7.50 | 5.26 | 13.85 | 1.218 | 1.17 | 6.15 | 2.70 |
|  |  | 3.500 |  | 1.750 | 1.570 | 17.16 | .102 | 15.39 | 9.46 | 8.00 | 5.10 | 12.95 | 1.321 | 1.19 | 6.06 | 2.60 |
|  |  | 4.000 |  | 2.000 | 1.693 | 17.09 | .117 | 14.47 | 8.80 | 8.90 | 5.26 | 12.10 | 1.416 | 1.20 | 6.28 | 2.92 |
|  |  | 4.500 |  | 2.250 | 1.813 | 17.05 | .132 | 13.73 | 8.27 | 9.60 | 5.29 | 11.30 | 1.492 | 1.22 | 6.44 | 3.10 |
|  |  | 5.000 |  | 2.500 | 1.920 | 17.01 | .147 | 13.06 | 7.82 | 9.80 | 5.10 | 10.60 | 1.558 | 1.23 | 6.29 | 3.20 |
|  |  | 5.500 |  | 2.750 | 2.020 | 17.08 | .161 | 12.55 | 7.50 | 10.50 | 5.20 | 10.20 | 1.642 | 1.23 | 6.40 | 3.20 |
|  |  | 6.000 |  | 3.000 | 2.110 | 16.95 | .177 | 11.92 | 7.10 | 11.00 | 5.21 | 9.65 | 1.708 | 1.24 | 6.44 | 3.30 |
|  | 0.102 | 1.000 | 2.000 | 0.500 | 0.970 | 15.63 | .032 | 30.3 | 15.40 | 4.20 | 4.33 | 21.25 | 0.680 | 1.42 | 6.17 | 2.51 |
|  |  | 1.500 |  | 0.750 | 1.180 | 15.63 | .048 | 24.58 | 12.57 | 5.20 | 4.41 | 17.30 | 0.830 | 1.42 | 6.27 | 2.50 |
|  |  | 2.000 |  | 1.000 | 1.354 | 15.87 | .063 | 22.49 | 11.14 | 6.10 | 4.51 | 15.35 | 0.967 | 1.40 | 6.31 | 2.44 |
|  |  | 2.500 |  | 1.250 | 1.543 | 16.23 | .077 | 20.04 | 10.30 | 6.80 | 4.40 | 14.15 | 1.088 | 1.42 | 6.24 | 2.50 |
|  |  | 3.000 |  | 1.500 | 1.724 | 16.48 | .091 | 18.95 | 9.63 | 7.60 | 4.41 | 13.20 | 1.200 | 1.44 | 6.34 | 2.56 |
|  |  | 3.000 |  | 1.500 | 1.720 | 16.30 | .092 | 18.70 | 9.47 | 7.50 | 4.36 | 12.95 | 1.191 | 1.44 | 6.30 | 2.58 |
|  |  | 3.500 |  | 1.750 | 1.890 | 16.36 | .107 | 17.66 | 8.81 | 8.20 | 4.34 | 12.10 | 1.293 | 1.46 | 6.34 | 2.75 |
|  |  | 4.000 |  | 2.000 | 2.040 | 16.53 | .121 | 16.86 | 8.37 | 8.80 | 4.31 | 11.40 | 1.379 | 1.48 | 6.38 | 2.72 |
|  |  | 4.500 |  | 2.250 | 2.152 | 16.42 | .137 | 15.71 | 7.82 | 9.40 | 4.37 | 10.60 | 1.452 | 1.48 | 6.47 | 2.70 |

Table 8--Continued

| (1) | (2) | (3) | (4) | (5) | (6) | (7) | (8) | (9) | (10) | (11) | (12) | (13) | (14) | (15) | (16) | (17) |
|---|---|---|---|---|---|---|---|---|---|---|---|---|---|---|---|---|
| B | 0.102 | 5.000 | 2.000 | 2.500 | 2.300 | 16.45 | 0.152 | 15.13 | 7.44 | 10.00 | 4.34 | 10.10 | 1.536 | 1.50 | 6.51 | 2.75 |
|  |  | 5.500 |  | 2.750 | 2.450 | 16.18 | .170 | 14.41 | 6.91 | 10.60 | 4.33 | 9.35 | 1.590 | 1.54 | 6.67 | 2.85 |
|  | 0.164 | 2.000 |  | 1.000 | 1.537 | 15.38 | .065 | 23.65 | 10.64 | 6.10 | 3.97 | 14.65 | 0.952 | 1.61 | 6.41 | 1.88 |
|  |  | 2.500 |  | 1.250 | 1.737 | 14.88 | .084 | 20.68 | 9.05 | 6.90 | 3.97 | 12.40 | 1.042 | 1.67 | 6.62 | 1.95 |
|  |  | 3.000 |  | 1.500 | 1.940 | 14.71 | .102 | 19.02 | 8.11 | 7.50 | 3.86 | 11.05 | 1.128 | 1.72 | 6.64 | 2.02 |
|  |  | 3.500 |  | 1.750 | 2.120 | 14.83 | .118 | 17.97 | 7.61 | 8.20 | 3.87 | 10.30 | 1.215 | 1.74 | 6.75 | 2.03 |
|  |  | 4.000 |  | 2.000 | 2.270 | 15.04 | .133 | 17.07 | 7.27 | 8.70 | 3.83 | 9.85 | 1.310 | 1.73 | 6.64 | 2.01 |
|  |  | 4.500 |  | 2.250 | 2.420 | 14.90 | .151 | 16.03 | 6.75 | 9.20 | 3.80 | 9.10 | 1.374 | 1.76 | 6.70 | 2.08 |
|  |  | 5.000 |  | 2.500 | 2.590 | 14.88 | .168 | 15.42 | 6.39 | 9.70 | 3.74 | 8.65 | 1.454 | 1.78 | 6.67 | 2.08 |
|  |  | 5.500 |  | 2.750 | 2.750 | 14.86 | .185 | 14.86 | 6.09 | 10.20 | 3.71 | 8.20 | 1.517 | 1.81 | 6.73 | 2.10 |
|  | 0.213 | 2.000 |  | 1.000 | 1.750 | 13.33 | .075 | 23.33 | 8.60 | 6.00 | 3.43 | 11.75 | 0.881 | 1.99 | 6.81 | 1.71 |
|  |  | 2.500 |  | 1.250 | 2.000 | 13.59 | .092 | 21.74 | 7.89 | 6.60 | 3.30 | 10.70 | 0.984 | 2.03 | 6.71 | 1.76 |
|  |  | 3.000 |  | 1.500 | 2.150 | 13.51 | .111 | 19.37 | 7.15 | 7.30 | 3.40 | 9.70 | 1.077 | 2.00 | 6.78 | 1.73 |
|  |  | 3.500 |  | 1.750 | 2.370 | 13.57 | .129 | 18.37 | 6.65 | 8.00 | 3.38 | 9.00 | 1.161 | 2.04 | 6.89 | 1.76 |
|  |  | 4.000 |  | 2.000 | 2.600 | 13.51 | .148 | 17.57 | 6.19 | 8.30 | 3.19 | 8.35 | 1.236 | 2.10 | 6.71 | 1.79 |
|  |  | 4.500 |  | 2.250 | 2.720 | 13.55 | .166 | 16.39 | 5.86 | 9.10 | 3.34 | 7.85 | 1.303 | 2.09 | 6.98 | 1.78 |
|  |  | 5.000 |  | 2.500 | 2.890 | 13.59 | .184 | 15.71 | 5.58 | 9.60 | 3.32 | 7.50 | 1.380 | 2.09 | 6.96 | 1.79 |
|  |  | 5.500 |  | 2.750 | 3.100 | 13.55 | .203 | 15.27 | 5.30 | 10.00 | 3.22 | 7.10 | 1.441 | 2.15 | 6.94 | 1.81 |
|  | 0.263 | 2.000 |  | 1.000 | 1.900 | 11.63 | .086 | 22.09 | 6.98 | 5.60 | 2.95 | 9.45 | 0.813 | 2.34 | 6.89 | 1.55 |
|  |  | 3.000 |  | 1.500 | 2.330 | 11.63 | .129 | 18.06 | 5.70 | 6.90 | 2.96 | 7.65 | 0.987 | 2.36 | 6.99 | 1.56 |
|  |  | 4.000 |  | 2.000 | 2.820 | 12.35 | .162 | 17.41 | 5.40 | 8.10 | 2.87 | 7.25 | 1.174 | 2.40 | 6.90 | 1.57 |
|  |  | 5.000 |  | 2.500 | 3.270 | 12.38 | .202 | 16.19 | 4.85 | 9.20 | 2.81 | 6.45 | 1.303 | 2.51 | 7.06 | 1.59 |
|  |  | 6.000 |  | 3.000 | 3.602 | 12.35 | .243 | 14.82 | 4.41 | 10.00 | 2.77 | 5.80 | 1.409 | 2.56 | 7.09 | 1.59 |
| D | 0.100 | 4.000 | 3.970 | 1.007 | 1.530 | 18.64 | .054 | 28.33 | 14.14 | 6.60 | 4.31 | 19.50 | 1.053 | 1.45 | 6.27 | 2.65 |
|  |  | 6.000 |  | 1.511 | 1.888 | 19.12 | .079 | 23.90 | 11.99 | 8.20 | 4.34 | 16.50 | 1.303 | 1.45 | 6.29 | 2.65 |
|  |  | 8.000 |  | 2.015 | 2.200 | 19.75 | .102 | 21.57 | 10.90 | 9.70 | 4.41 | 14.95 | 1.525 | 1.44 | 6.36 | 2.65 |
|  |  | 10.000 |  | 2.518 | 2.630 | 20.14 | .125 | 21.04 | 10.04 | 11.50 | 4.37 | 13.75 | 1.719 | 1.53 | 6.69 | 2.85 |
|  |  | 2.250 |  | 0.567 | 1.200 | 18.90 | .030 | 40.00 | 19.23 | 4.75 | 3.96 | 26.70 | 0.801 | 1.50 | 5.93 | 2.75 |

## Table 8—Continued

| (1) | (2) | (3) | (4) | (5) | (6) | (7) | (8) | (9) | (10) | (11) | (12) | (13) | (14) | (15) | (16) | (17) |
|---|---|---|---|---|---|---|---|---|---|---|---|---|---|---|---|---|
| D | 0.100 | 4.500 | 3.970 | 1.134 | 1.710 | 18.29 | 0.062 | 27.58 | 12.94 | 7.80 | 4.56 | 17.90 | 1.109 | 1.54 | 7.03 | 2.90 |
|   |   | 6.750 |   | 1.700 | 2.100 | 19.54 | 0.087 | 24.14 | 11.67 | 9.10 | 4.33 | 16.10 | 1.400 | 1.50 | 6.50 | 2.78 |
| F | 0.174 | 1.980 | 1.000 | 1.980 | 1.452 | 7.17 | .276 | 5.26 | 2.41 | 4.30 | 2.96 | 3.00 | 0.828 | 1.75 | 5.19 | 1.88 |
|   |   | 2.800 |   | 2.800 | 1.663 | 7.69 | .364 | 4.57 | 2.24 | 5.00 | 3.01 | 2.80 | 1.018 | 1.63 | 4.91 | 1.76 |
|   | 0.200 | 2.980 |   | 2.980 | 2.035 | 8.32 | .358 | 5.68 | 2.45 | 5.80 | 2.85 | 3.05 | 1.092 | 1.86 | 5.31 | 1.72 |
|   |   | 3.850 |   | 3.850 | 2.460 | 8.48 | .454 | 5.42 | 2.22 | 6.70 | 2.72 | 2.75 | 1.248 | 1.97 | 5.37 | 1.81 |
|   | 0.150 | 3.850 |   | 3.850 | 2.095 | 7.97 | .483 | 4.33 | 2.02 | 5.90 | 2.82 | 2.45 | 1.183 | 1.77 | 4.99 | 2.10 |
|   |   | 1.780 |   | 1.780 | 1.260 | 6.93 | .257 | 4.90 | 2.41 | 4.00 | 3.17 | 3.00 | 0.771 | 1.63 | 5.19 | 2.00 |
|   | 0.100 | 1.940 |   | 1.940 | 1.180 | 6.40 | .303 | 3.89 | 2.05 | 3.70 | 3.14 | 2.50 | 0.757 | 1.56 | 4.89 | 2.93 |
|   |   | 3.870 |   | 3.870 | 1.648 | 7.38 | .524 | 3.14 | 1.80 | 4.80 | 2.91 | 2.15 | 1.126 | 1.46 | 4.26 | 2.55 |
|   | 0.050 | 3.620 |   | 3.620 | 1.357 | 7.62 | .475 | 2.86 | 1.95 | 4.30 | 3.17 | 2.35 | 1.116 | 1.22 | 3.85 | 3.00 |
|   |   | 1.820 |   | 1.820 | 1.306 | 12.38 | .147 | 8.88 | 5.69 | 6.80 | 5.21 | 7.65 | 1.124 | 1.16 | 6.05 | 3.90 |
|   |   | 3.910 |   | 3.910 | 1.291 | 6.66 | .587 | 2.20 | 1.53 | 3.60 | 2.79 | 1.80 | 1.057 | 1.22 | 3.41 | 3.20 |
|   |   | 2.300 |   | 2.300 | 0.943 | 5.87 | .392 | 2.41 | 1.65 | 2.80 | 2.97 | 1.95 | 0.764 | 1.23 | 3.67 | 3.20 |

The small chart on Figure 31 was constructed using data from the larger chart, and shows, for a range of apron slopes, the ratio of tail water depth for a continuous sloping apron, to conjugate depth for a horizontal apron. As indicated on the small sketch in Figure 31, $D_2$ and TW are identical for a horizontal apron. The conjugate depth, $D_2$, listed in Column 14, Table 6, is the depth necessary for a jump to form on an imaginary horizontal floor beginning at Section 1, Figure 31.

The small chart, therefore, shows the extra depth, required for a jump of a given Froude number to form on a sloping apron, rather than on a horizontal apron. For example, if the tangent of the slope is 0.10, a tail water depth equal to 1.4 times the conjugate depth ($D_2$ for a horizontal apron) will occur at the end of the jump; while if the slope is 0.30, the tail water depth at the end of the jump will be 2.8 times the conjugate depth, $D_2$. The conjugate depth, $D_2$, used in connection with a sloping apron is merely a convenient reference figure which has no other meaning. It will be used throughout this discussion on sloping aprons.

## Length of Jump (Case D)

The length of jump for the Case D experiments has been presented in two ways. First, the ratio length of jump to tail water depth, Column 12, was plotted with respect to the Froude number on Figure 32 for sloping aprons having tangents from 0 to 0.25. Secondly, the ratio of length of jump to the conjugate tail water depth, Column 16, Table 8, has been plotted with respect to the Froude number for the same range of slopes on Figure 33. Although not evident on Figure 32, it can be seen from Figure 33 that the length of jump on a sloping apron is longer than that which occurs on a horizontal floor. For example, for a Froude number of 8, the ratio $\frac{L}{D_2}$ varies from 6.1, for a horizontal apron, to 7.0, for an apron with a slope of 0.25. Length determinations from Kindsvater[5] for a slope of 0.167 are also plotted on Figure 32. The points show a wide spread.

## Expression for Jump on Sloping Apron (Case D)

Several mathematicians and experimenters have developed expressions for the hydraulic jump on sloping aprons,[2,5,6,13] so there is no need to repeat any of these derivations here. An expression presented by Kindsvater[5] is the more common and perhaps the more practical to use.

$$\frac{D_2}{D_1} = \frac{1}{2 \cos \phi} \left[ \sqrt{\frac{8F_1^2 \cos^3 \phi}{1-2K \tan \phi} + 1} \ - 1 \right] \tag{5}$$

All symbols have been referred to previously, except for the coefficient K, a dimensionless parameter called the shape factor, which varies with the Froude number and the slope of the apron. Kindsvater and Hickox evaluated this coefficient from the profile of the jump and the measured floor pressures. Surface profiles and pressures were not measured in the current tests but, as a matter of interest, K was computed from Expression 5 by substituting experimental values and solving for K. The resulting values of K are listed in Column 17 of Table 8, and are shown plotted with respect to the Froude

FIGURE 32



HYDRAULIC JUMP STUDIES
STILLING BASIN "V" (CASE D)
LENGTH OF JUMP IN TERMS OF TW DEPTH
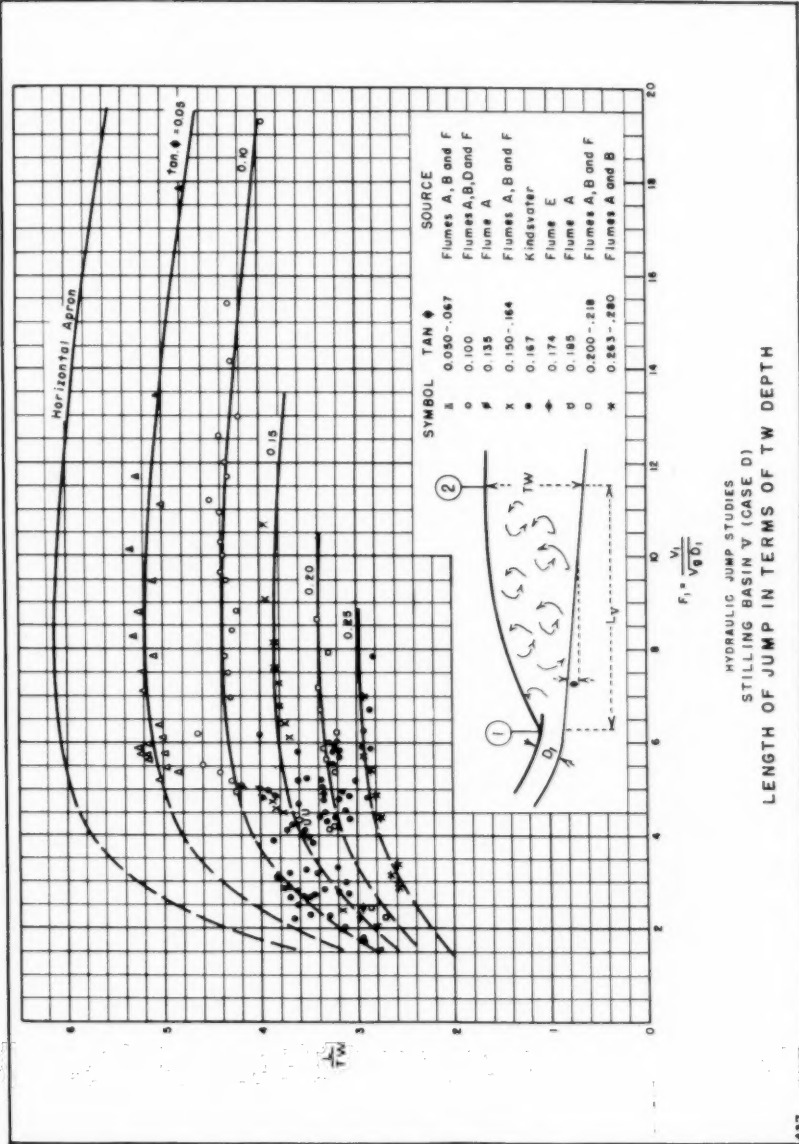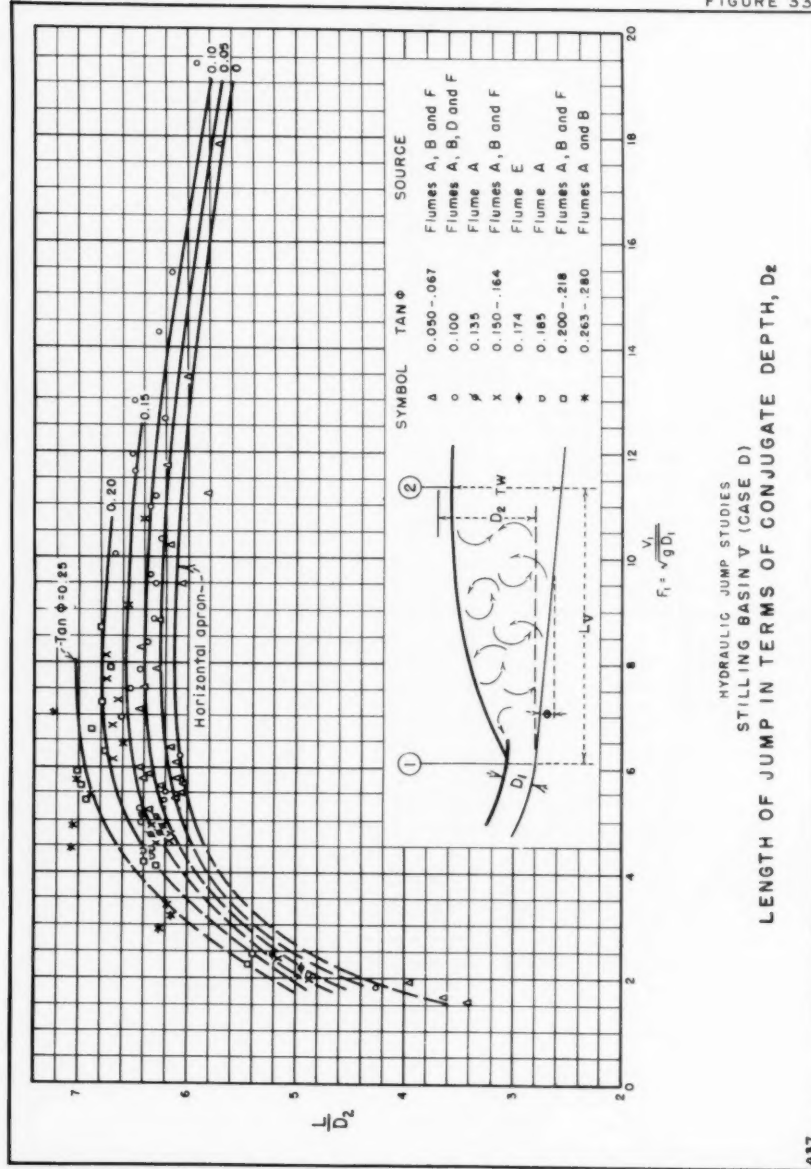
FIGURE 33



HYDRAULIC JUMP STUDIES
STILLING BASIN V (CASE D)
LENGTH OF JUMP IN TERMS OF CONJUGATE DEPTH, $D_2$

437

number for the various slopes on Figure 34A. Superimposed on Figure 34A are data from Kindsvater for a slope of 0.167, and data from Hickox on a slope of 0.333. The agreement is not particularly striking nor do the points plot well, but it should be remembered that the value K is dependent on the method used for determining the length of jump. The current experiments indicate that the Froude number has little effect on the value of K. Assuming this to be the case, values of individual points for each slope were averaged and K is shown plotted with respect to tan $\phi$ on Figure 34B. This phase is incidental to the study at hand and has been discussed only to complete the data analysis.

### Jump Characteristics (Case B)

Case B is the one usually encountered in sloping apron design where the jump forms both on the slope and over the horizontal portion of the apron. Although this form of jump may appear quite complicated, it can be readily analyzed when approached from a practical standpoint. The primary concern in sloping apron design is the tail water depth required to move the front of the jump up the slope to Section 1, Figure 30B. There is little to be gained with a sloping apron unless the entire length of the sloping portion is utilized.

Referring to the sketches on Figure 35A, it can be observed that for tail water equal to the conjugate depth, $D_2$, the front of the jump will occur at a point 0, a short distance up the slope. This distance is noted as $1_0$ and varies with the degree of slope. If the tail water depth is increased a vertical increment, $\Delta Y_1$, it would be reasonable to assume that the front of the jump would raise a corresponding increment. This is not true; the jump profile undergoes an immediate change as the slope becomes part of the stilling basin. Thus, for an increase in tail water depth, $\Delta Y_1$, the front of the jump moves up the slope to Point 1, or moves a vertical distance $\Delta Y_1'$, which is several times $\Delta Y_1$. Increasing the tail water depth a second increment, say $\Delta Y_2$, produces the same effect to a lesser degree, moving the front of the jump to Point 2. Additional increments of tail water depth produce the same effect but to a still lesser degree, and this continues until the tail water depth approaches $1.3D_2$. For greater tail water depths, the relation is geometric; an increase in tail water depth, $\Delta Y_4$, moves the front of the jump up the slope an equal vertical distance $\Delta Y_4$, from Point 3 to 4. Should the slope be very flat, as in Figure 35B, the horizontal movement of the front of the jump is even more pronounced.

The following studies were made to definitely tabulate the characteristics described above for conditions encountered in design since it has been necessary in the past to check practically all sloping apron designs by model studies to be certain that the entire sloping portion of the apron was utilized.

### Experimental Results (Case B)

The experiments for determining the magnitude of the profile characteristics were carried out on a large scale in Flume D, and the results are recorded in Table 9. A sloping floor was placed in the flume as in Figure 30B. A discharge was established (Column 3, Table 9) and the depth of flow, $D_1$ (Column 6), was measured immediately upstream from the front of the jump in each instance. The velocity entering the jump, $V_1$ (Column 7), and the Froude number (Column 8) were computed. Entering Figure 31 with the computed values of $F_1$, the ratio $\dfrac{D_2}{D_1}$ (Column 9) was obtained from the line labeled

FIGURE 34



$$\frac{D_2}{D'} = \frac{1}{2\cos\phi}\left(\sqrt{\frac{8F^2\cos^3\phi}{1-2K\tan\phi}+1} -1\right)$$
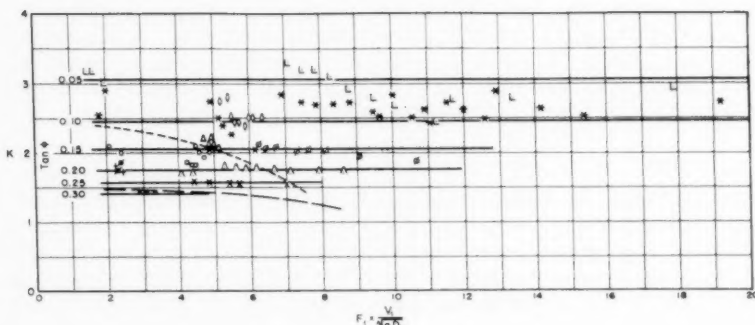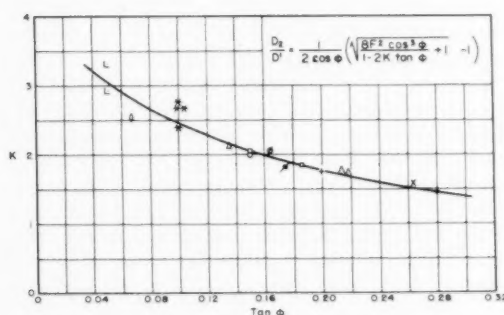
Above curve is based on assumption
that K is independent of $F_1$

**B**

| SYMBOL | Tan φ |
|---|---|
| L | 0 052 |
| 0 | .067 |
| * | .100 |
| Δ | .135 |
| o | .150 |
| ø | .164 |
| u | .174 |
| o | .185 |
| + | .200 |
| Λ | .215 |
| x | .263 |
| • |  |
| | .167 Kindsvator |
| - - - - - | .333 Hickox |

HYDRAULIC JUMP STUDIES

STILLING BASIN V (CASE D)

**SHAPE FACTOR K**
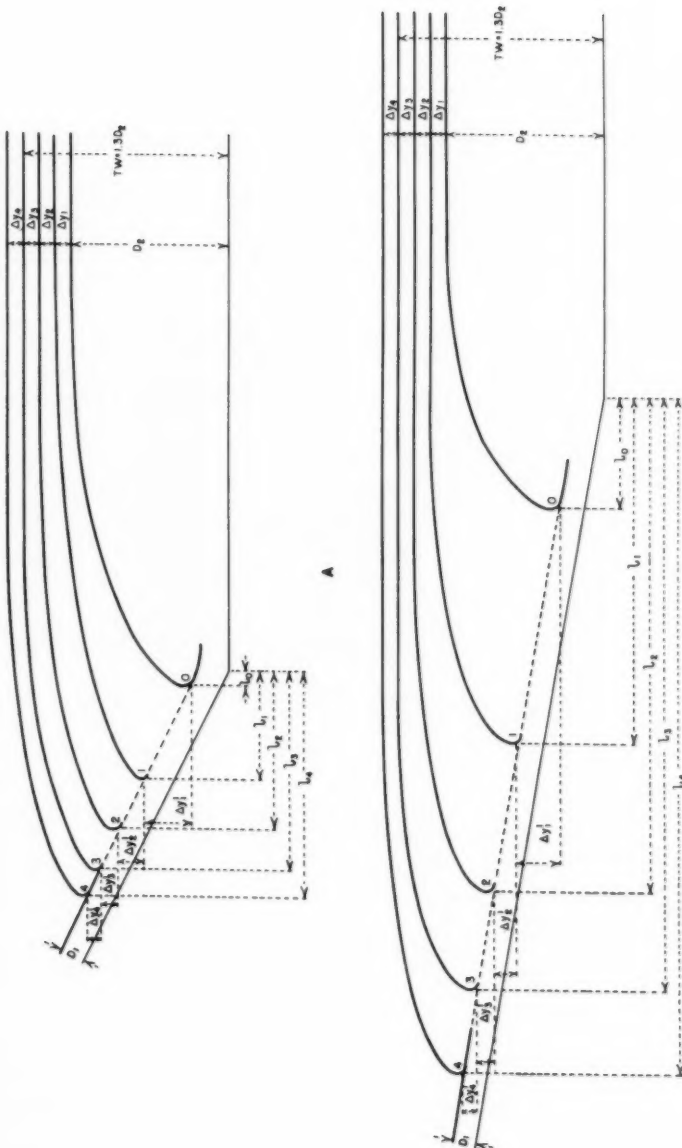
HYDRAULIC JUMP STUDIES

STILLING BASIN V (CASE B)

PROFILE CHARACTERISTICS

## Table 9

### STILLING BASINS WITH SLOPING APRONS
#### (Case B, Basin V)

| (1) Test flume | (2) Slope of $\tan\phi$ | (3) Total $Q$ of basin cfs | (4) Width $W$ of basin ft | (5) $q$ per ft of $W$ cfs | (6) $D_1$ ft | (7) $V_1$ ft/sec | (8) $F_1 = \dfrac{V_1}{\sqrt{gD_1}}$ | (9) $\dfrac{D_2}{D_1}$ | (10) $D_2$ Conj. of Jump: TW on slope ft | (11) Length of Jump on slope ft | (12) TW ft | (13) $\dfrac{l}{D_2}$ | (14) $\dfrac{TW}{D_2}$ | (15) $L_s$ Length of sloping floor ft |
|---|---|---|---|---|---|---|---|---|---|---|---|---|---|---|
| D | 0.05 | 5.050 | 3.970 | 1.272 | 0.063 | 20.19 | 14.18 | 19.51 | 1.229 | 6.00 | 1.390 | 4.88 | 1.13 | 4.0 |
| | | 8.070 | | 2.033 | .101 | 20.13 | 11.16 | 15.30 | .545 | 6.00 | 1.745 | 3.88 | 1.13 | |
| | | 11.555 | | 2.910 | .139 | 20.94 | 9.90 | 13.60 | .890 | 6.00 | 2.040 | 3.17 | 1.08 | |
| | 0.10 | 5.255 | | 1.324 | .067 | 19.76 | 13.46 | 18.60 | 1.246 | 4.80 | 1.440 | 3.85 | 1.16 | 4.0 |
| | | 8.090 | | 2.038 | .103 | 19.79 | 10.87 | 15.00 | 1.545 | 4.80 | 1.750 | 3.11 | 1.13 | |
| | | 11.560 | | 2.911 | .140 | 20.79 | 9.80 | 13.40 | 1.876 | 4.80 | 2.080 | 2.56 | 1.11 | |
| | | 5.000 | | 1.259 | .054 | 19.67 | 13.70 | 18.90 | 1.210 | 8.10 | 1.830 | 6.69 | 1.51 | 8.0 |
| | | | | | .065 | 19.37 | 13.38 | 18.40 | 1.196 | 6.30 | 1.660 | 5.26 | 1.39 | |
| | | | | | .067 | 18.79 | 12.80 | 17.65 | 1.183 | 4.70 | 1.510 | 3.97 | 1.28 | |
| | | | | | .068 | 18.51 | 12.50 | 17.20 | 1.169 | 4.00 | 1.410 | 3.42 | 1.21 | |
| | | | | | .070 | 17.98 | 11.99 | 16.50 | 1.155 | 3.20 | 1.340 | 2.77 | 1.16 | |
| | | 7.850 | | 1.977 | .101 | 19.57 | 10.86 | 15.00 | 1.515 | 7.80 | 2.070 | 5.15 | 1.37 | |
| | | | | | .102 | 19.38 | 10.70 | 14.70 | 1.499 | 6.00 | 1.940 | 4.00 | 1.29 | |
| | | | | | .103 | 19.19 | 10.54 | 14.50 | 1.494 | 5.30 | 1.880 | 3.55 | 1.26 | |
| | | | | | .104 | 19.01 | 10.39 | 14.25 | 1.482 | 4.40 | 1.770 | 2.96 | 1.19 | |
| | | 11.218 | | 2.825 | .139 | 20.32 | 9.61 | 13.15 | 1.828 | 8.30 | 2.410 | 4.54 | 1.32 | |
| | | | | | .141 | 20.04 | 9.41 | 12.88 | 1.816 | 6.20 | 2.260 | 3.41 | 1.24 | |
| | | | | | .142 | 19.89 | 9.30 | 12.80 | 1.818 | 4.80 | 2.180 | 2.64 | 1.20 | |
| | | 6.000 | | 1.511 | .076 | 19.88 | 12.70 | 17.50 | 1.330 | 2.20 | 1.375 | 1.65 | 1.03 | 2.0 |
| | | | | | .077 | 19.62 | 12.46 | 17.15 | 1.321 | 1.70 | 1.340 | 1.28 | 1.01 | |
| | | | | | .078 | 19.37 | 12.23 | 16.80 | 1.310 | 0.80 | 1.305 | 0.61 | 0.99 | |
| | | | | | | | | 17.50 | 1.321 | 0 | 1.260 | 0 | 0.98 | |
| | | 8.057 | | 2.029 | .098 | 20.70 | 11.66 | 16.00 | 1.568 | 2.40 | 1.625 | 1.53 | 1.04 | -- |
| | | | | | .099 | 20.49 | 11.48 | 15.80 | 1.564 | 1.90 | 1.600 | 1.22 | 1.02 | |

Table 9—Continued

| (1) | (2) | (3) | (4) | (5) | (6) | (7) | (8) | (9) | (10) | (11) | (12) | (13) | (14) | (15) |
|-----|-----|-----|-----|-----|-----|-----|-----|-----|------|------|------|------|------|------|
| D | 0.10 | | 3.970 | | 0.100 | 20.29 | 11.31 | 15.60 | 1.560 | 1.60 | 1.585 | 1.02 | 1.02 | |
| | | | | | .101 | 20.09 | 11.14 | 15.40 | 1.555 | 0.60 | 1.550 | 0.39 | 1.00 | |
| | | | | | .102 | 19.89 | 10.98 | 15.15 | 1.545 | 0 | 1.530 | 0 | 0.99 | |
| | 0.15 | 6.000 | | 1.511 | .075 | 20.15 | 12.96 | 17.85 | 1.339 | 0.50 | 1.335 | 0.37 | 1.00 | 1.2 |
| | | | | | .099 | 20.49 | 11.48 | 17.85 | 1.339 | 1.10 | 1.365 | 0.82 | 1.02 | |
| | | | | | .136 | 21.36 | 10.21 | 15.80 | 1.564 | 0.60 | 1.564 | 0.38 | 1.00 | |
| | | 8.057 | | 2.029 | | | | 14.00 | 1.564 | 1.20 | 1.600 | 0.77 | 1.02 | |
| | | | | | | | | 14.00 | 1.904 | 0.50 | 1.905 | 0.26 | 1.00 | -- |
| | | | | | | | | 14.00 | 1.904 | 1.50 | 1.970 | 0.79 | 1.03 | |
| | | 11.535 | | 2.905 | .069 | 19.32 | 12.97 | 17.85 | 1.232 | 4.00 | 1.530 | 3.25 | 1.24 | |
| | | | | | .104 | 19.57 | 10.70 | 14.70 | 1.529 | 4.20 | 1.810 | 2.75 | 1.18 | |
| | | | | | .141 | 20.64 | 9.69 | 13.25 | 1.868 | 4.20 | 2.150 | 2.25 | 1.15 | |
| | | 5.295 | | 1.333 | .064 | 19.58 | 13.64 | 18.75 | 1.200 | 5.30 | 1.660 | 4.42 | 1.38 | |
| | | | | | .065 | 19.27 | 13.32 | 18.35 | 1.193 | 5.10 | 1.590 | 4.27 | 1.33 | |
| | | | | | .066 | 18.98 | 13.02 | 18.00 | 1.188 | 4.00 | 1.505 | 3.37 | 1.27 | |
| | | | | | .067 | 18.70 | 12.74 | 17.55 | 1.176 | 3.10 | 1.420 | 2.64 | 1.21 | |
| | | 8.080 | | 2.035 | | | | 17.55 | 1.176 | 2.60 | 1.375 | 2.21 | 1.17 | |
| | | | | | .068 | 18.42 | 12.45 | 17.15 | 1.166 | 2.20 | 1.305 | 1.89 | 1.12 | |
| | | | | | | | | 17.15 | 1.166 | 1.80 | 1.230 | 1.54 | 1.05 | |
| | | 11.553 | | 2.910 | .103 | 19.62 | 10.77 | 14.85 | 1.530 | 5.30 | 1.940 | 3.46 | 1.27 | 5.3 |
| | | | | | | | | 14.85 | 1.530 | 4.30 | 1.875 | 2.81 | 1.23 | |
| | | | | | | | | 14.85 | 1.530 | 3.80 | 1.800 | 2.48 | 1.18 | |
| | | 4.976 | | 1.253 | .104 | 19.43 | 10.62 | 14.60 | 1.518 | 2.80 | 1.705 | 1.84 | 1.12 | |
| | | | | | | | | 14.60 | 1.518 | 2.20 | 1.640 | 1.45 | 1.08 | |
| | | | | | | | | 14.40 | 1.512 | 1.20 | 1.580 | 0.79 | 1.05 | |
| | | 8.025 | | 2.021 | .105 | 19.25 | 10.47 | 13.10 | 1.860 | 5.30 | 2.250 | 2.85 | 1.22 | |
| | | | | | | | | 13.10 | 1.860 | 4.30 | 2.190 | 2.31 | 1.18 | |
| | | 11.530 | | 2.904 | .142 | 20.45 | 9.57 | 13.10 | 1.860 | 3.60 | 2.120 | 1.94 | 1.14 | |

Table 9--Continued

| (1) | (2) | (3) | (4) | (5) | (6) | (7) | (8) | (9) | (10) | (11) | (12) | (13) | (14) | (15) |
|---|---|---|---|---|---|---|---|---|---|---|---|---|---|---|
| D | 0.20 | 5.393 | 3.970 | 1.358 | 0.071 | 19.13 | 12.65 | 17.35 | 1.232 | 4.60 | 1.790 | 3.73 | 1.45 | 5.3 |
|  |  |  |  |  |  |  |  | 17.35 | 1.232 | 4.40 | 1.720 | 3.58 | 1.40 |  |
|  |  |  |  |  | .072 | 18.86 | 12.40 | 17.05 | 1.228 | 4.00 | 1.680 | 3.25 | 1.36 |  |
|  |  |  |  |  |  |  |  | 17.05 | 1.228 | 3.60 | 1.605 | 2.93 | 1.31 |  |
|  |  |  |  |  |  |  |  | 17.05 | 1.228 | 3.00 | 1.550 | 2.44 | 1.26 |  |
|  |  |  |  |  |  |  |  | 17.05 | 1.228 | 2.60 | 1.490 | 2.12 | 1.21 |  |
|  |  |  |  |  | .073 | 18.60 | 12.13 | 16.65 | 1.212 | 2.30 | 1.420 | 1.90 | 1.17 |  |
|  |  |  |  |  |  |  |  | 16.60 | 1.215 | 1.50 | 1.350 | 1.24 | 1.11 |  |
|  |  |  |  |  |  |  |  | 16.60 | 1.215 | 1.20 | 1.280 | 0.99 | 1.05 |  |
|  |  | 8.080 |  | 2.035 | .105 | 19.38 | 10.54 | 14.50 | 1.523 | 4.60 | 2.010 | 3.02 | 1.32 |  |
|  |  |  |  |  |  |  |  | 14.50 | 1.523 | 4.00 | 1.955 | 2.63 | 1.28 |  |
|  |  |  |  |  |  |  |  | 14.50 | 1.523 | 3.30 | 1.890 | 2.17 | 1.24 |  |
|  |  |  |  |  | .104 | 19.57 | 10.70 | 14.70 | 1.529 | 3.10 | 1.830 | 2.03 | 1.20 |  |
|  |  |  |  |  |  |  |  | 14.70 | 1.529 | 2.50 | 1.730 | 1.64 | 1.13 |  |
|  |  |  |  |  |  |  |  | 14.70 | 1.529 | 1.80 | 1.670 | 1.18 | 1.09 |  |
|  |  | 11.573 |  | 2.915 | .145 | 20.10 | 9.30 | 12.80 | 1.856 | 4.40 | 2.310 | 2.37 | 1.24 |  |
|  |  |  |  |  |  |  |  | 12.80 | 1.856 | 3.70 | 2.230 | 1.99 | 1.20 |  |
|  |  |  |  |  |  |  |  | 12.80 | 1.856 | 3.30 | 2.175 | 1.78 | 1.17 |  |
|  |  | 4.820 |  | 1.214 | .063 | 19.27 | 13.53 | 18.70 | 1.178 | 3.70 | 1.605 | 3.14 | 1.36 | 4.0 |
|  |  | 8.089 |  | 2.037 | .105 | 19.40 | 10.55 | 14.50 | 1.523 | 3.90 | 1.900 | 2.56 | 1.25 |  |
|  |  | 11.565 |  | 2.913 | .143 | 20.37 | 9.50 | 13.05 | 1.866 | 3.90 | 2.180 | 2.09 | 1.17 |  |
| D | 0.25 | 5.344 |  | 1.346 | .071 | 18.96 | 12.54 | 17.25 | 1.225 | 4.20 | 1.825 | 3.43 | 1.49 | 5.3 |
|  |  |  |  |  |  |  |  | 17.25 | 1.225 | 4.10 | 1.755 | 3.35 | 1.43 |  |
|  |  |  |  |  |  |  |  | 17.25 | 1.225 | 3.50 | 1.680 | 2.86 | 1.37 |  |
|  |  |  |  |  | .070 | 19.22 | 12.81 | 17.75 | 1.242 | 3.00 | 1.600 | 2.42 | 1.29 |  |
|  |  |  |  |  |  |  |  | 17.75 | 1.242 | 2.60 | 1.525 | 2.09 | 1.23 |  |
|  |  |  |  |  |  |  |  | 17.75 | 1.242 | 2.20 | 1.445 | 1.77 | 1.16 |  |
|  |  |  |  |  |  |  |  | 17.75 | 1.242 | 1.60 | 1.375 | 1.29 | 1.11 |  |
|  |  |  |  |  |  |  |  | 17.75 | 1.242 | 0.90 | 1.290 | 0.72 | 1.04 |  |

Table 9--Continued

| (1) | (2) | (3) | (4) | (5) | (6) | (7) | (8) | (9) | (10) | (11) | (12) | (13) | (14) | (15) |
|---|---|---|---|---|---|---|---|---|---|---|---|---|---|---|
| D | 0.25 | 8.080 | 3.970 | 2.035 | 0.107 | 19.02 | 10.25 | 14.05 | 1.503 | 4.30 | 2.100 | 2.86 | 1.40 | |
| | | | | | .106 | 19.20 | 10.40 | 14.30 | 1.516 | 3.40 | 1.960 | 2.24 | 1.29 | |
| | | | | | | | | 14.30 | 1.516 | 2.90 | 1.860 | 1.91 | 1.23 | |
| | | | | | | | | 14.30 | 1.516 | 2.10 | 1.740 | 1.38 | 1.15 | |
| | | | | | .105 | 19.38 | 10.54 | 14.50 | 1.523 | 1.30 | 1.650 | 0.85 | 1.08 | |
| | | | | | | | | 14.50 | 1.523 | 0.50 | 1.550 | 0.33 | 1.02 | |
| | | 11.553 | | 2.910 | .147 | 19.80 | 9.10 | 12.45 | 1.830 | 4.30 | 2.410 | 2.35 | 1.32 | |
| | | | | | .146 | 19.93 | 9.20 | 12.60 | 1.840 | 4.10 | 2.320 | 2.22 | 1.26 | |
| | | | | | | | | 1.840 | 3.20 | 2.230 | 1.74 | 1.21 | |
| | | | | | .145 | 20.07 | 9.29 | 12.75 | 1.849 | 2.30 | 2.140 | 1.24 | 1.16 | |
| | | | | | | | | 1.849 | 1.60 | 2.090 | 0.87 | 1.13 | |
| | | | | | .144 | 20.21 | 9.39 | 12.85 | 1.850 | 1.20 | 2.010 | 0.65 | 1.09 | |
| | | | | | | | | 1.850 | 0.80 | 1.950 | 0.43 | 1.05 | |
| | | 6.005 | | 1.512 | .079 | 19.14 | 12.00 | 16.50 | 1.306 | 3.60 | 1.760 | 2.76 | 1.35 | |
| | | 8.057 | | 2.029 | .105 | 19.32 | 10.51 | 14.45 | 1.517 | 3.60 | 1.925 | 2.37 | 1.27 | 4.0 |
| | | 11.535 | | 2.905 | .144 | 20.21 | 9.37 | 12.85 | 1.850 | 3.60 | 2.210 | 1.95 | 1.29 | |
| | 0.30 | 8.105 | | 2.041 | .110 | 18.55 | 9.86 | 13.50 | 1.485 | 4.50 | 2.300 | 3.03 | 1.55 | |
| | | 5.410 | | 1.362 | .074 | 18.40 | 11.92 | 16.40 | 1.214 | 4.50 | 2.070 | 3.71 | 1.71 | 5.3 |
| | | 11.553 | | 2.910 | .150 | 19.40 | 8.83 | 12.05 | 1.808 | 4.50 | 2.570 | 2.49 | 1.42 | |
| | | 5.980 | | 1.506 | .079 | 19.06 | 11.95 | 16.45 | 1.300 | 3.40 | 1.840 | 2.62 | 1.42 | |
| | | 8.050 | | 2.028 | .106 | 19.13 | 10.36 | 14.25 | 1.510 | 3.40 | 2.025 | 2.25 | 1.34 | 4.0 |
| | | 11.538 | | 2.906 | .146 | 19.90 | 9.18 | 12.55 | 1.832 | 3.40 | 2.300 | 1.85 | 1.26 | |

"Horizontal apron." Multiplying this ratio by $D_1$ gives the conjugate depth for a horizontal apron which is listed in Column 10 of Table 9. The tail water was then set at conjugate depth (Point 0, Figure 35) and the distance, $l_0$, measured and tabulated. The distance, $l_0$, gives the position of the front of the jump on the slope, measured from the break in slope, for conjugate depth. The tail water was then increased, moving the front of the jump up to Point 1, Figure 35. Both the distance, $l_1$, and the tail water depth were measured, and these are recorded in Columns 11 and 12, respectively, of Table 9. The tail water was then raised, moving the front of the jump to Point 2 while the length, $l_2$, and the tail water depth were recorded. The same procedure was repeated until the entire apron was utilized by the jump. In each case, $D_1$ was measured immediately upstream from the front of the jump, thus compensating for frictional resistance on the slope. The velocity, $V_1$, and the Froude number were computed at the same location. The tests were made for slopes with tangents varying from 0.05 to 0.30, and in some cases, several lengths of floor were used for each slope, as indicated in Column 15 of Table 9.

The resulting lengths and tail water depths, divided by the conjugate depth, are shown in Columns 13 and 14 of Table 9, and these values have been plotted on Figure 36. The horizontal length has been used rather than the vertical distance, $\Delta Y$, as the former dimension is more convenient to use. Figure 36 shows that the straight lines for the geometric portion of the graph tend to intersect at a common point, $\frac{1}{D_2} = 1$ and $\frac{TW}{D_2} = 0.92$, indicated by the circle on the graph. The change in the profile of the jump as it moves from a horizontal floor to the slope is evidenced by the curved portion of the lines.

Case C, Figure 30, is the upper extreme of Case B; and as there is practically no difference in the performance for Cases D and C, data for Case D (Table 4) can again be utilized. By assuming that a horizontal floor begins at the end of the jump in Case D, Columns 15 and 16 of Table 8 can be plotted on Figure 36. In addition, data from experiments by D. D. Hindlaub of the University of California, for a slope of 0.217, have been plotted on Figure 36. The agreement of the information from the three sources is very satisfactory.

Length of Jump (Case B)

It is suggested that the length of jump for Case B be obtained from Figure 33. Actually, Figure 33 is for continuous sloping aprons, but these lengths can be applied to Case B with but negligible error. In some cases the length of jump is not of particular concern because it may not be economically possible to design the basin to confine the entire jump. This is especially true when sloping aprons are used in conjunction with medium or high overfall spillways where the rock in the riverbed is in fairly good condition. When sloping aprons are designed shorter than the length indicated on Figure 33, the rock in the river downstream must act as part of the stilling basin. On the other hand, when the quality of foundation material is questionable, it is advisable to make the apron sufficiently long to confine the entire jump, Figure 33.

FIGURE 36



HYDRAULIC JUMP STUDIES

STILLING BASIN V (CASE B)

TAILWATER REQUIREMENT FOR SLOPING APRONS
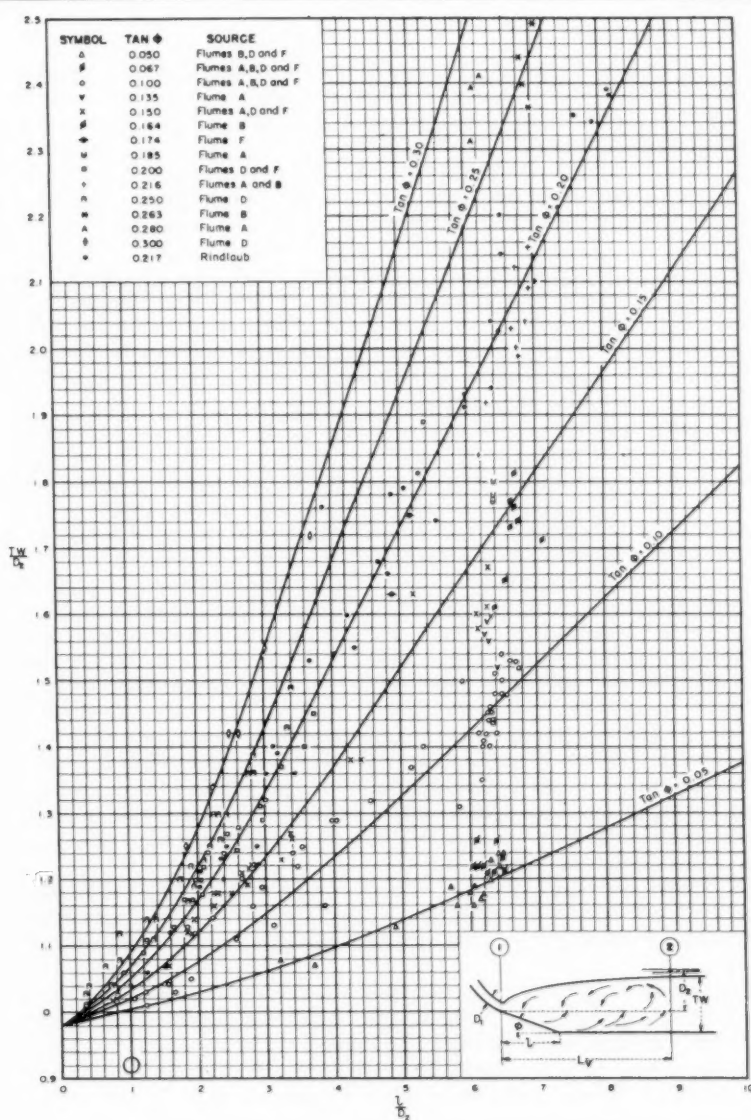
## Practical Applications

### Existing Structures

To determine the practical value of the methods given for the design of sloping aprons, existing basins employing sloping aprons were, in effect re-designed using the current experimental information. Pertinent data for 13 existing spillways are tabulated in Table 10. The slope of the spillway face is listed in Column 3; the tangent of the sloping stilling basin apron is listed in Column 4; the elevation of the upstream end of the apron, or front of the jump, is listed in Column 7; the elevation of the end of the apron is listed in Column 8; the fall from headwater to upstream end of apron is tabulated in Column 9; and the total discharge is shown in Column 11. Where outlets discharge into the spillway stilling basin, that discharge was also been included in the total. The length of the sloping portion of the apron is given in Column 14; the length of the horizontal portion of the apron is given in Column 15; and the overall length is given in Column 16. Columns 17 through 27 show computed values similar to those in the previous table.

The lower portions of the curves of Figure 36 have been reproduced to a larger scale on Figure 37. The coordinates from Columns 26 and 27 of Table 10 have been plotted on Figure 37 for each of the 13 spillways. Longitudinal sections through the basins are shown on Figures 38 and 39.

Each point in Figure 37 has been connected with an arrow to the $\tan\phi$ curve corresponding to the apron slope. Points which lie to the right and below the corresponding $\tan\phi$ curve indicate that if the tail water depth is correct the sloping portion of the apron is excessively long; if the length of the slope is correct the tail water is insufficient to move the jump upstream to Section 1 on the slope. Only the points for Capilano and Madden Dams show an excess of tail water depth for the length of slope used. In both these cases the jump will occur upstream from Section 1 as shown in Figures 38 and 39. Friant and Dickinson show almost perfect agreement with the derived curves while Bhakra (final) and Norris show agreement within practical limits. All other points indicate that the tail water depth is insufficient to move the toe of the jump upstream to Section 1. The rather large chute blocks on Keswick Dam may compensate for the discrepancy indicated by the point in the margin of Figure 37.

All of the structures listed in Table 10 and shown on Figures 38 and 39 were designed with the aid of model studies. The degree of conservatism used in each case was dependent on local conditions and the individual designer.

The overall lengths of apron provided for the above 13 existing structures are shown in Column 16 of Table 10. The length of jump for the maximum discharge condition for each case is tabulated in Column 29 of the same table. The ratio of total length of apron to length of jump is shown in Column 30. The total apron length ranges from 39 to 83 percent of the length of jump; or considering the 13 structures collectively, the average total length of apron is 60 percent of the length of the jump. Considering all aspects of the model tests on the individual structures and the current basin tests it is believed that 60 percent is sufficient for most installations. Longer basins are needed only when the downstream riverbed is in very poor condition. Shorter basins may be used where a solid bed exists.
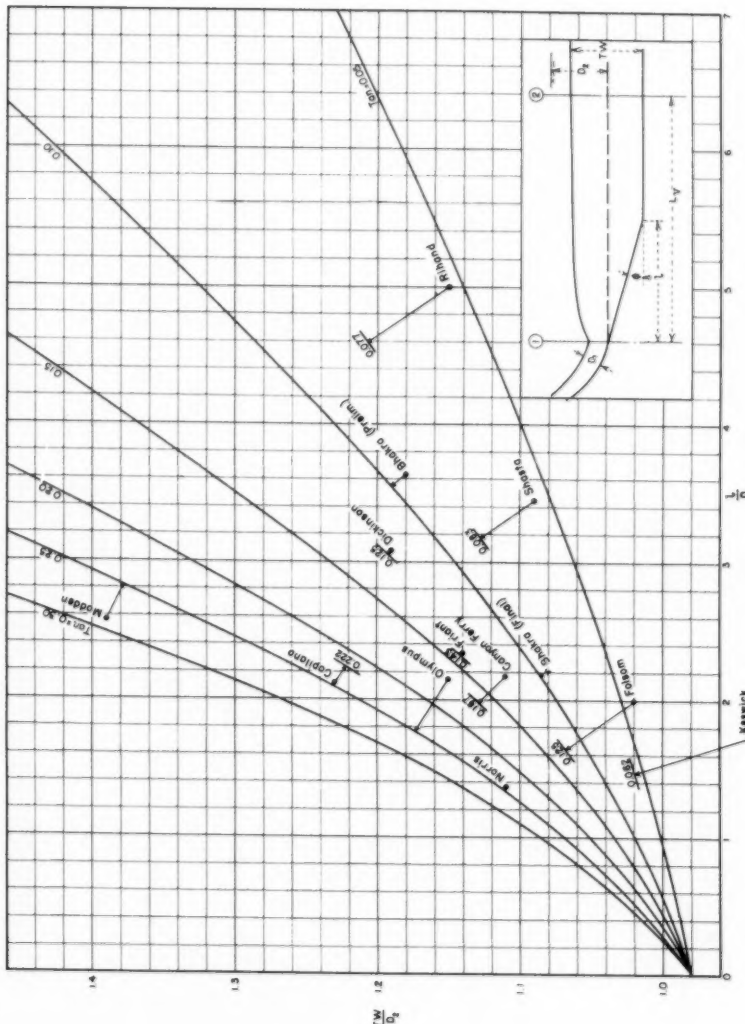
HYDRAULIC JUMP STUDIES

STILLING BASIN V (CASE B)

COMPARISON OF EXISTING SLOPING APRON DESIGNS WITH CURRENT EXPERIMENTAL RESULTS

FIGURE 38

HYDRAULIC JUMP STUDIES
STILLING BASIN V (CASE B)
EXISTING BASINS WITH SLOPING APRONS
SHEET 1 OF 2

103

HYDRAULIC JUMP STUDIES
STILLING BASIN V (CASE B)
EXISTING BASINS WITH SLOPING APRONS
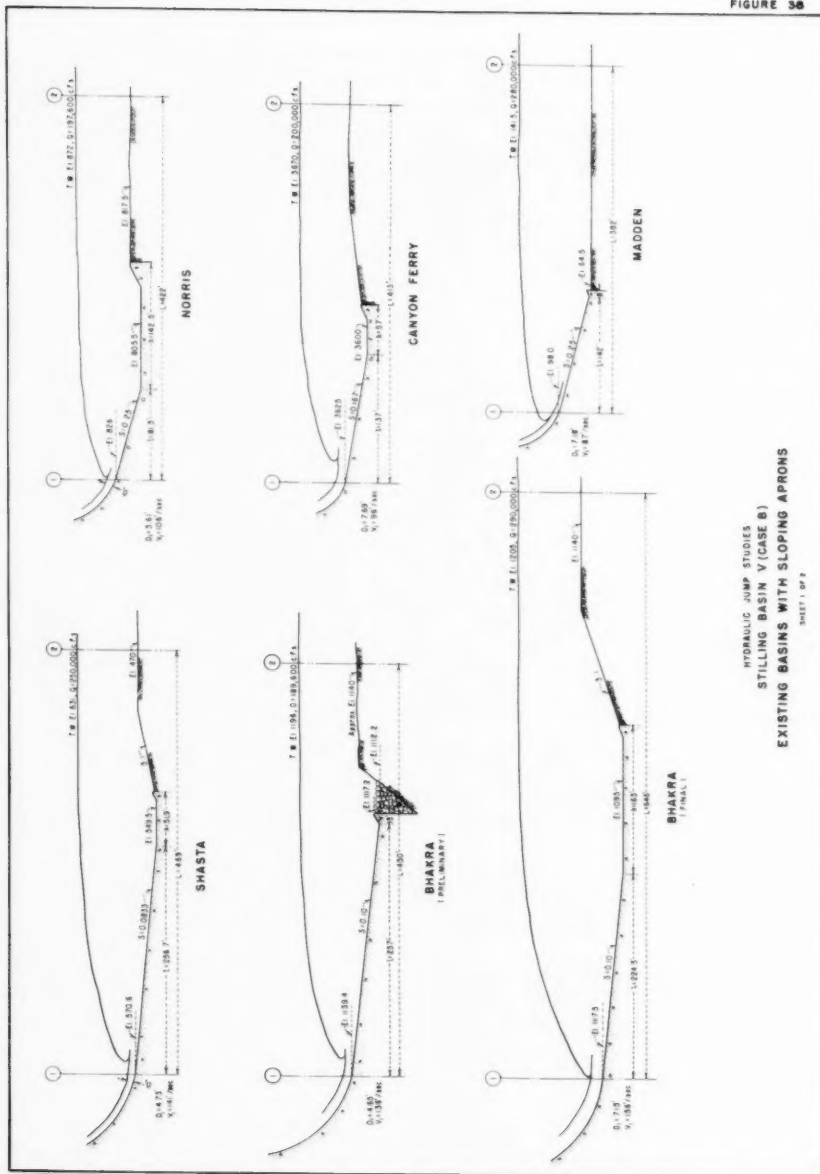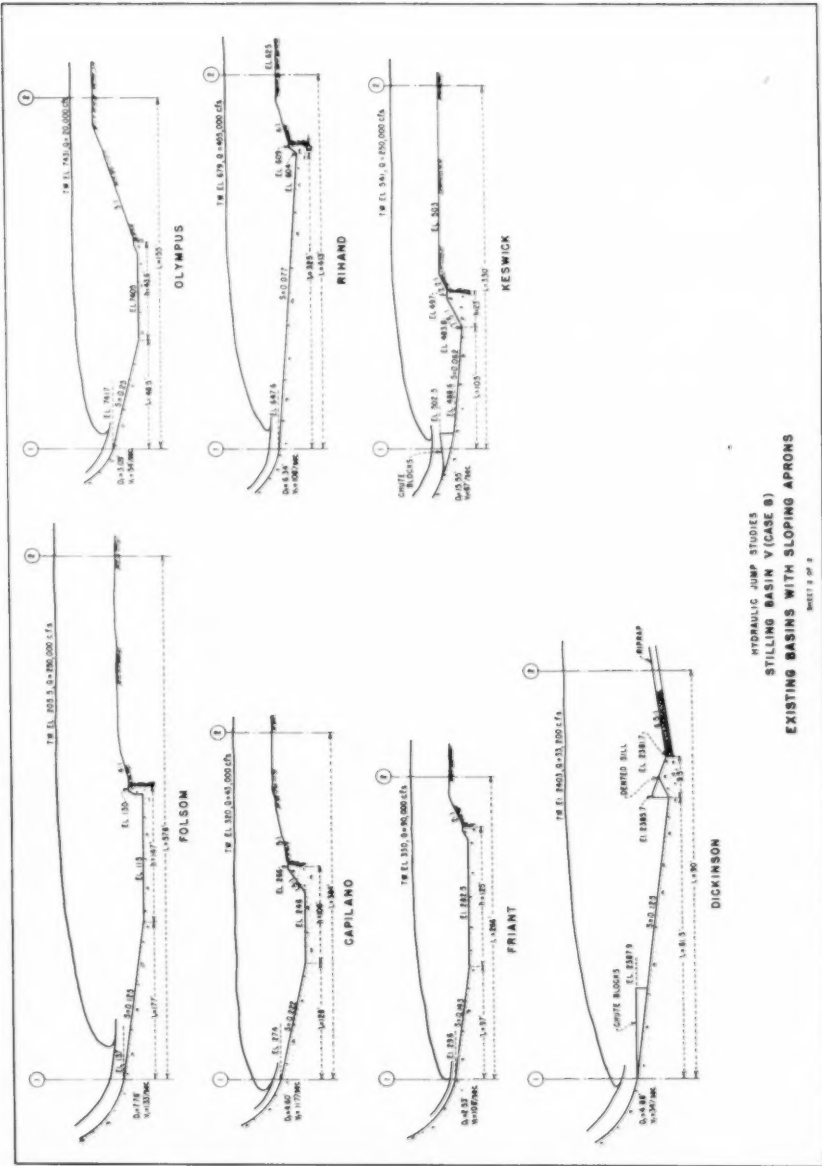
Table 10

EXISTING STILLING BASINS WITH SLOPING APRONS

| (1) Dam | (2) Location | (3) Slope of dam face: tan ø | (4) Slope of apron: el | (5) :Res: ft | (6) El: up end of apron: ft | (7) El: down end of apron: ft | (8) Fall: HW to: end of apron: ft | (9) HW to: up end of apron: ft | (10) Head on crest: ft | (11) Q Max cfs | (12) Max el TW ft | (13) TW depth ft | (14) l Length of sloping apron ft | (15) h Length of horizontal apron ft |
|---|---|---|---|---|---|---|---|---|---|---|---|---|---|---|
| Shasta | California | 0.8:1 | 0.083 | 1065 | 1037 | 570.6 | 549.5 | 494.4 | 28.0 | 250,000 | 631.0 | 81.5 | 256.7 | 51.9 |
| Norris | Tennessee | 0.7:1 | .250 | 1047 | 1020 | 826.0 | 805.5 | 221.0 | 27.0 | 197,600 | 872.0 | 66.5 | 81.5 | 142.5 |
| Bhakra (prelm) | India | 0.8:1 | .100 | 1560 | 1552 | 1139.4 | 1112.2 | 440.6 | 28.0 | 189,600 | 1196.0 | 83.8 | 257 | 15 |
| Canyon Ferry | Montana | Varies | .167 | 3800 | 3766 | 3625.0 | 3600.0 | 175.0 | 34.0 | 200,000 | 3670.0 | 70.0 | 137 | 57. |
| Bhakra (final) | India | 0.8:1 | .100 | 1685 | 1645 | 1117.5 | 1095.0 | 567.5 | 40.0 | 290,000 | 1205.0 | 110.0 | 224.5 | 165 |
| Madden | Canal Zone | 0.75:1 | .250 | 250 | 232 | 98.0 | 64.5 | 152.0 | 18.0 | 280,000 | 141.5 | 77.0 | 142 | 8 |
| Folsom | California | 0.67:1 | .125 | 466 | 418 | 137.0 | 115.0 | 329.0 | 48.0 | 250,000 | 205.5 | 90.5 | 177 | 147 |
| Olympus | Colorado | Varies | .250 | 7475 | 7460 | 7417.0 | 7405.0 | 58.0 | 15.0 | 20,000 | 7431.0 | 26.0 | 46.5 | 43.6 |
| Capilano | Br Columbia | 0.65:1 | .222 | 570 | 547 | 274.0 | 246.0 | 296.0 | 23.0 | 43,000 | 320.0 | 74.0 | 128 | 106 |
| Rihand | India | 0.7:1 | .077 | 888 | 852 | 647.6 | 604.0 | 240.4 | 36.0 | 455,000 | 679.0 | 75.0 | 325 | 10 |
| Friant | California | 0.7:1 | .143 | 578 | 560 | 296.0 | 282.5 | 282.0 | 18.0 | 90,000 | 330.0 | 47.5 | 97 | 125 |
| Keswick | California | Varies | .062 | 587 | 537 | 488.6 | 483.8 | 98.4 | 50.0 | 250,000 | 541.0 | 57.2 | 105 | 23 |
| Dickinson | North Dakota | 0.5:1 | .125 | 2426 | 2416 | 2388.0 | 2380.0 | 40.9 | 12.4 | 33,200 | 2404.7 | 23.0 | 61.5 | 9.5 |

Table 10--Continued

| Dam | Location | $1+h$ ft | $V_{th}$ Theoret-ical vel entering basin ft/sec | $\frac{V_A}{V_{th}}$ | $V_A = V_1$ Act vel entering basin ft/sec | W Width of basin ft | q per ft of W cfs | $D_1$ ft | $F_1 = \frac{V_1}{\sqrt{gD_1}}$ | $\frac{D_2}{D_1}$ | $D_2$ Conj depth ft | TW ft | $\frac{TW}{D_2}$ | $\frac{L}{D_2}$ | L Actual length of Jump ft | $\frac{1+h}{L}$ |
|---|---|---|---|---|---|---|---|---|---|---|---|---|---|---|---|---|
| | | (16) | (17) | (18) | (19) | (20) | (21) | (22) | (23) | (24) | (25) | (26) | (27) | (28) | (29) | (30) |
| Shasta | California | 308.6 | 176 | 0.81 | 141 | 375 | 667 | 4.73 | 11.42 | 15.75 | 74.5 | 3.44 | 1.09 | 6.30 | 469 | 0.66 |
| Norris | Tennessee | 224 | 116 | 0.91 | 106 | 332 | 595 | 5.61 | 7.88 | 10.70 | 60.0 | 1.36 | 1.11 | 7.03 | 422 | .53 |
| Bhakra (prelim) | India | 272 | 166 | 0.82 | 136 | 300 | 632 | 4.65 | 11.11 | 15.25 | 70.9 | 3.63 | 1.18 | 6.35 | 450 | .60 |
| Canyon Ferry | Montana | 194 | 101 | 0.95 | 96 | 271 | 738 | 7.69 | 6.10 | 8.20 | 63.1 | 2.17 | 1.11 | 6.55 | 413 | .47 |
| Bhakra (final) | India | 389.5 | 188 | 0.85 | 156 | 260 | 1115 | 7.15 | 10.27 | 14.20 | 101.5 | 2.21 | 1.08 | 6.36 | 646 | .60 |
| Madden | Canal Zone | 150 | 96 | 0.91 | 87 | 448 | 625 | 7.18 | 5.72 | 7.70 | 55.3 | 2.57 | 1.39 | 6.90 | 382 | .39 |
| Folsom | California | 324 | 140 | 0.95 | 133 | 242 | 1033 | 7.76 | 8.41 | 11.45 | 88.9 | 1.99 | 1.02 | 6.50 | 578 | .56 |
| Olympus | Colorado | 92.1 | 57 | 0.95 | 54 | 120 | 167 | 3.09 | 5.41 | 7.30 | 22.6 | 2.15 | 1.15 | 6.86 | 155 | .59 |
| Capilano | Br Columbia | 234 | 135 | 0.87 | 117 | 80 | 538 | 4.60 | 9.62 | 13.10 | 60.3 | 2.12 | 1.23 | 6.85 | 384 | .61 |
| Riband | India | 335 | 117 | 0.92 | 108 | 664 | 685 | 6.34 | 7.56 | 10.25 | 65.0 | 5.00 | 1.15 | 6.30 | 413 | .82 |
| Friant | California | 222 | 133 | 0.81 | 108 | 330 | 273 | 2.53 | 11.97 | 16.45 | 41.6 | 2.33 | 1.14 | 6.40 | 266 | .83 |
| Keswick | California | 128 | 69 | 1.00 | 69 | 240 | 1042 | 15.15 | 3.12 | 4.00 | 60.6 | 1.73 | 0.94 | 5.45 | 330 | .39 |
| Dickinson | North Dakota | 71 | 51 | -- | 48 | 200 | 166 | 3.50 | 4.44 | 5.70 | 20.0 | 3.08 | 1.19 | 6.00 | 120 | .59 |

Average 0.60

Evaluation of Sloping Aprons

Many sloping aprons have been designed so that the jump height curve matches the tail water curve for all discharge conditions. This procedure results in what has been designated a "tailor-made" basin. Some of the existing basins shown on Figures 38 and 39 were designed in this manner. As a result of the current experiments it was discovered that this course is not the most desirable. Matching of the jump height curve with the tail water curve should be a secondary consideration, except for the maximum discharge condition.

The first consideration in design should be to determine the apron slope that will require the minimum amount of excavation, the minimum amount of concrete, or both, for the maximum discharge and tail water condition. This is the prime consideration. Only then is the jump height checked to determine whether the tail water depth is adequate for the intermediate discharges. It will be found that the tail water depth usually exceeds the required jump height for the intermediate discharges resulting in a slightly submerged condition for intermediate discharges, but performance will be very acceptable. The extra depth will provide a smoother water surface in and downstream from the basin and greater stability at the toe of the jump. Should the tail water depth be insufficient for intermediate flows, it will be necessary to increase the depth by increasing the slope, or reverting to a horizontal apron. It is not necessary that the front of the jump form at the upstream end of the sloping apron for low or intermediate discharges provided the tail water depth and the length of basin available for energy dissipation are considered adequate. With this method, the designer is free to chose the slope he desires, since the current tests showed, beyond a doubt, that the slope itself had little effect on the performance of the stilling basin.

It is not possible to standardize design procedures for sloping aprons to the degree shown for the horizontal aprons; greater individual judgment is required. The slope and overall shape of the apron must be determined from economic reasoning, while the length must be judged by the type and soundness of the riverbed downstream. The existing structures shown on Figures 38 and 39 should serve as a guide in proportioning future sloping apron designs.

Sloping Apron Versus Horizontal Apron

The Bureau of Reclamation has constructed very few stilling basins with horizontal aprons for its larger dams. It has been the consensus that the hydraulic jump on a horizontal apron is very sensitive to slight changes in tail water depth. The current tests demonstrate this to be true for the larger values of the Froude number, but this characteristic can be remedied. Suppose a horizontal apron is designed for a Froude number of 10. The basin will operate satisfactorily for conjugate tail water depth, but as the tail water is lowered to $0.98D_2$ the front of the jump will begin to move. By the time the tail water is dropped to $0.96D_2$, the jump will probably be completely out of the basin. Thus, to design a stilling basin in this range the tail water depth must be known with certainty or a factor of safety provided in the design. To guard against deficiency in tail water depth, the same procedure used for Basins I and II (papers 1401 and 1402) is suggested here. Referring to the minimum tail water curve for Basins I and II on Figure 11, (paper 1402) the margin of safety can be observed for any value of the Froude number. It is

recommended that the tail water depth for maximum discharge be at least 5 percent larger than the minimum shown on Figure 11. For values of the Froude number greater than 9, a 10 percent factor of safety may be advisable as this will not only stabilize the jump but will improve the performance of the basin. With the additional tail water depth, the horizontal apron will perform on a par with the sloping apron. Thus, the primary consideration in design need not be hydraulic but structural. The basin, with either horizontal or sloping apron, which can be constructed at the least cost is the most desirable.

### Effect of Slope of Chute

A factor which occasionally affects stilling basin operation is the slope of the chute upstream from the basin. The foregoing experimentation was sufficiently extensive to shed some light on this factor. The tests showed that the slope of chute upstream from the stilling basin was unimportant, as far as jump performance was concerned, so long as the velocity distribution in the jet entering the jump was reasonably uniform. In the case of steep chutes or short flat chutes, the velocity distribution can be considered normal. Difficulty is experienced, however, with long flat chutes where frictional resistance on the bottom and side walls is sufficient to produce a center velocity greatly exceeding that on the bottom or sides. When this occurs, greater activity results in the center of the stilling basin than at the sides, producing an asymmetrical jump with strong side eddies. This same effect is also witnessed when the angle of divergence of a chute is too great for the water to follow properly. In either case the surface of the jump is unusually rough and choppy and the position of the front of the jump is not always predictable.

When long chutes precede a stilling basin the practice has been to make the upstream portion unusually flat, then increase the slope to 2:1, or that corresponding to the natural trajectory of the jet, immediately preceding the stilling basin. Figure 1A, (paper 1401) which shows the model spillway for Trenton Dam, illustrates this practice. Bringing an asymmetrical jet into the stilling basin at a steep angle usually helps to redistribute the flow to stabilize the jump. This is not effective, however, where very long flat slopes have caused the velocity distribution to be completely out of balance.

The most adverse condition has been observed where long canal chutes terminate in stilling basins. A typical example is the chute and basin at Station 25+19 on the South Canal, Uncompahgre Project, Colorado, Figure 40. The operation of this stilling basin is not particularly objectionable, but it will serve as an illustration. The above chute is approximately 700 feet long with a slope of 0.0392. The stilling basin at the end is also shown on Figure 40. A photograph of the prototype basin operating at normal capacity is shown on Figure 41. The action is of the surging type; the jump is unusually rough, with a great amount of splash and spray. Two factors contribute to the rough operation: the unbalanced velocity distribution in the entering jet, and excessive divergence of the chute in the steepest portion.

A definite improvement can be accomplished in future designs where long flat chutes are involved by utilizing the Type III basin described in Paper 1403. The baffle piers on the floor tend to alter the asymmetrical jet, resulting in an overall improvement in operation.

FIGURE 40



HYDRAULIC JUMP STUDIES
SOUTH CANAL CHUTE STA. 25+19
UNCOMPAHGRE PROJECT, COLO.
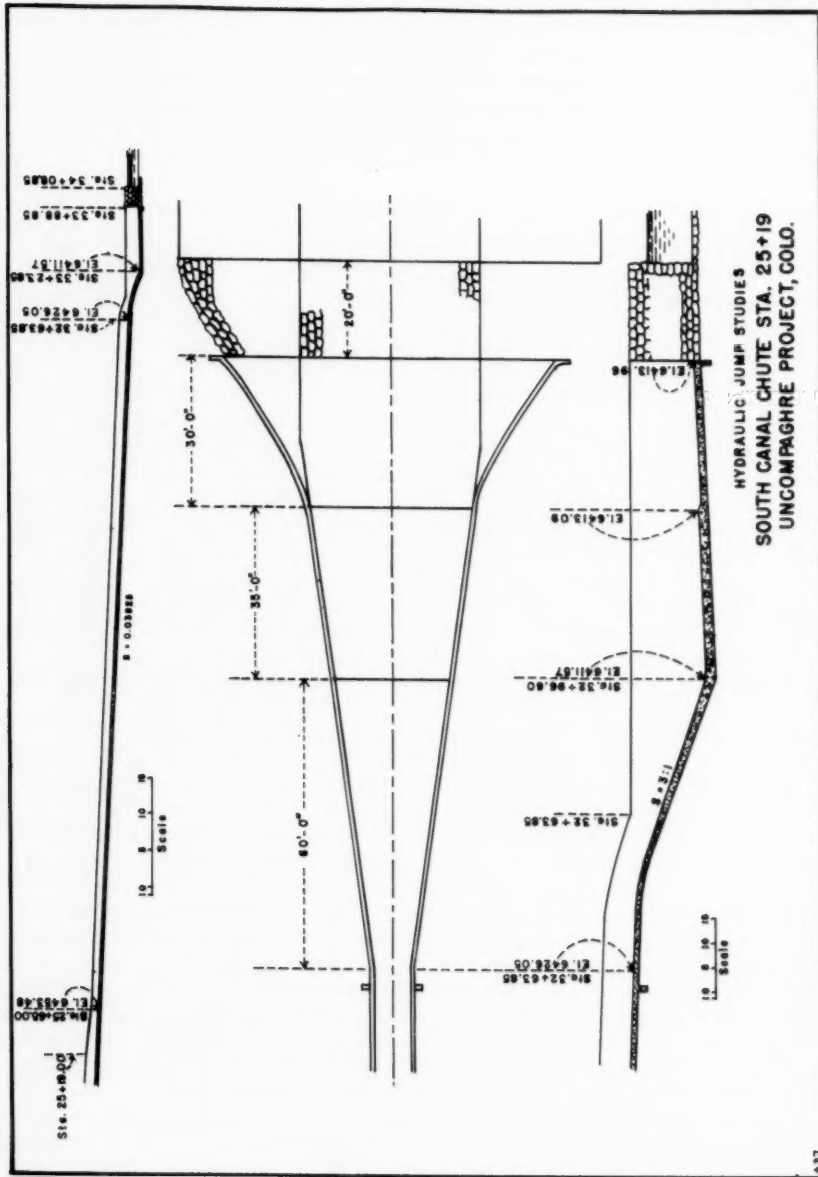
## Recommendations

The following rules have been devised for the design of the sloping aprons developed from the foregoing experiments:

1. Determine an apron arrangement which will give the greatest economy for the maximum discharge condition. This is the governing factor and the only justification for using a sloping apron.

2. Position the apron so that the front of the jump will form at the upstream end of the slope for the maximum discharge and tail water condition by means of the information on Figure 37. Several trials will usually be required before the slope and location of the apron are compatible with the hydraulic requirement. It may be necessary to raise or lower the apron, or change the original slope entirely.

3. The length of the jump for maximum or partial flows can be obtained from Figure 33. The portion of the jump to be confined on the stilling basin apron is a decision for the designer. In making this decision, Figures 38 and 39 may be helpful. The average overall apron in Figures 38 and 39 averages 60 percent of the length of jump for the maximum discharge condition. The apron may be lengthened or shortened, depending upon the quality of the rock in the riverbed and other local conditions. If the apron is set on loose material and the downstream channel is in poor condition, it may be advisable to make the total length of apron the same as the length of jump.

4. With the apron designed properly for the maximum discharge condition, it should then be determined that the tail water depth and length of basin available for energy dissipation are sufficient for, say, 1/4, 1/2, and 3/4 capacity. If the tail water depth is sufficient or in excess of the jump height for the intermediate discharges, the design is acceptable. If the tail water depth is deficient, it may then be necessary to try a flatter slope or reposition the sloping portion of the apron. It is not necessary that the front of the jump form at the upstream end of the sloping apron for partial flows. In other words, the front of the jump may remain at Section 1 (Figure 30B), move upstream from Section 1, or move down the slope for partial flows, providing the tail water depth and length of apron are considered sufficient for these flows.

5. Horizontal and sloping aprons will perform equally well for high values of the Froude number if the proper tail water depth is provided.

6. The slope of the chute upstream from a stilling basin has little effect on the hydraulic jump when the velocity distribution and depth of flow are reasonably uniform on entering the jump.

7. A small solid triangular sill, placed at the end of the apron, is the only appurtenance needed in conjunction with the sloping apron. It serves to lift the flow as it leaves the apron and thus acts to control scour. Its dimensions are not critical; the most effective height is between $0.05D_2$ and $0.10D_2$ and a slope of 3:1 to 2:1 (see Figures 38 and 39).

8. The spillway should be designed to operate with as nearly symmetrical flow in the stilling basin as possible. (This applies to all stilling basins.) Asymmetry produces large horizontal eddies that can carry riverbed material onto the apron. This material, circulated by the eddies, can abrade the apron

and appurtenances in the basin at a very surprising rate. Eddies can also undermine wing walls and riprap. Asymmetrical operation is expensive operation, and operating personnel should be continually reminded of this fact.

9. Where the discharge over high spillways exceeds 500 cfs per foot of apron width, where there is any form of asymmetry involved, and for the higher values of the Froude number where stilling basins become increasingly costly and the performance less acceptable a model study is advisable.

# Journal of the
# HYDRAULICS DIVISION

## Proceedings of the American Society of Civil Engineers

### HYDRAULIC DESIGN OF STILLING BASINS: SMALL BASINS FOR PIPE OR OPEN CHANNEL OUTLETS—NO TAIL WATER REQUIRED (BASIN VI)

J. N. Bradley[1] M. ASCE and A. J. Peterka[2] M. ASCD
(Proc. Paper 1406)

---

## FOREWORD

This is one of a group of six papers on the hydraulic design of stilling basins and their associated appurtenances. Although original data from hydraulic models are presented in tabular form, the papers emphasize practical design procedures. Basin sizes and dimensions are given in easy-to-use dimensionless forms so that dependable stilling basins may be designed without the need for exceptional judgment or extensive experience. Sample problems are included.

The "Introduction" and "Experimental Equipment" are included in Paper 1401 but apply to all papers in this group. Paper 1401 is an academic study of the hydraulic jump on a flat floor. Useful information is presented concerning energy losses, applicability of the hydraulic jump formula, length of jump, and a new classification of the various types of jumps.

Paper 1402 covers the design of a short hydraulic jump stilling basin having an end sill and chute blocks. Paper 1403 describes a shorter stilling basin which utilizes baffle piers. In both papers information is given to determine the critical dimensions of the stilling basin, the tail water range, and the water surface profile in the basin.

Paper 1404 describes a special type of hydraulic jump basin for use when the Froude number of the incoming flow is low, and the jump produces waves in the downstream channel. An alternate design and two types of wave suppressors are also developed.

Paper 1405 describes the design of a stilling basin having a sloping apron. The extra tail water depth required and the merits of a sloping apron are evaluated, as is the basin length for a range of apron slopes.

Paper 1406 develops the design of impact basins for discharges up to 340

second feet and incoming velocities up to 30 feet per second. No tail water is required. The bibliography in this paper applies to all papers in this group.

## ABSTRACT

An impact-type stilling basin is developed which will handle 21 to 340 cubic feet per second. No tail water is required and incoming velocities may be as great as 30 feet per second. General design rules and a table listing critical dimensions and proper riprap sizes for 9 different basin sizes are presented.

## INTRODUCTION

The stilling basin developed in these tests is an impact-type energy dissipator, contained in a relatively small boxlike structure, which requires no tail water for successful performance. Although the emphasis in this discussion is placed on use with pipe outlets, the entrance structure may be modified for use with an open channel entrance.

Generalized design rules and procedures are presented to allow determining the proper basin size and all critical dimensions for a range of discharges up to 339 feet per second and velocities up to about 30 feet per second. Greater discharges may be handled by constructing multiple units side by side. The efficiency of the basin in accomplishing energy losses is greater than a hydraulic jump of the same Froude number.

The development of this short impact-type basin was initiated by the need for some 50 or more stilling structures on a single irrigation project. The need was for relatively small basins providing energy dissipation independent of a tail water curve or tail water of any kind.

Since individual model studies on 50 small stilling structures were too costly a procedure, tests were made on a single setup which was modified as necessary to generalize the design for the range of expected operations.

### Test Procedure

Hydraulic Models

Hydraulic models were used to develop the stilling basin, determine the discharge limitations, and obtain dimensions for the various parts of the basin. Basins 1.6 to 2.0 feet wide were used in the tests. The inlet pipe was 6 3/8 inches, inside diameter, and was equipped with a slide gate located well upstream from the basin entrance so that the desired relations between head, depth, and velocity could be obtained. The pipe was transparent so that backwater effects in the pipe could be studied. Discharges of over 3 cubic feet per second and velocities up to 15 feet per second could be obtained during the tests. Hydraulic model-prototype relations were used to scale up the results to predict performance for discharges up to 339 second-feet and velocities up to 30 feet per second.

The basin was tested in a tail box containing gravel formed into a

trapezoidal channel. The size of the gravel was changed several times during the tests. The outlet channel bottom was slightly wider than the basin and had 1:1 side slopes. A tail gate was provided at the downstream end to evaluate the effects of tail water.

## Development of Basin

The shape of the basin evolved from the development tests was the result of extensive investigations on many different arrangements. These tests are discussed briefly to show the need for the various parts of the adopted design.

With the many combinations of discharge, velocity, and depth possible for the incoming flow, it became apparent during the early tests that some device was needed at the stilling basin entrance to convert the many possible flow patterns into a common pattern. The vertical hanging baffle proved to be this device, Figure 42. Regardless of the depth or velocity of the incoming flow (within the prescribed limits) the flow after striking the baffle acted the same as any other combination of depth and velocity. Thus, some of the variables were eliminated from the problem.

The effect of velocity alone was then investigated, and it was found that for velocities 30 feet per second and below the performance of the structure was primarily dependent on the discharge. Actually, the velocity of the incoming flow does affect the performance of the basin, but from a practical point of view it could be eliminated from consideration. Had this not been done, a prohibitive amount of testing would have been required to evaluate and express the effect of velocity.

For velocities of 30 feet per second or less the basin width W was found to be a function of the discharge, with other basin dimensions being related to the width, Figure 42. To determine the necessary width, erosion test results, judgment, and operating experiences were all used, and the advice of laboratory and design personnel was used to obtain the finally determined limits. Since no definite line of demarcation between a "too wide" or "too narrow" basin exists, it was necessary to work between two more definite lines, shown on Figure 42 as the upper and lower limits. These lines required far less judgment to determine than a single intermediate line.

Various basin sizes, discharges, and velocities were tested taking note of the erosion, wave heights, energy losses, and general performance. When the upper and lower limit lines had been established a line about midway between the two was used to establish the proper width of basin for various discharges. The exact line is not shown because strict adherence to a single curve would result in difficult to use fractional dimensions. Accuracy of this degree is not justifiable. Figure 43 shows typical performance of the recommended stilling basin for three limits. It is evident that the center photograph represents a compromise between the upper limit operation which is very mild and the lower limit operation which is approaching the unsafe range.

Using the middle range of basin widths, other basin dimensions were determined, modified, and made minimum by means of trial and error tests on the several models. Dimensions for nine different basins are shown in Table 11. These should not be arbitrarily reduced since in the interests of economy the dimensions have been reduced as far as is safely possible.

## Performance of Basin

Energy dissipation is initiated by flow striking the vertical hanging baffle

and being turned upstream by the horizontal portion of the baffle and by the floor, in vertical eddies. The structure, therefore, requires no tail water for energy dissipation as is necessary for a hydraulic jump basin. Tail water as high as $d + \frac{g}{2}$, Figure 42, however, will improve the performance by reducing outlet velocities, providing a smooth water surface, and reducing tendencies toward erosion. Excessive tail water, on the other hand, will cause some flow to pass over the top of the baffle. This should be avoided if possible.

The effectiveness of the basin is best illustrated by comparing the energy losses within the structure to those which occur in a hydraulic jump. Based on depth and velocity measurements made in the approach pipe and in the downstream channel (no tail water), the change in momentum was computed as explained in Paper 1401 for the hydraulic jump. The Froude number of the incoming flow was computed using the $D_1$ obtained by converting the flow area in the partly full pipe into an equivalent rectangle as wide as the pipe diameter. Compared to the losses in the hydraulic jump, Figure 44, the impact basin shows greater efficiency in performance. Inasmuch as the basin would have performed just as efficiently had the flow been introduced in a rectangular cross section, the above conclusion is valid.

## Basin Design

Table 11 and the key drawing, Figure 42, may be used to obtain dimensions for the usual structure operating within usual ranges. However, a further understanding of the design limitations may help the designer to modify these dimensions when necessary for special operating conditions.

The basin dimensions, Columns 4 to 13, are a function of the maximum discharge to be expected, Column 3. Velocity at the stilling basin entrance need not be considered except that it should not greatly exceed 30 feet per second.

Columns 1 and 2 give the pipe sizes which have been used in field installations. These may be changed as necessary, however. The suggested sizes were obtained by assuming the velocity of flow to be 12 feet per second. The pipes shown would then flow full at maximum discharge or they would flow half full at 24 feet per second. The basin operates as well whether a small pipe flowing full or a larger pipe flowing partially full is used. The pipe size may therefore be modified to fit existing conditions, but the relation between structure size and discharge should be maintained as given in the table. In fact, a pipe need not be used at all; an open channel having a width less than the basin width will perform equally as well.

The invert of the entrance pipe, or open channel, should be held at the elevation shown on the drawing of Figure 42, in line with the bottom of the baffle and the top of the end sill, regardless of the size of the pipe selected. The entrance pipe may be tilted downward somewhat without affecting performance adversely. A limit of 15⁰ is a suggested maximum although the loss in efficiency at 20⁰ may not cause excessive erosion. For greater slopes use a horizontal or sloping pipe (up to 15⁰) 2 or more diameters long just upstream from the stilling basin.

For submerged conditions a hydraulic jump may be expected to form in the downstream end of the pipe, sealing the exit end. If the upper end of the pipe is also sealed by incoming flow, a vent may be necessary to prevent pressure fluctuation in the system. A vent to the atmosphere, say one-sixth the pipe diameter, should be installed upstream from the jump.

The notches shown in the baffle are provided to aid in cleaning out the basin after prolonged nonuse of the structure. When the basin has silted level full of sediment before the start of the spill, the notches provide concentrated jets of water to clean the basin. If cleaning action is not considered necessary the notches need not be constructed. The basin is designed, however, to carry the full discharge, shown in Table 11, over the top of the baffle if for any reason the space beneath the baffle becomes clogged, Figure 45C. Performance is not as good, naturally, but acceptable. With the basin operating normally, the notches provide some concentration of flow passing over the end sill, resulting in some tendency to scour, Figure 45A. Riprap as shown on the drawing will provide ample protection in the usual installation, but if the best possible performance is desired, it is recommended that the alternate end sill and 45° end walls be used, Figures 45B and 42. The extra sill length reduces flow concentration, scour tendencies, and the height of waves in the downstream channel.

Figure 46 shows the performance of a prototype structure designed from Table 11. The basin, designed for a maximum discharge of 165 second-feet, is shown discharging 130 second-feet with a higher than recommended entrance velocity of about 39 feet per second. Performance is entirely satisfactory.

## CONCLUSIONS AND RECOMMENDATIONS

The following procedures and rules pertain to the design of Basin VI:

1. Use of Basin VI is limited to cases where the velocity at the entrance to the stilling basin does not greatly exceed 30 feet per second.

2. From the maximum expected discharge, determine the stilling basin dimensions, using Table 11, Columns 3 to 13. The use of multiple units side by side may prove economical in some cases.

3. Compute the necessary pipe area from the velocity and discharge. The values in Table 11, Columns 1 and 2, are suggested sizes based on a velocity of 12 feet per second and the desire that the pipe run full at the discharge given in Column 3. Regardless of the pipe size chosen, maintain the relation between discharge and basin size given in the table. An open channel entrance may be used in place of a pipe. The approach channel should be narrower than the basin with invert elevation the same as the pipe.

4. Although tail water is not necessary for successful operation, a moderate depth of tail water will improve the performance. For best performance set the basin so that maximum tail water does not exceed $d + \frac{g}{2}$, Figure 42.

5. Suggested thicknesses of various parts of the basin are given in Columns 14 to 18, Table 11.

6. The suggested sizes for the riprap protective blanket, given in Column 19 of Table 11, show the minimum size of individual stones which will resist movement when critical velocity occurs over the end sill. Since little is known regarding the effect of interlocking rock pieces, most of the riprap should consist of the sizes given or larger. An equation[34,35] for determining minimum stone sizes, which appears from a limited number of experiments and observations to be accurate, is given below.

$$V_b = 2.6\sqrt{d}$$

where

$$V_b = \text{bottom velocity in feet per second}$$

$$d = \text{diameter of rock in inches}$$

The rock is assumed to be of the ordinary variety having a specific gravity of about 2.65. The accuracy of the equation is not known for velocities above 16 feet per second.

7. The entrance pipe or channel may be tilted downward about 15° without affecting performance adversely. For greater slopes use a horizontal or sloping pipe (up to 15°) 2 or more diameters long just upstream from the stilling basin. Maintain proper elevation of invert at entrance as shown on the drawing.

8. If a hydraulic jump is expected to form in the downstream end of the pipe and the pipe entrance is sealed by incoming flow, install a vent about one-sixth the pipe diameter at any convenient location upstream from the jump.

9. For best possible operation of basin use alternate end sill and 45° wall design shown on Figure 42. Erosion tendencies will be reduced as shown on Figure 45.

## BIBLIOGRAPHY

1. Bakhmeteff, B. A. and Matzke, A. E., "The Hydraulic Jump in Terms of Dynamic Similarity," Transactions ASCE, Vol. 101, p. 630, 1936.

2. Puls, L. G., "Mechanics of the Hydraulic Jump," Bureau of Reclamation Technical Memorandum No. 623, Denver, Colorado, October 1941.

3. Dr. Ing. Kurt Safranez, "Untersuchungen uber den Wechselsprung" (Research Relating to the Hydraulic Jump), Bausinginieur, 1929, Heft. 37, 38. Translation by D. P. Barnes, Bureau of Reclamation files, Denver, Colorado. Also Civil Engineer, Vol. 4, p. 262, 1934.

4. Woycicki, K., "The Hydraulic Jump and its Top Roll and the Discharge of Sluice Gates," a translation from German by I. B. Hosig, Bureau of Reclamation Technical Memorandum No. 435, Denver, Colorado, January 1934.

5. Kinsvater, Carl E., "The Hydraulic Jump in Sloping Channels," Transactions ASCE, Vol. 109, p. 1107, 1944.

6. Bakhmeteff, B. A. and Matzke, A. E., "The Hydraulic Jump in Sloped Channels," Transactions ASME, Vol. 60, p. 111, 1938.

7. Rindlaub, B. D., "The Hydraulic Jump in Sloping Channels," Thesis for Master of Science degree in Civil Engineering, University of California, Berkeley, California.

8. Blaisdell, F. W., "The SAF Stilling Basin," United States Department of Agriculture, Soil Conservation Service, St. Anthony Falls Hydraulic Laboratory, Minneapolis, Minnesota, December 1943.

9. Bakhmeteff, B. A., "The Hydraulic Jump and Related Phenomena," Transactions ASME, Vol. 54, 1932, Paper APM-54-1.

10. Chertonosov, M. D. (Some Considerations Regarding the Length of the Hydraulic Jump), Transactions Scientific Research Institute of Hydrotechnics, Vol. 17, 1935, Leningrad. Translation from Russian in files of University of Minnesota.

11. Einwachter, J., Wossersprung and Deckwalzenlange (The Hydraulic Jump and Length of the Surface Roller) Wasserkraft und Wasserwirtschaft, Vol. 30, April 17, 1935.

12. Ellms, R. W., "Computation of Tail-water Depth of the Hydraulic Jump in Sloping Flumes," Transactions ASME, Vol. 50, Paper Hyd. 50-5, 1928.

13. Ellms, R. W., "Hydraulic Jump in Sloping and Horizontal Flumes," Transactions ASME, Vol. 54, Paper Hyd. 54-6, 1932.

14. Hinds, Julian, "The Hydraulic Jump and Critical Depth in the Design of Hydraulic Structures," Engineering News-Record, Vol. 85, No. 22, p. 1034, November 25, 1920.

15. King, H. W., "Handbook of Hydraulics," McGraw-Hill Book Company, Second Edition, p. 334, 1929.

16. Blaisdell, F. W., "Development and Hydraulic Design, Saint Anthony Falls Stilling Basin," Transactions ASCE, Vol. 113, p. 483, 1948.

17. Lancaster, D. M., "Field Measurements to Evaluate the Characteristics of Flow Down a Spillway Face with Special Reference to Grand Coulee and Shasta Dams," Bureau of Reclamation Hydraulic Laboratory Report Hyd. 368.

18. Rouse, Hunter, Engineering Hydraulics, John Wiley & Sons, 1950, p. 571.

19. Newman, J. B. and LaBoon, F. A., "Effect of Baffle Piers on the Hydraulic Jump," Master of Science Thesis, Massachusetts Institute of Technology, 1953.

20. Higgins, D. J., "The Direct Measure of Forces on Baffle Piers in the Hydraulic Jump," Master of Science Thesis, Massachusetts Institute of Technology, 1953.

21. Forchhemier, Ueber den Wechselsprung, The Hydraulic Jump, Die Wasserkraft, Vol. 20, 1925, p. 238.

22. Kennison, K. R., "The Hydraulic Jump in Open Channel Flow," Transactions ASCE, 1916.

23. Kozeny, J., Der Wassersprung, The Hydraulic Jump, Die Wasserwirtschaft, Vol. 22, 1929, p. 537.

24. Rehbock, T., Die Wasserwalze als Regler des Energie—Haushaltes der Wasserlaufe, The Hydraulic Roller as a Regulator of the Energy Content of a Stream, Proceedings 1st International Congress for Applied Mechanics, Delft, 1924.

25. Schoklitsch, A., Wasserkraft and Wasserwirtschaft, Vol. 21, 1926, p. 108.

26. Woodward, S. M., "Hydraulic Jump and Backwater Curve, Engineering News-Record, Vol. 8, 1918, p. 574, Vol. 86, 1921, p. 185.

27. Moore, W. L., "Energy Loss at the Base of a Free Overfall," Transactions ASCE, Vol. 109, 1943, p. 1343.

28. "Hydraulic Model Studies, Fontana Project," Technical Monograph 68, Tennessee Valley Authority, p. 99.

29. Rhone, T. J., "Hydraulic Model Studies on the Wave Suppressor Device at Friant-Kern Canal Headworks," Bureau of Reclamation Hydraulic Laboratory Report Hyd. 395.

30. Beichley, G. L., "Hydraulic Model Studies of the Outlet Works at Carter Lake Reservoir Dam No. 1 Joining the St. Vrain Canal," Bureau of Reclamation Hydraulic Laboratory Report Hyd. 394.

31. Peterka, A. J., "Impact Type Energy Dissipators for Flow at Pipe Outlets, Franklin Canal," Bureau of Reclamation Hydraulic Laboratory Report Hyd. 398.

32. Simmons, W. P., "Hydraulic Model Studies of Outlet Works and Wasteway for Lovewell Dam," Bureau of Reclamation Hydraulic Laboratory Report Hyd. 400.

33. Schuster, J. C., "Model Studies of Davis Aqueduct Turnouts 15.4 and 11.7, Weber Basin, Utah," Bureau of Reclamation Hydraulic Laboratory Paper No. 62.

34. Mavis, F. T. and Laushey, L. M., A Reappraisal of the Beginnings of Bed Movement-Competent Velocity, Proceedings of the International Association for Hydraulic Structures Research, 1948, Stockholm, Sweden.

35. Berry, N. K., The Start of Bed Load Movement, Thesis, University of Colorado, 1948.

FIGURE 41
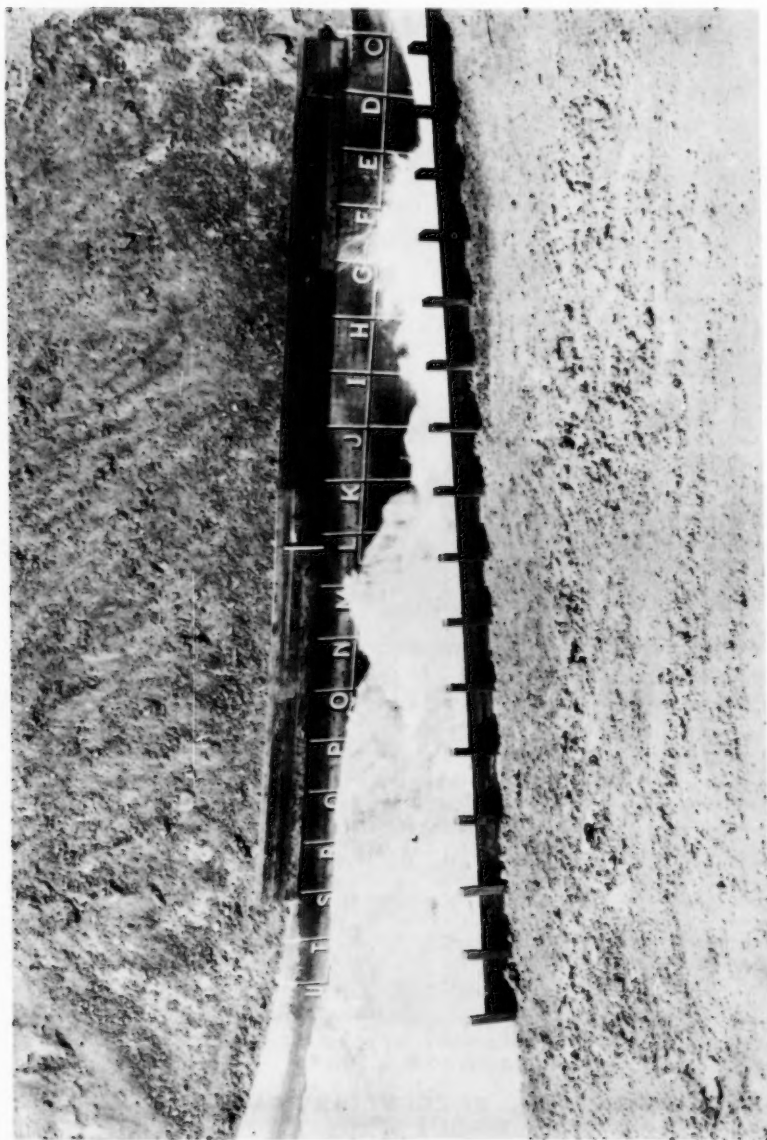


**CHUTE STILLING BASIN ON SOUTH CANAL**
UNCOMPAHGRE PROJECT

FIGURE 42

SEC. A-A

PLAN

PLAN

STILLING BASIN DESIGN

SECTION
ALTERNATE
END SILL

DISCHARGE LIMITS

DISCHARGE IN C.F.S.

WIDTH IN FEET (W)

UPPER LIMIT

LOWER LIMIT

IMPACT TYPE ENERGY DISSIPATOR
BASIN VI
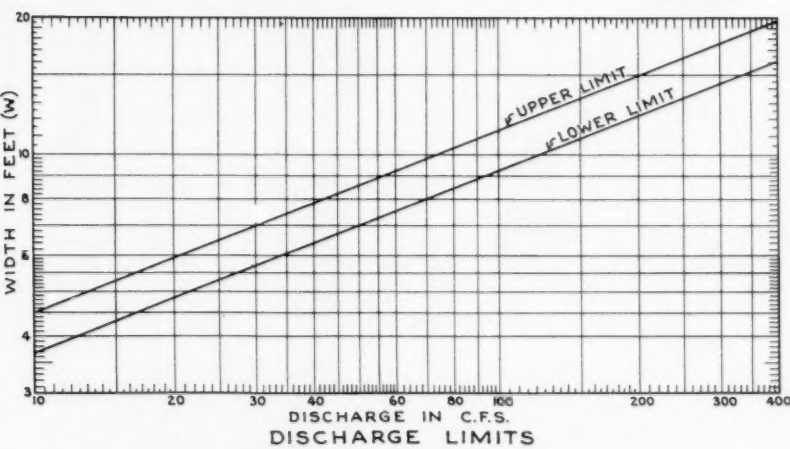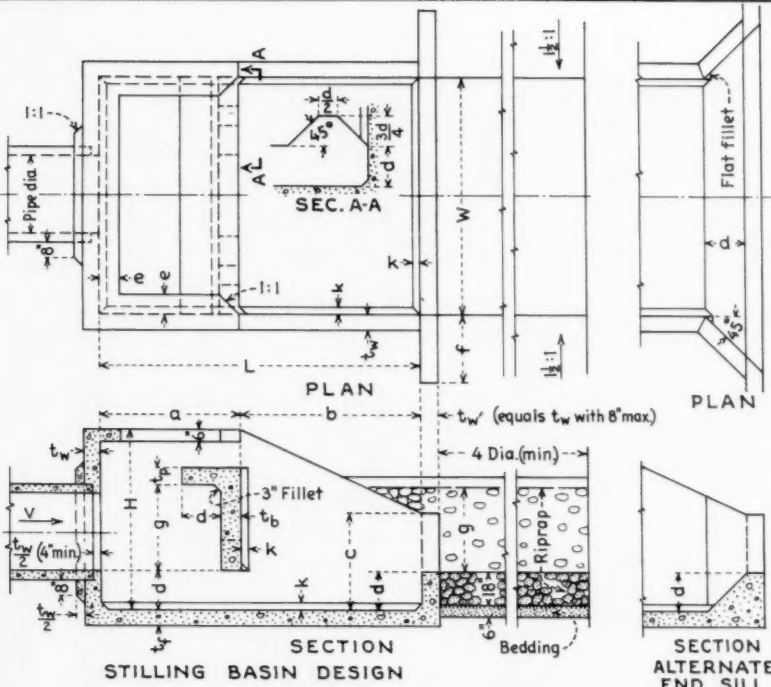
FIGURE 43
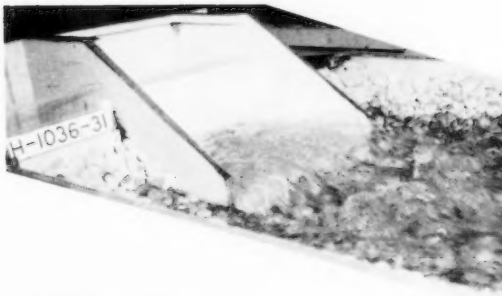


Lowest value of maximum
discharge - Corresponds
to upper limit curve
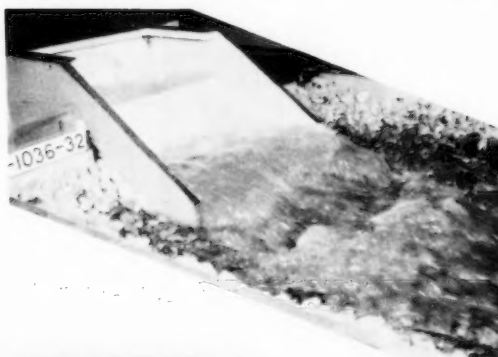
Intermediate value of
maximum discharge -
Corresponds to tabular
values
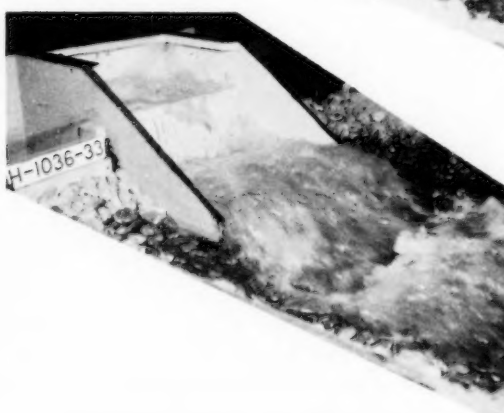
Largest value of maxi-
mum discharge - Corre-
sponds to lower limit
curve

Typical Performance at Maximum Discharges - No Tailwater
Impact Type Energy Dissipator - Basin VI
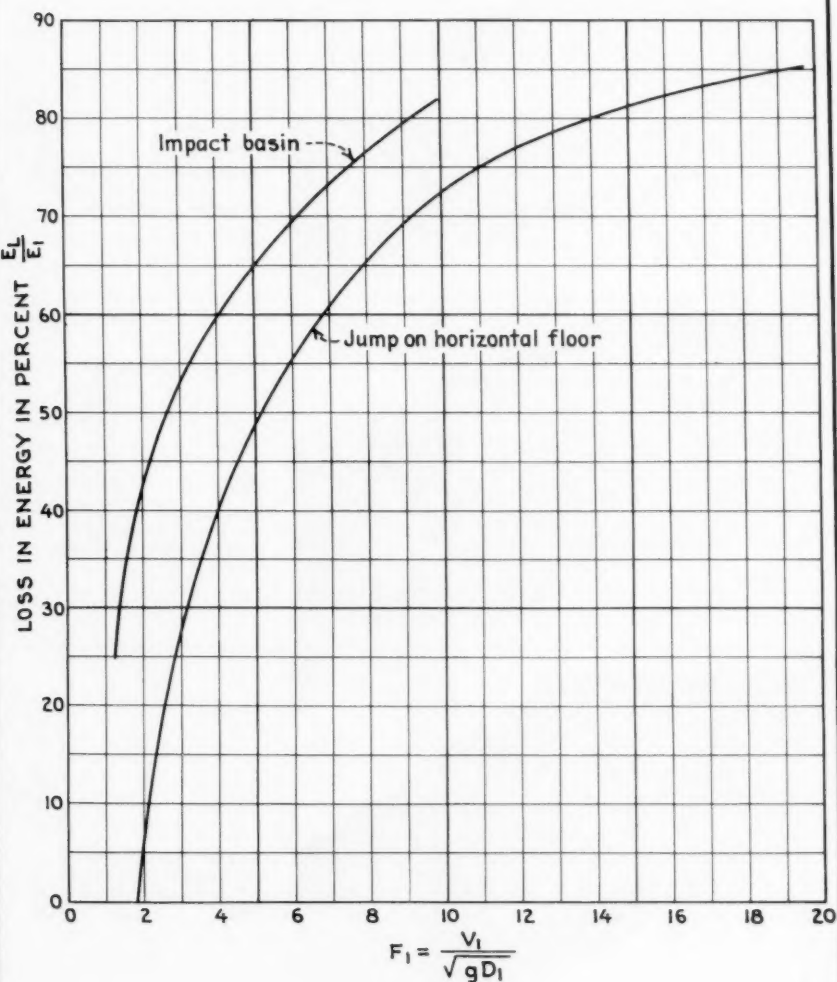
FIGURE 44



COMPARISON OF ENERGY LOSSES
IMPACT BASIN AND HYDRAULIC JUMP

FIGURE 45



A. Erosion of channel bed-standard wall and end sill.

B. Less erosion occurs with alternate end sill and wall design.

C. Flow appearance when entire maximum discharge passes over top of baffle during emergency operation.
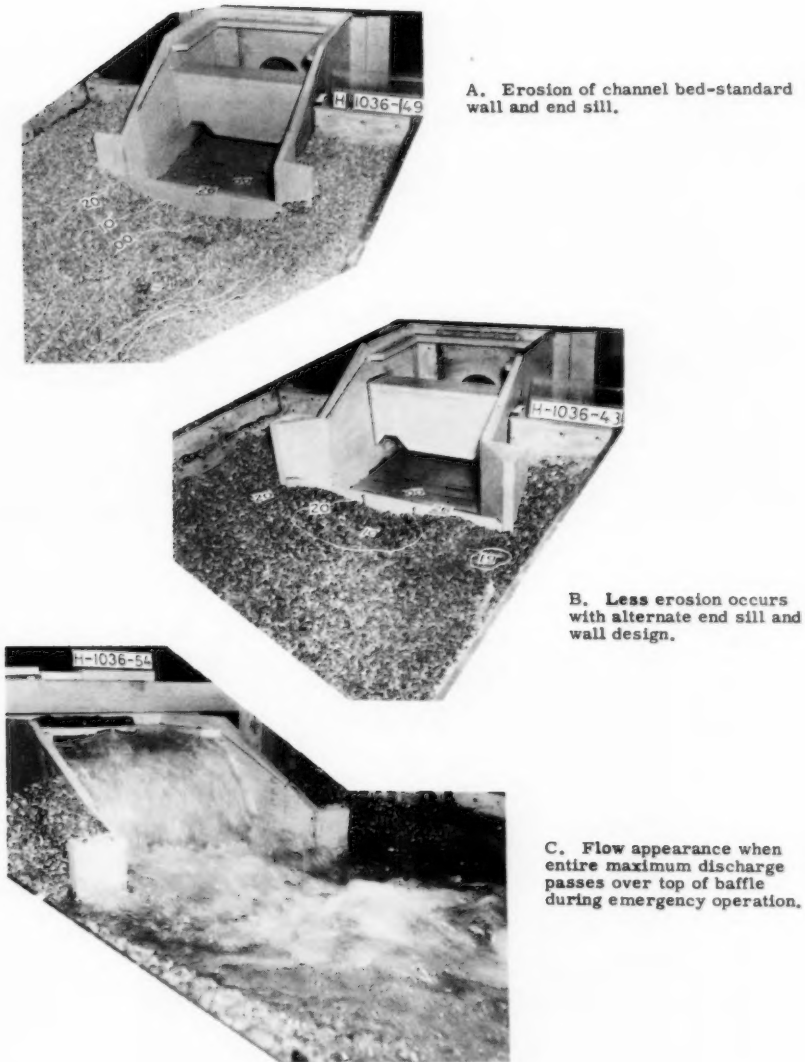
Channel Erosion and Emergency Operation for Maximum Tabular Discharge
No Tailwater
Impact Type Energy Dissipator - Basin VI

Figure 46
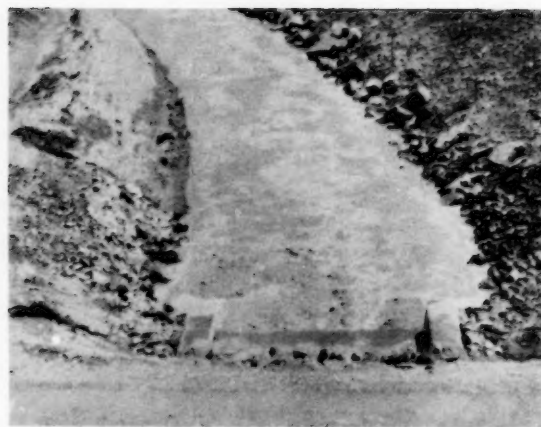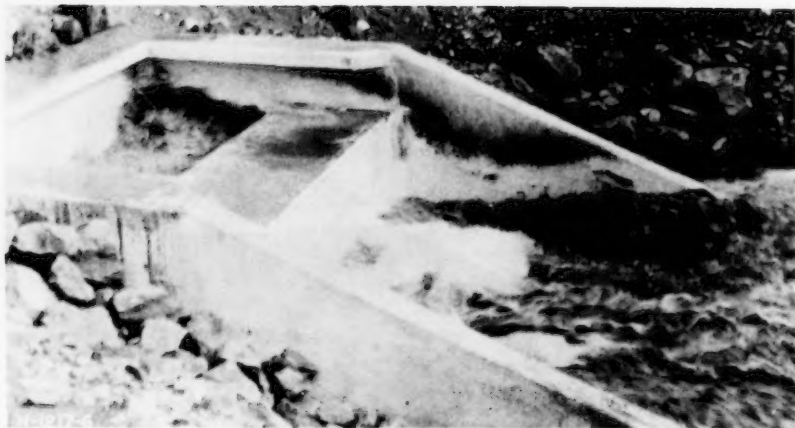




Prototype Performance of Basin VI
Discharge 130 c.f.s. (80 percent of maximum)

## Table 11

### STILLING BASIN DIMENSIONS
### Impact-type Energy Dissipator
### (Basin VI)

| Suggested pipe size* | Area | Max dis-charge | | | | Feet and inches | | | | | | | Inches | | | | | Suggested |
| Dia in | (sq ft) | Q | W | H | L | a | b | c | d | e | f | g | $t_w$ | $t_f$ | $t_b$ | $t_p$ | K | riprap size |
| (1) | (2) | (3) | (4) | (5) | (6) | (7) | (8) | (9) | (10) | (11) | (12) | (13) | (14) | (15) | (16) | (17) | (18) | (19) |
|---|---|---|---|---|---|---|---|---|---|---|---|---|---|---|---|---|---|---|
| 18 | 1.77 | **21 | 5-6 | 4-3 | 7-4 | 3-3 | 4-1 | 2-4 | 0-11 | 0-6 | 1-6 | 2-1 | 6 | 6-1/2 | 6 | 6 | 3 | 4.0 |
| 24 | 3.14 | 38 | 6-9 | 5-3 | 9-0 | 3-11 | 5-1 | 2-10 | 1-2 | 0-6 | 2-0 | 2-6 | 6 | 6-1/2 | 6 | 6 | 3 | 7.0 |
| 30 | 4.91 | 59 | 8-0 | 6-3 | 10-8 | 4-7 | 6-1 | 3-4 | 1-4 | 0-8 | 2-6 | 3-0 | 6 | 6-1/2 | 7 | 7 | 3 | 8.5 |
| 36 | 7.07 | 85 | 9-3 | 7-3 | 12-4 | 5-3 | 7-1 | 3-10 | 1-7 | 0-8 | 3-0 | 3-6 | 7 | 7-1/2 | 8 | 8 | 3 | 9.0 |
| 42 | 9.62 | 115 | 10-6 | 8-0 | 14-0 | 6-0 | 8-0 | 4-5 | 1-9 | 0-10 | 3-0 | 3-11 | 8 | 8-1/2 | 9 | 8 | 4 | 9.5 |
| 48 | 12.57 | 151 | 11-9 | 9-0 | 15-8 | 6-9 | 8-11 | 4-11 | 2-0 | 0-10 | 3-0 | 4-5 | 9 | 9-1/2 | 10 | 8 | 4 | 10.5 |
| 54 | 15.90 | 191 | 13-0 | 9-9 | 17-4 | 7-4 | 10-0 | 5-5 | 2-2 | 1-0 | 3-0 | 4-11 | 10 | 10-1/2 | 10 | 8 | 4 | 12.0 |
| 60 | 19.63 | 236 | 14-3 | 10-9 | 19-0 | 8-0 | 11-0 | 5-11 | 2-5 | 1-0 | 3-0 | 5-4 | 11 | 11-1/2 | 11 | 8 | 6 | 13.0 |
| 72 | 28.27 | 339 | 16-6 | 12-3 | 22-0 | 9-3 | 12-9 | 6-1 | 2-9 | 1-3 | 3-0 | 6-2 | 12 | 12-1/2 | 12 | 8 | 6 | 14.0 |

*Suggested pipe will run full when velocity is 12 feet per second or half full when velocity is 24 feet per second. Size may be modified for other velocities by Q = AV, but relation between Q and basin dimensions shown must be maintained.

**For discharges less than 21 second-feet, obtain basin width from curve of Figure 42. Other dimensions proportional to W; $H = \frac{3W}{4}$, $L = \frac{4W}{3}$, $d = \frac{W}{6}$, etc.

SUMMARY OF

## STILLING BASIN I
### NOTES
Jump occurs on flat floor with no chute blocks, baffle piers or end sill in basin. Usually not a practical basin because of expensive length. Elements and characteristics of jumps for complete range of Froude numbers is determined to aid designers in selecting more practical basins II, III, IV, V and VI.

HYDRAULIC JUMP ON HORIZONTAL FLOOR (FIGURE 4)

RATIO OF TW DEPTH TO $D_1$ (FIG. 5)

$\frac{D_2}{D_1} = \frac{1}{2}(\sqrt{1+8F^2}-1)$
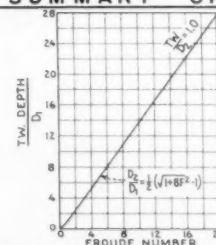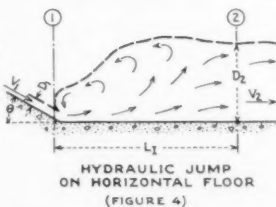
## STILLING BASIN II
### NOTES
Jump and basin length reduced about 33 percent with chute blocks and dentated end sill. For use on high spillways, large canal structures, etc. for Froude numbers above 4.5.

(FIGURE 14)

MINIMUM TAILWATER DEPTHS (SWEEPOUT) (FIG. 11)
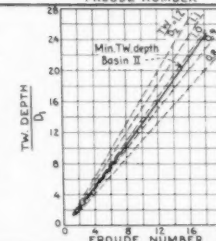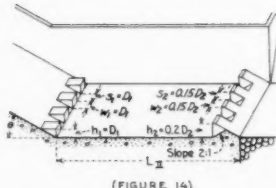
## STILLING BASIN III
### NOTES
Jump and basin length reduced about 60 percent with chute blocks, baffle piers, and solid end sill. For use on small spillways, outlet works, small canal structures where $V_1$ does not exceed 50-60 feet per second and Froude number is above 4.5.

(FIGURE 17)

MINIMUM TAILWATER DEPTHS (SWEEPOUT) (FIG. 11)
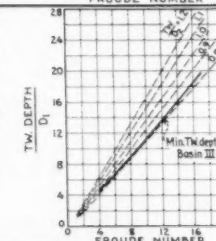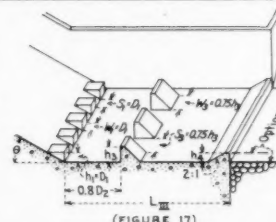
## STILLING BASIN IV
### NOTES
For use with jumps of Froude number 2.5 to 4.5 which usually occur on canal structures and diversion dams. This basin reduces excessive waves created in imperfect jumps. May also use alternate design and/or wave suppressors shown to right, or Basin VI

(FIGURE 22)

ALTERNATE DESIGN (FIGURE 23)
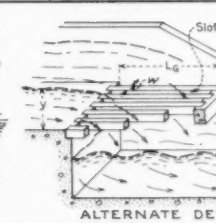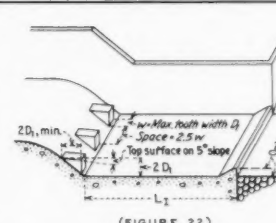
## STILLING BASIN V
### NOTES
For use where structural economies dictate desirability of sloping apron, usually on high dam spillways.
Needs greater tailwater depth than horizontal apron.

CASE B

CASE D (FIG. 30)

LENGTH OF JUMP (CASE D) (FIGURE 32)

TAILWATER DEPTH RELATED TO CONJUGATE DEPTH (CASE D) (FIGURE 31)

Fig. 47.

# STILLING BASIN CHARACTERISTICS



LENGTH OF JUMP

(FIGURE 7 OR 12)

LOSS OF ENERGY IN JUMP,
(FIGURE 8)

$F_1 = 1.7 - 2.5$, PRE JUMP

$F_1 = 2.5 - 4.5$, TRANSITION

$F_1 = 4.5 - 9.0$, RANGE OF GOOD JUMPS

$F_1 = 9.0$ UPWARD, EFFECTIVE BUT ROUGH

JUMP FORMS (FIG. 9)

LENGTH OF JUMP

(FIGURE 12)

WATER SURFACE & PRESSURE PROFILES
(FIGURE 13)

Profile for greater than
conjugate depth
Pressure profile for
conjugate depth

LENGTH OF JUMP

(FIGURE 12)

HEIGHT OF BAFFLE BLOCKS & END SILLS
(FIGURE 18)

Profile for
conjugate depth

WATER SURFACE AND
PRESSURE PROFILES

(FIGURE 19)

Gate structure
Radial gate
Rafts

RAFT TYPE

UNDERPASS TYPE

WAVE SUPPRESSORS

(FIGURE 24)          (FIGURE 29)

## SUMMARY SHEET
### NOTES
This sheet summarizes the main
features discussed in this report,
and shows some of the important
charts. More charts are given
in the report. This sheet should
be used as a reference guide only;
the entire report should be read
before attempting to use any of
the material contained herein.

## STILLING BASIN VI
### NOTES
For use on pipe or open channel
outlets, sizes and discharges
from table. $V_1$ should not exceed
30 feet per second. No tailwater
required. Froude number usually
1.5 to 7 but not important.
May substitute for Basin IV.
Energy loss greater than in com-
parable jump, figure 44.

W = Distance between
side walls.

(FIGURE 42)

| PIPE DIA. IN | AREA SQ FT | Q | FEET AND INCHES | | | | | | | |
|---|---|---|---|---|---|---|---|---|---|---|
| | | | W | H | L | a | b | c | d | g |
| 18 | 1.77 | 21 | 5-6 | 4-3 | 7-4 | 3-3 | 4-1 | 2-4 | 0-11 | 2-1 |
| 24 | 3.14 | 38 | 6-9 | 5-3 | 9-0 | 3-11 | 5-1 | 2-10 | 1-2 | 2-6 |
| 30 | 4.91 | 59 | 8-0 | 6-3 | 10-8 | 4-7 | 6-1 | 3-4 | 1-4 | 3-0 |
| 36 | 7.07 | 85 | 9-3 | 7-3 | 12-4 | 5-3 | 7-1 | 3-10 | 1-7 | 3-6 |
| 42 | 9.62 | 115 | 10-6 | 8-0 | 14-0 | 6-0 | 8-0 | 4-5 | 1-9 | 3-11 |
| 48 | 12.57 | 151 | 11-9 | 9-0 | 15-8 | 6-9 | 8-11 | 4-11 | 2-0 | 4-5 |
| 54 | 15.90 | 191 | 13-0 | 9-9 | 17-4 | 7-4 | 10-0 | 5-5 | 2-2 | 4-11 |
| 60 | 19.63 | 236 | 14-3 | 10-9 | 19-0 | 8-0 | 11-0 | 5-11 | 2-5 | 5-4 |
| 72 | 28.27 | 339 | 16-6 | 12-3 | 22-0 | 9-3 | 12-9 | 6-11 | 2-9 | 6-2 |

(TABLE 11)

Fig. 47.

# Journal of the

# HYDRAULICS DIVISION

## Proceedings of the American Society of Civil Engineers

### CONTENTS

### DISCUSSION
(Proc. Paper 1417)

Page

Discussion of
"FLOOD PROTECTION OF CANALS BY LATERAL SPILLWAYS"

by Harald Tults
(Proc. Paper 1077)

HARALD TULTS,[1] A.M. ASCE.—The discussion of this paper by Professor
Ven Te Chow describes the application of the momentum and energy princi-
ples to the flow with increasing and decreasing discharges.

Professor Chow states that the water level variation in spacially varied
flow may be computed either by the energy or momentum principles.

The energy principle is generally applicable when the change of the energy
in the flow is computable. That is the case with the flow along the lateral
spillway crest, which is subject to friction loss only. However, the kinetic
energy of spilled water is almost entirely lost at the drop into a side channel
as demonstrated by the laboratory tests. Thus, the statement by Professor
Chow that "the energy due to the added discharge dQ per elementary distance
dx should be added to the total energy along the length of the channel during
the time interval dt" is not substantiated. The flow in the side channels is in-
vestigated by Messrs. W. H. R. Nimmo,[11] H. Favre,[17] J. Hinds,[12] and T. R.
Camp,[18] but none of them attempts to compute the water level in the side
channels by the Bernouilli energy equation.

Unfortunately, Professor Chow does not show how his Eq. (D-1) is derived
and how it can be transformed to Eq. (D-2). A superficial analysis indicates,
that Eq. (D-1) may be applicable only for rectangular canals because the term
"D" is defined as hydraulic depth equal to the cross sectional area, A, divided
by its top width.

Furthermore, Eq. (D-3) for lateral spillway flow represents only the super-
critical flow (Cases d and e in Fig. 1) as shown by the discussion of the dif-
ferential equation (Eq. 18) for lateral spillway flow. This differential equa-
tion for the lateral spillway was omitted in the writers paper because the
application of the $(\bar{y},Q)$-curves is much simpler in practical design. However,
in regard to the discussion by Professor Chow, it would be expedient to in-
clude the development of the differential equation of lateral spillway flow into
the closure of the paper.

For the differentiation of the Bernouilli equation, the friction term, $S_F$, as
a function of the velocity, of the cross section, and of the wetted perimeter is
eliminated by equating it to the bottom slope, S.

The first derivative of the simplified version of Eq. 10,

$$H_g = \bar{y} + C_v \frac{Q^2}{2gA^2} \ , \ \text{is}$$

1. Hydr. Engr., Bechtel Corp., Vernon, Calif.
17. "Contributions a l'Etude des Eaux Currents," Editor Rascher & Cie.,
    Zurich, Leipzig and Stuttgart, 1933.
18. "Lateral Spillway Channels," ASCE Transactions, Vol. No. 105, 1940,
    pp. 636-637.

$$\frac{dH_s}{dx} = \frac{d}{dx}\left(\bar{y} + C_v \frac{Q^2}{2gA^2}\right) = gA^3 \frac{d\bar{y}}{dx} - C_v Q^2 \frac{dA}{dx} + C_v QA\frac{dQ}{dx} \tag{15}$$

is zero because of the constancy of the energy head, $H_s$, of lateral spillway flow.

This general equation applied to a rectangular uniform lateral spillway canal is transformed by replacing $\frac{dA}{dx}$ by $b\frac{d\bar{y}}{dx}$ to

$$\frac{d\bar{y}}{dx} = \frac{C_v QA}{C_v Q^2 b - gA^3} \frac{dQ}{dx} \tag{16}$$

in which the spillway discharge per increment of length, $\frac{dQ}{dx}$, is

$$\frac{dQ}{dx} = -C(\bar{y} - z)^{3/2} \tag{17}$$

As the value of $\frac{dQ}{dx}$ is always negative, the water level variation, $\frac{d\bar{y}}{dx}$, may be positive or negative depending on the sign of the factor $C_v Q^2 b - gA^3$.

When the value of $C_v Q^2 b - gA^3$ is negative, the water level along the spillway canal is rising in the downstream direction as in the subcritical flow, shown in Fig. 1 -a, b, and c.

In case, when $C_v Q^2 b - gA^3$ is positive, the water level along the spillway crest is subsiding as in the case of supercritical flow, Fig. 1 - d and e. In this case, Eq. 16 is fully identical with Eq. (D-3) by Professor Chow, when S is made equal to $S_0$.

For the integration, Eq. 16 is transformed using Eqs. 11 and 17 into the following form:

$$\frac{d\bar{y}}{dx} = -\frac{2C}{b\sqrt{2g}} \frac{\sqrt{C_v(H_s - \bar{y})}}{2H_s - 3\bar{y}}(\bar{y} - z)^{3/2} \tag{18}$$

Integration of Eq. 18 between the limits x and $x_0$ ($x_0$ - the abscissa at which $\bar{y}$ is equal to $H_s$, i.e. Q is equal to zero according to Eq. 11) results in the following equation as shown by Professor A. Schocklitsch[13] and modified by writer:

$$-\frac{b}{2C}\sqrt{\frac{2g}{C_v}}\int_{\bar{y}}^{H_s} \frac{2H_s - 3\bar{y}}{\sqrt{(H_s-\bar{y})(\bar{y}-z)^3}}dx = \frac{b}{C}\sqrt{\frac{2g}{C_v}}\left|\frac{2H_s-3z}{H_s-z}\sqrt{\frac{H_s-\bar{y}}{H_s-z}} - 3\sin^{-1}\sqrt{\frac{H_s-\bar{y}}{H_s-z}}\right|_{\bar{y}}^{H_s} \tag{19}$$

The required length of the lateral spillway, replacing

$$\frac{2H_s - 3z}{H_s - z} \sqrt{\frac{H_s - \bar{y}}{H_s - z}} - 3\sin^{-1}\sqrt{\frac{H_s - \bar{y}}{H_s - z}} \quad \text{by} \quad \phi(\frac{\bar{y}}{H_s}), \text{ is}$$

$$L = \frac{b}{C}\sqrt{\frac{2g}{C_v}}\left\{\phi\left(\frac{\bar{y}_2}{H_s}\right) - \phi\left(\frac{\bar{y}_1}{H_s}\right)\right\} \tag{20}$$

It is obvious from the mathematical work required that the application of Eq. 11 for the computation of the dimensions of a lateral spillway is much simpler than the integration of the fundamental differential Eq. 18 derived for the lateral spillway flow in canals of rectangular cross-section. Besides that, integration of Eq. 15, adapted to a more complex spillway cross section than to the rectangular one, is very complicated, perhaps even impossible. However, it is possible for any kind of canal cross-section to establish an equation $Q = f(A, H_s, y)$ of the same type as Eq. 11.

The writer is obliged to Professor Ven Te Chow for corrections, particularly in connection with the derivation of Eq. 6. Eq. 6 itself is correct, but the sign error during typing of Eq. 3 caused the writer to change "subtracted" to "added" at last check.

Actually, the writer expected more discussions, particularly field observations about the performances of lateral spillways and about the priming of the spillway at the filling of the canal.

It is hoped that the writers paper and closure will contribute to the understanding of lateral spillway flow and of its application for flood protection of open canals.
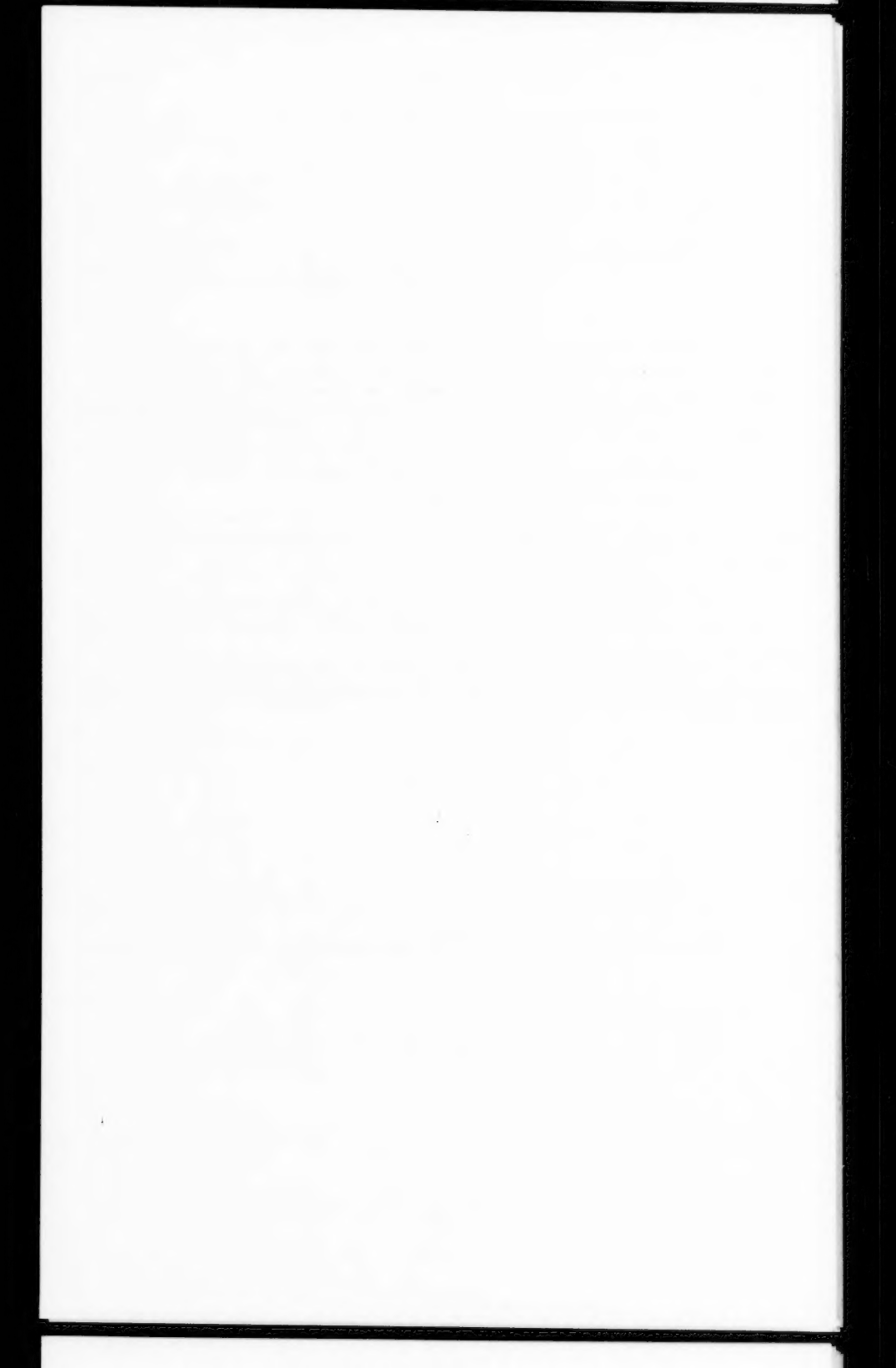
Discussion of
## "GRAPHICAL DETERMINATION OF WATER-SURFACE PROFILES"

by Francis F. Escoffier
(Proc. Paper 1114)

FRANCIS F. ESCOFFIER,[1] A.M. ASCE.—Mr. Ven Te Chow has pointed out how the accuracy of the graphical method is affected by the variation of the critical slope and proposes a different graphical construction in which he plots as the abscissa the product wB rather than the quantity B. The differential equation which serves as the starting point for both methods can be written.

$$S_o dx = dy - y_o w dB \tag{22}$$

When this is integrated from $x_1$ to $x_2$ there is obtained

$$S_o(x_2 - x_1) = y_2 - y_1 - y_o \int_{x_1}^{x_2} w dB \tag{23}$$

The writer followed Bakhmeteff in assuming, as an approximation, that w remains constant. The solution proposed by Mr. Chow replaces eq. (23) by

$$S_o(x_2 - x_1) = y_2 - y_1 - y_o (wB)_2 + y_o (wB)_1 \tag{24}$$

To compare eq.'s (23) and (24) we consider the identity

$$\int_{B_1}^{B_2} w dB + \int_{w_1}^{w_2} B dw = (wB)_2 - (wB)_1 \tag{25}$$

which can be recognized as a variation of the formula for integration by parts. On appropriate substitution from eq. (25) into eq. (24) there is obtained

$$S_o(x_2 - x_1) = y_2 - y_1 - y_o \int_{B_1}^{B_2} w dB - y_o \int_{w_1}^{w_2} B dw \tag{26}$$

On comparing eq. (26) with eq. (23) it is seen that eq. (26) contains the extraneous term

$$\int_{w_1}^{w_2} B dw$$

---

1. Hydr. Engr., Corps of Engrs., U. S. Dept. of the Army, Mobile Dist., Mobile, Ala.

and that therefore eq.'s (24) and (26) are in error to that extent.

Mr. Chow has outlined a graphical method in which he uses the varied-flow functions published by him. Another method similar to that shown in fig. 7 can also be used with these functions. In this method the abscissa is $\frac{i}{n} B_0$ the ordinate in the lower diagram is $B - \eta$ and that in the upper diagram is $\eta$. The slope w is

$$ w = \beta_o = \left(\frac{y_c}{y_o}\right)^{m} $$

The two methods are mathematically equivalent and will therefore give the same numerical results. However, Mr. Chow's method requires a replotting of the curves for each change in discharge whereas that of the writer does not.

Mr. Chow's tables of varied-flow functions for adverse slopes represent a distinct advance over Matzke's table not only because of the wider range of exponents that are included but also because of the wider range in the depth variable $\eta$ and because of the smaller intervals in both the exponent and the depth variable.

Mr. Chow refers to a chart in his own papers similar to the chart in fig. 8. His chart (fig. 2 in his paper) includes a larger number of side slopes for trapezoidal channels than fig. 8 and can be read more accurately. Attention should also be directed at this point to figs. 3, 4, and 5 in his paper. Fig. 3 is similar to fig. 2 but gives the exponent m instead of the exponent n. Fig. 4 is useful in determining the normal depth and fig. 5, in determining the critical depth. These four charts will prove invaluable to anyone engaged in computing water-surface profiles in trapezoidal or circular channels.

The writer wishes to thank Mr. Chow for his most interesting discussion.

<center>Discussion of
"MECHANICS OF SEDIMENT-RIPPLE FORMATION"

by H. K. Liu
(Proc. Paper 1197)</center>

THOMAS MADDOCK, JR.,[1] M. ASCE.—Dr. Liu has presented an important addition to our slowly growing understanding of the sediment movement problem. From Dr. Liu's work one would conclude that ripple formation is limited to those conditions during which the flow around the sediment grains is neither laminar or viscous nor turbulent, but is in that area which Horton called "mixed."

In conventional hydraulics "mixed" flow is relatively unimportant and has been the subject of little study. It appears likely that an understanding of this type of flow is a prerequisite to a resolution of sediment problems since it may be that ripple forms are simply the visual evidence of unstable flow conditions around the grains. The lengthening of the ripple form as the flow changes from laminar to turbulent in terms of the Reynolds number $U_*d/\nu$ as noted by Shields,[26] might be explained in an oversimplified fashion, as being due to changes in the cycle of formation of vortices in the boundary layer.

Thus, we are not interested in the values of a Reynolds number at which flow around the grains becomes fully turbulent nor fully laminar but in learning what happens in between these stages. It is not clear to the writer that those authorities cited by the author fully discuss what happens during the transition stage.

One of the most interesting presentations by Dr. Liu is his fig. 10 showing the relation between his values for the beginning of ripples and the Shields curve for the beginning of bed-load movement. The two curves appear to coincide in the turbulent range but should not coincide in the laminar range. There is a considerable amount of sediment in movement at the time ripples form—enough to affect the hydraulics of the channel. Nevertheless, it might be assumed that ripples are found as soon as enough sediment becomes available to form them. Thus, it is easy to presume that the flow conditions related to the ripple existed at some smaller value of $U_* d/\nu$ but, lacking adequate movement of sediment, there was no way to distinguish them. However, ripple formation might also be related to velocity distributions in the cross section of the channel.

The shape of the curves on figs. 9 and 10 bears a considerable similarity to the usual Drag Coefficient ($C_D$) - Reynolds Number plot of particles falling in water. It is to be noted that $U_*/w$ becomes constant at high Reynolds numbers. So does the drag coefficient, hence, it may be possible to presume that

$U_*/w \propto C_D^n$     . Now, if the Liu and Shields curves on fig. 10 are extended in the laminar range, we find that    $U_*/w \propto \nu/U_*d$   or, because both sides

of the equation are functions of    $\nu, \; U_*^2 d \propto w$     and $U_* d^{1/2} \propto w^{1/2}$

or $U_*/w \propto 1/w^{1/2}d^{1/2}$  At small Reynolds numbers $w \propto d^2$ so

<hr>

1. Bureau of Reclamation, U. S. Dept. of the Interior, Washington, D. C.

$U_*/\omega \propto 1/\omega^{3/4}$ . But in this size $C_D \propto 1/\omega^{3/2}$ . So it can be concluded that $U_*/\omega \propto C_D^{1/2}$

Since from equation (8) $U_*/\omega \propto C_2^{1/2} C_1^{1/2}$ and since $C_2 = C_D, C_1$ must also be proportional to $C_D$ in spite of the way in which it is derived. More importantly, however, this expression indicates a strong relationship between $U_*$ and d.

$$C_D = \frac{4}{3} \frac{(\rho_s - \rho) g d}{\rho \omega^2} \qquad \text{and}$$

$$\frac{U_*^2}{\omega} \propto \frac{(\rho_s - \rho) g d}{\rho \omega^2} \qquad \text{so}$$

$$RS \propto \frac{(\rho_s - \rho) d}{\rho_f} \qquad \text{but}$$

$$\psi = \frac{(\rho_s - \rho) d}{\rho RS}$$

where $\psi$ is generally called the flow intensity.

The data from the Liu and Shields curves indicate, therefore, that

$U_*/gd$ or $1/\psi$ is roughly constant over a wide range of particle sizes at the time sediment movement begins or ceases. It should be noted that the ratios of $U_*/d^{1/2}$ found in Table I are 1.23, 1.14, 1.07, 1.10, 0.93, and 0.975.

This relationship is confirmed to some extent by inspection of the curves of the Einstein bed-load function and the Meyer-Peter formula. Both show constant values of $\psi$ for low values of $\phi$, the intensity of bed-load transport. Furthermore, fig. 11 shows that there is no direct relationship between

$\tau/(\gamma_s - \gamma) d$ and $U_* d/\nu$. While there is considerable scatter, there is no regular variation apparent in $\tau/(\gamma_s - \gamma) d$ . This latter value is equivalent to $RS/(\frac{\rho_s - \rho}{\rho}) d$ or $1/\psi$

There is enough scatter in fig. 11, however, to indicate that $RS/(\frac{\rho_s - \rho}{\rho}) d$ cannot be assumed to be precisely constant at the time movement begins. Part of the scatter may be caused by variation in channel shape or the un-recognized effect of particle shape on settling velocity. Certainly sediment load is responsible for part. There are also indications that another parameter may be involved since Shields[26] concluded that $\tau_c/(\gamma_s - \gamma) d$ was not a constant at the beginning of sediment movement. The writer believes that Dr. Liu has answered his own question and that $\tau_c/(\gamma_s - \gamma) d$ is not a

satisfactory parameter to define the beginning of sediment movement. It is too constant to be used as a variable and too variable to be used as a constant.

The evidence presented by Dr. Liu indicates that $U_*/\omega$ is a better parameter when related to $U_* d/\nu$. The discussion here indicates that $\left(\frac{\rho_s - \rho}{\rho}\right) \frac{gd}{\omega^2}$ could be used as a substitute. However, it would be effective only if precise information were available to describe conditions at the beginning of the movement.

It could be assumed that if $\psi$ is reasonably constant at the beginning of movement of a wide range of sediment sizes, it would be a satisfactory parameter to describe the rate of sediment movement. As a matter of fact, Ning Chien (1956) showed that

$$\phi = \left(\frac{4}{\psi} - 0.188\right)^{3/2}$$

which is in accord with such an assumption.

However, the same Journal carrying Dr. Liu's paper contains Brook's closure of his very fine paper, "Mechanics of Streams with Movable Beds of Fine Sand." In it he shows a poor relation between $\psi$ and sediment movement and concludes "Because of enormous changes in roughness have been observed to occur with almost negligible changes in bed shear, it appears that the latter is a poor choice of independent variable." Thus, there is strong evidence to indicate that $RS/\frac{\rho_s - \rho}{\rho} d$ is a poor independent parameter to be used to describe either the beginning or the rate of sediment movement.

It is worthy of note that Durand (1953) who has presented the only really definitive description of the movement of sediment, in this case as it flows in pipes, did not use the shear velocity as an independent parameter. This paper, which does not seem to have attracted the attention it deserves, is noteworthy for its use of the drag coefficient of the sediment with respect to its fall velocity as an independent parameter. The purpose of this discussion is to show that Dr. Liu's paper indicates that this parameter should have an equal application to the movement of sediment in open channels.

In his equation (5) Dr. Liu presents the conventional relationship presumed to exist in a flow near a smooth boundary. At the time sediment just begins to move, such an assumption may be satisfactory. However, there is a growing mass of evidence that once sediment is moving these conventional relations no longer hold.

## REFERENCES

"The Present Status of Research on Sediment Transport," by Ning Chien, Trans. A.S.C.E., vol. 121, 1956, p. 853.

"Basic Relationships of the Transportation of Solids in Pipes—Experimental Research," by R. Durand, Proceedings Minnesota International Hydraulics Convention, 1953.
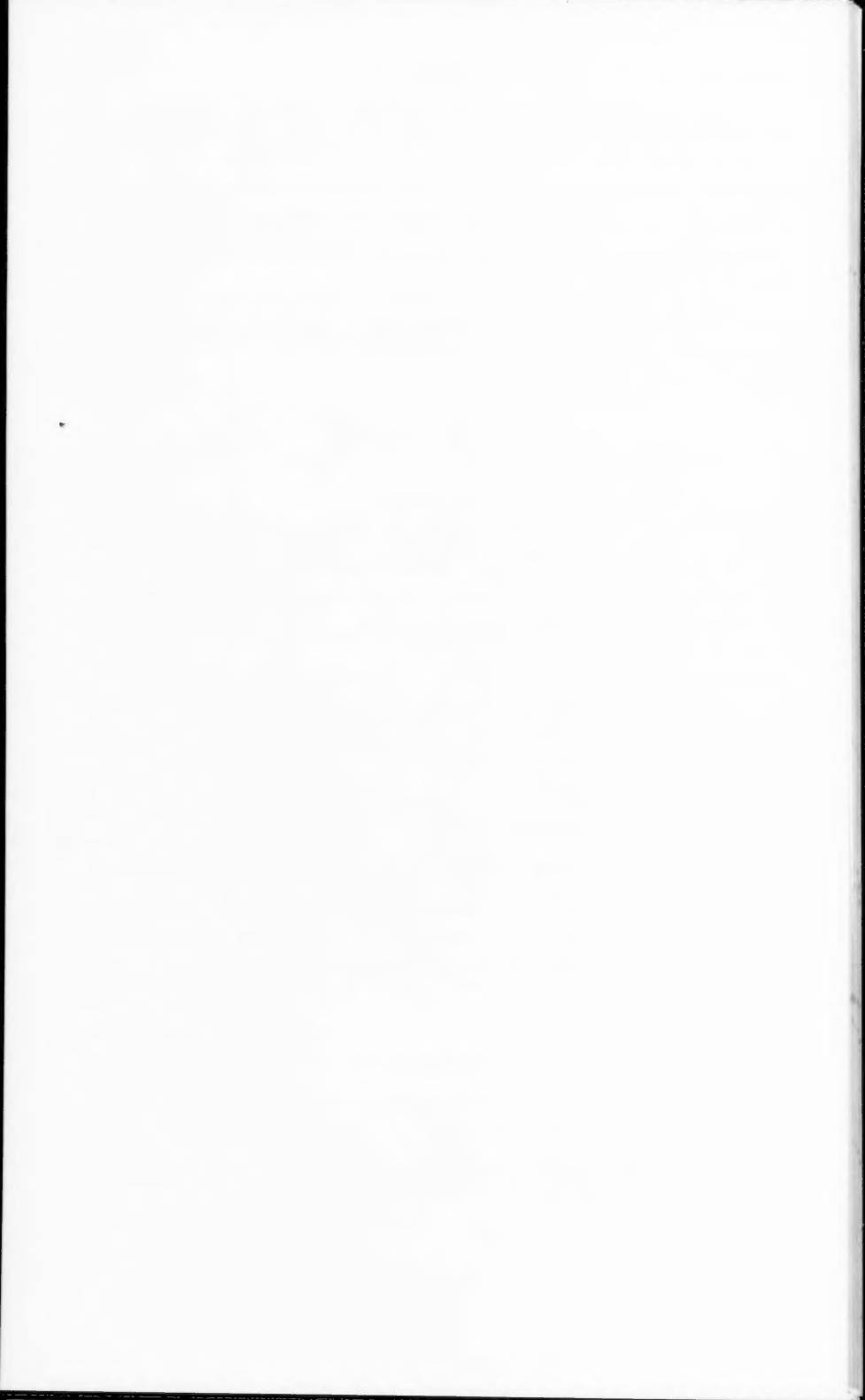
Discussion of
"CHARACTERISTICS OF A LARGE THROATED SIPHON"

by J. C. Stevens
(Proc. Paper 1198)

E. F. RICE,[1] M. ASCE.—The Sullivan siphon is of boldly novel design and
unprecedented dimensions. As a solution to a difficult engineering problem,
the design could hardly have been improved upon for economy, performance,
or dependability.

Some question might be raised as to the use of the terms "efficiency" and
"discharge coefficient." "Efficiency" can be defined as the ratio of estab-
lished merit to unattainable ideal. The word should not be applied to siphon
spillways, for few authors would agree as to what should be their established
merit or unattainable ideal. If "efficiency" is to be regarded as the ratio of
energy used in passing the designed flow to the energy available for such use,
one could, with some justification, conclude that the "efficiency" is always
100 per cent: All the energy available for producing flow is dissipated either
in friction within the spillway or in eddies downstream from the structure.
If efficiency is somehow to be regarded as a measure of the extent of the re-
duction of unwanted friction losses, a similar conclusion could be reached.
For each obstruction to flow that is removed or reduced, there will result a
corresponding increase in the flow that may be passed through the siphon for
a given head. This increased flow is a product of higher velocities which also
result in increased friction losses until the total head loss again becomes the
total operating head; the entire head is used up and no rational expression for
efficiency results. If efficiency were to be defined as the ratio of energy re-
covered to that expended, then the efficiency would be zero, for the siphon
spillway cannot recover energy from falling water, but can only use it to ac-
celerate the water along its way. Several writers have chosen to abandon any
definition of efficiency in terms of energy in favor of more general criteria
describing the utility of various designs. Frequently the "efficiency" is taken
to be the coefficient of discharge, although in many cases designers have not
agreed upon which dimensions should be used to determine this value. As a
result, coefficients of discharge have been reported from about 0.33 to over
1.5, i.e., 33 per cent "efficiency" to 150 per cent for various designs of
siphon spillways. The wide range of values and the extremely low apparent
efficiencies of some of the best designs have been the sources of consider-
able controversy. The difficulty arises in the selection of the area to be used
in the equation $Q = CA\sqrt{2gH}$ , where C is the disputed discharge co-
efficient and A the area upon which the dispute hinges. If the cross-sectional
area is constant there is no problem, but for the designer who hopes to in-
crease the flow by making the lower leg divergent, as a draft tube, the choice
becomes more difficult. Since the majority of designers have chosen the
throat area as the basis for computing C it will be well to examine here the
reason for the presence in occasional siphons of an "efficiency" exceeding
100 per cent.

1. Prof. of Civ. Eng., Univ. of Alaska, College, Alaska.

A siphon with a divergent lower leg fitted with a normally converging entrance is somewhat like a bent Venturi tube. Equating energy at the forebay to that of any point in the interior of the siphon using the outlet elevation as datum,

$$H = \frac{V^2}{2g} + C_L \frac{V^2}{2g} + z$$

Where $C_L$ is a coefficient embodying all losses upstream from the point considered, z is the elevation of the point considered, and V is the mean velocity of the liquid passing the cross-section in which the point is located. Writing the same equation for the cross-section at the exit

$$H = \frac{V^2}{2g} + C_L \frac{V^2}{2g}$$

$$\frac{V^2}{2g} = \frac{H}{1 + C_L}$$

$$V = \sqrt{\frac{2gH}{1 + C_L}}$$

$$Q = AV = A\sqrt{\frac{2gH}{1+C_L}} = CA\sqrt{2gH}$$

where
$$C = \sqrt{\frac{1}{1 + C_L}}$$

H is the full operating head. C is the coefficient of discharge of the siphon and is frequently expressed as a percentage and called the efficiency. If there were no losses, C would be unity, corresponding to 100 per cent efficiency or 100 per cent conversion of the available energy into velocity head. (If efficiency were to be defined as the ratio of output energy, $\frac{V^2}{2g}$, to input energy, H, then efficiency, N, would be $C^2$.)

No coefficient greater than unity is possible if the area, A, used in the equations above is the outlet area of the siphon tube. However, most authors have used, instead, the area of greatest constriction (usually the throat area at the spillway crest) as the area in the equation

$$Q = CA\sqrt{2gH}$$

Thus, the arbitrarily reduced A demands a proportionally increased C, for unchanged flow and head. This new coefficient may be much greater than unity and "efficiencies" greater than 100 per cent may be reported.

A coefficient based on any area other than the area of the issueing cross-section of liquid has no merit as a measure of the extent to which losses have

been eliminated. The erroneous use of the throat area is common, however, and is justified wherever the outlet area is not well defined, as in an incompletely submerged draft tube of trumpet shape which discharges horizontally.

Mr. Stevens has long held that the efficiency of a siphon can be defined as the ratio between the average velocity across the throat of the siphon and the velocity theoretically obtainable under a head of 1 atmosphere. This measure of efficiency has the advantage that it accurately portrays the extent to which losses have been eliminated in the design of a siphon. Its legitimacy is based on two criteria: (1) the throat of a siphon is the highest, frequently most constricted, part, and (2) the flow through it cannot be greater than the flow due to a head of 1 atmosphere. To be completely correct the "1 atmosphere" should perhaps be reduced by the partial pressures of gases and the water vapor pressure. Should the term efficiency be used at all with regard to siphons, this definition will be found the least objectionable, even though it varies for varying heads on the structure.

Since the true discharge coefficients (i.e., coefficients based on outlet area) of most siphons vary between 0.4 and 0.8, siphons compare with any other short tubes. It is something of a paradox that divergent tubes have low coefficients while straight or convergent tubes have high ones, although the reasons for this are fairly apparent upon reflection. Speaking of divergent tubes, King, Wisler and Woodburn, in a standard hydraulics text, have this to say:

> "Experiments indicate that even under favorable conditions the value of $C_V$ based on velocity at outlet is small. Venturi and Eytelwein, experimenting with the flow of water in a tube eight inches long, one inch in diameter at the throat and 1.8 inches at the outer end, obtained a value of $C_V$ of about 0.46. The lost head was therefore approximately 0.79 H. Even with this large loss of head the discharge was about 2 1/2 times the discharge from a sharp-edged orifice having the same diameter as the throat of the tube."

This last statement illustrates the fallacy of assuming that a low discharge coefficient is evidence of a low degree of hydraulic effectiveness. Unless based on outlet area, a coefficient of discharge is not even a valid basis for comparison of various designs. The tube cited above, though 2 1/2 times as effective as an orifice, would show less "efficiency," even by Mr. Stevens' criterion.

From a practical standpoint, very little attention should be paid to reducing the hydraulic losses by extreme refinements in design, because a slight increase in the cross-sectional area of the siphon will increase the flow enough to compensate for a profile of high loss. By this means any desired capacity may be achieved, up to a flow of nearly 200 cubic feet per second per foot of crest attained in the Sullivan siphon.

The author's correction of an obviously erroneous energy gradient is questionable. A cursory study of the literature would seem to show that the velocity-head correction, $\alpha$, rarely exceeds 2.0 even in natural streams, whose uneven distributions of velocity might imply the largest possible values. It remains to determine $\alpha$ for tortuous, man-made conduits such as the Sullivan siphon.

Prior to undertaking the model tests on the Sullivan siphon for Mr. Stevens, the writer made some velocity traverses in a siphon model of simple design with the results shown in Figure 1. At section (2) the velocity

Fig. 1　VELOCITY DISTRIBUTION in SIPHON MODEL
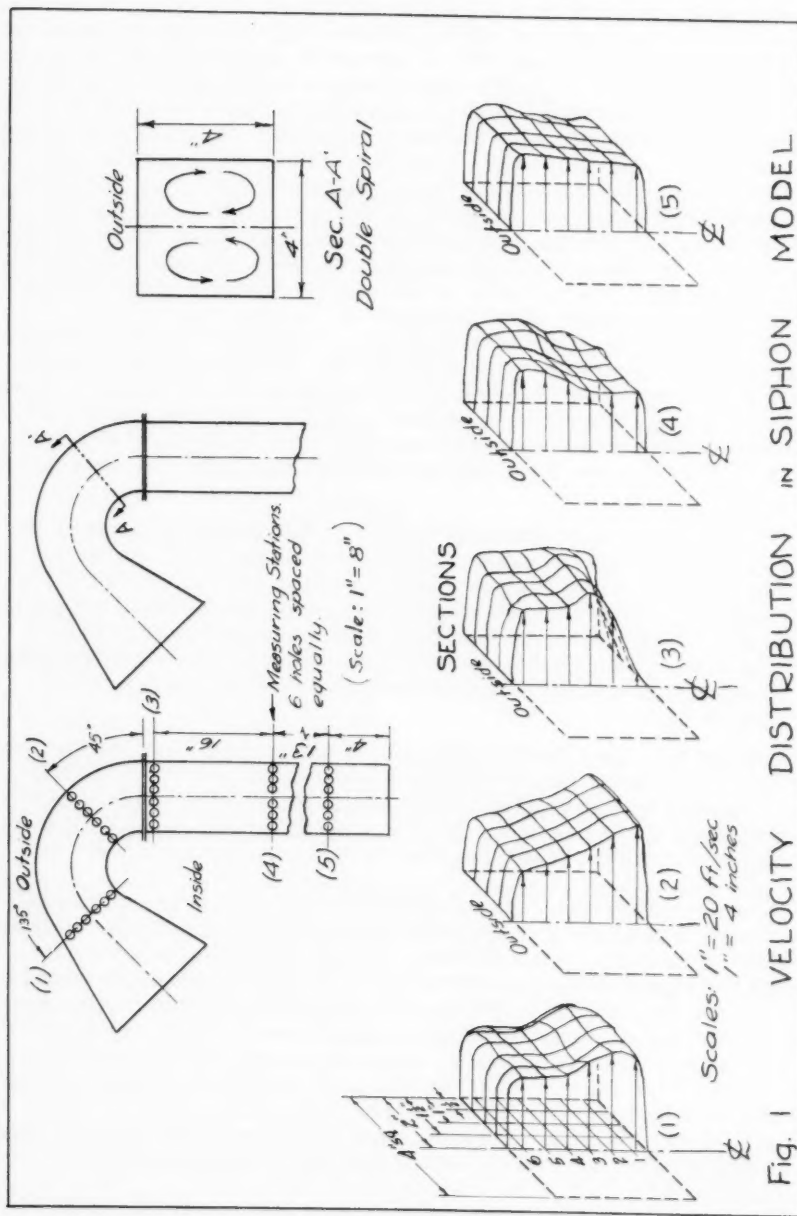
distribution closely obeyed the so-called free-vortex law, wherein the product of velocity and radius is constant for all stream-tubes. (While the diagram shown does not take into account the deviation of the streamlines from true radial lines, it nevertheless shows the relative velocities obtaining at each of the measuring points. The value of $\alpha$ for this region (assuming free-vortex distribution) is calculated to be 1.5. The values of $\alpha$ for sections (3) and (4) are hardly greater, and at sections (1) and (5), $\alpha$ approaches unity. Even if the velocity distribution in the Sullivan siphon was equivalent to a unifrom variation from zero on one side to maximum at the other, would be no greater than 2.

To postulate that $\alpha$ is much higher than 2 at any section would be to imply eddies so strong as to reverse the flow in some portions of the siphon. No such reversals were present either in the low head or high head models, and it is hardly possible that they existed in the prototype—certainly not at piezometer set No. 1.

Therefore, uneven velocity distribution is not likely to be the true explanation for the misaligned energy gradient as measured with the piezometer tubes.

The 11 per cent error of prediction of design flow of the Sullivan siphon by model studies warrants some explanation, especially since the prediction errs on the unsafe side (which is unusual in hydraulic models). Such an error is often acceptable since it may be well within other factors of uncertainty. In this case, the 11 per cent error includes not only the "model error," but also considerable variation due to design changes, for Mr. Stevens wisely used the model as a basis for modifications rather than as a mere "checking" device.

Figure 2 shows the changes made in the design. Both the addition of the air relief valves and the redesign of the outlet were dictated by factors determined by the model's priming characteristics. Under conditions of high tailwater, the sheet of falling water could not exhaust the air, for the low velocities prevailing during free fall over the crest were unable to sweep the bubbles out through the descending leg. Also, the rising forebay displaced air within the siphon, causing a rise in the air pressure inside, inhibiting priming by depressing that part of the forebay within the siphon inlet. Air check valves proved able to correct the priming; the change in the descending leg was made to assure higher velocities for carrying air through the siphon. While they affected the discharge coefficient adversely, these modifications were expected to improve priming and to make possible much better low-flow characteristics.
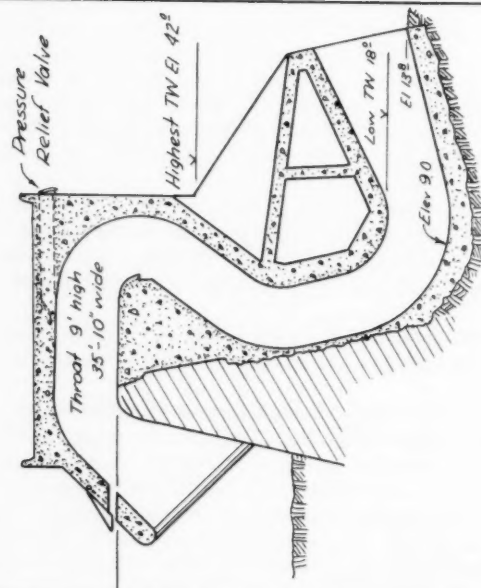
WILLAMETTE FALLS SIPHON SPILLWAY

Pressure Relief Valve

Highest TW El 42º

Low TW 18º

El 13⁸

Elev 90

Throat 9' high
35'-10" wide

Fig. 2(b)   FINAL   DESIGN

AS BUILT

Crest Elev. 58.0'

Existing Wall

42º

Lowest TW
Elev. 18.0'

Elev. 4º
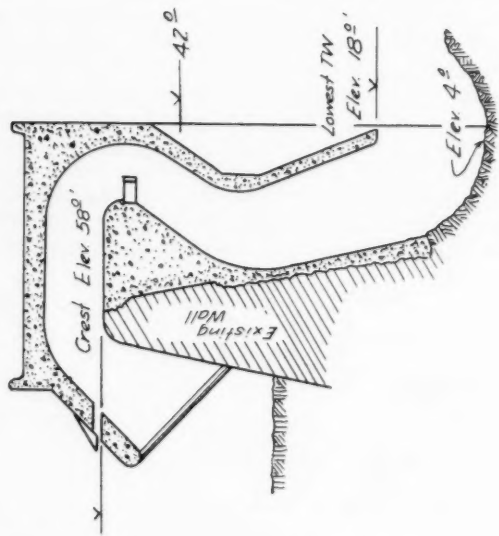
AS TESTED

Fig. 2 (a) ORIGINAL DESIGN

Discussion of
## "OCEAN WAVE FORCES ON CIRCULAR CYLINDRICAL PILES"

by R. L. Wiegel, K. E. Beebe and James Moon
(Proc. Paper 1199)

T. E. STELSON,[1] J.M. ASCE.—Large scale model tests such as the ones described in this paper are of great value in obtaining immediate design data as well as providing a basis for evaluating both theoretical relationships and the results of smaller scale model studies. When so much time, money and skill result in data that show such tremendous variation, non-uniformity and scatter, however, something is lacking, either in experimental method or theoretical understanding. Measured values for apparently identical experimental conditions vary by factors of more than ten as shown in Figures 11, 12, and 13. A paper such as this provides the stimulus to evaluate our present knowledge in this field considering both basic theory and supporting experimental data.

One example of such an area of deficient understanding is that of inertia drag. The added mass coefficient, $C_M$, as defined in equation (3) would have a theoretical value of one* for a circular cylinder of infinite length, accelerated in an ideal fluid of infinite extent in irrotational motion at rest at infinity. This theoretical coefficient was erroneously given as two on pages 22 and 23.

The experimental data summarized in Figure 13 would then show that 91 per cent of the measured values for the mass coefficients were in excess of the theoretical value. The mean experimental value of 2.5 is 150 per cent in excess of the theoretical value. Furthermore, the data presented in Table 3 shows the maximum coefficient to be more than seven times the minimum coefficient.

Some deviations from the theoretical value would be expected because of divergence in physical conditions such as (1) limited length of the test cylinder, (2) wake formation behind the pile, (3) non-uniform movement within the wave and incorrect determination of acceleration, and (4) presence of the free surface as well as the variation in turbulence as mentioned by the authors. None of these items, however, offer any reasonable explanation for such great diversity and scatter of data unless it could possibly be item (3) above.

The coefficient of drag as shown in Figure 11 also showed tremendous variation with the larger values being more than twenty times the smaller values for the same pile and Reynolds' number.

The forces computed using mean values of drag and mass coefficients and plotted in Figures 16 and 17 still show considerable scatter indicating that (1) measured forces are incorrect, (2) mean coefficients are incorrect, or (3) understanding of the phenomena is inadequate. The tendency for computed forces to be higher than measured forces when forces are low and for

---

1. Asst. Prof. of Civ. Eng. and Acting Dept. Head, Carnegie Inst. of Technology, Pittsburgh, Pa.
* Milne-Thomson, L. M. Theoretical Hydrodynamics, 3rd ed., The Macmillan Company, New York (1955) P. 233.

computed forces to be lower than measured forces when forces are high (a
dangerous tendency), may point to the cause of some of the irregularity.
Force due to fluid inertia varies as the height of the waves whereas force due
to drag varies as the square of the height of the waves. Thus, acceleration
dependent forces seem to be too large and velocity dependent forces too small
since the larger forces are associated with the higher waves. This again
would indicate that mean coefficients of mass are too large and that mean
coefficients of drag are too small. Lower values for the mass coefficients
would make them more consistent with theory, and the possibility of higher
drag forces has been stated by the authors on page 22.

A possible conclusion from this paper is that if the experimental measure-
ments are correct, a re-evaluation of all concepts of wave movement, fluid
inertia and viscous drag should be made. They certainly do not begin to pro-
vide an adequate basis for reasonable correlation for the reported data. So
much divergence cannot be tolerated in most engineering situations unless
large safety factors are consistently used. Thus designs tend to be conserva-
tive and expensive and fewer projects are economically feasible.

Discussion of
"THE ESTIMATION OF THE FREQUENCY OF RARE FLOODS"

by Benjamin A. Whisler, M. ASCE, and Charles J. Smith, A. M. ASCE
(Proc. Paper 1200)

LEO R. BEARD.[1]—The equation given by the authors for relating the
probability of monthly flows to annual flows is apparently based on the as-
sumption that flow probabilities during each month of the year are equal for
equal flows, which condition is rarely, if ever, attained under actual condi-
tions. As a consequence of the inequity of the monthly probabilities in most
regions of this country, the relationship is complex, and it is believed that
the authors' conclusions should be reexamined in the light of empirical rela-
tionships among the frequency curves for the various calendar months.
These relationships will be different for different geographical regions.

The authors' findings that frequency curves of annual flows curve upward
on logarithmic-probability paper and that those of monthly flows are straight
are not borne out by the examples given and might well be tested using data
from other parts of the United States. The Washington District, Corps of En-
gineers, has made such a test for the annual-event curve and has found[2] that
frequency curves of annual maximum flows for 108 of the streams throughout
the United States having the longest records of unregulated runoff average
very nearly a straight line. While frequency curves of annual flows on
streams in some regions, particularly in the northeastern United States, do
have a tendency to curve upward, those on streams in some other regions
show the opposite tendency. Whether these regional irregularities are due to
regional characteristics or to accidental excess or deficiency of floods or
droughts in the period of record is a question.

One of the advantages claimed for the authors' method is that it is based
on more numerous data than the annual-event method, but this advantage may
not be as great as appears at first sight. The writer questions whether a
curve based on monthly maximum flows can actually be extrapolated much
more accurately than a curve based on annual maximum flows. Extrapolation
must start at the same magnitude, since the largest observed flow is common
to both series. Also, by the authors' table it can be seen that while the
monthly series has 12 events (1 percent) in 100 years above a given magni-
tude, the annual series has 11.4 on the average above that same magnitude.
Therefore, in the region where the trend of the frequency curve is critical
for extrapolation purposes, the numerical advantage of the monthly-event
curve is small.

It is hoped that the advantages of statistical techniques over graphical
techniques are greater than the authors infer. Certainly the authors have not
exaggerated the unreliability of estimates based entirely on a single record.
No method, no matter how ingenious, can make up for an accidental deficiency

---

1. Hydr. Engr., Corps of Engrs., U.S. Dept. of the Army, Sacramento, Calif.
2. Stream Flow Volume-Duration-Frequency Studies, June 1955, Office of the
   District Engineer, Washington District, Washington 25, D. C.

or excess of large floods during the period of record at one location, without
comparing the experience at that location with experience at other locations.
Statistical methods provide an effective vehicle for comparing frequency
characteristics and for differentiating between accidental and characteristic
variations. The writer believes that statistical techniques, improved from
time to time by new ideas, such as those suggested by the authors, and tested
in the light of experience, as is being done under the Corps of Engineers
Civil Works Investigations Program, will pave the way to much more precise
frequency estimates in the future.

MANUEL A. BENSON,[1] A.M. ASCE.—The authors' ideas are ingenious and
certainly well worth investigation. Their discussion of some present-day
methods of using mathematical statistics in flood-frequency analysis is dis-
cerning and points out the weaknesses and assumptions involved. The writer
would like to express complete agreement with and reemphasize their obser-
vations that

"... many investigators utilized mathematical techniques involving the
coefficient of variation and the coefficient of skew to fit skew curves to
peak annual flow data that plotted as a curve. This technique becomes
little more than a mathematical method of fitting an empirical curve to
the data and is little, if any, better than drawing such a curve graphical-
ly by eye through the plotted points, and may actually be worse."

The authors' contention that the series of annual flood peaks is not a
proper series for statistical analysis is debatable. They have said, "It is
faulty statistical technique to use selected data in studying any phenomenon
which is presumed to follow the basic laws of probability." There is nothing
inherently incorrect in selecting data to be subjected to statistical analysis,
particularly such selection as is represented by the highest event in a time
series. Some types of selection are proper, others are not. There may be
something inherently incorrect, however, about assuming that any phenome-
non follows any of the basic laws of probability if basic law is intended to
mean a frequency distribution. This applies equally to phenomena for which
"all" the data are considered.

It must be recognized that a "flood peak" per se is not as clear cut an item
as most of the phenomena ordinarily subjected to statistical analysis. A flood
peak needs to be defined before it can be determined. By "flood peak" most
people would mean the single momentary maximum or daily maximum occur-
ring during a rise caused by a flood of damaging or notable magnitude. The
annual flood comes as close to fitting this definition as is possible. The con-
cept of "floods above a base" attempts to include all the high or damaging
floods regardless of the period of time within which they occur, but in doing
so introduces uncertainty because flood crests often occur in rapid succession
and may be part of the same general rise. The authors' definition of "all"
peaks will mean the use of many events occurring at low flows, most of which
are not ordinarily considered as flood peaks at all. It also involves consider-
ing each of the separate crests during a flood rise as being independent events.

There does not seem to be any reason for expecting that a series of such
events, defined arbitrarily, should follow a log-normal or any other statistical
distribution, despite the fact that "all" such events are being considered. As

---

1. Hydr. Engr., U. S. Geological Survey, Wash. 25, D. C.

the authors realize, any such contention must be shown to conform to actual streamflow data in order to justify the use of a fitted distribution which averages the data within the defined range. Whether the distribution is or is not a good fit within the range of data, extrapolation is risky and not justified unless as a minimum condition the evidence is numerous and shows a definite and undeniable tendency. Even then, the possibility exists of a change in relationship beyond the range of data.

Langbein (1949) has demonstrated the relation between the annual flood series and "floods above a base." The same relation holds true between the annual series and the series of "all" peaks, since "all" peaks represent the floods above a zero base. As Langbein shows, there is virtually no difference between the frequency curves derived from the two above a recurrence interval of about 10 years. The additional floods included in the partial-duration (or complete-duration) series serve only to add information at the lower end, where it is not badly needed. For this reason there is no advantage in considering "all" floods or monthly floods, unless the relationship shown by such a series is to be extrapolated beyond the range of data, as the authors have done.

The plotted data for the three stations analyzed by the authors do not show clear-cut evidence of having produced better methods of fitting the data than are now available. Their final computed curves of annual peak flow do not appear to give any better fit of the data than do the computed straight lines of best fit in the case of Lehigh River and Iowa City (authors' fig. 1, 3). Their curve is not as good a fit for Tunkhannock Creek (authors' fig. 2).

The curves for Lehigh River (authors' fig. 1) have been cited as demonstrating "the great errors in the determination of the recurrence interval of rare floods which are made in assuming that annual peak flows follow the logarithmically normal laws of probability." It would be equally as valid to show by means of the curves for Tunkhannock Creek (authors' fig. 2) "the great errors which are made in assuming that monthly peak flows follow the log-normal laws." Actually, neither the monthly nor annual peaks are demonstrated by the fit of the data as being representative of the log-normal law.

Data for all the peaks on Lehigh River show a slight positive curvature (concave upward) for Lehigh, a definite negative curvature for Tunkhannock. The monthly peaks for Iowa River exhibit a slight negative curvature. It is therefore not at all certain, particularly in view of only three gaging-station records, that "all" peaks or monthly peaks exhibit a log-normal distribution.

The method has been tested by the writer using unregulated records at 8 stations in California (unpublished records of monthly peak discharges available at District office of U. S. Geological Survey, Menlo Park, Calif.) and 6 stations in Great Britain (1937-45, 1945-53, 1953-54). For these stations records of momentary monthly and annual peaks are available. Daily peaks have but a limited use in engineering design involving storage, whereas momentary peaks are the important factor in the design of most hydraulic structures and in problems of flood prediction and flood damage. For this reason no attempt was made to analyze "all" peaks and investigation of the authors' methods was confined to momentary peaks.

The longest record is that for Kern River near Bakersfield, Calif., for which monthly peaks have been published in water-supply papers from October 1912 to December 1950. The other California stations have records from 10 to 18 years in length. The records in Great Britain are 17 years long.

The curves for Kern River near Bakersfield, Calif., are shown in figure 1

% of Values Greater Than

KERN RV. NR. BAKERSFIELD CALIF.

- • Actual monthly peak flow
- ✗ Actual annual peak flow
- —— Straight line of best fit, monthly and annual peaks
- – – Probability of annual peak flow from monthly peak flows

Flow in cfs

FIG. 1

Recurrence Interval (years)
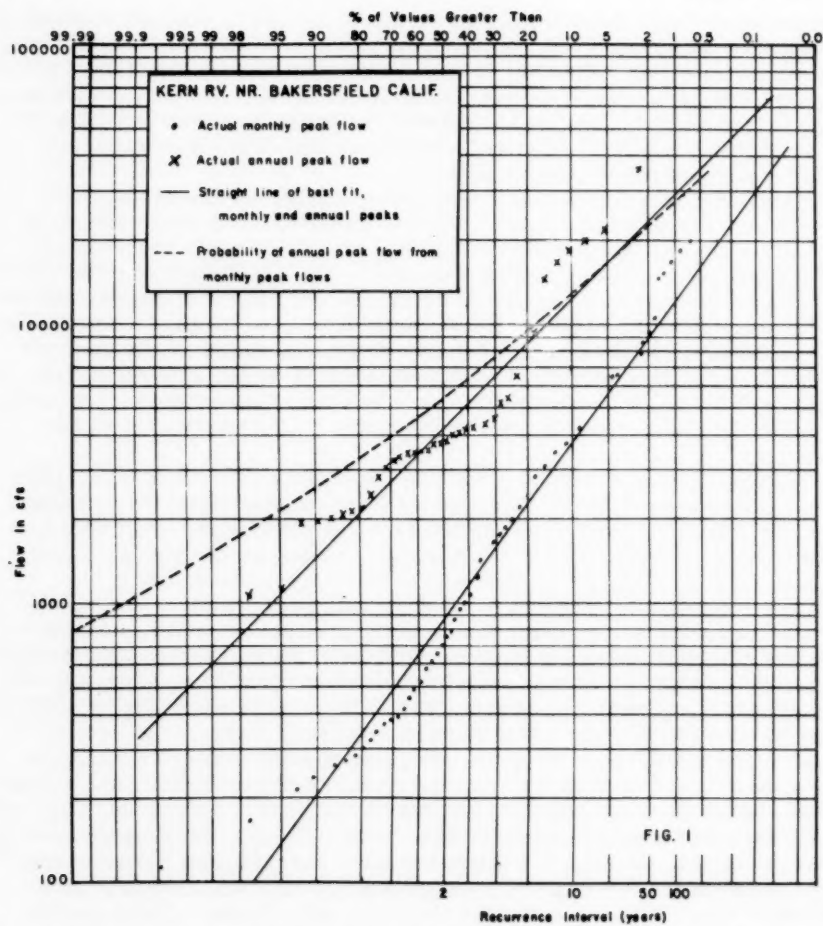
and those for River Avon at Evesham, England in figure 2. The data for River Avon are typical of those for all the English stations and the remainder of the California stations. In all cases the actual monthly peaks appear to define an S-curve. In all cases (except Kern River) the top points are well to the right of the least squares line through the monthly peaks. At every station but Kern River, the actual annual peaks are well to the right of the transformed annual peak curve. (Note that in figures 1 and 2 only one in ten of the monthly peaks are shown within the middle range, for clarity).

The following table shows the recurrence interval from the theoretical (transformed) annual peak curve, of 10-, 50-, and 100-year peaks on the annual peak least-squares line.

The table on page 25 shows the extremely large difference between the annual peak least-squares lines and the authors' derived annual peak curves. For example, at River Avon, the discharge with 100-year recurrence interval on the least-squares line has a 14.3-year recurrence interval on the authors'

FIG. 2
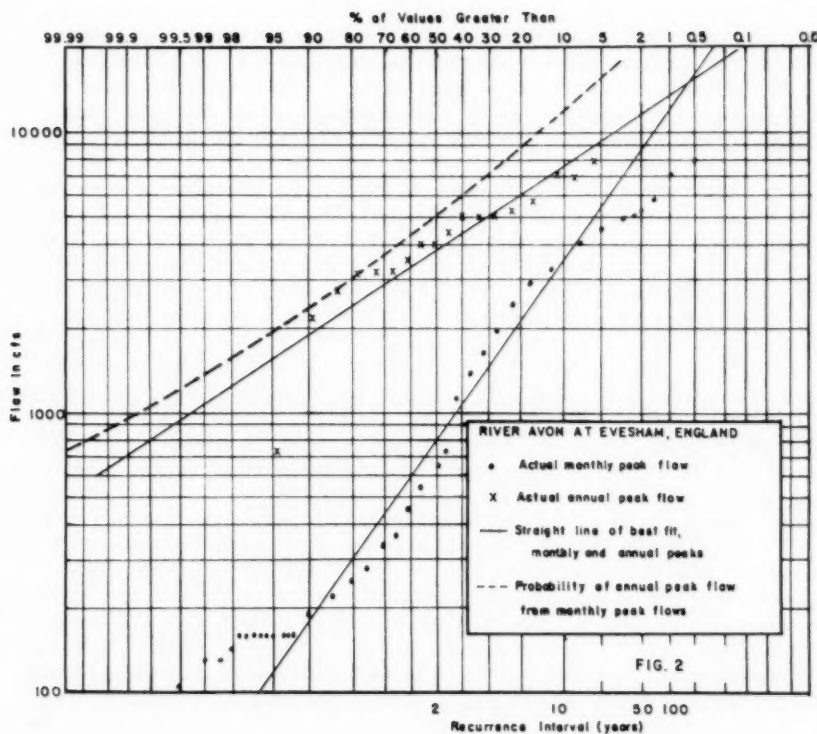
| Station | Recurrence interval from least-squares line (years) | | |
|---|---|---|---|
| | 10 | 50 | 100 |
| **England** | | | |
| R. Avon at Evesham | 3.7 | 9.1 | 14.3 |
| R. Brenig at Birkenhead | 1.5 | 1.8 | 2.0 |
| R. Dee at Woodend | 3.4 | 7.2 | 9.3 |
| R. Irfon at Abernant | 1.5 | 1.8 | 2.0 |
| R. Lugg at Lugwardine | 1.4 | 1.6 | 1.6 |
| R. Wye at Rhayadar | 2.1 | 3.0 | 3.4 |
| **California** | | | |
| Deer Cr. below East Fork | 2.9 | 5.0 | 6.1 |
| Dinkey Cr. at Dinkey Meadow | 2.1 | 3.0 | 3.6 |
| Dinkey Cr. at mouth | 1.8 | 2.5 | 2.9 |
| Helms Cr. at Sand Meadow | 3.6 | 5.7 | 6.7 |
| Kern R. nr. Bakersfield | 9.1 | 62.5 | 139 |
| N.F. Kings R. above Dinkey Cr. | 2.2 | 2.9 | 3.2 |
| N.F. Kings R. blw. Meadowbrook | 2.4 | 3.0 | 3.3 |

annual peak curve. The closer agreement, shown by the table, between the two curves for Kern River should not hide the fact that the actual annual peaks define a quite different relation than either of the two curves (see fig. 1). The writer considers the least-squares line through the peaks to be a better means of predicting future annual peaks than the authors' transformed curve. However, a graphically-fitted line through the upper points would be even better.

Some explanation seems necessary to account for the large discrepancies between the actual annual peak floods experienced and the authors' derived annual flood curves. There appears to be a basic accumption in making the transformation from monthly to annual peaks that is not borne out by the facts. The statement reads, "If $P_m$ is the probability of a given event occurring in any one month, the probability, $P_y$, that it will occur in a year is much greater and can be expressed as $P_y = 1-(1 - P_m)^{12}$." In actuality, the probability of a peak of a given magnitude being a monthly peak is not the same in any two consecutive months and is far from the same in 12 consecutive months. This is well illustrated by the record on the Kern River near Bakersfield, Calif., where all 39 annual peaks occurred during the 8-month period from November through June. Monthly peaks of the magnitudes occurring in the 4-month period from July through October have only an extremely small chance (if any) of being the annual peaks. Or, working backwards, annual peaks which occur with high frequency (high probability) in November-June have practically no probability of occurring during July-October. It might be thought that this situation could be handled by computing the probability of, say, a 1,000 cfs peak occurring in each of the 12 months and multiplying these. However, even this is not correct, since the principle of independence of probabilities which is assumed in the combining process does not actually exist. For example, if all annual peaks occurred in May, the probability of May peaks and annual peaks would be identical, and all the other monthly peaks would have no effect on the probability of the annual peak. The situation at Bakersfield and any other river is analogous, though not as extreme.

In summary:

1. The authors' method of extrapolation beyond the range of data is dependent on the validity of the log-normal distribution for "all" peaks (approximated by distribution of monthly peaks). Conformance to this distribution cannot be predicated by theory and is not borne out by actual streamflow records.

2. The method of transforming from monthly to annual probabilities is based on assumptions which are not in accord with the hydrologic facts.

## REFERENCES

Langbein, W. B. (1949), Annual floods and the partial-duration flood series, Amer. Geophy. Union, Trans. v. 30, p. 879.

The Surface Water Year-Book of Great Britain (1937-45, 1945-53, 1953-54), London, Her Majesty's Stationery Office.

Discussion of
"HIGH HEAD CAVITATION TEST STAND FOR HYDRAULIC TURBINES"

by W. G. Whippen and G. D. Johnson
(Proc. Paper 1201)

LESLIE J. HOOPER,[1] M. ASCE.—The authors are to be complimented on
their clear presentation of a carefully worked out design which seems to be
admirably adapted to the purpose intended.  The provision in the design for
mounting the water wheel casings and dynamometer in one frame work seems
to be particular noteworthy.  In this way it is hard to see how deflections
caused by changes in pressure or changes in the loading on the pipe can pos-
sibly affect the alignment of the shaft and friction readings of the rotating
parts.  This is an important feature bearing upon the repeatability of tests.

With respect to repeatability of tests it is noted that the repeatable
accuracy of any test point appears to be within $\pm$ 1/4 of 1%.  It is presumed
that this refers to a single test set-up where the gate and speed are read-
justed to the same operating conditions.  It would be interesting to know what
the discrepancies might be when a unit has been tested, completely torn down
and then reinstalled at a later date and tested again.

There are one or two questions that come to mind that probably can be
very easily answered.  It is noted at one point that "since equipment is avail-
able to cool both fresh and de-aerated water, the effect of air content upon
performance and cavitation may be studied."  Inasmuch as no provision has
been made in the design to re-absorb air that might be liberated in a passage
through the test circuit it is difficult to see how the studies on the effect of
air content can be made when the air content is not controlled.

A second question that arises is concerned with the prediction of full scale
prototype efficiency of model test results.  It is noted in Fig. 4 that model
test efficiencies of the order of 91.5% are being obtained.  Assuming a 12"
diameter model, a 240" diameter prototype and the Moody step-up formula
with the 1/4 power of the diameter ratio there results a predicted efficiency
of 96%.  If the 1/5 power of the diameter ratio is assumed the resulting
efficiency is still 95.4%.  Either of these results is very complimentary to the
design of the water wheel but do seem a little difficult to obtain by field test-
ing methods.

There is no question that laboratory tests can be made more accurately
than field tests because the control and possibilities of calibration are much
better.  However, there is still a place for field tests inasmuch as a model
test can never duplicate all of the conditions that exist in the field and it
would seem that the step-up formulas now in use still leave a little to be
desired.

B. L. VANDER BOEGH.[2]—The S. Morgan Smith high head test stand offers

1. Prof. of Hydraulic Eng., Worcester Polytechnic Inst., Worcester, Mass.
2. Hydr. Engr., Newport News Shipbuilding and Dry Dock Co., Newport News,
   Va.

a means heretofore unavailable by which the answer to several baffling problems may well be determined.

Mention is made of the lower head flume. A comparison of performance test results of homologous models between the low head and the new high stand would certainly be of interest. A later comparison with a prototype test might indicate the need or, conversely, the lack of a requirement that all model testing be done at field heads if possible.

A visual comparison of cavitation formation at high and low heads is not possible inasmuch as this feature is not incorporated in the new stand. It would seem that this comparison would be of definite value in outlining the surfaces to be overlaid with stainless steel, and in the observance of tip cavitation as well as trailing edge flow patterns.

It is assumed that provision for the study of the hydraulic moment and forces on the vanes of a Kaplan model has been made in the low head stand inasmuch as no mention is made of this feature in the high head stand. This might well have been considered in the high stand as the moments are known to vary with sigma, and this stand should give more accurate sigma values.

It would seem that a filling of the system with city water for each test would make it difficult to maintain a uniform air content over the extent of the test. At low sigmas, it has been suggested that the air content may definitely affect the performance to varying degrees. A storage tank for the reuse of the water might seem desirable.

The cooling system for the stand is definitely interesting. It would be helpful to know the effect of temperature change of the water on the cavitation results, (inasmuch as the water vapor pressure is included in the sigma formula) with a suggestion or recommendation as to the reliable temperature range for accurate cavitation testing.

Many of the newer test stands use head and discharge tanks. The question is raised as to whether the flow conditions into the case inlet of the model are affected without the use of an inlet section or penstock.

In general, the new stand seems to be well designed, incorporating provisions for exceptionally accurate testing, and the test results should be both interesting and reliable.

Discussion of
"IS THE WRITING OF FLOOD INSURANCE FEASIBLE?"

by John F. Neville
(Proc. Paper 1202)

E. M. LAURSEN,[1] A.M. ASCE, and A. TOCH,[2] J.M. ASCE.—The three
papers (Proc. Papers 1164, 1165, and 1202) of this series describe very
clearly the difficulties involved in the various aspects of writing flood in-
surance—the first two papers dealing primarily with the technical problems,
this paper with the practical problem of selling insurance. The conclusion
that appears to be inescapable is that such insurance would be possible tech-
nically but impossible practically. It would seem, however, that the conclu-
sion "insurance against the peril of flood applicable to fixed property cannot
successfully be written" is based on a possibly shaky premise as to the type
of insurance program to be evolved. That flood insurance must be written on
the basis of the average annual loss incurred by each property is not pre-
ordained. However, if this assumption is made it does become necessary for
the insurance company to make hydrologic and damage studies (as outlined by
Foster in the second paper of the series) which will cover each individual
property to be insured. Not only is the average annual loss high for any
property on the flood plain, but there is then a sizable "expense loading"
added to the premium.

Average annual losses should be thought of, quite properly, as part of the
price paid for the benefits derived from occupation of the flood plain. The
cost of repairing damage caused by flood stages which occur frequently can
and should be paid just like taxes or any other cost.

The following hypothetical problem of determining the location of steam-
power plant will serve to illustrate this assertion. Given two alternate loca-
tions, one on the flood plain next to the river and another on high ground out
of danger of flooding, certain advantages will be inherent in each site. Con-
struction and operating costs for the condenser-water supply will be less at
the flood-plain location, as may be storage costs for the coal supply. Costs
attributable to flood damage will be least at the high-ground location. Other
costs, such as land acquisition, foundations, and spur trackage, will be less
for one or the other site depending on local conditions. An economic analysis
will determine the best site, with average annual flood damage taken into ac-
count either as an operating cost or by inclusion of proper structural safe-
guards.

Thus there is no advantage in having insurance against floods of frequent
occurrence, since the premiums must necessarily be greater than the
"losses" due to those floods. Insurance against the unusual damage caused
by a very large—and therefore very infrequent—flood may be desirable, how-
ever, because a considerable reserve fund would otherwise be needed in

1. Research Engr., Iowa Inst. of Hydr. Research, Iowa City, Iowa.
2. Research Engr. and Research Associate, Iowa Inst. of Hydr. Research,
   Iowa City, Iowa.

order to overcome such a catastrophic loss. Insurance can be substituted for all or part of this reserve. The amount of insurance does not need to be related precisely to the damage which actually occurs, but can be an arbitrary amount which will cushion the effect of the flood damage. Since only floods of rare frequency would be involved, the premium should be much smaller than would be required to cover the average annual loss. Stage-probability and stage-damage studies for the individual property do not need to be as precise, and the burden of these studies can be placed on the insured. The policies could be written simply on the occurrence of floods of various magnitudes as determined at the nearest gaging station, and stage-probability relationships for these stations would form the basis for the determination of risk and corresponding premium per dollar of coverage.

The argument for considering flood losses as a cost of doing business is readily apparent in the case of a steam-power plant. It is equally true for any other business. If the benefits derived from a flood-prone location do not outweigh the costs resulting from flood damages, a move to high ground is indicated. If the benefits do outweigh the average annual "losses," it would be utter folly to pay an insurance premium greater than these "losses" except as a cushion against extreme cases of catastrophic losses due to very rare floods. Farming would differ from other business enterprises only in that the timing and duration of a flood might assume, to the insured, as much importance as stage. It is difficult to see any benefits of a flood-prone location accruing to dwellings except that of cheap land. If the damages exceed this benefit, moving the house to high ground or putting it on stilts would seem preferable to buying flood insurance for frequent floods.

In order to protect the insurance company from opportunists, two safeguards could easily be used: a time lapse of several months between the date of payment of premium and the date the policy goes into effect, to eliminate policies bought after a definite flood prediction has been made; and a "house cut" of sufficient magnitude to discourage mere gambling on the probable river stage. Long-term policies could be encouraged, on the other hand, by reducing the premium every year for several years on policies kept in force continuously.

It would be interesting to know whether the type of insurance proposed here would be more feasible and practicable from the underwriters' viewpoint than the average-annual-loss type assumed by the author.

Discussion of
## "THE EFFICACY OF FLOOR SILLS UNDER DROWNED HYDRAULIC JUMPS"

by Ahmed Shukry
(Proc. Paper 1260)

A. RYLANDS THOMAS,[a] M. ASCE.—The provision of a sill, lip wall or de-
flector, at the end of the floor to reduce scour downstream of low-head struc-
tures is regarded as standard practice in many countries. The height of sill
is generally about one-tenth of maximum tailwater depth. It is believed that
this device has been used on many of the barrages and other hydraulic works
in Egypt, so the author's preference for a sill at an intermediate position is
all the more surprising. In this he appears to have ignored the evidence of
Fig. (2), which shows the beneficial effect of the end sill in reducing scour
and preferred that of the velocity distribution of Figs. (8) and (11), and cer-
tain earlier tests not quoted.

It would, however, appear that the rigid floor in Figs. (8) and (11) was con-
tinuous beyond section V and therefore the flow pattern at that section was not
representative of conditions where scour occurs immediately downstream of
the sill. There is no reason why the effect of an end sill in the case where the
hydraulic jump is drowned should differ from that where the jump is clear,
provided that in both cases measures are taken to normalize the flow up-
stream of the floor end. These measures may include the provision of a sill,
baffle blocks or baffle piers at an intermediate position and their function is
separate and distinct from that of the end sill which is required in addition.

Rehbock[b] showed that the effect of an end sill was to create a roller with
horizontal axis which swept bed material back towards the end of the floor,
thus reducing the depth of scour at that point, and this action has been con-
firmed in numerous experiments with models, including those of Butcher and
Atkinson.[6] Experience in India and Pakistan with full size structures has
been favourable, though in the case of larger works the effect is generally
masked by the presence of concrete blocks laid downstream as an additional
safety measure. It is only when these blocks have sunk in the sand or have
been washed downstream, which should not occur under design conditions,
that the effect of the end sill in reducing scour becomes apparent.

The author's contention that an end sill is not beneficial would carry more
weight if supported by observations of scour in models and, if available, on
full size structures. It would also be useful if details were given of the gate
regulation, discharge and tailwater depth in the tests to which Figs. (8) to (11)
relate.

---

a. Consultant, Barclay's Bank, Abbey House, London, England.
b. "Bekampfung der Sohlenauskolkung bei Wehren durch Zahnschwellen" by
   Th. Rehbock. Zeitschrift des Vereins Vereins Ingenieure, No. 69,
   p. 1382, 1925.
6. Reference quoted on page 9 of Paper.
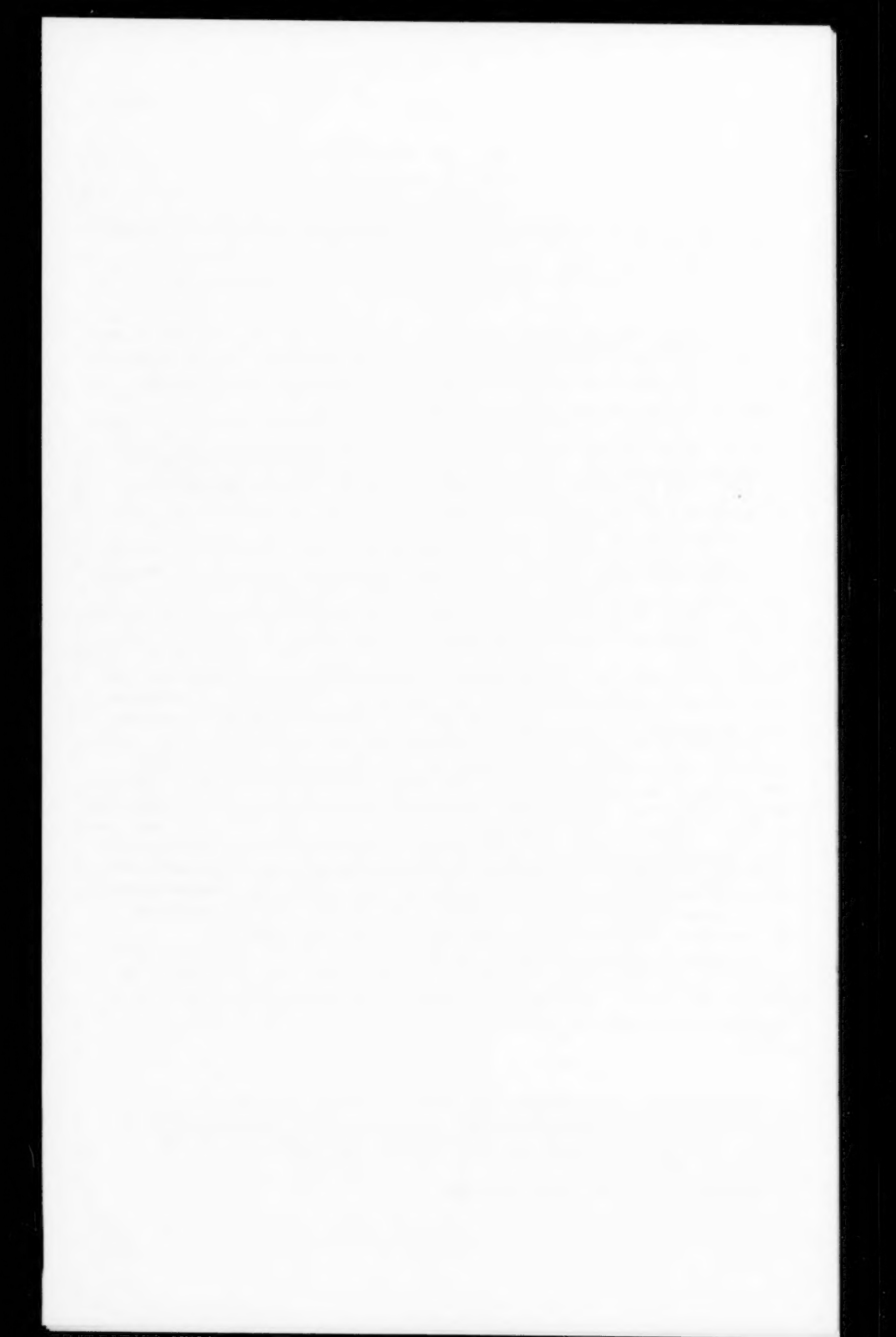
Discussion of
"A STUDY OF BUCKET-TYPE ENERGY DISSIPATOR CHARACTERISTICS"

by M. B. McPherson and M. H. Karr
(Proc. Paper 1266)

E. A. ELEVATORSKI,[a] J.M. ASCE.—The authors have presented useful information on the characteristics of solid roller bucket-type energy dissipators. There is a regretable lack of information on this subject and certainly more is needed. In part, the lack of information can be attributed to the difficulty of relating the many variables which affect the performance of the bucket. It is the purpose of this discussion to list the pertinent factors and relate them in a convenient dimensionless form.

Probably the two most important factors in the design of a solid roller bucket are the size of the bucket radius and the tailwater depth. A combination of the minimum allowable bucket radius and minimum tailwater depth exists, which will permit satisfactory bucket action. Below these limits, the bucket will not perform satisfactorily. Buckets larger than the minimum allowable bucket radius will only slightly improve the bucket performance while being far more costly to construct. It is therefore evident that there is a minimum bucket size which will still perform properly and be the most economical design.

This writer proposes that the minimum allowable bucket radius is a function of the following variables.

$$R_{min.} = f \ ( \ v_1, d_1, s, g, y )$$ (1)

In equation (1), $v_1$ and $d_1$, represent the computed velocity and depth, respectively, for a point at the intersection of the spillway face and tailwater surface. The symbols s, g, and y represent the slope of the spillway face, acceleration due to gravity, and vertical distance between the bucket lip and channel bed, respectively.

With the aid of dimensional analysis, the variables in equation (1) can be reduced to dimensionless form

$$\frac{R_{min.}}{d_1} = f' \ ( \ \frac{v_1^2}{gd_1} \ , \ \frac{s}{y} \ )$$ (2)

Studies conducted by the Bureau of Reclamation[1] indicate that both s and y do not, within ordinary limits, affect the bucket size. It was pointed out, however, that frictional resistance on the spillway face affects the minimum allowable bucket radius, as a result of the velocity reduction. Eliminating $\frac{s}{y}$ from equation (2) we find

---

a. Hydr. Engr., Bureau of Reclamation, U. S. Dept. of the Interior, Salt Lake City, Utah.

$$\frac{R_{min.}}{d_1} = f''(\lambda) \tag{3}$$

where

$$\lambda = \frac{v_1^2}{gd_1}$$

This is contrary to recommendation (d) of the authors, which states that the size of the bucket exerts no influence on bucket action. Investigations by Okada and Ishibashi[2] substantiate the functional relationship given by equation (3) and further state that "the discharge per unit width of spillway is the predominant influence on the bucket size."

When the tailwater is insufficient, the high-velocity flow entering the bucket will break through the supernatant water blanket, leaving the bucket in the form of a jet. The depth at which this action takes place is known as the "sweepout" depth. Considerable scour occurs at the point where the jet strikes the riverbed, making this type of action undesirable. The tailwater depth just safely above the sweepout depth will, hereafter, be called the minimum tailwater depth. Factors affecting the minimum tailwater depth are given in equation (4).

$$t.w._{min.} = f(v_1, d_1, s, R, y, g) \tag{4}$$

Again, by dimensional analysis, equation (4) is reduced to dimensionless form

$$\frac{t.w._{min.}}{d_1} = f'(\lambda, \frac{R}{d_1}, \frac{s}{y}) \tag{5}$$

Within ordinary limits, $\frac{s}{y}$ can be neglected. Consequently,

$$\frac{t.w._{min.}}{d_1} = f''(\lambda, \frac{R}{d_1}) \tag{6}$$

Equations (3) and (6) express the minimum allowable bucket radius and tailwater depth as a function of dimensionless parameters. A relationship between the parameters can be determined with the use of laboratory models.

Some designers may be concerned with the degree of submergence or maximum allowable tailwater depth for satisfactory bucket performance. Evidence obtained from both laboratory and prototype tests seems to indicate that the condition of "diving" flow, for solid roller buckets is impossible except perhaps for rare cases.

Of interest to the designer will be the dimensions of existing solid roller buckets listed in Table 1. As noted in the table, almost all of the buckets

have 45-degree lip slopes. Experiments indicate that a 45-degree lip slope renders best results.(3) If the lip slope is made steeper than 45-degrees, the impact of the flow on the lip wall will disrupt roller action, while for flatter slopes the high-velocity flow downstream from the bucket was found to be submerged.

## REFERENCES

1. Bureau of Reclamation, Progress Report II, Research Study on Stilling Basins, Energy Dissipators, and Associated Appurtenances, Section 7, Slotted and Solid Buckets for High, Medium, and Low Dam Spillways, Hydraulic Laboratory Report No. 415, p. 39, 1956.

2. Okada, O. and Ishibashi, T., Hydraulic Model Tests of Sakuma Dam, Technical Research Laboratory, Central Research Institute of Electric Power Industry, Japan, June 1, 1956, p. 6.

3. Hydraulic Design, Spillways—Engineering Manual, Civil Works Construction (Preliminary), Part CXVI, Chapter 3, Department of the Army, Office of the Chief of Engineers, March 1953, p. 41.

Table 1

SOLID ROLLER BUCKET PROTOTYPE DIMENSIONS

| Structure (1) | Location (2) | Bucket radius (feet) (3) | Maximum discharge (c.f.s.) (4) | Max. q (c.f.s. per ft. of bucket width) (5) | Head (feet) [1] (6) | Bucket lip slope (7) | Tailwater depth (feet) [2] (8) | Remarks (9) |
|---|---|---|---|---|---|---|---|---|
| Buggs Island | Virginia-No.Carolina | 40 | 770,000 | 705 | 167 [1] | 45° | 70 | |
| Center Hill | Tennessee | 50 | 457,000 | 973 | 226 [1] | 45° | 86.4 | bucket invert varies |
| Clark Hill | Georgia-So.Carolina | 50 | 1,058,000 | 964 | 185 | 45° | 69.2 | |
| Davis | Arizona-California | 75 | 192,000 | 781 | 177 | 45° | 70 [4] | |
| Grand Coulee | Washington | 50 | 1,000,000 | 606 | 422 | 45° | 161.5 | |
| Greensboro | No.Carolina | 17 | 32,000 | 540 | 72 | 45° | 33.0 | |
| Headgate Rock | Arizona-California | 40 | 200,000 | 500 | 83 | 45° | 55.6 | |
| Murdock | Utah | 5 | 5,000 | 500 | 21 | 37° | --- | |
| Penn Forest | Pennsylvania | 17 | 12,000 | 300 | 132.5 [5] | 45° | --- | |
| Sakuma | Japan | 63.1 | 346,000 | 1,315 | 389 [5] | 45° | 90 | |
| Stewarts Ferry | Tennessee | 40 | 199,250 | 607 | 122 [5] | 45° | 60.5 | bucket invert varies |
| Wolf Creek | Kentucky | 50 | 535,000 | 907 | 227 | 45° | 102.6 | |

[1] From maximum pool level to bucket invert.
[2] At maximum discharge.
[3] From spillway crest to bucket invert.
[4] Approximate.
[5] Varies.

Discussion of
"MEASUREMENT OF SEDIMENTATION IN TVA RESERVOIRS"

by E. H. McCain
(Proc. Paper 1277)

LLOYD C. FOWLER,[a] J.M. ASCE and ROBERT H. LIVESEY.[b]—There has
been, in recent years, considerable improvement in the equipment and pro-
cedures available for hydrographic surveys; however, there has been little
correlation or standardization in the use of the newer more accurate and
efficient equipment and procedures. The author's dissemination of informa-
tion on the procedures of the TVA surveys should contribute to the general
advancement.

The adoption of the sonic sounding to replace the laborious and time-
consuming sounding by hand line is unquestionably a major forward step in
sub-aqueous surveys. Instead of a series of point elevations, the sonic
sounder produces a continuous and permanent record of the bottom configura-
tion. High frequency sounders will accurately show the surface of low-
density deposits, and low frequency sounders can penetrate deposited sedi-
ments, recording the surfaces between superimposed strata of increasing
density.

Sounder accuracy of $\pm 3$ inches between depths of 3 to 50 feet, and $\pm 6$ inches
for greater depths, is adequate for most hydrographic surveys over relatively
flat or gently sloping terrain. However, two sources of error are introduced
immediately when traversing steep slopes or vertical banks; both originate
with the transmission of the sound wave in a diverging cone from the trans-
ducer (antenna) and increase with depth of water. First, an error in depth is
introduced because the recorded echo was reflected from the shallowest sur-
face within the radius of the cone, and second, a positioning error due to the
increasing radius of the cone with depth. Assuming, for example, the cone
apex is $30^O$ (it can vary from $7 1/2^O$ to $50^O$ depending on the type of trans-
ducer), then at a depth of 50 feet the recorded echo could have theoretically
originated from the shallowest depth anywhere within a circle 27 feet in
diameter, discounting any signal loss due to absorption or radiation.

The several districts within the Missouri River Division of the Corps of
Engineers have had considerable experience in the development and improve-
ment of the equipment and procedures used in hydrographic survey work on
both rivers and reservoirs. Their experience has indicated that the proper
craft for work of this nature depends on the conditions imposed by the river
or reservoir. A skiff with an outboard motor is best used in shallow water
along the shores of a reservoir, in its headwaters, or in the open river while
a relatively large inboard cabin cruiser capable of withstanding heavy weather
and seas may be best for the sounding of long and deep reservoir ranges.

---

a. Hydr. Engr., Missouri River Div., Corps of Engrs., U. S. Dept. of the
   Army, Omaha, Nebr.
b. Head, Reservoir Sedimentation Unit, Omaha Dist., Corps of Engrs., U. S.
   Dept. of the Army, Omaha, Nebr.

Some craft may be specially designed to meet specific needs.  For instance,
Figure 7 shows a shallow draft river survey boat designed especially to ob-
tain data on sediment transport, velocity distribution, and bed form roughness
in the open river.

In the boats, launches, or skiffs, used regularly for sounding, the trans-
ducers should be mounted within the hull.  One exception is a scow bow boat
(see Figure 8).  The skiff illustrated in Figure 1, is not generally considered
as having a scow bow.  Transducers mounted inside the hull of scow bow
boats have proven to be unsatisfactory for sonic sounding because of the pas-
sage. of entrained air under the hull.  The transmission of sound through this
aerated lamina results in a severe reduction and usually a complete attenua-
tion of the transmitted signal and returning echo.  With a scow bow boat the
outrigger "shoe" enclosing the antenna is essential (Figure 8).

Seaworthiness, maneuverability, and draft are relatively constant factors
inherent in the design of a specific survey boat; however, weight and bulk of
equipment, plus survey "know how" are variables which directly influence the
safety, accuracy, and economy of reservoir and river hydrographic surveys.
Considering the skiff described by the author, removal of the outrigger "shoe"
with its enclosing well would produce a sizeable reduction in both weight and
bulk.  Early experience with mounting the "shoe" in an open well, similar to
that illustrated in Figure 2, resulted in a reduction in maximum boat speed of
almost 50 percent and severely limited the maximum sounding speed by intro-
ducing aeration below the transducers.  All of the boat speed was returned
and higher sounding speeds were possible when the bottom of the well was
closed by a smooth steel plate mounted flush with the bottom of the skiff.
The "shoe" was then placed just above the steel plate and submerged in a few
inches of water.  However, constant attention was required to keep the outside
surface of the plate smooth to prevent the accumulation of entrained air which
would obliterate the sounding trace.

Even greater efficiency and excellent results have been obtained by replac-
ing the awkward well and "shoe" by separate transmitting and receiving mag-
neto-restriction transducer units mounted in individual tanks attached to the
inside of the hull.  Figure 9a illustrates the interior transducer mounting in a
38 foot steel launch and Figure 9b shows the installation in a 16 foot fiber-
glas skiff.  The individual transducer tanks were mounted athwart-ship near
the keel and just forward of the center of the boat.  Each tank was tailored to
fit the dead rise of the hull so that the transducer reflector cone rested in the
horizontal plane.  After installation of the transducers, the tanks were filled
with castor oil which doubles as the sounding medium and anti-freeze.

Utilization of this type of installation requires only the transfer of the re-
cording unit and battern when changing the survey work from one craft to an-
other.  It also makes possible reconnaissance soundings at speeds of 15 to 20
miles per hour.  During a recent reconnaissance survey, the sounding of the
thalweg profile of a 100 mile reach of submerged river channel, plus the
sounding of 20 reservoir ranges, which totalled about 20 miles in length,
(positioning along the ranges was determined by current meter) was accom-
plished by two men in 12 hours.

The accurate location of the boat on the range poses a problem which has
been ingeniously solved on the TVA surveys by the use of stretched piano wire
as described by the author.  However, the question is raised:  can the weight
and bulk of this equipment be justified to obtain a distance measurement ac-
curate to 2 feet in 6000 feet when a simultaneous depth measurement of 50

feet could have been reflected from any point within a 27 foot diameter circle? It is believed that the 6000 foot distance as measured by means of the piano wire approaches the maximum feasible distance for this method; certainly it would be unsuitable for Missouri River reservoirs where the ranges frequently exceed three miles in length, and for use in the open river.

In the Missouri River Division the distance along the range line is fixed by one of three methods:

a) By direct stadia measurement on short ranges (Figure 10). This method is extensively used on the open river where the sight distance is less than 2000 feet.

b) By current meter measurement on long ranges in still water. Insofar as the writers know, this method of distance measurement was initiated by the Southwest Division of the Corps of Engineers. The current meter is suspended from a boom near the bow of the boat (Figure 11) and calibrated under field conditions. (The distance computed from the standard current meter formula will vary from the field distance by an amount depending on the field installation). Using the field calibration, check measurements have indicated a maximum error of 1 per cent for this method.

c) By Raydist measurement. This is an electronic device which after calibration measures the distance between a master station on the boat and a relay station on the shore (Figure 12). Over open water it is accurate to within 0.02 percent (1 in 5000); however, its accuracy decreases sharply when used within about 600 feet of the shore. It has proved to be very effective over long ranges but as its initial cost is high the Raydist unit could not be justified except for very large reservoirs.

With both the current meter and Raydist measurements, the distance at the ends of the sounding ranges near the shores must be measured by some other means such as stadia or a range finder. The sounding boat is kept on the range by sighting range markers, and where greater accuracy is required, by transit and radio.

The use of portable radio equipment, as described by the author, has been found to be highly beneficial in surveying, both on land and water. They provide a real economy of operation as well as convenience.

Figure 7a. River survey boat Santee. A shallow draft
boat especially designed for the study of sediment
transport in the open river. Note the large amount of
special measurement equipment on foredeck.



Figure 7b. River survey boat Santee in position for
sediment transport measurement on a 1200 foot tag line
stretched above the river. Tag line is not used when
sounding the river bed.

Figure 8. River survey boat Terrapin. With the scow
bow it is necessary to use the outrigger sonic sounder
antenna. Note the outrigger mounting at stern of boat;
the "shoe" is in the water.



Figure 9a. Installation of transducer wells inside the
steel hull of the reservoir survey launch Dakota.

Figure 9b.  Installation of transducer wells inside the
fiberglas hull of a 16 foot skiff.  The wells are
located out of the way beneath a seat.



Figure 9c.  Transducer wells in hull of fiberglas skiff.
One transducer has been removed from the well.

Figure 10a.  Fiberglas skiff sounding a river range.
Distance measurement to "fixes" on range measured by
stadia.  Fixes marked and reported by portable radio.
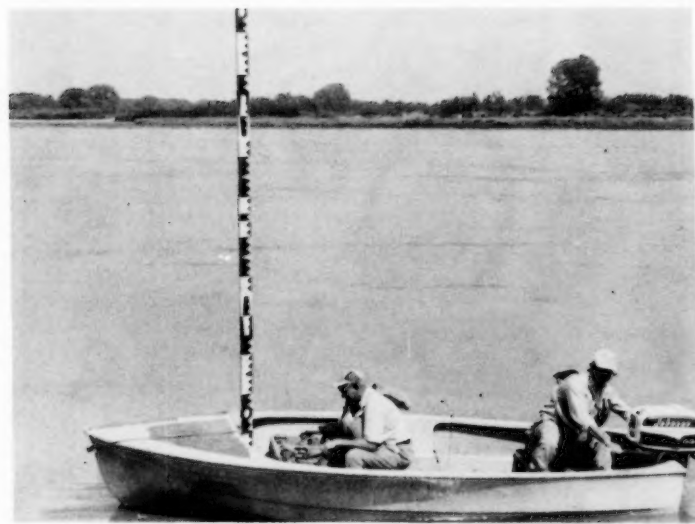


Figure 10b.  Fiberglas skiff sounding a river range.

Figure 10c.  Sonic sounding equipment in fiberglas skiff.



Figure 10d.  Launching fiberglas skiff.  Note convenience
of hitch mounted on front bumper of power wagon.

Figure 11. Current meter used to measure distance along reservoir ranges as mounted on bow of reservoir survey launch Dakota.



Figure 12a. Raydist distance measuring equipment mounted on Santee. Master control station is inside the cabin and the transmitter is mounted on the stern. Note large number of antennas.

Figure 12b.  Raydist phase meter used to indicate
distance from boat to relay stations on shore.



Figure 12c.  Raydist relay stations on shore.  Transit
is used to keep boat on range and provide "fixes" when
the boat is less than 600 feet from shore.

## PROCEEDINGS PAPERS

The technical papers published in the past year are identified by number below. Technical-division sponsorship is indicated by an abbreviation at the end of each Paper Number, the symbols referring to: Air Transport (AT), City Planning (CP), Construction (CO), Engineering Mechanics (EM), Highway (HW), Hydraulics (HY), Irrigation and Drainage (IR), Pipeline (PL), Power (PO), Sanitary Engineering (SA), Soil Mechanics and Foundations (SM), Structural (ST), Surveying and Mapping (SU), and Waterways and Harbors (WW), divisions. Papers sponsored by the Board of Direction are identified by the symbols (BD). For titles and order coupons, refer to the appropriate issue of "Civil Engineering." Beginning with Volume 82 (January 1956) papers were published in Journals of the various Technical Divisions. To locate papers in the Journals, the symbols after the paper numbers are followed by a numeral designating the issue of a particular Journal in which the paper appeared. For example, Paper 1113 is identified as 1113 (HY6) which indicates that the paper is contained in the sixth issue of the Journal of the Hydraulics Division during 1956.

### VOLUME 82 (1956)

OCTOBER: 1070(EM4), 1071(EM4), 1072(EM4), 1073(EM4), 1074(HW3), 1075(HW3), 1076(HW3), 1077(HY5), 1078(SA5), 1079(SM4), 1080(SM4), 1081(SM4), 1082(HY5), 1083(SA5), 1084(SA5), 1085(SA5), 1086(PO5), 1087(SA5), 1088(SA5), 1089(SA5), 1090(HW3), 1091(EM4)^C, 1092 (HY5)^C, 1093(HW3)^C, 1094(PO5)^C, 1095(SM4)^C.

NOVEMBER: 1096(ST6), 1097(ST6), 1098(ST6), 1099(ST6), 1100(ST6), 1101(ST6), 1102(IR3), 1103 (IR3), 1104(IR3), 1105(IR3), 1106(ST6), 1107(ST6), 1108(ST6), 1109(AT3), 1110(AT3)^C, 1111(IR3)^C, 1112(ST6)^C.

DECEMBER: 1113(HY6), 1114(HY6), 1115(SA6), 1116(SA6), 1117(SU3), 1118(SU3), 1119(WW5), 1120(WW5), 1121(WW5), 1122(WW5), 1123(WW5), 1124(WW5)^C, 1125(BD1)^C, 1126(SA6), 1127 (SA6), 1128(WW5), 1129(SA6)^C, 1130(PO6)^C, 1131(HY6)^C, 1132(PO6), 1133(PO6), 1134(PO6), 1135(BD1).

### VOLUME 83 (1957)

JANUARY: 1136(CP1), 1137(CP1), 1138(EM1), 1139(EM1), 1140(EM1), 1141(EM1), 1142(SM1), 1143(SM1), 1144(SM1), 1145(SM1), 1146(SM1), 1147(ST1), 1148(ST1), 1149(ST1), 1150(ST1), 1151(ST1), 1152(CP1)^C, 1153(HW1), 1154(EM1)^C, 1155(SM1)^C, 1156(ST1)^C, 1157(EM1), 1158 (EM1), 1159(SM1), 1160(SM1), 1161(SM1).

FEBRUARY: 1162(HY1), 1163(HY1), 1164(HY1), 1165(HY1), 1166(HY1), 1167(HY1), 1168(SA1), 1169(SA1), 1170(SA1), 1171(SA1), 1172(SA1), 1173(SA1), 1174(SA1), 1175(SA1), 1176(SA1), 1177(HY1)^C, 1178(SA1), 1179(SA1), 1180(SA1), 1181(SA1), 1182(PO1), 1183(PO1), 1184(PO1), 1185(PO1)^C.

MARCH: 1186(ST2), 1187(ST2), 1188(ST2), 1189(ST2), 1190(ST2), 1191(ST2), 1192(ST2)^C, 1193 (PL1), 1194(PL1), 1195(PL1).

APRIL: 1196(EM2), 1197(HY2), 1198(HY2), 1199(HY2), 1200(HY2), 1201(HY2), 1202(HY2), 1203 (SA2), 1204(SM2), 1205(SM2), 1206(SM2), 1207(SM2), 1208(WW1), 1209(WW1), 1210(WW1), 1211(WW1), 1212(EM2), 1213(EM2), 1214(EM2), 1215(PO2), 1216(PO2), 1217(PO2), 1218 (SA2), 1219(SA2), 1220(SA2), 1221(SA2), 1222(SA2), 1223(SA2), 1224(SA2), 1225(PO)^C, 1226 (WW1)^C, 1227(SA2)^C, 1228(SM2)^C, 1229(EM2)^C, 1230(HY2)^C.

MAY: 1231(ST3), 1232(ST3), 1233(ST3), 1234(ST3), 1235(IR1), 1236(IR1), 1237(WW2), 1238(WW2), 1239(WW2), 1240(WW2), 1241(WW2), 1242(WW2), 1243(WW2), 1244(HW2), 1245(HW2), 1246 (HW2), 1247(HW2), 1248(WW2), 1249(HW2), 1250(HW2), 1251(WW2), 1252(WW2), 1253(IR1), 1254(ST3), 1255(ST3), 1256(HW2), 1257(IR1)^C, 1258(HW2)^C, 1259(ST3)^C.

JUNE: 1260(HY3), 1261(HY3), 1262(HY3), 1263(HY3), 1264(HY3), 1265(HY3), 1266(HY3), 1267 (PO3), 1268(PO3), 1269(SA3), 1270(SA3), 1271(SA3), 1272(SA3), 1273(SA3), 1274(SA3), 1275 (SA3), 1276(SA3), 1277(HY3), 1278(HY3), 1279(PL2), 1280(PL2), 1281(PL2), 1282(SA3), 1283 (HY3)^C, 1284(PO3), 1285(PO3), 1286(PO3), 1287(PO3)^C, 1288(SA3)^C.

JULY: 1289(SM3), 1290(EM3), 1291(EM3), 1292(EM3), 1293(EM3), 1294(HW3), 1295(HW3), 1296(HW3), 1297(HW3), 1298(HW3), 1299(SM3), 1300(SM3), 1301(SM3), 1302(ST4), 1303 (ST4), 1304(ST4), 1305(SU1), 1306(SU1), 1307(SU1), 1308(ST4), 1309(SM3), 1310(SU1)^C, 1311(EM3)^C, 1312 (ST4), 1313(ST4), 1314(ST4), 1315(ST4), 1316(ST4), 1317(ST4), 1318 (ST4), 1319(SM3)^C, 1320(ST4), 1321(ST4), 1322(EM3), 1323(AT1), 1324(AT1), 1325(AT1), 1326(AT1), 1327(AT1), 1328(AT1)^C, 1329(ST4)^C.

AUGUST: 1330(HY4), 1331(HY4), 1332(HY4), 1333(SA4), 1334(SA4), 1335(SA4), 1336(SA4), 1337(SA4), 1338(SA4), 1339(CO1), 1340(CO1), 1341(CO1), 1342(CO1), 1343(CO1), 1344(PO4), 1345(HY4), 1346(PO4)^C, 1347(BD1), 1348(HY4), 1349(SA4)^C, 1350(PO4), 1351(PO4).

SEPTEMBER: 1352(IR2), 1353(ST5), 1354(ST5), 1355(ST5), 1356(ST5), 1357(ST5), 1358(ST5), 1359(IR2), 1360(IR3), 1361(ST5), 1362(IR2), 1363(IR2), 1364(IR2), 1365(WW3), 1366(WW3), 1367(WW3), 1368(WW3), 1369(WW3), 1370(WW3), 1371(HW4), 1372(HW4), 1373(HW4), 1374(HW4), 1375(PL3), 1376(PL3), 1377(IR2)^C, 1378(HW4)^C, 1379(IR2), 1380(HW4), 1381(WW3)^C, 1382(ST5)^C, 1383(PL3)^C, 1384(IR2), 1385(HW4), 1386(HW4).

OCTOBER: 1387(CP2), 1388(CP2), 1389(EM4), 1390(EM4), 1391(HY5), 1392(HY5), 1393(HY5), 1394(HY5), 1395(HY5), 1396(PO5), 1397(PO5), 1398(PO5), 1399(EM4), 1400(SA5), 1401(HY5), 1402(HY5), 1403(HY5), 1404(HY5), 1405(HY5), 1406(HY5), 1407(SA5), 1408(SA5), 1409(SA5), 1410(SA5), 1411(SA5), 1412(EM4), 1413(EM4), 1414(PO5), 1415(EM4)^C, 1416(PO5)^C, 1417 (HY5)^C, 1418(EM4), 1419(PO5), 1420(PO5), 1421(PO5), 1422(SA5)^C, 1423(SA5), 1424(EM4), 1425(CP2).

C. Discussion of several papers, grouped by Divisions.